Friedreich ataxia: investigating the relationships between mismatch repair gene expression, *FXN* gene expression and GAA repeat instability in human and mouse cells and tissues.

A thesis submitted for the degree of Doctor of Philosophy by

Vahid Ezzatizadeh

December 2012

Division of Biosciences
School of Health Sciences and Social Care

Declaration

I hereby declare that the research presented in this thesis is my own work, except where otherwise specified, and has not been submitted for any other degree.

Vahid Ezzatizadeh

Abstract

Friedreich ataxia (FRDA) is the most common inherited ataxia disorder, caused by a GAA repeat expansion mutation within the first intron of the *FXN* gene. The subsequent deficiency of frataxin protein leads to neurological disability, increased risk of diabetes mellitus, cardiomyopathy and premature death. The exact FRDA disease mechanism is not yet clear, despite some understanding of epigenetic, transcriptional and DNA repair system effects that lead to frataxin reduction. Previous studies have shown that mismatch repair (MMR) genes can affect other trinucleotide repeat disorders by destabilisation of the repeats. Furthermore, it has been proposed that frataxin deficiency might lead to cell malignancy by an as yet undefined mode of action. Therefore, the principle aim of this thesis was to use human and genetically altered mouse cells and tissues to understand the effects of MMR proteins on GAA repeat instability and *FXN* transcription, and also to identify potential changes in MMR transcription that might cause malignancy in *FXN*-defective human cells.

Firstly, by using *FXN* and MMR genetically altered mice, MMR proteins were shown to be involved in both intergenerational and somatic GAA repeat instability, although their effects in the two systems were different. Thus, Msh2 or Msh3 were both found to protect against intergenerational transmission of GAA contractions, while loss of Msh2 or Msh3 reduced somatic GAA repeat expansions and increased levels of *FXN* transcription in brain and cerebellum tissues. Loss of Msh6 induced both intergenerational GAA repeat expansions and contractions, while the frequency of somatic GAA repeat expansions was reduced. Curiously, the level of *FXN* transcription was also reduced in Msh6-deficient brain and cerebellum tissues. On the other hand, Pms2 was found to protect against both intergenerational and somatic GAA repeat expansions, with loss of Pms2 causing increased GAA repeat expansions and decreased levels of *FXN* transcription in brain and cerebellum tissues.

Finally, loss of Mlh1 led to a reduced frequency of both intergenerational and somatic GAA repeat expansions, but the level of *FXN* transcription was also reduced in brain and cerebellum tissues. Furthermore, upregulation of MMR mRNA expression was detected in human FRDA fibroblast cells, but downregulation was seen in FRDA cerebellum tissues, suggesting tissue-dependent control of *FXN* and MMR expression. In summary, these studies indicate that the MMR system can affect GAA repeat expansion instability and *FXN* transcription through different mechanisms of action. Furthermore, frataxin deficiency can also affect the levels of MMR mRNA expression in a tissue-dependent manner. These findings will assist future investigations aimed at identifying novel FRDA therapies.

Acknowledgments

Foremost, I would like to give my sincere gratitude to my supervisor, Dr. Mark Pook, for his patience, guidance, friendship and most importantly his kind and unforgettable support during this project. Thanks also to Dr. Mariann Rand-Weaver, my second supervisor.

In addition, I gratefully thank Dr. Sahar Al-Mahdawi for her careful attention to my work and her instruction on some practical techniques that undoubtedly elevated my dissertation. Her worthy comments in meetings increased my knowledge and experience, and her keen insight, great experience, and thoughtful reflection on the different aspect of research are outstanding abilities to which I aspire.

My other laboratory colleagues, Dr. Ricardo Mouro Pinto and Dr. Chiranjeevi Sandi, have also provided excellent guidance. Conversations and consultations with Ricardo Mouro Pinto helped me become more familiar with the project issues, and critical scientific points explained by Chiranjeevi Sandi have supported my research. I must also thank our present PhD students, Sara Anjomani and Madhavi Sandi, for being nice colleagues.

I am grateful to Steve Pash, Julie Walker and Sue Toogood for their invaluable assistance in successful maintenance of animal husbandry.

I would also like to acknowledge Prof. Robert Newbold for kindly referring me to Prof. Christos Paraskeva who generously provided HCT-116 cell line for this project.

It is my pleasant honour to thank Ataxia UK, GoFAR (Italy), FARA (USA) and the NIH who financially supported the work presented in this thesis.

Finally, and most importantly, after thanks to my GOD, I deeply acknowledge my family, particularly my parents and older brother, whose support helped me to follow my study.

This dissertation is dedicated to my parents who always supported me, who always made education one of their top priorities, and who taught me to love learning.

Table of contents

List of figures

List of tables

List of the abbreviations

5-aza-dC	5-aza-2'-deoxycytidine
ADL	activities of daily living
AID	activation-induced cytidine deaminase
AT	ataxia telangiectasia
BAC	bacterial artificial chromosome
bp	base pair
C.elegans	*Caenorhabditis elegans*
CAT	catalase
CBP	CREB binding protein
cDNA	complementary DNA
CoQ_{10}	coenzyme Q_{10}
CRC	colorectal cancer
DEPC	diethylpyrocarbonate
DFP	deferiprone
DM1	myotonic dystrophy type 1
DMEM	Dulbecco's modified eagle medium
DMPK	myotonic dystrophy protein kinase
DNMT	DNA methyltransferase
DSB	double strand break
dsDNA	double-strand DNA
E.coli	*Escherichia coli*
EGFP	enhanced green fluorescent protein
ERK	extracellular-signal-regulated kinase
ETC	electron transport chain
FARR	FRDA with retained tendon reflexes
FCS	foetal calf serum
FRDA	Friedreich ataxia
GFP	green fluorescent protein
GGR	global genome repair
G-PCR	gradient-PCR
GPX	glutathione peroxidase
G-RT-PCR	gradient-reverse transcriptase-PCR
HAT	histone acetyltransferase
hCD2	human CD2
HD	Huntington disease
HDAC	histone deacetylase
HDACi	HDAC inhibitor
Het	heterozygous
HIF	hypoxia-inducible factor
HMGB1	high mobility group box 1
hMLH1	human MLH1
HNPCC	hereditary non-polyposis colorectal cancer
HP1	heterochromatin protein 1
HR	homologous recombination
HRE	hypoxia-responsive element
iPSC	induced pluripotent stem cell

IRP1	iron regulatory protein-1
ISC	iron sulfur cluster
kb	kilobase
KO	knockout
LOH	loss of heterozygosity
MBP	methyl CpG binding proteins
MCK	muscle creatine kinase
MCK-KO	muscle creatine kinase conditional frataxin knockout
MEF	mouse embryonic fibroblast
MLH1	human MutL homologue 1
MMR	mismatch repair
mRNP	messenger ribonucleoprotein
MSH2	MutS homolog 2
MSI	microsatellite instability
NER	nucleotide excision repair
NSE	neuron-specific enolase
PCNA	proliferating cell nuclear antigen
PCR	polymerase chain reaction
PD	population doubling
Pen	*penicillin*
PEV	position effect variegated
PMS2	post meiotic segregation increased 2
Pur.Pyr	poly-purine.poly-pyrimidine
qRT-PCR	quantitative reverse transcriptase-PCR
RFC	replication factor C
RNAi	RNA interference
ROS	reactive oxygen species
RPA	replication protein A
RQ	relative quantification
RT-PCR	reverse transcriptase-PCR
SAHA	suberoylanilide hydroxamic acid
SCA1	spinocerebellar ataxia 1
SIX5	sine oculis homeobox homologue 5
SOD	superoxide dismutase
SSB	ssDNA binding protein
ssDNA	single-strand DNA
SSR	simple sequence repeats
Strep	*streptomycin*
TBE	tris-borate-EDTA
TCR	transcription-coupled repair
TE	tris-EDTA
TNR	trinucleotide repeats
TSA	trichostatin A
UV	ultraviolet
WT	wild-type
YAC	yeast artificial chromosome
Yfh1	yeast frataxin homologue gene 1

Chapter 1 - Introduction: Friedreich ataxia (FRDA) and DNA mismatch repair

1.1 - Ataxia

The word ataxia comes from the Greek “a-taxia”, meaning literally “no order”. Indeed, it is a blanket term referring to a loss of muscle control. Sometimes, loss of position sense may result from de-afferentation, with subsequent ataxia (called sensory ataxia). This problem generally occurs because of defects in parts of the nervous system that control coordination of movement, particularly the cerebellum. Ataxia can be a symptom of many disorders, such as multiple sclerosis or cerebellar palsy. However, it is the principle symptom of a group of neurological disorders termed “cerebellar ataxias”.

Generally, diseases of ataxia are sub-divided into two different groups: sporadic and hereditary (Table 1.1). Hereditary ataxia is a form that occurs via genetic defects and is associated with a familial history. In general, the inherited ataxias are classified into two types: early onset disorders (under 25 years old) that are usually autosomal recessive in inheritance, such as Friedreich ataxia, and later onset cases of cerebellar degeneration that are most often dominantly inherited (Klockgether 2007). Although, classification of the hereditary ataxias remains a matter of controversy, they can also be divided into types caused by metabolic defect, such as ataxia telangiectasia and abetalipoproteinaemia, and those which fit the features of a named disease, such as Friedreich ataxia and spinocerebellar ataxia (Cellini *et al.* 2001; Nardin and Johns 2001; Klockgether 2007; Sas *et al.* 2007; de Souza-Pinto *et al.* 2008).

Table 1.1 - Classification of progressive ataxias (Klockgether 2007)**.**

- ***Hereditary ataxias***
  - **Autosomal recessive ataxias**
    - Friedrich ataxia (FRDA)
    - Ataxia telangiectasia (AT)
    - Autosomal recessive ataxia with oculomotor apraxia type 1 (AOA1)
    - Autosomal recessive ataxia with oculomotor apraxia type 2 (AOA2)
    - Spinocerebellar ataxia with axonal neuropathy (SCAN1)
    - Abetalipoproteinaemia
    - Ataxia with isolated vitamin E deficiency (AVED)
    - Refsum disease
    - Cerebrotendinous xanthomatosis
    - Other autosomal recessive ataxias
  - **Autosomal dominant ataxias**
    - Spinocerebellar ataxias
- ***Non-hereditary degenerative ataxias***
  - Multiple system atrophy, cerebellar type (MSA-C)
  - Sporadic adult-onset ataxia of unknown origin (SAOA)
  - Acquired ataxias
  - Alcoholic cerebellar degeneration
  - Ataxia due to other toxins
  - Ataxia caused by acquired vitamin deficiency or metabolic disorders
  - Paraneoplastic cerebellar degeneration
  - Immune-mediated ataxias

1.2 - Friedreich ataxia

Friedreich ataxia (FRDA; OMIM 229300) is a progressive autosomal recessive inherited disorder, with usual onset in childhood or adolescence, mainly caused by spinocerebellar degeneration.

1.2.1 - Prevalence

FRDA is the commonest hereditary ataxia, accounting for approximately half of all inherited ataxias. It is recognised as a rare disease with a prevalence of 1-2 per 100,000 individuals. The carrier rate was initially reported to be 1:110 in the USA and UK, but lower in Far-East

Asian and sub-Saharan African societies. However, accessibility to molecular diagnostic techniques has helped to identify affected individuals and carriers more precisely, so that the estimated incidence has now increased to 1:30,000 persons and the estimated carrier rate is now 1:60-1:90 (Cossee *et al.* 1997; Epplen *et al.* 1997; Pandolfo and Montermini 1998; Bidichandani *et al.* 2000; Delatycki *et al.* 2000; Labuda *et al.* 2000; Puccio and Koenig 2000). FRDA is generally first observed under 25 years of age (the average age of onset is 10-12 years), with an equal range in both genders; although cases of later onset or very late onset may also occur rarely (Bidichandani *et al.* 2000; Berciano *et al.* 2005; Bhidayasiri *et al.* 2005; Condo *et al.* 2006).

1.2.2 - Clinical features

The natural history of FRDA is gradual development of neurological symptoms, followed by muscular deficiencies. The main presenting symptoms include gait and limb ataxia (first in the lower extremities, followed by all limbs), associated with optic atrophy, deafness, severe dysarthria, defect or absence in vibration and position sense (however the temperature and pain senses are preserved), loss of reflexes (particularly in the lower extremities), the presence of spasticity and extensor plantar responses and muscle atrophy and weakness, together with a hypertrophic obstructive cardiomyopathy in most of the patients. Since the disorder is aggressive, most of patients are wheelchair bound by 15 years after onset, followed by death in the third to fifth decades of life. Following clinical consideration, FRDA is diagnosed by molecular analysis (Alper and Narayanan 2003; Koeppen 2011).

1.2.3 - Pathology

The crucial sites affected in FRDA are dorsal root ganglia (DRG), dentate nucleus of the cerebellum, posterior columns and corticospinal tracts of the spinal cord, and heart.

Generally, the FRDA lesion causes several changes throughout the entire DRG, but mainly in the sub-capsular regions (Figure 1.1).

Figure 1.1 - Pathology of DRG in FRDA and Normal cells (Koeppen 2011).

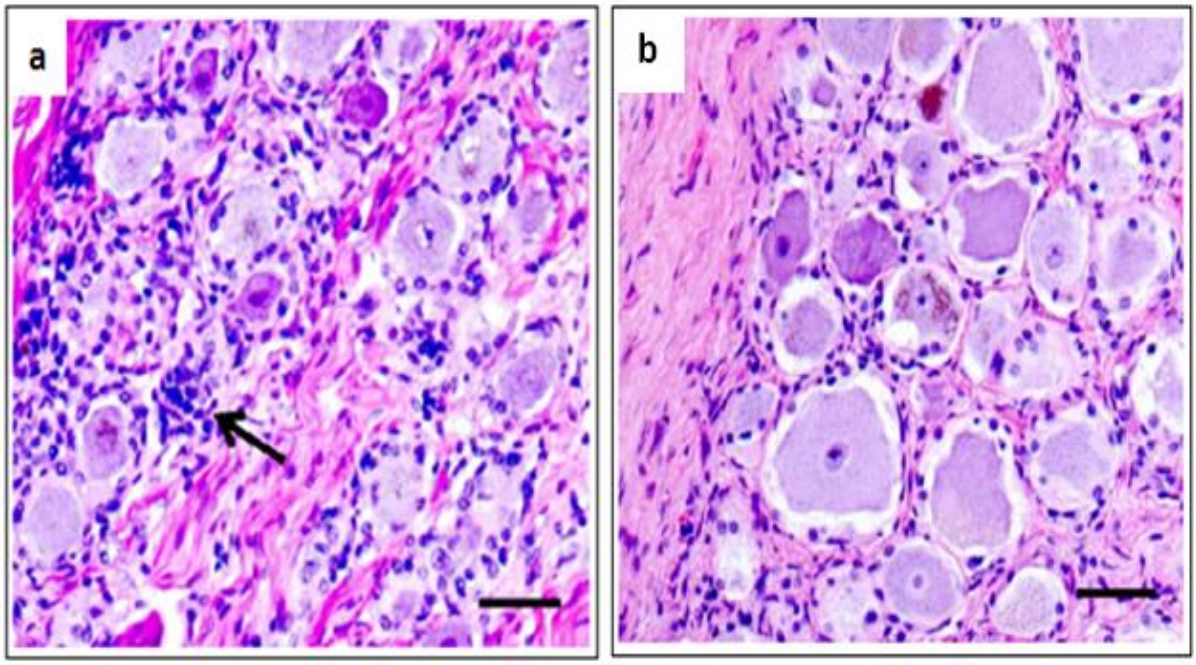

Haematoxylin and eosin staining of DRG in **(a)** FRDA and **(b)** unaffected individuals show a reduced size of sub-capsular neurons in FRDA. The arrow **(a)** shows a nodule of Nageotte.

Macroscopically, a small spinal cord is detectable, with reduced dorsal columns, spinocerebellar and pyramidal tracts in FRDA. The nervous system changes result in axonal atrophy and loss of sensory axons (particularly large myelinated fibres) in peripheral nerves. Loss of the large sensory neurons is particularly prominent in the DRG and de-myelination is detectable in the posterior columns of the spinal cord. There is only mild neuronal loss in the cerebellar cortex. Reduction of phospholipid levels can also be detected in the cerebellar and occipital cortex of the brain (Pandolfo 1999; Condo *et al.* 2006).

1.2.4 - Frataxin protein

FRDA is caused by deficiency of a conserved mitochondrial protein that is found ubiquitously in all cells from bacteria to humans, called frataxin (Figure 1.2). The precursor form of frataxin is a 210 amino acid protein, containing an N-terminal transit amino-acid sequence that conducts its transport into the mitochondria, where two cleavages occur. These two proteolytic steps convert the precursor protein to a 19kDa intermediate and a 17kDa mature form of frataxin, respectively. The final protein in mitochondria is recognised as the mature form of frataxin (Condo *et al.* 2007). The first idea of frataxin maturation was obtained by physical interaction between the mouse frataxin precursor and mouse mitochondrial processing peptidase β (MPP-β). It was recognised that by binding MPP-β, frataxin was initially cleaved between residues 41-42 to make the initial intermediate form of frataxin (amino-acids 42-210) (Koutnikova *et al.* 1998; Condo *et al.* 2007). Subsequently, the second cleavage on human frataxin *in vitro* was observed between residues Ala55 and Ser56 by MPP. This was the first reported mature form of frataxin (m56-210) (Cavadini *et al.* 2000; Condo *et al.* 2007). Later, other independent *in vivo* studies identified two mature forms of frataxin, cleaved at residues Leu78-Arg79 (m79-210) and Lys80-Ser81 (m81-210). Mass spectrometry investigations showed that the m79-210 product is caused by natural degradation leading to a non-functional 14.5kDa frataxin. In contrast to m79-210, the m81-210 form is recognised as a functional protein, which is not produced from m56-210 frataxin degradation. This protein has the capability to bind and transfer ferrous iron in iron sulfur cluster (ISC) and heme biosynthesis.

Figure 1.2 - Multiple alignments of predicted protein sequences of frataxin (Long *et al.* 2008)**.**

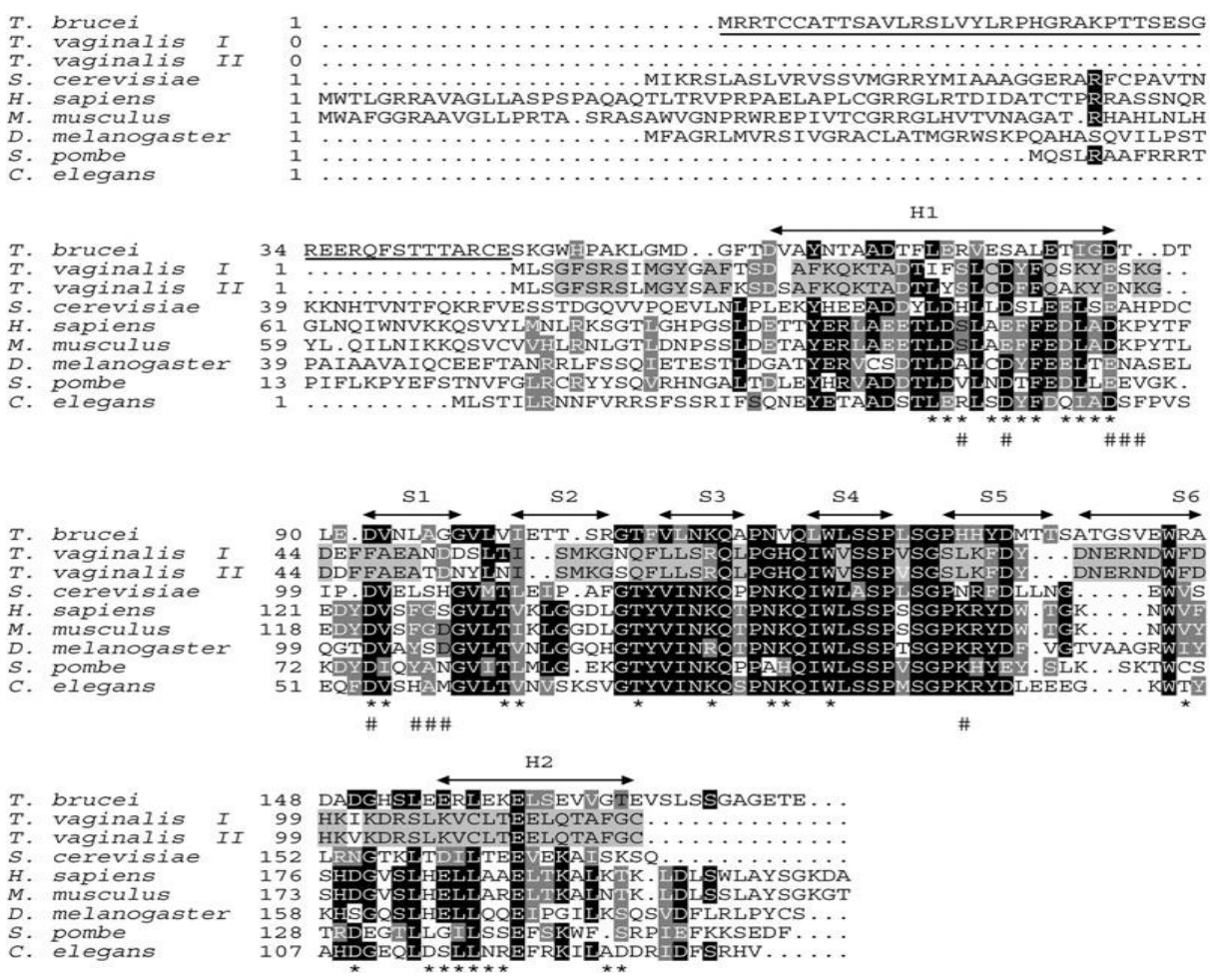

The figure shows multiple alignments of predicted frataxin protein sequences from different cells. The number of amino acids mentioned at the left of the respective sequences. Black highlight sequences are conserved positions conservatively substituted in grey, and variable positions are white. Gaps were introduced to optimise the alignment. The mitochondrial targeting sequence of *T.brucei* frataxin is underlined. Asterisks and hash marks denote residues implicated in iron and ferrochelatase binding. The position of α-helices (H1and H2) and β-sheets (S1–S6) are indicated above the alignment.

The mature form of frataxin (m81-210) can also recover metabolic defects, such as deficiency of aconitase activity, caused by the absence of m56-210 frataxin. Overall, these studies suggest that m81-210 is the primary mature form *in vivo* (Figure 1.3), while m56-210 can be proteolytically established from the precursor *in vivo* when generation of the m81-210 form is prevented by the blocking of residues 80-81 (Condo *et al.* 2007; Yoon *et al.* 2007; Schmucker *et al.* 2008).

Figure 1.3 - Different forms of human frataxin (Schmucker *et al.* 2008)**.**

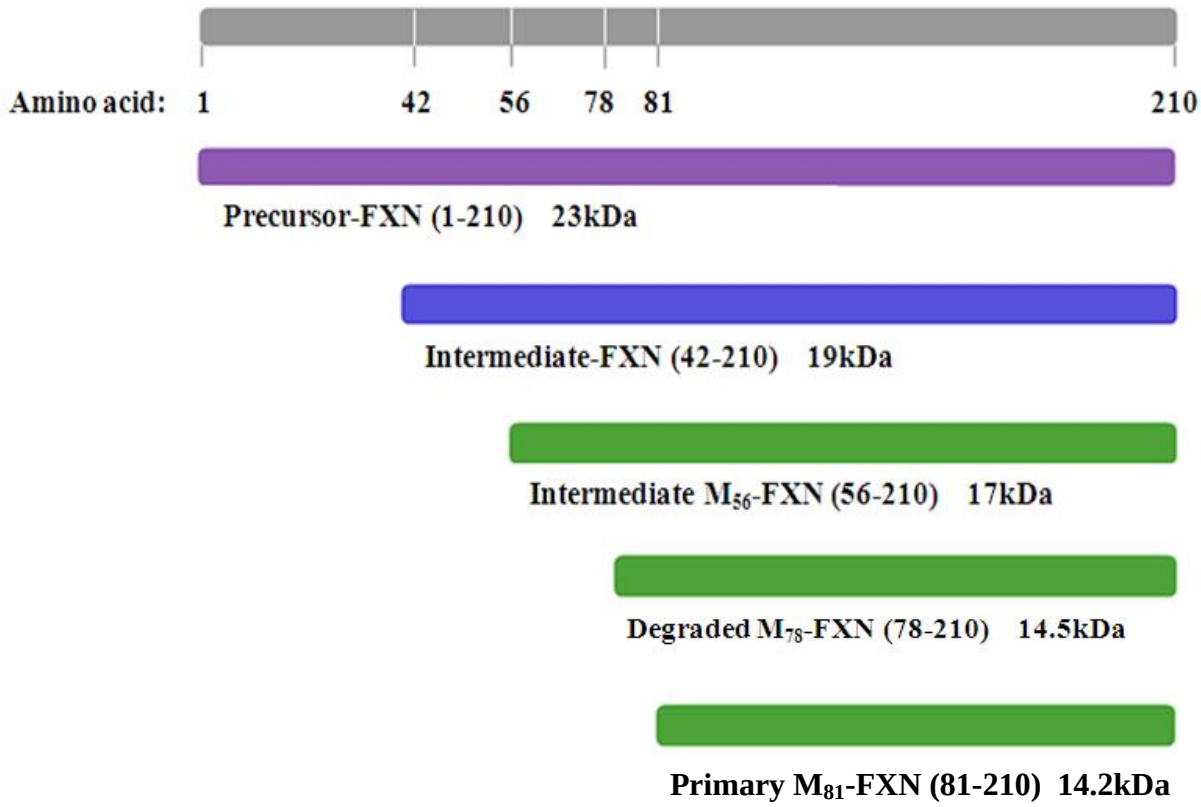

The precursor form is targeted to the mitochondria and undergoes a two-step cleavage process; the intermediate form and one of three mature forms starting at the amino acid 56 (intermediate-mature form), 78 (degraded-mature form) or 81 (primary-mature form).

Interestingly, recent data shows that a mature form of frataxin can also be found in the cytoplasm. In this study, Condo and colleagues recognised a direct interaction of the human extra-mitochondrial frataxin with cytosolic aconitase/iron regulatory protein-1 (IRP1), a bi-functional protein involved in enzymatic and RNA-binding function through the 'iron-sulfur switch' mechanism (Condo *et al.* 2010).

Analysis of the crystal structure of mature frataxin (Figure 1.4) shows a compact of αβ sandwich, including 7 β-sheets (β_1-β_5, β_6 and β_7) interacting with 2 α-helices (α_1 and α_2). The α_1- and α_2-helices are almost parallel to each other and the large β-sheets (β_1-β_5). The β_6 and β_7 are composed of the β_5 C-terminus site (Dhe-Paganon *et al.* 2000).

Figure 1.4 - Structure of frataxin (Dhe-Paganon *et al.* 2000)**.**

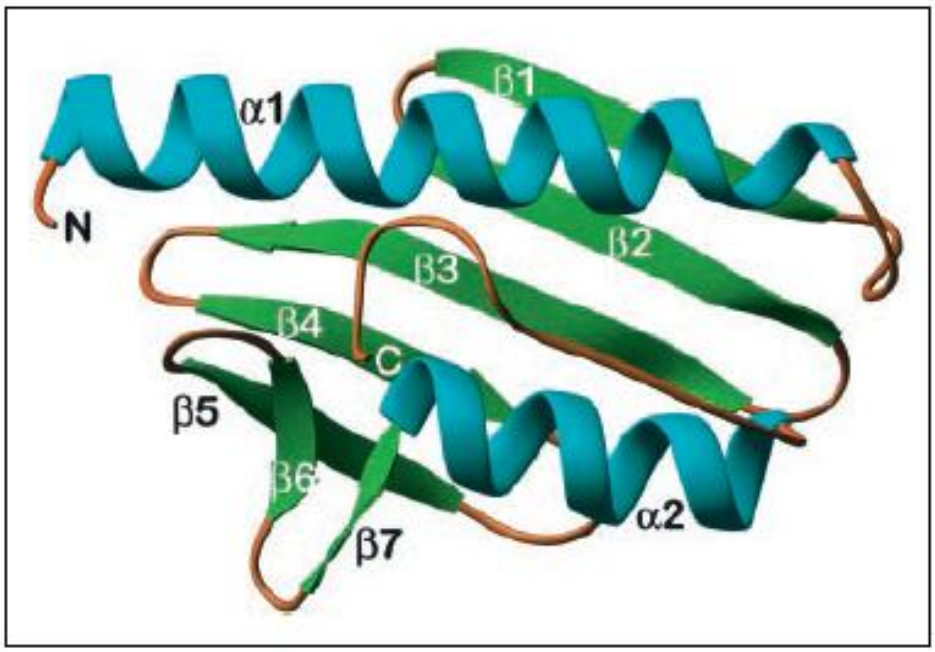

Ribbon diagram showing the fold of frataxin, a compact αβ sandwich, with helices coloured turquoise and β strands in green.

The function of frataxin is not completely clear yet, but several gene targeting studies indicate that loss of this protein results in cell death, and consequently endangers life. Thus, by deletion of frataxin in the hearts of conditional KO mouse model (MCK-KO) and comparing to wild-type (WT) mice, frataxin deficiency in the knockout models results in development of cardiomyopathy, which is the most prominent cause of death in most of FRDA patients (Calabrese *et al.* 2005). Frataxin depletion in mice also revealed the crucial role of this protein in DRG neurons, as one of the most sensitive tissues to frataxin deficiency (Sutak *et al.* 2008). Furthermore, the complete deficit of frataxin results in early mouse embryonic lethality and developmental arrest in the nematode *Caenorhabditis elegans* (Cossee *et al.* 2000; Ventura *et al.* 2005; Sutak *et al.* 2008).

These observations can be extended to all eukaryotic cells, emphasising the fundamental role of frataxin in cell survival (Koutnikova *et al.* 1997; Pianese *et al.* 1997). However, a similar

essential function for frataxin has not always been observed in many prokaryotes (Li *et al.* 1999; Vivas *et al.* 2006). Absence of frataxin results in aberration of many cellular functions. Studies of yeast showed that the yeast frataxin homologue gene 1 (*Yfh1*) deficiency leads to dysregulation of mitochondrial and even cytosolic iron levels (Wong *et al.* 2000). Other investigations of yeast suggested a fundamental role for frataxin in iron efflux from mitochondria (Radisky *et al.* 1999; Puccio and Koenig 2000).

In normal conditions in eukaryotes, frataxin binds ferrous iron through negatively charged amino acids on its surface. It promotes the mitochondrial synthesis of iron containing molecules, specifically ISCs and heme. Frataxin interacts with the scaffold protein Isu1 at the first step of ISC assembly, and is a Fe(II) donor for ferrochelatase in the ultimate step of heme synthesis (Park *et al.* 2003; Yoon and Cowan 2003; Yoon and Cowan 2004; Di Prospero and Fischbeck 2005; Gakh *et al.* 2006; Martelli *et al.* 2007; Long *et al.* 2008). Two hypotheses have been proposed to explain the role of frataxin in these procedures. The first hypothesis suggests that frataxin acts as an iron chaperone, providing proficient iron for Fe-S and heme assembly. The second hypothesis suggests an iron storage function for frataxin, scavenging toxic iron into a sheltered form. Studies of the *Escherichia coli* (*E.coli*) frataxin orthologue (CyaY) have shown that frataxin is not only an iron chaperone with an intrinsic function in the ISC enzymatic processes, but it can also act as a molecular regulator to inhibit formation of 2Fe-2S and store iron in a bio-available form (Figure 1.5) (Adinolfi *et al.* 2009).

Figure 1.5 - Schematic model of the frataxin molecular mechanism in mitochondria (Adinolfi *et al.* 2009)**.**

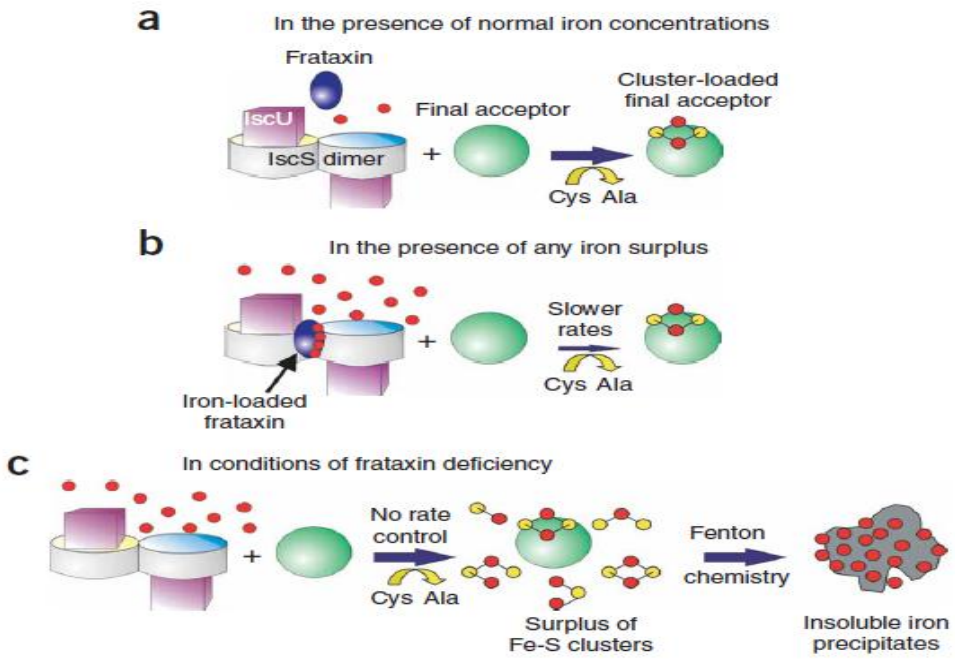

Schematic representation of the frataxin molecular mechanism in: **(a)** normal iron concentrations, **(b)** excess iron concentrations and **(c)** frataxin deficit.

1.2.4.1 - Frataxin and iron homeostasis

To date, further to ISC assembly, it is accepted that frataxin is an iron-binding protein in eukaryotes, contributing in cellular iron homeostasis (Bradley *et al.* 2000; Lodi *et al.* 2001). It has been reported that frataxin interaction with another protein that contributes to ISC transfer, called HSC20, is crucial for the biogenesis of ISCs and iron homeostasis in mammals (Shan and Cortopassi 2012).

1.2.4.2 - Frataxin and ISC enzymes

In mammalian cells, frataxin also acts as an iron-chaperone modulating many ISC containing enzymes, including aconitase activity in both mitochondria and cytosol, together with ferrochelatase and succinate dehydrogenase activities (Bulteau *et al.* 2004; Condo *et al.* 2010; Shan and Cortopassi 2012). Studies of the frataxin MCK-KO mouse models have shown that mitochondrial iron accumulation occurs only after onset of the pathology and Fe-S dependent

enzyme inactivation (Puccio *et al.* 2001), suggesting a direct effect of frataxin on the Fe-S dependent enzyme activity. Further investigations of FRDA patients' mitochondrial heart muscle and dentate nuclei showed consistent iron accumulation and reduction of aconitase activities, However, respiratory chain and aconitase activity changes were not significant in skeletal muscles, brain and cerebellum tissues (Waldvogel *et al.* 1999; Bradley *et al.* 2000; Koeppen *et al.* 2007).

1.2.4.3 - Frataxin and oxidative stress

It has been shown that overexpression of frataxin leads to Ca^{2+}-induced upregulation of tricarboxylic acid cycle flux and respiration and subsequently mitochondrial membrane potential ($\Delta\psi m$) and a cellular ATP content elevation. This finding shows key roles for frataxin in the regulation of mitochondrial energy conversion, oxidative phosphorylation and anti-oxidant defence (Ristow *et al.* 2000). To investigate the role of frataxin in reactive oxygen species (ROS) formation in the liver, Ristow and colleagues established a hepatocyte-specific frataxin deficient mouse model. They demonstrated that frataxin depletion enhances the ROS formation in liver, although no change was observed in the cellular buffering capacity against ROS. This data suggests that oxidative stress probably plays a confined role in FRDA phenotypic development (Thierbach *et al.* 2005). To date, it is believed that oxidative damage, as a secondary effect of impaired iron homeostasis and respiratory chain dysfunction, is caused by frataxin deficiency via imperfection of ISCs and/or heme protein biosynthesis (Yoon and Cowan 2003; Rai *et al.* 2008). Moreover, it has also been shown that frataxin not only functions to protect against oxidative stress, but also determines antioxidant responses, in the presence or absence of excess iron (O'Neill *et al.* 2005). By affecting the iron level, disruption of frataxin leads to multiple enzyme deficiencies, mitochondrial dysfunction and oxidative damage. In other words, loss of frataxin culminates in accumulation of iron in mitochondria. This abnormality can induce a pathogenic mechanism

culminating in elevation of free radical production and subsequently oxidative stress by down-regulating antioxidant elements (Puccio and Koenig 2000). Increasing the susceptibility to oxidative stress (Figure 1.6) can also cause decline in oxidative phosphorylation, because of a defect in mitochondrial proteins containing iron sulphur clusters (Lu and Cortopassi 2007; Martelli *et al.* 2007). Frataxin deficiency particularly affects ISC synthesis and culminates in reduction of some ISC-containing enzyme activities. Controlling the ability of iron to perform redox chemistry is another function of the frataxin (Rotig *et al.* 1997; Chen *et al.* 2002; Pandolfo 2002; Yoon and Cowan 2004; O'Neill *et al.* 2005; O'Neill *et al.* 2005; Lu and Cortopassi 2007).

Figure 1.6 - Frataxin function and oxidative stress in Friedreich ataxia (Pandolfo 2008)**.**

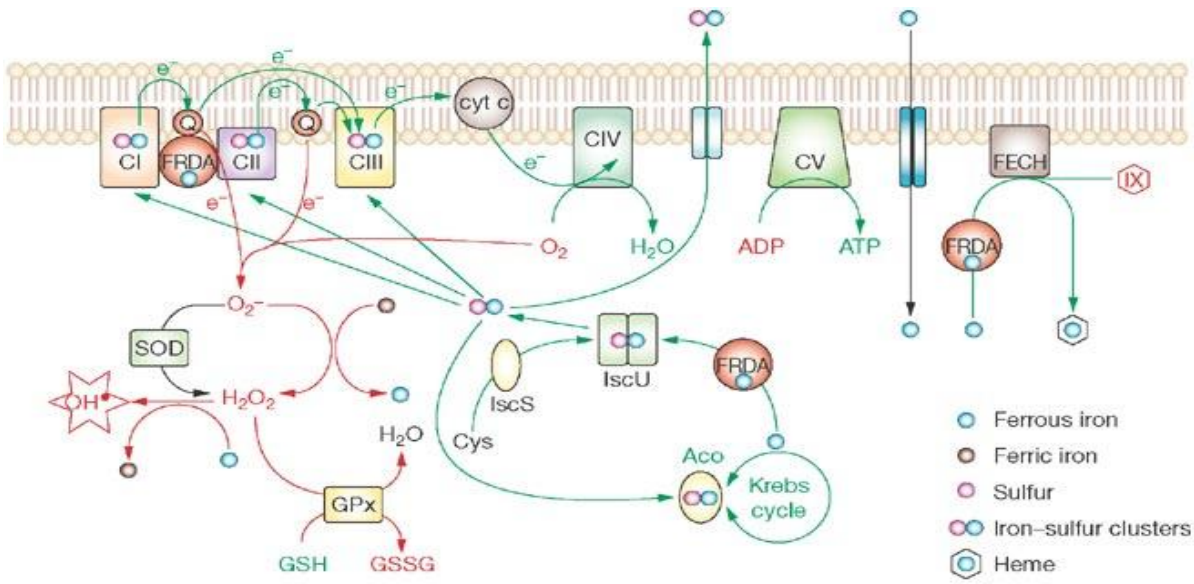

Several of the postulated functions of frataxin are represented, including the provision of iron for iron–sulfur clusters and heme synthesis, and direct interaction with respiratory chain complexes. Green arrows and text indicate molecules and pathways that have decreased activity in frataxin deficiency; red arrows and text indicate molecules and pathways that have increased activity in frataxin deficiency. Abbreviations: Aco, aconitase; CI, respiratory chain complex I; CII, respiratory chain complex II; CIII, respiratory chain complex III; CIV, respiratory chain complex IV; CV, respiratory chain complex V; Cys, cysteine; cyt c, cytochrome c; e^-, electron; FECH, ferrochelatase; FRDA, frataxin; GPx, glutathione peroxidase; GSH, reduced glutathione; GSSG, oxidised glutathione; H_2O_2, hydrogen peroxide; IscS, cysteine desulfurase; IscU, iron–sulfur cluster scaffold protein; IX, protoporphyrin IX; OH●, hydroxyl radical; Q, coenzyme Q; SOD, superoxide dismutase.

1.2.4.4 - Frataxin and cell malignancy

Although cell malignancy is not considered as a typical feature of the disease, various types of atypical cancer have been detected in the FRDA patients at a young age (Ristow 2004; Thierbach *et al.* 2012). The first FRDA patient case study in 1986 described a primary small bowel ganglio-neurobalstoma in a 26 year-old pregnant patient. In this study, Barr and colleagues reported that the small bowel tumour had arisen from autonomic nerve cells in the myenteric plexus of Auerbach; however, the chance of metastasis from a primary tumour elsewhere was not excluded (Barr *et al.* 1986). Another study then described two siblings with FRDA who both presented with gastric adenocarcinoma at an early age, suggesting the inheritance of a mutant tumour suppressor gene, which could be a DNA repair gene (Ackroyd *et al.* 1996). Aberration of DNA repair genes may cause many different genetic mutations and subsequently different diseases, such as FRDA and different types of cancer (Ku *et al.* 2010). Another FRDA patient, a 16 years old male, was shown to suffer from a lymphoblastic T-cell non-Hodgkin lymphoma (De Pas *et al.* 1999). Yet, another case study described the presence of breast cancer in two FRDA patient sisters, whilst the other brother and sister of family, with almost the same age, did not show any history of the FRDA or breast cancer. The authors of this study could not explain any potential correlation between FRDA and breast cancer. Nevertheless, due to the low incidence of FRDA combined with breast cancer, they suggested that due to the cardiomyopathy in early life, FRDA patients do not generally live long enough to develop breast cancer (Kidd *et al.* 2001).

Investigations of the hepatocyte-specific frataxin conditional KO (Alb $Fxn^{-/-}$) mouse liver tissue demonstrated reduced activity of ISC enzymes and ATP levels, as well as elevated oxidative stress, impaired respiration, apoptosis and cell proliferation. Almost 50% of these mice died up to 30 weeks of life. Unexpectedly, the surviving mice after 30 weeks developed multiple apparent hepatic tumours at late life stages. In this study, apoptosis was typically

observed following ATP reduction and sometimes after ROS induction (Thierbach *et al.* 2012). On the other hand, study of the same conditional KO mice showed that frataxin deficit may promote tumour formation through impairment of activation and phosphorylation of the p38 MAP kinase, as a critical ISC tumour suppressor protein for growth and tumourigenesis particularly in liver. It has been suggested that the cell proliferation in these mice could be due to induction of impaired phosphorylation of p38 MAP kinase and even enhanced formation of ROS (Thierbach *et al.* 2005). Considering the fact that frataxin is vitally important for mitochondrial ISC biosynthesis and that ISCs are required for the proper function of some DNA repair proteins, it has been suggested that one of the mechanisms by which a frataxin defect may cause tumourigenesis could be aberration of the ISC function containing DNA repair enzymes and subsequently an increased gene mutation rate (Thierbach *et al.* 2012).

In 2006, investigating the role of frataxin in colon cancer confirmed the Otto Warburg hypothesis indicating that cancer might be caused by reduction of mitochondrial energy metabolism and increased glycolytic flux. In this study, overexpression of frataxin in various colon cancer cell lines exhibited an increase in oxidative metabolism and aconitase activity, mitochondrial membrane potential, cellular respiration, ATP content and population doubling (PD) times, as well as reduced growth rates and prevention of colony formation capacity in soft agar. Injecting each of these cell lines into nude mice also showed a decline in the capacity of tumour formation. In addition, to reduce the phosphorylation of extracellular signal-regulated kinase (ERK), the authors confirmed that overexpression of frataxin raises p38 MAP kinase phosphorylation. Considering the increased oxidative metabolism caused by frataxin, and its role in suppressing malignant growth in the mammalian cells, this study also suggested a tumour suppressor role for frataxin (Schulz *et al.* 2006).

A reduced level of frataxin was observed in neoplastic astrocytic brain tissues and malignant cell lines compared with normal astrocyte cells. Overexpression of frataxin in glioblastoma (U87-FXN) cells showed surprisingly increased ROS levels in cytoplasm, whilst reduced mitochondrial ROS was observed, as predicted. The higher cytoplasmic ROS levels suggested that cytoplasmic antioxidant defences were altered in these cells. Further studies demonstrated that higher cytoplasmic ROS levels reduced cytoplasmic antioxidant capacity in U87-FXN cells, causing enhanced susceptibility of these cells against oxidative stress induced by H_2O_2 or L-buthionine-S,R-sulfoximine (BSO). In contrast to colon and liver cells, U87-FXN cells exhibited faster growth in both *in vitro*, under hypoxic and growth factor restricted conditions, and *in vivo* models. These data may go against the former hypothesis that frataxin generally acts as a tumour suppressor, based on its proposed antioxidant function (Kirches *et al.* 2011). It has also been reported that frataxin expression might contribute to malignant cell survival by the regulation of the antioxidant response under hypoxic conditions and that it may influence metabolic pathways by modulating the hypoxia-induced p53 stress response (Guccini *et al.* 2011). Hypoxic stress is a characteristic feature that promotes most tumours either into the angiogenic switch for tumour survival or cell death through necrosis or apoptosis. Hypoxia-inducible factors (HIFs) are essential elements in preserving a balance between adaptation to hypoxia and cell death by regulating the hypoxia responsive genes (Semenza 2010). It has also been demonstrated that there is a link between hypoxia in malignant cells and promoting the leakage of ROS from the mitochondrial electron transport chain and regulation of tumour suppressor p53 (Guccini *et al.* 2011). In contrast, Malisan and colleagues showed that frataxin is increased in human glioblastoma and colon carcinoma tumours *in vivo*. Hypoxic stress was shown to increase frataxin expression in several malignant cell lines by regulating HIF expression and p53 activation was observed in a condition of frataxin upregulation in these malignant cells. These data indicate that

frataxin is involved in the hypoxia-induced responses in tumours, and thus modulation of frataxin expression can play critical role in malignant cell survival and/or progression (Guccini *et al.* 2011). Taken together, it would appear that frataxin could act as a double-edged sword in different malignant cells; overexpression of frataxin can play an anti-apoptotic role, whilst it can also behave as a tumour suppressor.

1.2.5 - Molecular genetics

The human FRDA gene (*FXN*) was mapped to chromosome 9 in 1988 by linkage analysis of families (Chamberlain *et al* 1988) (Figure 1.7).

Figure 1.7 - Molecular location of the FRDA gene.

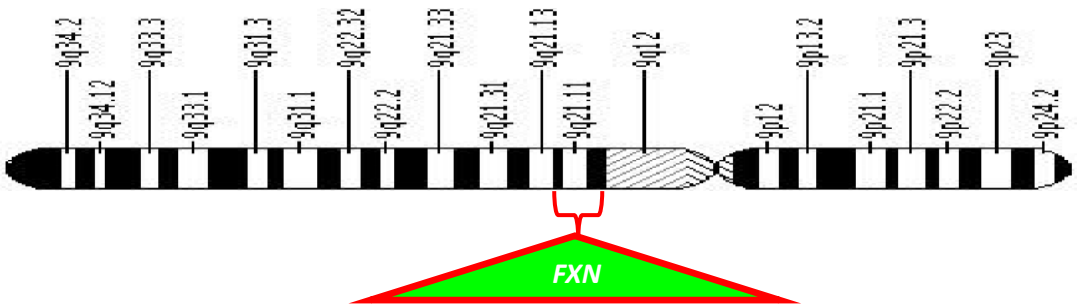

Schematic representation of the *FXN* gene located on the long (q) arm of the chromosome 9 from position 13 to 21.1.

The location of the FRDA gene was narrowed down to 9q13-21.1 by physical mapping investigations, followed by identification of the mutated gene in 1996 (Fujita *et al.* 1989; Hanauer *et al.* 1990; Campuzano *et al.* 1996). The *FXN* gene, which was initially called *X25*, contains seven exons (1-5a, 5b, and 6) spread across 95kb of genomic DNA, in which exon 6 is non-coding (Figure 1.8). The major transcript arises from exons 1-5a, which culminates in the generation of a 210 amino acid frataxin protein. By alternative splicing, a 171 amino-acid protein can be transcribed from exons 1-5b (Campuzano *et al.* 1996; Cossee *et al.* 1997).

Figure 1.8 - Schematic illustration of the *FXN* exons and splicing patterns.

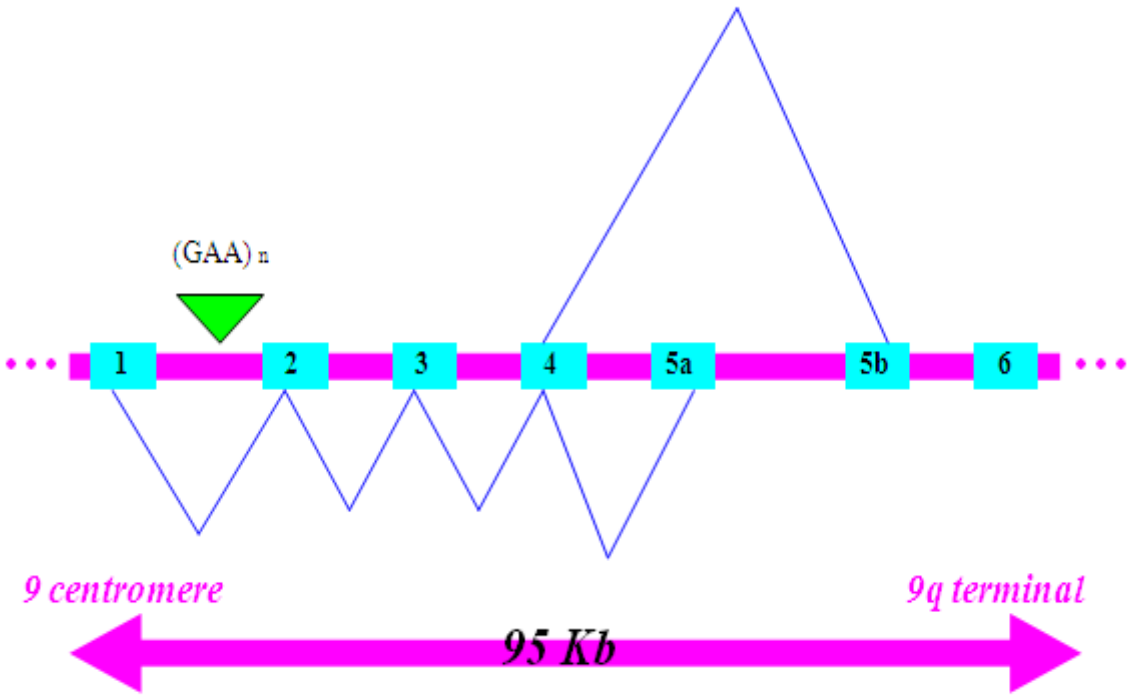

The gene extends from centromere to telomere of the 9q chromosome. In normal conditions exons 1-5a transcribe and translate into 210 amino acids protein; called frataxin. Alternative splicing might produce different lengths of proteins. The GAA repeats are situated in intron 1.

The human *FXN* gene is expressed in all cells, but at various levels in different tissues. Frataxin expression is generally higher in mitochondria-rich cells, such as cardiomyocytes and neurons. It has been shown that frataxin is abundant in the cerebellar cortex, cerebellum, DRG and spinal cord (Campuzano *et al.* 1996; Simon *et al.* 2004; Al-Mahdawi *et al.* 2006; De Biase *et al.* 2007; Gottesfeld 2007). However, other studies have shown that frataxin is also highly expressed in non-central nervous system tissues with a high metabolic rate, including heart, liver, kidney, brown fat, skeletal muscle, kidney and pancreas (Koutnikova *et al.* 1997; Pandolfo 2008). Investigation of the *FXN* mRNA levels in the

peripheral blood samples have shown that FRDA patients have 13% to 30% of normal levels and FRDA carriers have 40% of normal levels (Campuzano *et al.* 1996; Pianese *et al.* 2004). Molecular studies of FRDA have revealed that several *FXN* mutations may lead to frataxin dysfunction. A GAA trinucleotide repeat expansion within intron 1 of the *FXN* gene is the most common mutation, resulting in disruption of *FXN* transcription (Figure 1.9) and a subsequent decrease of frataxin protein levels (Becker and Richardson 2001; Sakamoto *et al.* 2001; Clark *et al.* 2007; De Biase *et al.* 2007; Llorens *et al.* 2007).

Figure 1.9 - Schematic presentation of frataxin expression.

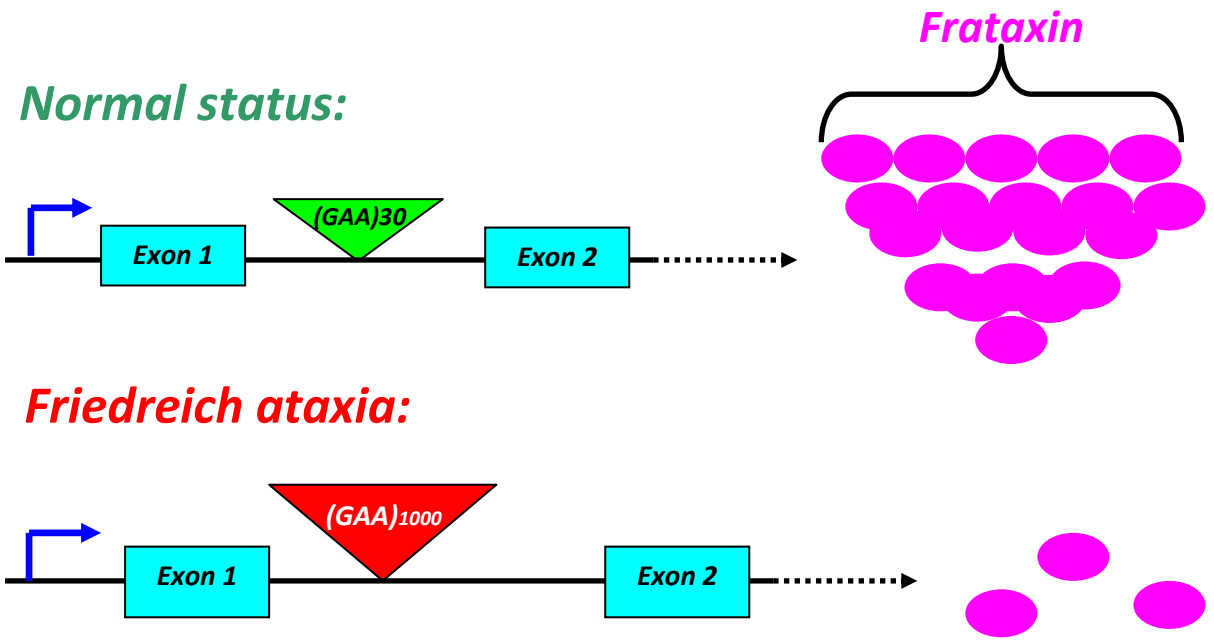

In most FRDA patients, frataxin expression is reduced because of a GAA repeat expansion within intron 1 of the *FXN* gene.

Studies have shown that 96% of FRDA patients carry GAA repeat expansions in both alleles (Bidichandani *et al.* 2000; Grabczyk and Usdin 2000; Potaman *et al.* 2004; Lobmayr *et al.* 2005). In addition to GAA repeat expansion, cases of missense, nonsense and splice-site mutations in the *FXN* gene may also lead to this disorder. About 4% of FRDA patients are compound heterozygous for a point mutation on one allele and a GAA repeat expansion on

the other allele. Thus far, 17 different point mutations have been discovered, the most prevalent of which are I154F, M1I, and G130V. The I154F mutation is associated with a typical FRDA phenotype, while the other mutations present with atypical features, such as late onset (Alper and Narayanan 2003). No patient has yet been reported to carry point mutations in both alleles of the frataxin gene, indicating that this scenario is incompatible with survival.

1.3 - Repeat instability

Repetitive nucleotide sequences, which comprise approximately 30% of the human genome, are hot spots for recombination, resulting in insertion (expansion) or deletion (contraction) (Potaman *et al.* 2004). Repeat instability is a crucial form of mutation that has been detected in more than 40 neurological, neurodegenerative and neuromuscular disorders. In contrast to other mutations, which are stably transmitted to offspring, a repeat mutation is a dynamic process that increases or decreases within tissues and across generations (Kovtun and McMurray 2008).

Abnormal nucleotide repeat expansions consist of different types, including microsatellites (e.g. FRDA), minisatellites (e.g. insulin-dependent *diabetes*) and megasatellites (e.g. fascioscapulohumeral muscular dystrophia 1A). Microsatellites, or simple sequence repeats (SSRs), generally comprise the multiple repeated sequences of 1-6 nucleotides, which could be found in both coding and non-coding region of the genome (Tautz 1989; Beckman and Weber 1992; Jurka and Pethiyagoda 1995; Toth *et al.* 2000; Potaman *et al.* 2004; Pearson *et al.* 2005; Gaspari *et al.* 2007; Mrazek *et al.* 2007). Repeat expansions can cause disorders as dinucleotides (e.g. Norrie's disease), tetranucleotides (e.g. dystrophia myotonica type 2) or pentanucleotides (e.g. spinocerebellar ataxia 10). However, trinucleotide repeats (TNRs) are

the largest category of microsatellites, contributing to many human disorders (Djian *et al.* 1996; Kovtun and McMurray 2008).

1.3.1 - Trinucleotide repeats

TNR expansion is a mutational mechanism that contributes to several inherited disorders, including myotonic dystrophy type 1 (DM1), Huntington disease (HD) and FRDA (Cossee *et al.* 1997). About 10% of all human genes carry at least one trinucleotide sequence of four units. Normally TNR positions are divided between two regions; coding, and non-coding regions. Generally, disorders related to non-coding TNR expansion typically result in loss of gene function or toxic effects at the mRNA level, while TNR expansions within coding regions usually cause either a polyglutamine or polyalanine tract in the protein products, culminating in protein toxicity in the absence or presence of normal protein function (Pizzi *et al.* 2007).

Studies indicate that more than 14 hereditary neuromuscular diseases are caused by TNR expansions localised in particular genes (Jasinska *et al.* 2008). Expansion of CAG and CTG multiple repeats, for instance, lead to HD and DM1 diseases, respectively (Cummings and Zoghbi 2000; Savouret *et al.* 2003; Jasinska *et al.* 2008). In addition, fragile X syndrome (FRAXA) is caused by a GCC/GGC expansion. FRDA is the only disorder known to be caused by a GAA/TTC repeat expansion (Cummings and Zoghbi 2000; Al-Mahdawi *et al.* 2006; De Biase *et al.* 2007; Gottesfeld 2007).

TNR instability can be classified into either somatic or germline instability. Somatic repeat instability exhibits different lengths of TNR repeats in different tissues (Pearson *et al.* 2005). It is suggested that tissue-specific and age-dependent repeat instability might be regulated by *cis*-acting factors (*cis*-elements) and *trans*-acting factors (*trans*-elements). Thus, by integration of the human *FXN* locus into transgenic mice, it has been demonstrated that *cis*-elements are necessary for somatic instability of GAA repeats in human FRDA cells

(Pearson *et al.* 2005; Clark *et al.* 2007). Evidence indicates that tissue-specific repeat instability may be affected by DNA repair, DNA replication, epigenetic marks, chromatin packaging or transcription of the disease gene. Such effects might be different for each genetic locus, different tissues, and even different ages of individuals (Figure 1.10). Interestingly, age-dependent instability is a factor in post-mitotic neuronal tissues which seems to be the result of genome maintenance repair (Pearson *et al.* 2005). TNR diseases also exhibit germline instability during transmission of the repeat mutation from parent to offspring. DNA metabolic activities involved in DNA replication, repair, recombination or transcription may contribute to such TNR germline instability during gametogenesis. Intergenerational TNR instability can be inherited with either a paternal or maternal expansion or contraction bias. Paternal expansion bias might be caused by mutations in the mitotic cycles of spermatogenesis. For example, it has been reported that CAG repeats in HD patients undergo expansions before meiosis, with expansions already detected in mitotic germ cells. FRDA is the other example of a disorder that shows paternal contraction bias, although the main cause of this contraction is not yet clear (Pearson *et al.* 2005).

In contrast to male germ cells that carry little DNA repair proteins, post-meiotic female germ cells bear DNA repair and recombination activities, which can culminate in age-related TNR instability due to mutations in oogenic meiosis. This type of expansion has been observed in CAG, CGG, and CTG expansions of spinocerebellar ataxia 1 (SCA1), FRAXA and DM1, respectively (Pearson *et al.* 2005).

Figure 1.10 - Unstable repeat tracts and the processes associated with repeat instability (Pearson *et al.* 2005)**.**

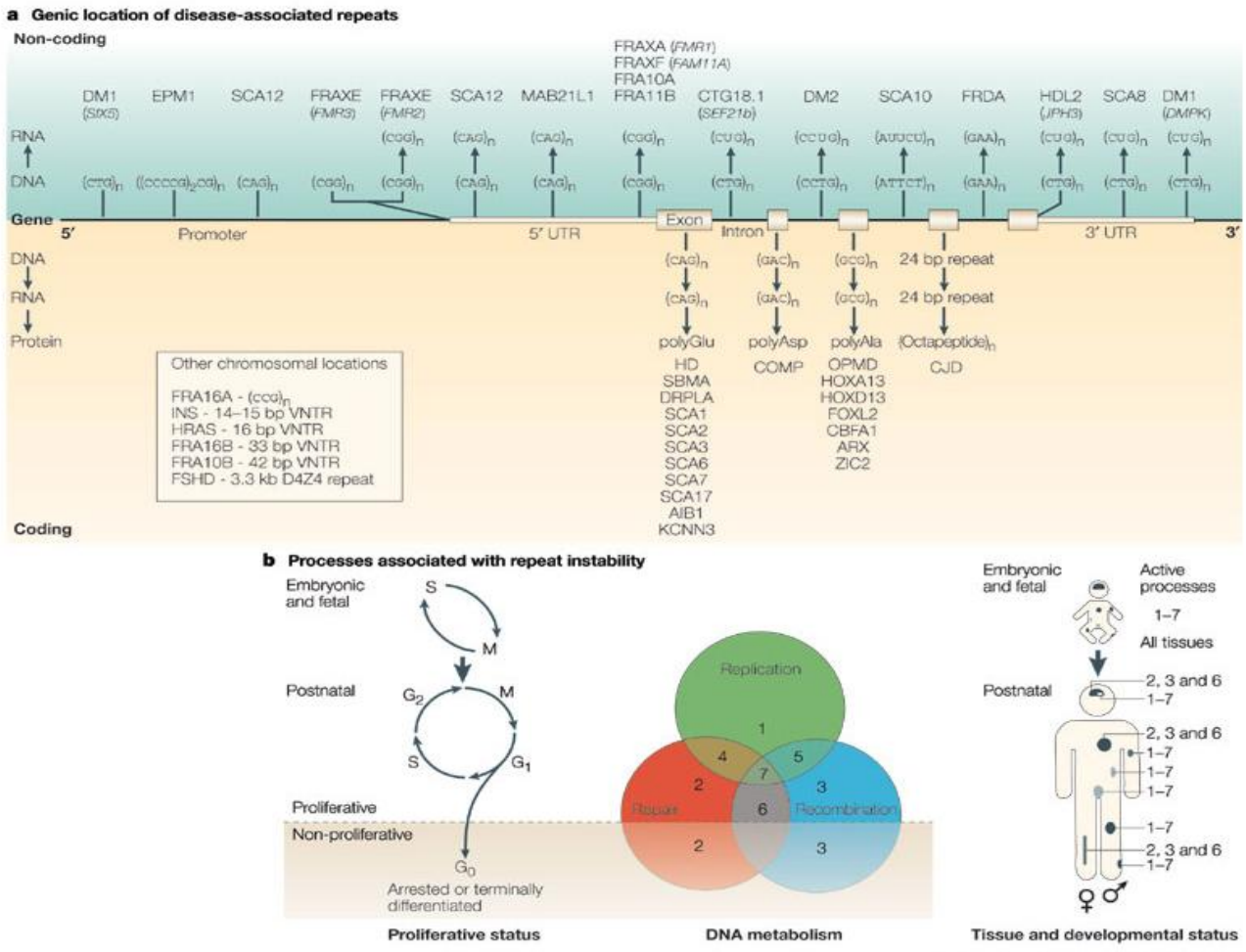

(a) A representation of the genetic location of non-coding (top) and coding (bottom) disease-associated repeats (promoter, 5' UTR, exons, introns, 3' UTR or other chromosomal locations (includes undetermined locations). The DNA, RNA and amino acid sequence for each repeat is noted. For DM1, the CTG tract is located in the 3' UTR of the myotonic dystrophy protein kinase (*DMPK*) gene, as well as the promoter of the sine oculis homeobox homologue 5 (*SIX5*) gene. **(b)** The processes associated with repeat instability are shown. Instability occurs in proliferative (above the dotted line) and non-proliferative (below the dotted line) tissues. The DNA metabolic processes of DNA replication, repair and recombination are associated with repeat instability, either independently or in conjunction with other processes. The involvement of various processes varies depending on tissue and developmental stage (bottom right). The numbers in the tissue and developmental status section correspond to those in the DNA metabolism section.

1.3.1.1 - GAA repeat instability

Screening patients who carried a mutation in the *FXN* gene identified a GAA repeat within the first intron of this gene (Figure 1.9) as the major cause of FRDA (Campuzano *et al.* 1996). The normal *FXN* gene carries between 7 and 35 GAA repeats; however, this elevates from 66 to 1700 repeats in FRDA patients. Based on the length of the expanded GAA repeat (also termed E-allele), the rate and severity of the disease are changed. Thus, E-alleles in FRDA patients, who exhibit classical symptoms, are between 500 and 1700 GAA repeats. Patients who carry shorter GAA expansion mutations (fewer than 500 triplet repeats) usually present with a milder disease (De Biase *et al.* 2007). Late onset of FRDA is an atypical disease that is generally classified into 3 sub-groups. In the first group, late onset FRDA (LOFA 25-39 years) and very old onset FRDA (VLOFA ≥ 40 years) possess up to 500 GAA repeats. The second group, FRDA with retained tendon reflexes (FARR), has fewer than 300 repeats and contains at least one E-allele. Acadian FRDA is the third atypical age-dependent group, exhibiting an unusually gradual disease progression with a mean age of onset of 27 years, accompanied by wheelchair confinement (Durr *et al.* 1996; Filla *et al.* 1996; Montermini *et al.* 1997; Bidichandani *et al.* 2000; Berciano *et al.* 2002).

Origin of GAA repeat expansions: There is no clear explanation how the GAA repeat became expanded in FRDA patients. To find out the cause of the GAA repeat expansions, Pandolfo analysed the GAA repeats in the normal chromosomes. He recognised that 83% of normal chromosomes contain 6-10 GAA repeats, whilst 17% of chromosomes showed larger normal triplets of 12-36 repeats. These results suggested that polymorphism of normal GAA alleles is generated by two events. The small changes, most probably deriving from occasional events of polymerase 'stuttering' during DNA replication, may cause size heterogeneity within small or large normal groups. Shifting from small to large normal triplets was suggested by linkage disequilibrium results due to the different marker haplotype

association to small and large normal alleles. The same conditions were observed during investigation of large normal alleles containing more than 34 uninterrupted GAA triplets that undergo hyper-expansions to hundreds of triplets in one generation, leading to GAA hyper-expansions in the *FXN* (Pandolfo 1998).

Molecular mechanism of GAA repeat expansions: Studies have shown that FRDA patients who carry expanded GAA repeats in both alleles have very low level of the mature *FXN* mRNA and protein (Sakamoto *et al.* 2001). Further investigations have demonstrated that a decrease in mRNA expression level is the principle cause of dysfunction of the frataxin gene and not a problem with post-transcriptional RNA processing. It has been reported that the *FXN* mRNA expression level is inversely correlated to GAA repeat expansion size (Delatycki *et al.* 2000). So far, *in vitro* and *in vivo* investigations suggest two different mechanisms by which GAA expansions might produce reduction in the level of the *FXN* mRNA expression: non-B DNA conformation and/or heterochromatin mediated gene silencing. Non-B DNA conformation can occur due to triplex or sticky DNA structures (Mariappan *et al.* 1999; Sakamoto *et al.* 1999; Sakamoto *et al.* 2001). The first report of triplex DNA structures came from observing a retarded profile in agarose gel caused by plasmids containing long GAA expansions. The GAA.TTC tract is recognised as poly-purine.poly-pyrimidine (Pur.Pyr) sequence, containing only purines (R) in one strand and pyrimidine (Y) on the other. *In vitro* and *in vivo* studies have shown that GAA expansions can form intramolecular triple helical structures (Ohshima *et al.* 1998; Schmucker and Puccio 2010). Mechanistically, a DNA triple-helix structure is formed upon binding a "Y" or "R" single stranded DNA to the normal grove of double stranded DNA (Figure 1.11a), resulting in RRY or YRY structures (Grabczyk and Usdin 2000). In FRDA, GAA repeat expansions form a triplex containing two GAA repeat strands along with a single strand of TTC repeats; RRY. This form of the DNA triplex can form higher-order conformations inhibiting *FXN* transcription, called sticky DNA

(Figure 1.11b). This type of triplex DNA can be detected by decreasing mobility of the GAA content DNA restriction fragments and probably arises from intramolecular association of GAA expanded repeat triplexes (Gottesfeld 2007; Schmucker and Puccio 2010).

Figure 1.11 - Schematic structure of a DNA triplex and sticky DNA (Son *et al.* 2006)**.**

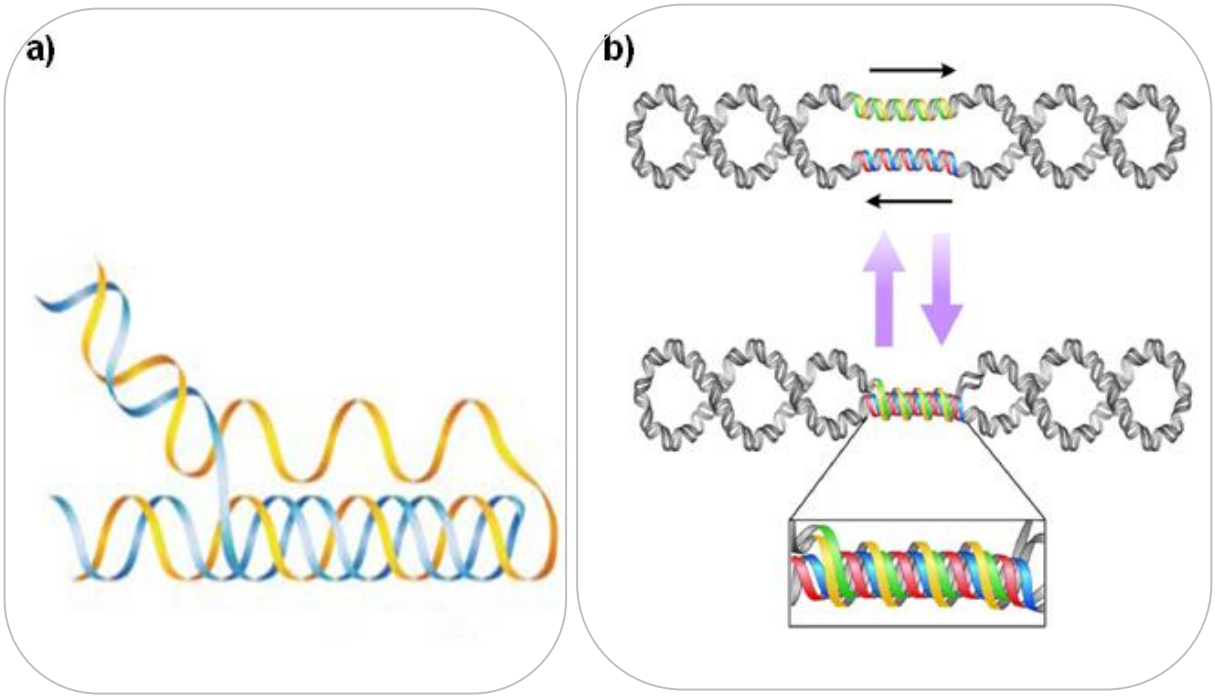

(a) Diagram showing a triple-helix DNA (H-DNA) (Zhao *et al.* 2010). **(b)** A sticky DNA model in a plasmid presenting the association of two GAA.TTC expanded repeat sequences in one DNA molecule. This interaction is dynamic and facilitated by negative supercoiling and divalent cations. The green and yellow represent one duplex and the red and blue show the second duplex.

It is not clear yet whether or not a sticky DNA structure is directly involved in inhibition of *FXN* mRNA transcription. A persistent RNA-DNA hybrid formation, arising during transcription of expanded GAA repeats, is the other proposed model, which could result in transcriptional arrest at the promoter distal duplex-triplex junction. It has been shown that GAA expansions start from a threshold length of 44 repeats. This length correlates with the shortest length of GAA repeat expansion in which RNA-DNA hybrid formation was

observed. Thus, it is proposed that formation of the transcription-dependent RNA-DNA hybrid structure might also cause repeat instability in the cell (Grabczyk *et al.* 2007).

In contrast to a DNA structure basis, it has also been proposed that GAA repeat expansions could result in chromatin remodelling by forming heterochromatin structures and subsequently cause silencing of *FXN* transcription. Studies of the heterochromatin-sensitive human CD2 (hCD2; lymphoid cell surface marker protein) showed that GAA repeat expansions cause chromatin packaging and silencing in transgenic mice via position effect variegation (PEV) (Saveliev *et al.* 2003). PEV is recognised as a phenomenon that happens when a gene is abnormally located within or near a chromatin silencing region. Silent heterochromatin is generally characterised by reduced promoter accessibility and increased levels of histone deacetylases (HDACs), DNA methyltransferases, polycomb group proteins and certain types of histone modifications, such as histone H3-lysine 9 (H3-K9) tri-methylation and histone hypo-acetylation. To support the effect of chromatin structure on the GAA repeat-associated gene silencing, investigations on heterochromatin-sensitive hCD2 cells showed that GAA repeat expansions inhibit promoter accessibility and DNase I digestion (Saveliev *et al.* 2003). Besides, it is believed that the classical modifier PEV heterochromatin protein 1 (HP1), as a highly conserved chromo-domain protein associated directly with pericentric heterochromatin, can also regulate transcriptional silencing caused by GAA repeat expansions (Elgin and Grewal 2003). In addition, investigations showed that overexpression of HP1β protein led to remarkably reduced proportion of the hCD2 expression in T cells of transgenic mice carrying GAA repeat expansions, whilst no effect of HP1β overexpression on the level of hCD2-expressiong T cells was reported in the mice without GAA repeat expansions. Thus, these results further support the hypothesis implicating the role of GAA repeat expansions on the gene silencing via generation of heterochromatin structure (Figure 1.12) (Saveliev *et al.* 2003).

Figure 1.12 - Putative heterochromatin-mediated silencing pathway in FRDA (Festenstein 2006)**.**

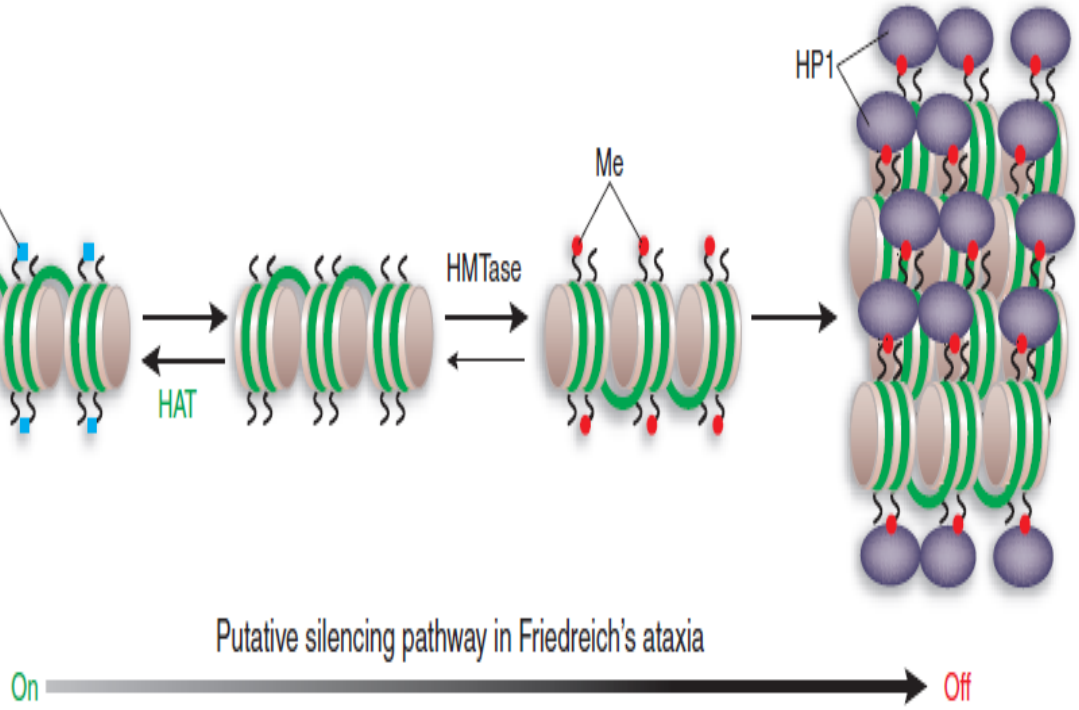

The chromatin organisation of a normal *FXN* (left) has acetylated histone tails (Ac, acetyl). GAA repeat expansions might cause heterochromatin formation via deacetylation of the lysines on histones, providing a substrate for histone methyltransferases. Methylation (Me) of the histone H3 tail (on Lys9) would provide a binding site for HP1. HP1 dimers might condense a higher-order heterochromatin structure that prohibits access of the transcriptional machinery to the *FXN* locus.

Further studies of GAA repeat expansion-induced heterochromatin-mediated gene silencing have shown a critical role of other epigenetic factors. Usdin and colleagues demonstrated increased DNA methylation of specific *FXN* gene CpG residues in FRDA patient lymphoblastoid cells compared with unaffected cells. In particular, they found three DNA methylated CpG sites upstream of the expanded GAA repeat in FRDA patient cells, while these residues were almost methylation-free sites in normal cells. One of these three sites,

located within an E-box, is a critical enhancer of frataxin expression that influences promoter activity (Greene *et al.* 2007). Further studies of lymphoblastoid cells indicated a role for histone modifications in GAA repeat expansion-induced gene silencing. These changes consist of elevation of di- and tri-methylation of the H3K9 and hypo-acetylation at particular lysine residues on histones H3 and H4 (H3K14, H4K5 and H4K12) (Herman *et al.* 2006). These findings were confirmed by studies of human FRDA patient tissues and YG8 and YG22 FRDA transgenic mouse models (Al-Mahdawi *et al.* 2008). In these studies, Pook and colleagues also showed that upstream *FXN* GAA CpG sites become hyper-methylated, while downstream GAA CpG sites become consistently hypo-methylated in different tissues of FRDA patients, implicating DNA hypermethylation of the upstream GAA region in downregulation of frataxin transcription (Al-Mahdawi *et al.* 2008).

1.4 - FRDA drug therapy

1.4.1 - Current therapies

Many FRDA therapeutic strategies are now being pursued, based on the findings that different epigenetic pathways can affect frataxin expression, together with the subsequent effects of oxidative stress and mitochondrial dysfunction (Figure 1.13).

Figure 1.13 - Schematic pipeline representation of FRDA treatments.

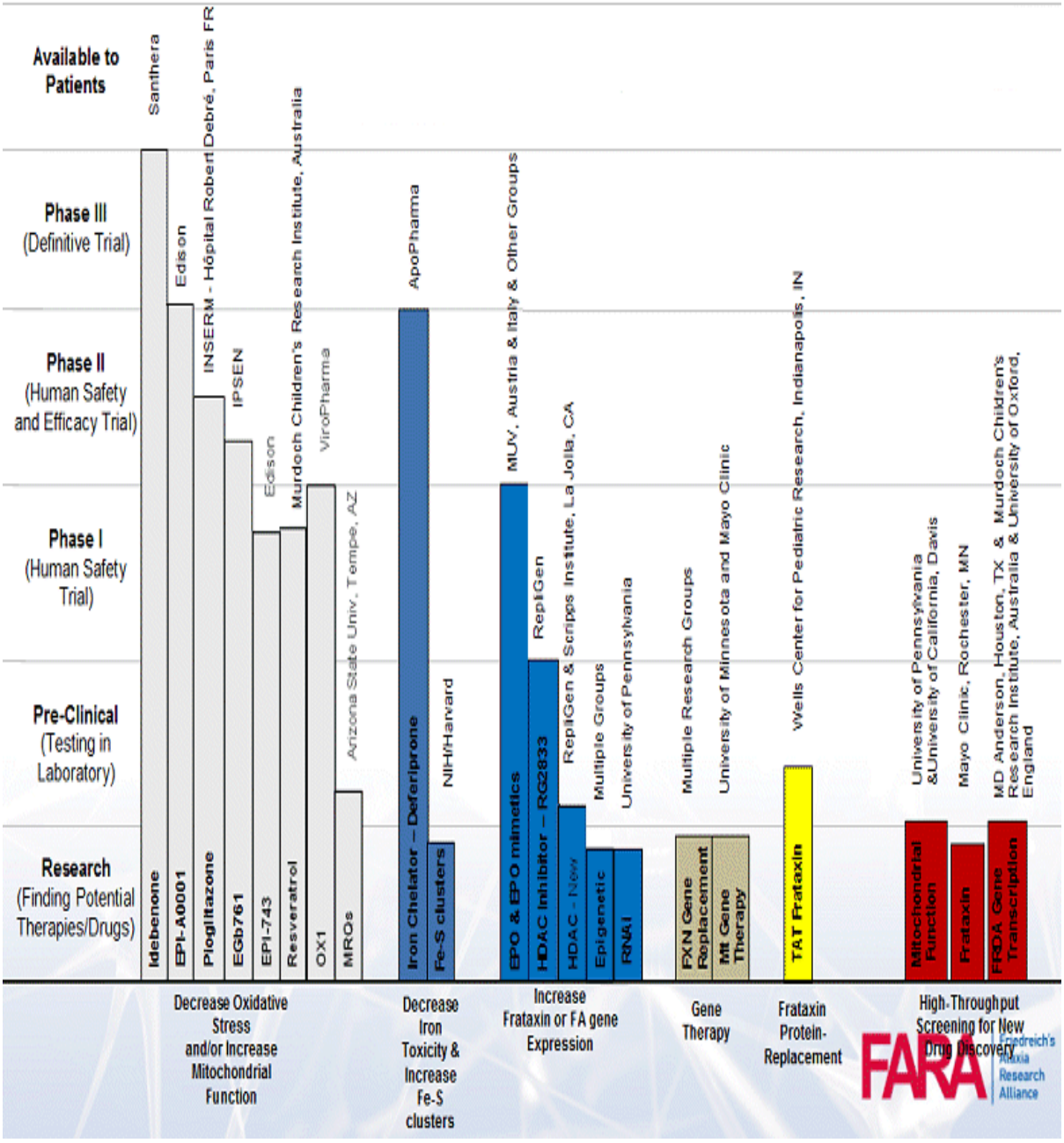

The pipeline shows the potential therapies being developed to treat FRDA. Each bar shows a different agent, highlighted by its mechanism of action on FRDA in the horizontal axis and the milestone of preclinical and clinical development in the vertical axis (adapted from http://www.curefa.org/pipeline.html).

1.4.1.1 - Iron chelators

Disruption of frataxin causes dysfunction of ISC formation and a subsequent susceptibility to oxidative stress and late mitochondrial iron accumulation. Thus, both mitochondrial iron chelator-based and antioxidant therapies have been considered for FRDA. Desferrioxamine (DFO), the only widespread iron chelator clinically trialled at that time, was initially studied as a potential drug to treat FRDA. However, it proved to be ineffective, because it did not target mitochondrial iron. Recently, a new generation of drugs are being considered. Deferiprone (DFP) is one of the most potent iron chelator drugs used specifically to target mitochondrial iron. It has been demonstrated that DFP reduces iron accumulation and overload in the liver and heart. It has also been shown to cross the blood-brain barrier to reduce brain iron levels in FRDA patients (Hadziahmetovic *et al.* 2011). However, studies of the DFP-treated FRDA fibroblasts has shown that it can also impair aconitase activity, one of the main affected ISC enzymes in FRDA (Goncalves *et al.* 2008). Therefore, some caution should be taken when using DFP for FRDA therapy.

1.4.1.2 - Antioxidants

Investigations have suggested that frataxin deficiency may cause a delay in antioxidant defence responses, particularly coenzyme Q_{10} (CoQ_{10}) and vitamin E. Recent investigations showed that a high percentage of FRDA patients have a reduced level of serum CoQ_{10} (Cooper *et al.* 2008). This data supports the hypothesis that CoQ_{10} and vitamin E could be good therapeutic agents in FRDA patients. A short-term clinical study of ten FRDA patients showed that using combined CoQ_{10} and vitamin E treatment caused significant improvement of ATP production in cardiac and skeletal muscle (Lodi *et al.* 2001). Other CoQ_{10} and vitamin E treatments of the same number of patients over 47 months showed increased mitochondrial energy synthesis in cardiac and skeletal muscle and improvement in cardiac function (Hart *et al.* 2005; Cooper and Schapira 2007).

Idebenone is a CoQ_{10} analogue that reduces the cardiac hypertrophy in FRDA. *In vitro* studies reported that idebenone acts as an electron carrier, supporting mitochondrial ATP function, as well as an anti-oxidative agent preventing mitochondrial membrane damage. So far, several studies have been carried out to determine the toxicity and efficiency of idebenone on FRDA pathogenesis (Meier and Buyse 2009). Pilot clinical studies of this agent at a dose of 5mg/kg/day showed the efficiency of idebenone in cardiomyopathy and controlling early onset cardiac hypertrophy of FRDA patients (Hausse *et al.* 2002). Another long-term follow up study showed that using low dose of idebenone (5-20mg/kg/day) could not only control FRDA-associated cardiomyopathy in both paediatric (8-18 years old) and adult patients, but also significantly improve left ventricular mass in adult. However, these observations demonstrated that neurological dysfunction is only stabilised in paediatric FRDA patients (Pineda *et al.* 2008). To find out whether neurological dysfunction could be improved in presence of higher doses of idebenone, Fischbeck and colleagues randomised 48 paediatric FRDA patients and classified them into 4 sub-groups double-blindly receiving placebo, 5 mg/kg/day, 15 mg/kg/day or 45 mg/kg/day. The results showed that higher doses of this agent are associated with neurological benefits and improvement of functional capacity and ameliorating activities of daily living (ADL) in paediatric FRDA patients, indicating that higher doses of idebenone might have beneficial effects on neurological function (Di Prospero *et al.* 2007).

1.4.2 - Epigenetic therapy

There are three different epigenetic systems that may contribute to human disorders: histone modifications, DNA methylation and siRNA-associated silencing (Figure 1.14). Aberration of one or more of these interacting systems might cause perturbation of expression or gene silencing, and subsequently lead to an epigenetic disorder. It has been demonstrated that

FRDA is an epigenetic disorder that might be caused by abnormal chromatin and subsequent disruption of frataxin expression (Egger *et al.* 2004).

Figure 1.14 - Interaction between RNA, histone modification and DNA methylation in heritable silencing (Egger *et al.* 2004)**.**

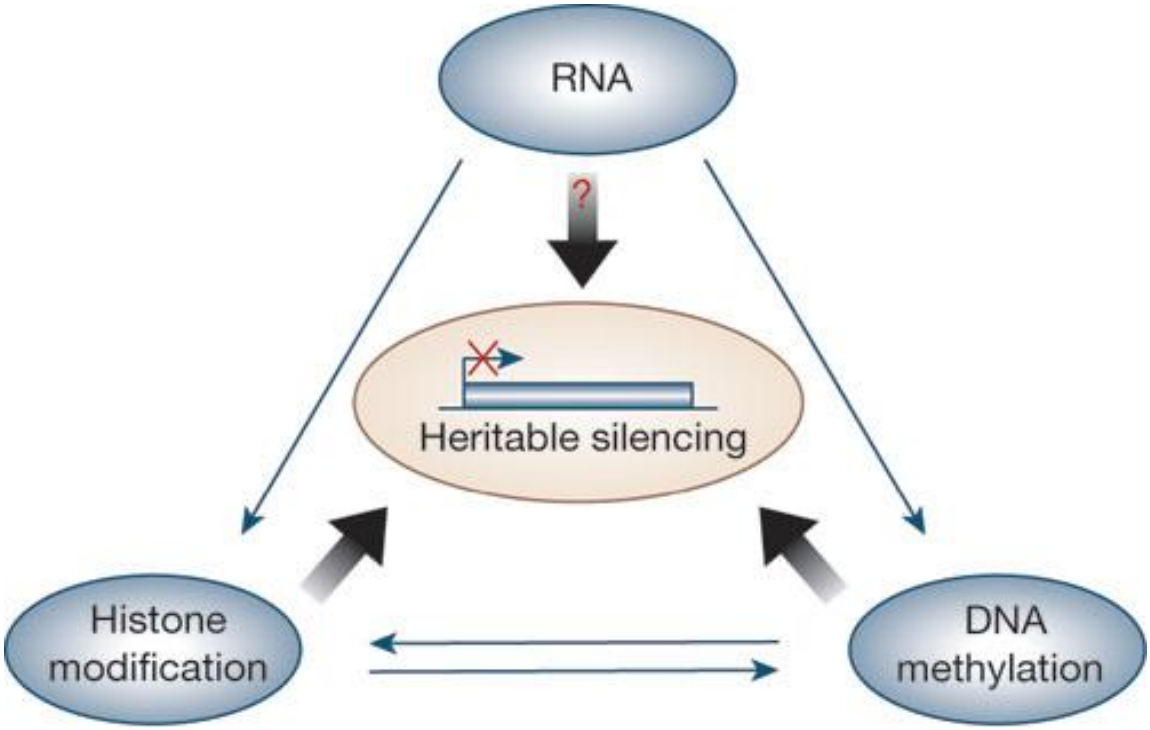

Histone deacetylation and methylation of H3K9 residues cause chromatin condensation and block transcriptional initiation. Histone modification can also attract DNA methyltransferases to initiate cytosine methylation, which in turn can reinforce histone modification patterns conducive to silencing. Experiments in yeast and plants have clearly shown the involvement of RNA interference in the establishment of heterochromatic states and silencing. siRNA triggering of heritable quiescence might therefore also be involved in higher organisms.

1.4.2.1 - DNA methylation

DNA methylation in mammals occurs by modification of position C5 of the cytosine base in CpG dinucleotides. Two components participate in gene silencing by DNA methylation of CpG sites: DNA methyltransferases (DNMTs) and methyl CpG binding proteins (MBPs). DNMTs establish and maintain DNA methylation as an intrinsic mechanism for

transcriptional repression of particular genes and viral sequences against genome instability, while MBPs bind to methylation marks to reinforce gene silencing. Recent investigations suggest that DNA methylation may regulate the expression of microRNAs, small RNA molecules which suppress translation of many genes (Hadnagy *et al.* 2008). By preventing specific transcription factor binding and engaging MBP-associated repressive chromatin remodelling activity, DNA methylation suppresses transcription. Aberrant DNA methylation is one of the main epigenetic abnormalities, leading to disorders such as cancer, imprinting disorders and neurodegenerative disorders caused by microsatellite instability (MSI). DNMT inhibitors, including nucleoside or non-nucleoside analogues of cytidine, are the main classes of epigenetic drug under investigation of targeting hypermethylation. While non-nucleoside analogues can inhibit DNMTs without incorporation of DNA, nucleoside analogues need DNA incorporation to block DNMTs (Hadnagy *et al.* 2008). Studies of FRAXA showed that 5-aza-2'-deoxycytidine (5-aza-CdR) reactivates *FMR1* transcription by removing the transcriptional blockade caused by promoter methylation, although some side effects have also been reported. Firstly, long-term use of 5-aza-CdR is highly toxic. Secondly, it is not recommended for post-mitotic neurons, because its action is based upon incorporation into dividing cells (Di Prospero and Fischbeck 2005). High instability (even in normal pH, because of a fast decomposition of triazine ring) is another negative point reported for this agent (Marquez *et al.* 2005; Hadnagy *et al.* 2008). Another DNMT inhibitor is a 5-aza-CdR derivative named zebularine. Higher stability and less toxicity are two advantages of this drug in comparison with 5-aza-CdR. However cytotoxicity is still a side-effect of zebularine caused by its incorporation into DNA (Hadnagy *et al.* 2008). Since several studies have shown elevation of DNA methylation in the 5'UTR and upstream of GAA repeat regions of FRDA-associated *FXN* alleles, it is hypothesised that 5-aza-CdR and zebularine might be

good therapeutic agents for FRDA treatment (Greene *et al.* 2007; Al-Mahdawi *et al.* 2008; Castaldo *et al.* 2008).

1.4.2.2 - Histone deacetylase (HDAC) inhibitors

Histones, the major proteins within the nucleosome, can undergo post-translation modifications, specially acetylation, phosphorylation and methylation at the terminal side of amino acid tails (Figure 1.15) (Zhang and Reinberg 2001; Kondo *et al.* 2003). Acetylation of histones bound to DNA is essential for transcription. This mechanism is regulated by two enzymes: histone acetyltransferases (HATs) and histone deacetylases (HDACs). Acetylation of core histones (H2A, H2B, H3, and H4) is catalysed by transcriptional co-activators that carry HAT activity, such as CREB binding protein (CBP) (Abel and Zukin 2008). Unlike HAT proteins, HDACs play the opposite role in acetylation of many proteins. Thus, HDACs can recognise the lysine/arginine amino acids situated at the N-terminal of many proteins (particularly core histones), and cause removal of acetyl groups from the protein. This action culminates in silencing of gene expression. Regulation is the other function of HDACs by which they play a critical role in cell growth, differentiation, and apoptosis. Therefore, transcriptional activity might be reduced by HDACs (Carey and La Thangue 2006; Wilson *et al.* 2006; Abel and Zukin 2008).

To date, 17 types of human HDACs have been detected carrying out various specificities within the cell. Generally these are categorised into four subgroups; classes I-IV. Class I, which are completely situated in the nucleus, include HDACs 1, 2, 3, and 8 and have high homology to HDAC-*Rpd3* in yeast. Class II (homologue of HDAC-*Hda1* in yeast) contains HDACs 4, 5, 6, 7A, 9, and 10, which shuttle between the nucleus and the cytoplasm and are expressed in a tissue and cell specific manner. In comparison with class I HDACs, which are Zn-dependent enzymes, class II HDACs are independent of Zn. Class III (also named sirtuins; homologues of HDAC-*Sir2* in yeast) is a highly conserved gene family classified

into 7 members; SIRT 1-7. SIRT-4 and SIRT-6 catalyse protein ribosylation by their NAD^+-dependent ADP ribosylation domain. Finally, HDAC 11 is the only recognised member of HDAC class IV (Carey and La Thangue 2006; Abel and Zukin 2008; Spurling *et al.* 2008).

Figure 1.15 - Sites of post-translational modifications on the histone tails (Zhang and Reinberg 2001)**.**

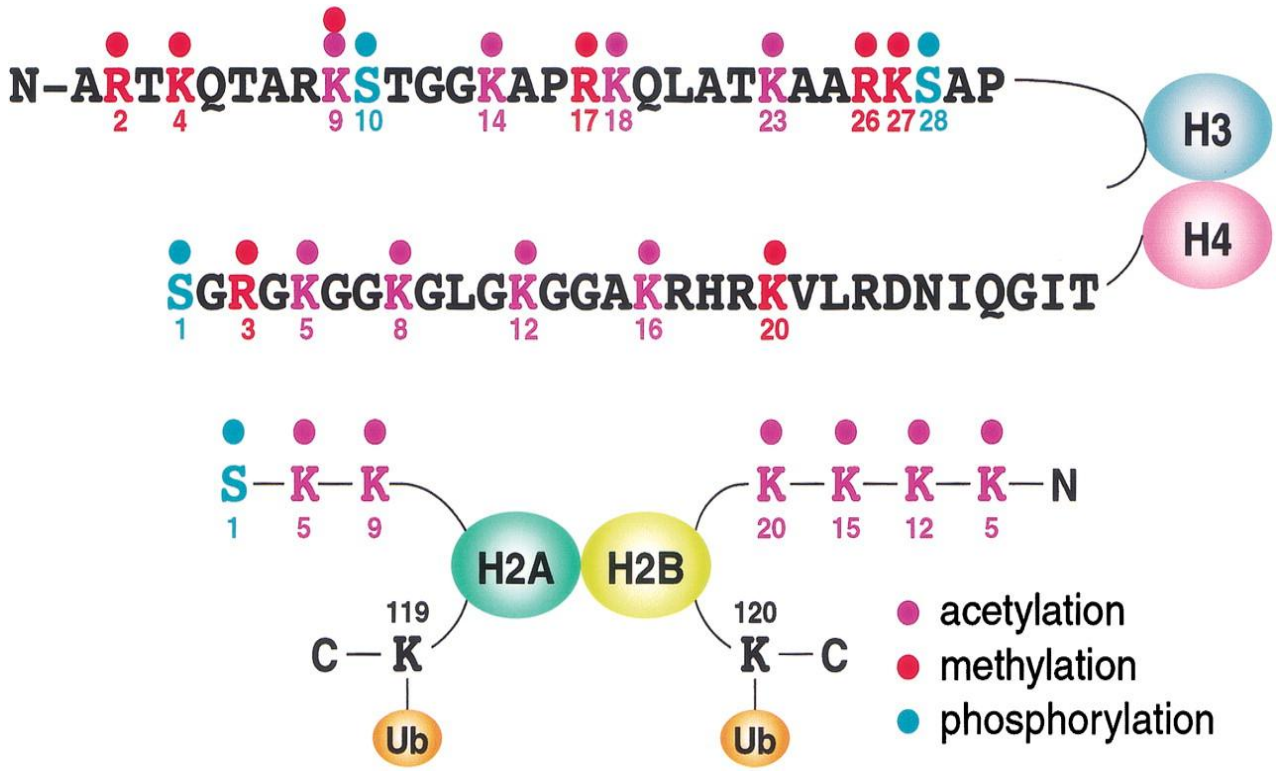

The modifications shown include acetylation (purple), methylation (red), phosphorylation (blue), and ubiquitination (orange). Note that Lys 9 in the H3 tail can be either acetylated or methylated.

The diversity of HDAC functions has made them potential therapeutic targets to treat many aberrations, unlike HATs. Thus, HDAC inhibitors (HDACi) have been recognised as a new mechanism-based therapy for many disorders. HDACis are generally categorised into four different subgroups: 1) short chain fatty acids (e.g. sodium butyrate), 2) hydroxamic acids

(e.g. trichostatin A (TSA) and suberoylanilide hydroxamic acid (SAHA)), 3) epoxyketones (e.g. trapoxin) and 4) benzamides (Figure 1.16). Several investigations have shown the positive effects of HDACis in cancer therapy by induction of differentiation, arrest of cell growth, apoptosis, and de-repression of different genes by their anti-proliferative activities (Carey and La Thangue 2006; Minucci and Pelicci 2006; Abel and Zukin 2008).

Figure 1.16 - Structure of representative compounds from the major classes of HDACis (Carey and La Thangue 2006)**.**

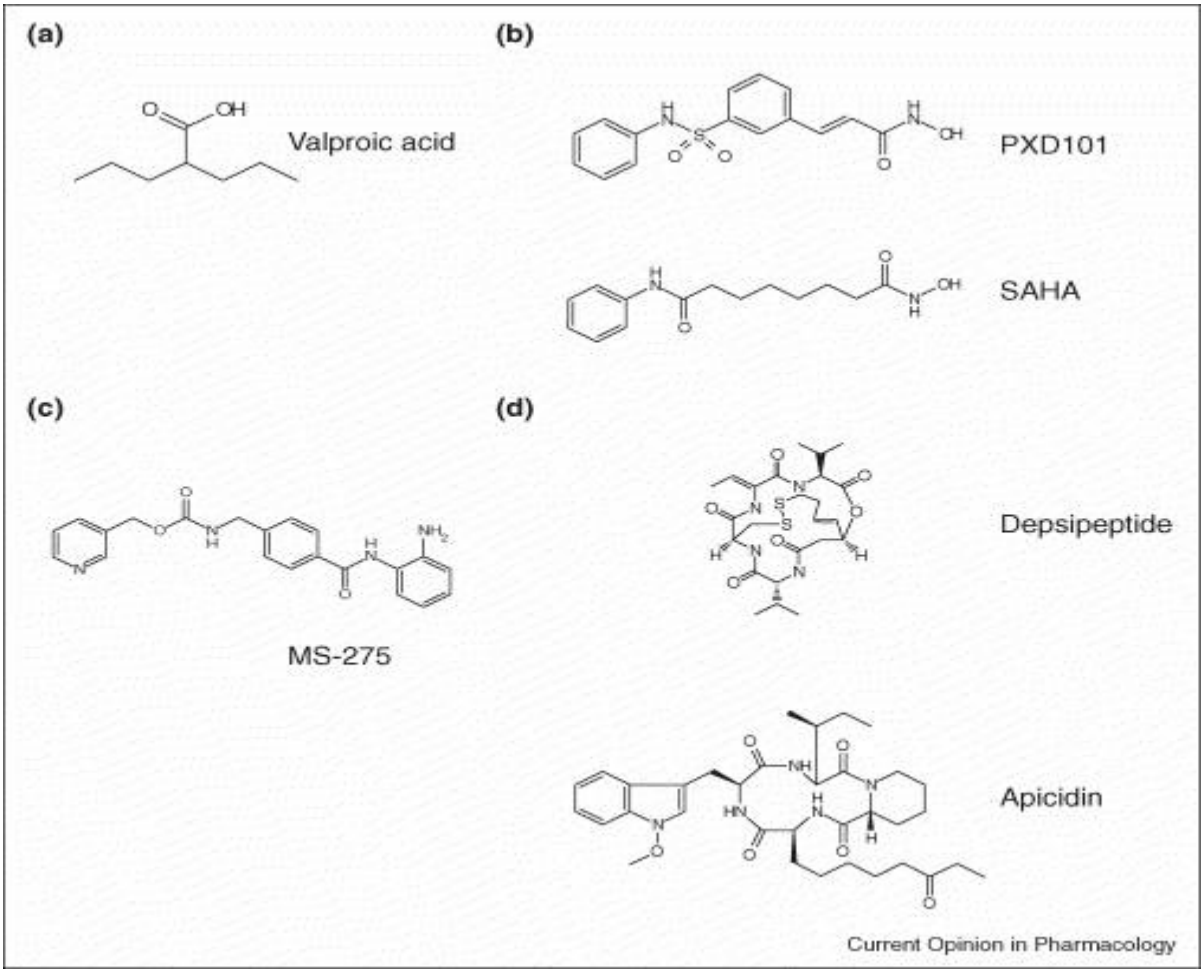

(a) Small chain fatty acids: valproic acid is in Phase II oncology trials. **(b)** Hydroxamate small molecule inhibitors SAHA and PXD101 are both in Phase II oncology trials. **(c)** Non-hydroxamate small molecule inhibitors: MS-275 is in Phase II oncology trials. **(d)** Cyclic peptides: depsipeptide is in Phase III oncology trials.

Interestingly, investigations suggest that inhibition of HDACs (particularly classes I and II) might be targeted as a treatment for many neurodegenerative disorders. Applying different drugs of the HDACi family, such as sodium butyrate, phenylbutyrate, TSA and SAHA, have revealed positive effects on the treatment of a Huntington disease *Drosophila* model by elevating histone acetylation (Steffan *et al.* 2001; Abel and Zukin 2008). Extending these studies to mouse models has emphasised the modifier role of HDACis by increasing motor function and reduction of neuronal loss (Ferrante *et al.* 2003; Hockly *et al.* 2003; Gardian *et al.* 2005; Abel and Zukin 2008).

It is recognised that hypoacetylation of histones H3 and H4 may cause *FXN* silencing in FRDA patients carrying expanded GAA trinucleotide repeats. Although the use of some HDACi drugs is not recommended because of their toxicity, several studies indicate a beneficial effect of commercial HDACi drugs in reverting the effects caused by GAA expansions in lymphoblastoid cells. For instance, BML-210 is a benzamide HDACi that can increase the level of frataxin expression almost two-fold (Herman *et al.* 2006; Wells 2008). Also the HDACi drug 4b (an analogue of BML-210) can increase *FXN* mRNA and frataxin expression levels in FRDA patient lymphoid cell lines and primary lymphocytes without any cytotoxicity. Furthermore, HDACi 106, another member of the benzamide HDACi drug family, has been used in *FXN*-GAA knock-in mice to restore frataxin levels and the gene expression profile to that of wild-type mice. HDACi 106 has been proposed to work by increasing H3 and H4 lysine (H3K14, H4K5 and H4K12) acetylation in chromatin positioned near the GAA nucleotide repeat (Herman *et al.* 2006; Rai *et al.* 2008).

Recent studies suggest the potential therapeutic effects of HDACi class III compounds in the treatment of trinucleotide repeat disorders. For example, sirtinol is an HDACi III drug characterised by high potency and selective inhibition of SIRT-1 and SIRT-2 that may affect SIRT-1 in neurons. SIRT-1 is recognised as a protein that may contribute to FRAXA by

reducing *FMR1* transcription. It has also been reported that SIRT-1 is involved in H4K16 and H3K9 acetylation. Usdin and colleagues have shown that nicotinamide (vitamin B_3), a class III HDACi, can increase *FMR1* transcription 3-fold in FRAXA patient cells (Biacsi *et al.* 2008). Splitomicin, another class III HDAC inhibitor, has also been shown to increase acetylation of H3K9 on *FMR1*. In other words, splitomicin can reverse the *FMR1* gene silencing caused by SIRT-1 via inhibiting deacetylation of H3K9 (Bedalov *et al.* 2001; Biacsi *et al.* 2008). Furthermore, splitomicin therapy may indirectly inhibit DNA methylation of the *FMR1* promoter; so it might be more useful than 5-aza-CdR to reverse *FMR1* gene silencing in neurons which no longer divide (Biacsi *et al.* 2008). Regarding potential FRDA therapy, Pook and colleagues have shown that adding low concentration (0.2µM) of 5-aza-CdR to FRDA fibroblast cells significantly elevates *FXN* mRNA expression level after 24 hours compared to vehicle-treated samples, while no increase was observed in higher (0.5 and 1µM) concentration of this agent. Therefore, it is proposed that higher concentration of this agent caused cell toxicity. Furthermore, DNA methylation was also reduced in FRDA fibroblasts treated with 5-aza-CdR compared to vehicle-treated cells (C. Sandi, personal communication). Taken together, these findings suggest that low concentration of 5-aza-CdR could be beneficial to improve frataxin levels in FRDA patients.

1.5 - Development of models for FRDA

Since FRDA is a neurodegenerative disease, mainly affecting the DRG, cerebellum, heart and pancreas, investigation of the many molecular aspects of this disorder in patients is not feasible. However, the highly conserved evolution of frataxin across various organisms has enabled scientists to develop different *in vitro* and *in vivo* models. Thus, human cell lines or

animal models have provided insights into FRDA disease molecular pathophysiology and have been used for relevant pilot therapeutic studies.

1.5.1 - *Saccharomyces cerevisiae* model

Many studies have been carried out on the *Saccharomyces cerevisiae* yeast frataxin homologue, *YFH1*, and the corresponding protein Yfh1. The results showed that Yfh1 is an essential mitochondrial protein, playing role in mitochondrial DNA maintenance. It has been reported that Yfh1 deficiency causes impaired respiratory complex function due to accumulation of iron in mitochondria and loss of mitochondrial DNA. To confirm the latter finding, investigations showed that introducing a missense mutation, corresponding to one of the FRDA patients' mutations, into *YFH1* leads to a reduction of yeast respiratory function (Wilson and Roof 1997; Foury 1999). Isaya and colleagues showed that lack of Yfh1 culminates in mitochondrial iron accumulation, suggesting that Yfh1 is required for iron uptake. This also suggests that oxidative stress, as a secondary effect of frataxin deficiency, could also be caused by defect of Yfh1 (Branda *et al.* 1999). In contrast, another study has shown that iron accumulation, due to reduced Yfh1 function, does not significantly affect cell growth or cell viability. Further investigations of the same yeast model showed that aberration of Yfh1 protein level was not associated with changing the level of soluble iron distribution. In addition, this study demonstrated that increased level of iron in mitochondria was not accompanied with expression of Yfh1 (Seguin *et al.* 2010).

1.5.2 - *Caenorhabditis elegans* model

Several investigations have been carried out on *C. elegans* nematode worm models by modifying the relevant frataxin homologue, *frh-1*, but the results differ. Using RNAi in *C. elegans*, three investigations have shown that downregulation of many mitochondrial genes results in prolonged lifespan (Feng *et al.* 2001; Dillin *et al.* 2002; Lee *et al.* 2003).

Interestingly, Johnson and colleagues have also demonstrated that RNAi-mediated deficiency of frh-1 protein leads to lifespan longevity; however, the worms presented with a smaller body size, less fertility and different responses to oxidative stress (Ventura *et al.* 2005). In contrast, other studies have reported that RNAi-mediated deficiency of frh-1 incrementally leads to lifespan shortening and increasing sensitivity to oxidative stress, suggesting oxidative stress could be the principle cause of reducing lifespan (Vazquez-Manrique *et al.* 2006; Zarse *et al.* 2007). In addition, Palau and colleagues demonstrated that frh-1 defect causes a constant pleiotropic phenotype, including slow growth, abnormal pharyngeal pumping, egg laying defects and lethargic behaviour (Vazquez-Manrique *et al.* 2006). To explain the conflicting lifespan results observed in different studies, Johnson established a novel RNAi dilution strategy to significantly reduce the expression of 5 major genes involved in the mitochondrial electron transport chain (ETC), one of which was *frh-1*. The results showed that the mitochondrial ETC phenotype is dependent on the RNAi dose as well as particular period of development. They demonstrated that intermediate suppression leads to lifespan extension whilst using high dose of RNAi causes shortening lifespan (Rea *et al.* 2007).

1.5.3 - *Drosophila melanogaster* model

To generate a transgenic *Drosophila* fly model mimicking FRDA patients, Philips and colleagues used a UAS-GAL4 transgene-based RNAi technique to reduce expression of the frataxin homologue, *dfh*, in different tissues. Suppression of the *dfh* showed distinguishable phenotypes in larvae and adult *Drosophila*, including giant long-lived larvae and conditional short-lived adults. In parallel to this finding, they recognised that *dfh* silencing causes differential dysregulation of ferritin expression in adults but not in larvae. They also showed that *dfh* silencing leads to downregulation of many heme and ISC enzyme activities, defect of intracellular iron homeostasis and increased susceptibility to iron toxicity. Finally, they found that *dfh* silencing has no effect on larvae development of peripheral nerves, but significantly

reduces the lifespan of these cells in adults. Furthermore, overexpression of the anti-oxidant enzymes cytosolic superoxide dismutase (SOD1), mitochondrial superoxide dismutase (SOD2) and catalase (CAT) did not improve the *dfh*-defective phenotype, suggesting a minimal role of oxidative stress in this model (Anderson *et al.* 2005).

Later, to determine the role of frataxin and oxidative stress in FRDA patients, Molto and colleagues induced post-transcriptional silencing of *dfh* by using double stranded RNAi. They generated transgenic flies that expressed 30% residual frataxin and showed shorter life span, reduced climbing ability in adulthood and elevated sensitivity to oxidative stress. In addition, there was a significant decrease in aconitase activity, caused by hyperoxia, while no change was observed in succinate dehydrogenase and respiratory complex I-IV activities. Curiously, further studies demonstrated that overexpression of frataxin could also cause oxidative stress induced impairment of aconitase activity (Llorens *et al.* 2007). Yet more studies of the RNAi transgenic flies showed that loss of frataxin leads to toxicity caused by accumulation of lipid peroxides in glial cells, lifespan shortening, increased sensitivity to oxidative stress, impaired locomotor activity and progressive vacuolisation of glia, suggesting that lipid peroxidation can somehow cause FRDA-like symptoms in glial cells (Navarro *et al.* 2010).

1.5.4 - FRDA mouse models

Many useful results have been obtained by the investigation of FRDA mouse models, using both gene targeting technology and transgenic mice to cause frataxin deficiency.

1.5.4.1 - Knockout mouse models

To explore frataxin function and the mechanism of FRDA disease, a mouse model was generated by inactivation of the mouse *FXN* homologue, *Fxn*. In this study, Koenig and colleagues' investigations to target exon 4 of *Fxn* did not result in a viable FRDA mouse model, due to the fact that $Fxn^{-/-}$ mice die before birth, indicating the critical role of frataxin for life (Cossee *et al.* 2000). To overcome this early embryonic lethality, as well as to study

the effect of a frataxin defect on different tissues, Koenig and colleagues subsequently generated two lines of conditional *Fxn*-KO mice: muscle frataxin deficient and neuron/cardiac muscle frataxin deficient lines. To obtain these lines, homozygous mice with a conditional allele of *Fxn* ($Fxn^{L3/L3}$) were crossed with mice heterozygous for a deletion located in exon 4 of *Fxn* that carried a tissue specific Cre transgene under control of the muscle creatine kinase (MCK) or the neuron-specific enolase (NSE) promoters to develop $Fxn^{L3/\Delta}$-MCK-Cre^{+} or $Fxn^{L3/\Delta}$-NSE-Cre^{+} lines, respectively. NSE mutated mice showed low birth weight, early onset progressive neurological features, such as ataxia, and short lifespan. In contrast, weight loss was observed later in MCK models, followed by progressive features of fatigue and early death. in the MCK and NSE mutant mouse lines developed progressive biochemical and pathophysiological signs, similar to FRDA in humans, including iron accumulation caused by ISC enzyme deficiencies, dysfunction of large sensory neurons with no alteration of the small sensory and motor neurons, loss of activities of MRC complexes and aconitase, cardiac hypertrophy and premature death (Puccio *et al.* 2001).

Later, another conditional knockout mouse model that lacked frataxin in pancreatic β cells was established. The levels of reactive oxygen species and frequency of apoptosis were increased in these mice, together with a reduced rate of pancreatic β cell proliferation. They also showed impaired glucose tolerance, progressing to overt diabetes mellitus, caused by defective insulin secretion due to loss of β cell mass (Ristow *et al.* 2003).

1.5.4.2 - Knock-in mouse models

To mimic the mechanisms of human FRDA in mice, $(GAA)_{230}$ repeats were directly inserted into the mouse *Fxn* intron1 region to generate a FRDA knock-in mouse model. By crossing the knock-in mice with frataxin KO mice, studies showed that the resulting knock-in/knockout (KIKO) mice expressed 25-36% of the normal levels of frataxin. However

no GAA repeat instability, motor co-ordination abnormality, iron metabolism response due to iron loading, or premature death was observed (Miranda *et al.* 2002).

1.5.4.3 - *FXN* YAC transgenic mouse models

To investigate human frataxin function in a mouse background, Chamberlain and colleagues generated transgenic mice containing a human WT-*FXN* yeast artificial chromosome (YAC) with no endogenous mouse frataxin. Interestingly, the results showed that mice with loss of endogenous frataxin were rescued from embryonic lethality due to functional human frataxin expressed from the *FXN*-YAC transgene (Pook *et al.* 2001). To identify the mechanism of GAA repeat expansion, two lines of FRDA-YAC transgenic mice were established, YG8 and YG22, by integrating a GAA repeat expansion-containing 370kb human YAC clone. The difference between YG8 and YG22 lines is that there are 190 GAA repeats in YG22 and two arrays of 90 and 190 GAA repeats in YG8 (Al-Mahdawi *et al.* 2004). The results showed expansions of GAA repeat transmission from parent to offspring in these transgenic mice, similar to other TNR instability disorders (Figure 1.17, Table 1.2). These findings were consistent with a previous study carried out on transgenic mice carrying a 200 GAA repeat inserted into tandem arrays of hCD2 reporter constructs (Saveliev *et al.* 2003), which showed GAA repeat instability over generations.

Figure 1.17 - Intergenerational GAA repeat instability in FRDA YAC transgenic mice (Al-Mahdawi *et al.* 2004)**.**

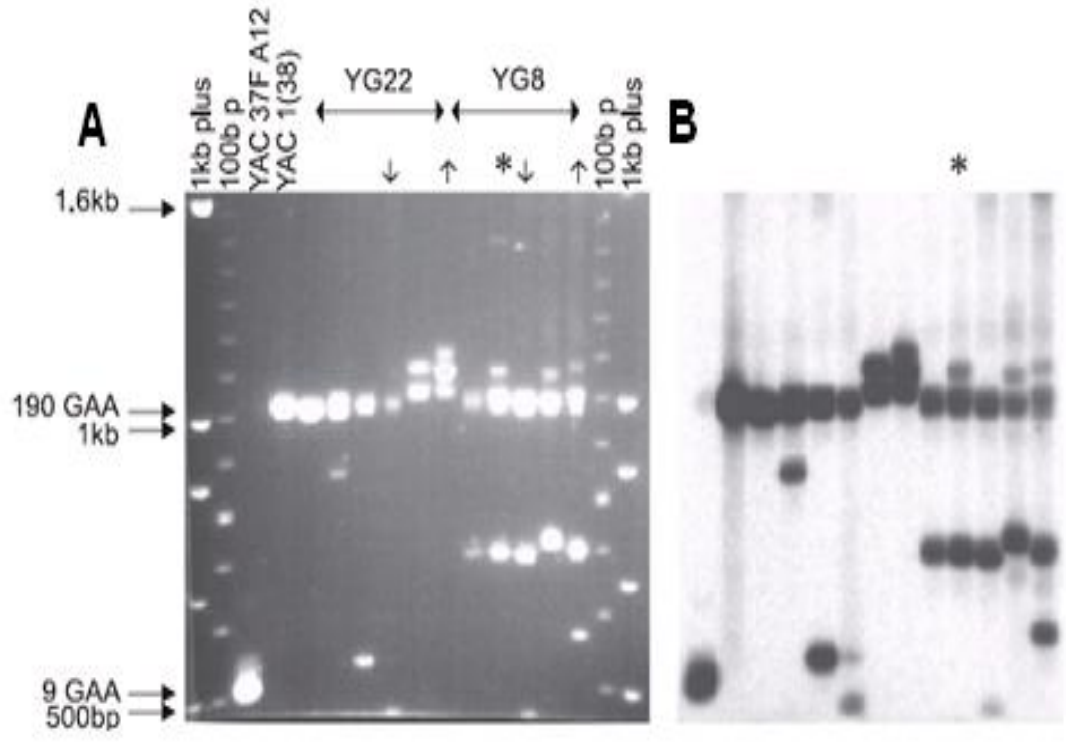

(A) Ethidium bromide-stained agarose gel and **(B)** Southern blot autoradiograph of GAA PCR products from representative YG22 (190 repeats) and YG8 (90 + 190 repeats) transgenic mice showing expansions (↑) up to 235 repeats (YG22) or 223 repeats (YG8) and contractions (↓) down to fewer than 9 repeats (both lines). An example of a discrete PCR product potentially corresponding to 340 repeats that failed to hybridize with a GAA probe is indicated by an asterisk. Each PCR product also contains 451 base pairs (bp) of non-GAA *FXN* intron 1 sequence flanking the actual GAA repeat. $1Kb^{+}$ and 100bp DNA markers and PCR products from wild-type YAC 37FA12 (9 repeats) and modified YAC 1(38) (190 repeats) are shown for comparison.

Table 1.2 - Parental age-related effect on GAA instability (Al-Mahdawi *et al.* 2004)**.**

Parental age	Instability	*GAA* alteration per transmission *(%)*	
		YG22	***YG8***
< 3 months	***Expansion***	4/60 (7%)	4/37 (11%)
	Contraction	6/60 (10%)	1/37 (3%)
4-6 months	***Expansion***	7/100 (7%)	7/41 (17%)
	Contraction	14/100 (14%)	2/41 (5%)
> 7 months	***Expansion***	9/66 (14%)	ND
	Contraction	11/66 (17%)	ND
Total	***Expansion***	20/226 (9%)	11/78 (14%)
	Contraction	31/226 (14%)	3/78 (4%)

ND: not determined. ***** Significant expansion bias upon transmission from older parents ($p < 0.05$). All nine cases of expansions were derived from male parents and none from females.

Nonetheless, any comparable fluctuation of expansion or contraction was not detected in different offspring gender carrying YG8 or YG22 (Table 1.3).

Table 1.3 - Effect of offspring gender on GAA instability (Al-Mahdawi *et al.* 2004)**.**

Offspring gender	Instability	*GAA* alterations per transmission *(%)*	
		YG22	***YG8***
Male	***Expansion***	13/226 (6%)	6/78 (8%)
	Contraction	16/226 (7%)	1/78 (1%)
Female	***Expansion***	7/226 (3%)	5/78 (6%)
	Contraction	15/226 (7%)	2/78 (3%)

In addition, somatic GAA repeat expansions were also observed in the YG8 and YG22 transgenic mice, particularly in CNS tissues such as cerebellum and spinal cord. Such somatic instability has previously been observed in FRDA patient lymphoblastoid cell lines and blood samples (Campuzano *et al.* 1996; Simon *et al.* 2004). However, YG8 and YG22 mice demonstrated for the first time that GAA repeat instability could also be dependent on age (Figure 1.18), particularly in cerebellar tissue (Al-Mahdawi *et al.* 2004).

Figure 1.18 - Somatic GAA repeat instability in FRDA YAC transgenic mice (Al-Mahdawi *et al.* 2004)**.**

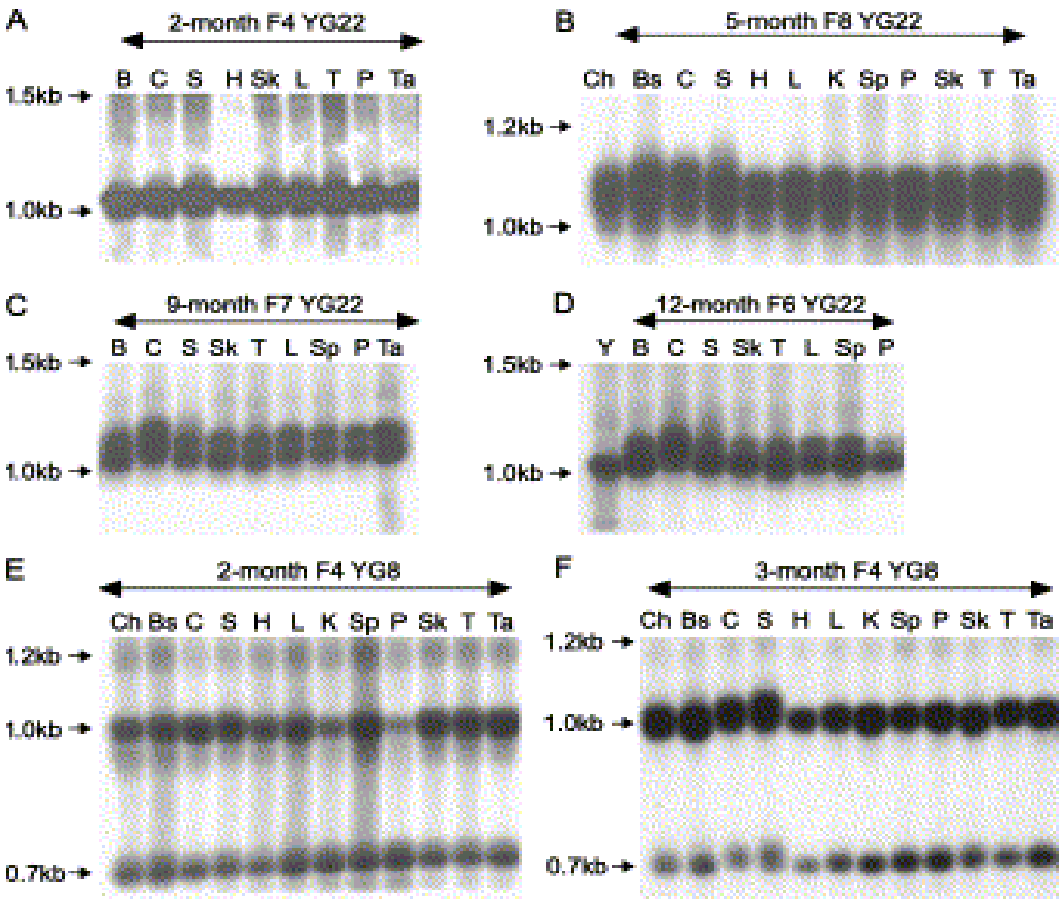

GAA PCR products from somatic tissues of representative transgenic mice. **(A)** 2-month F4 YG22, **(B)** 5-month F8 YG22, **(C)** 9-month F7 YG22, **(D)** 12-month F6 YG22, **(E)** 2-month F4 YG8, and **(F)** 3-month F4 YG8. No GAA repeat instability is detected in either 2-month-old YG22 or 2-month-old YG8 mice. Instability is greatest in the cerebellum of 9- and 12-month-old YG22 mice and the cerebellum and spinal cord of 3-month-old YG8 mice. Y, YAC 1(38); B, whole brain; Ch, cerebral hemisphere; Bs, brain stem; C, cerebellum; S, spinal cord; H, heart; L, liver; K, kidney; Sp, spleen; P, pancreas; Sk, skeletal muscle; T, testis; Ta, tail.

1.5.5 - Human cell culture models

FRDA cell lines are needed to identify the potential effects of novel therapeutic approaches. The generation of readily available FRDA cell lines, such as fibroblasts and lymphoblasts, has aided the understanding of molecular disease mechanisms, including epigenetic silencing of *FXN* expression. However, because they are not the primary affected cells in FRDA patients, these cells may not show the disease effects caused by FRDA. To produce more relevant disease-like cell models with reduced levels of frataxin mRNA and/or protein, different cell lines have been manipulated by siRNA or shRNA-mediated silencing. By generating stable *FXN*-transfected clones, researchers have recognised that frataxin defect causes increasing apoptosis in retinoic acid-stimulated cells, suggesting that frataxin depletion makes cells more susceptible to apoptosis during appropriate stimulation (Santos *et al.* 2001). In another study, it was shown that reduction of frataxin protein by transfecting human HeLa cells with RNAi caused reduction of Fe/S enzyme activities, such as aconitase and succinate dehydrogenase, but non-Fe/S enzyme activities remained unchanged. This study confirmed that frataxin is a constituent element of human ISC assembly machinery that plays an essential role in the maturation of both mitochondrial and cytosolic ISC (Stehling *et al.* 2004). Meanwhile, Ioannou and colleagues constructed a bacterial artificial chromosome (BAC) genomic reporter containing two in-frame fusions between *FXN* and enhanced green fluorescent protein (EGFP). This was a good approach to detect and evaluate novel compounds that may have an effect on frataxin expression. However, due to the short GAA repeats (only 6 GAA repeats), this experiment was only useful for evaluating molecules that affect a WT promoter region and not an expanded GAA repeat promoter region (Sarsero *et al.* 2003). Following this study, Herbert and colleagues constructed green fluorescent protein (GFP) cell lines containing part of *FXN* intron 1 with either 15 or 148 GAA repeats, fused to the GFP coding sequence. Analysis of the GFP signal

by using fluorescent microscopy and western blotting showed significant reduction in the cell lines with 148 GAA repeats compared to the cell lines with 15 GAA repeats. These data suggested that the reduced GFP signal was caused by the expanded GAA repeat, although other factors like a transgene integration site may have also had roles to play (Grant *et al.* 2006).

Since FRDA is a tissue selective disease, investigating various cell types can help to understand the mechanisms of disease. However, unlike fibroblasts and lymphocytes, the generation of human neuronal and cardiomyocyte cell lines is not easily achieved. Recently, the ability to reprogram somatic cells into induced pluripotent stem cells (iPSCs) has aided the potential generation of patient-specific FRDA-relevant cell lines, including neurons and cardiomyocytes. Several FRDA iPSC lines have been generated to date (Ku *et al.* 2010; Liu *et al.* 2011). Gottesfeld and colleagues have demonstrated that iPSCs can be derived from FRDA patients' skin fibroblasts. They showed that the *FXN* level is consistently reduced in iPSCs and their derivative cells, indicating that iPSCs could be a useful option to investigate high-throughput therapeutic screening (Ku *et al.* 2010; Liu *et al.* 2011).

1.6 - DNA mismatch repair

DNA is damaged by both endogenous and exogenous agents, resulting in cancer, due to hyper-proliferation, or neurodegenerative disorders, due to cell death. However, DNA repair proteins may enable DNA-damaged cells to survive by repair of the aberrant genes. DNA repair activities are generally classified into 5 different mechanisms: homologous recombination (HR), non-homologous end joining (NHEJ), nucleotide excision repair (NER), base excision repair (BER) and mismatch repair (MMR) (Sancar *et al.* 2004; Savas *et al.* 2004). MMR corrects genomic mismatch alterations that occur during DNA replication.

MMR genes play a critical role in genomic stability by influencing cell cycle checkpoints and programmed cell death. Thus, MMR genes induce apoptosis in severely damaged cells, by which tumourigenesis is blocked (Figure 1.19).

Figure 1.19 - Various functions of mismatch repair (MMR) proteins (Jun *et al.* 2006)**.**

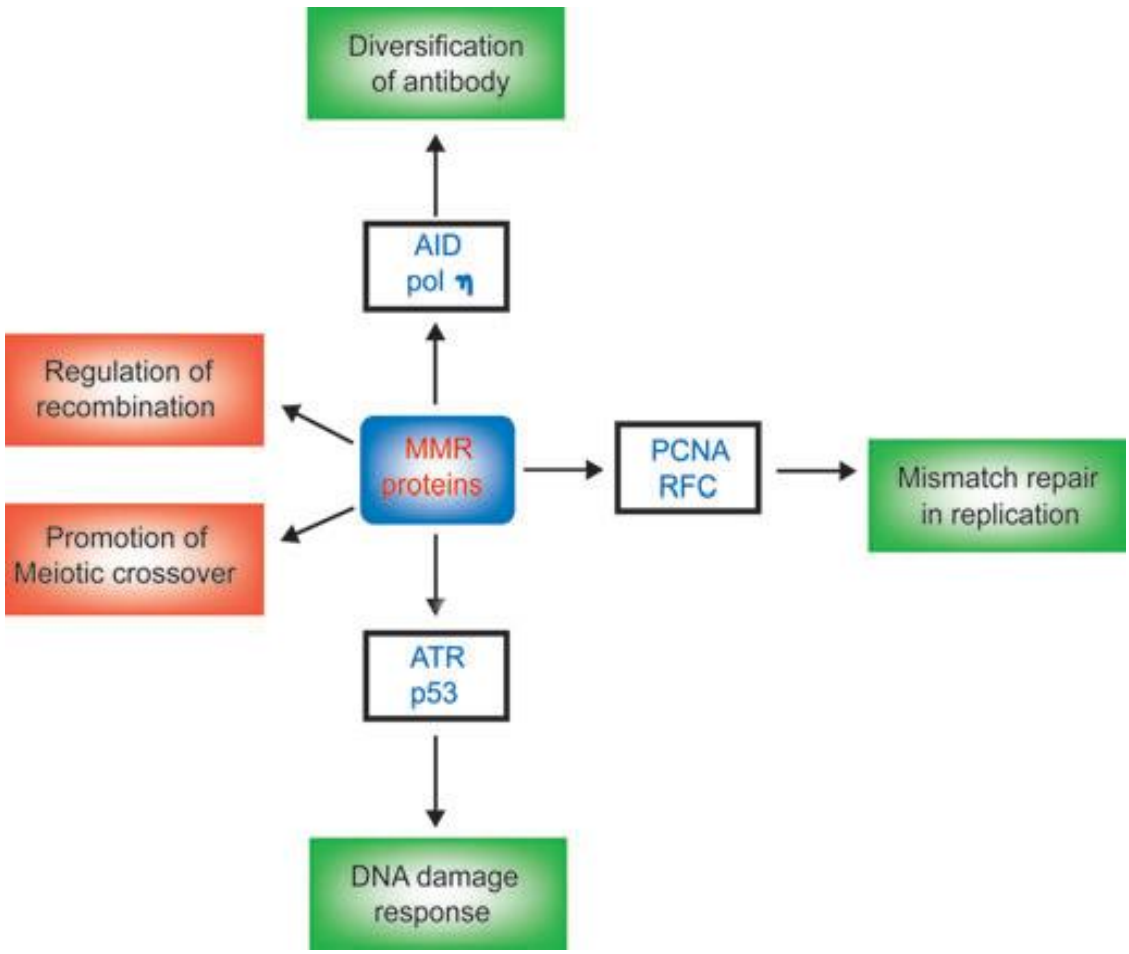

MMR proteins are involved in diverse genetic pathways through interactions with different proteins. MMR proteins increase replication fidelity by repairing errors generated during replication. Proliferating cell nuclear antigen (PCNA) and replication factor C (RFC) work with MMR proteins during mismatch repair in replication. Various kinds of DNA damage trigger MMR protein-dependent DNA damage responses that are implemented through the activation of ataxia telangiectasia mutated and Rad3-related (ATR) and p53. Antibody diversification is formed by mutations in immunoglobulin genes that are introduced by MMR proteins in conjunction with activation-induced cytidine deaminase (AID) and DNA polymerase. In addition, MMR proteins regulate recombination and promote meiotic crossover.

More than 30 years ago, the first evidence of MMR was obtained from *S.pneumoniae* studies, but most bacterial investigations are now based on *Escherichia coli* (*E.coli*). In 1989, three different MMR proteins were identified in *E.coli*, called MutS, MutL and MutH. MutS proteins have an intrinsic ATPase activity and play a role in recognising and binding as homodimers to both base-base mismatches and small nucleotide insertion/deletion loops (IDLs). Physical interaction of MutL with MutS results in elevation of mismatch recognition. Mechanistically, the mismatch repair pathway starts by binding MutS to the mismatch. In the presence of ATP and MutL, DNA helicase II (UvrD) unwinds double-strand DNA (dsDNA) towards the mismatch, culminating in single-strand DNA (ssDNA) generation. This ssDNA is protected from nuclease attack by ssDNA binding protein (SSB). In the next step, MutH determines and makes a strand-specific nick in hemi-methylated dGATC DNA. Depending on the position of the nick in the strand, different exonuclease enzymes (ExoI/ExoX for 3′→5′ exonuclease or ExoVII/RecJ for 5′→3′ exonuclease) excise past the mismatch sequence. Finally, the cleaved ssDNA is resynthesised by interaction of MutL, DNA polymerase III (δ and γ subunits), SSB and DNA ligase (Li 2008). High stability and strong interaction of the DNA polymerase III complex with MutL suggest that another protein (clamp loader) is being recruited during the resynthesis step of MMR (Li *et al.* 2008). Repairing mismatches in *E.coli* is dependent on ATP, suggesting a critical role of MutL and particularly MutS ATPase activities. Defect in MutL entirely prevent the MMR function in *E.coli* (Li 2008). Studies have shown that defective ATP hydrolysis in MutL, but not MutS, can activate MutH, although it is not able to stimulate the MutH in response to a mismatch or MutS, suggesting the crucial role of MutL ATP hydrolysis to mediate the activation of MutH by MutS (Junop *et al.* 2001).

MMR is a highly conserved process from prokaryotes to eukaryotes. However, the *E.coli* MutS and MutL proteins act as homodimeric complexes, whereas their human counterparts are heterodimers (Table 1.4).

Table 1.4 - MMR components and their functions (Li 2008)**.**

E.coli	***Human***	***Function***
(MutS)2	hMutSα (MSH2-MSH6)[a] hMutSβ (MSH2-MSH3)	DNA mismatch/damage recognition
(MutL)2	hMutLα (MLH1-PMS2)[a] hMutLβ (MLH1-PMS1) hMutLγ (MLH1-MLH3)	Molecular matchmaker; endonuclease, termination of mismatch-provoked excision
MutH	?[b]	Strand discrimination
UvrD	?[b]	DNA helicase
ExoI, ExoVII, ExoX, RecJ	ExoI	DNA excision; mismatch excision
Pol III holoenzyme	Pol δ	DNA re-synthesis
	PCNA	Initiation of MMR, DNA re-synthesis
SSB	RPA	ssDNA binding/protection; stimulating mismatch excision; termination of DNA excision; promoting DNA re-synthesis
	HMGB1	Mismatch-provoked excision
	RFC	PCNA loading; 3' nick-directed repair; activation of MutLα endonuclease
DNA Ligase	DNA ligase I	Nick ligation

[a] Major components in cells. [b] Not yet identified.

In humans, three MutS proteins form two complexes: MSH2/MSH3 form hMutSβ and MSH2/MSH6 form hMutSα. The hMutSα complex recognizes base-base mismatches and IDLs of one or two nucleotides, whereas the hMutSβ complex detects larger IDLs. In addition, hMutSα and hMutSβ, like MutS in *E.coli*, also play a role in MMR initiation via ATPase activity (Zhang *et al.* 2005; Jascur and Boland 2006; Hsieh and Yamane 2008). In both prokaryotes and eukaryotes, a defect of base-base mismatch repair culminates in single base substitutions. However, deficiency in the repair of IDLs results in MSI (Abdel-Rahman *et al.* 2006). MutL comprises 4 different homologues, including hMLH1, hMLH3, hPMS1, and hPMS2. Human MLH1 (hMLH1) can form three heterodimeric complexes by interaction with hPMS2, hPMS1 or hMLH3, comprising hMutLα, hMutLβ, or hMutLγ, respectively. It has been demonstrated that hMutLα is used in MMR and hMutLγ is involved in meiosis, but the function of hMutLβ is not clear yet. The hMutLα protein complex, like MutL in *E.coli*, carries an ATPase activity (Li 2008).

Eukaryotic DNA MMR consists of MutSα or MutSβ, MutLα, DNA polymerase δ and ligase I. However, existence of some other proteins is necessary to initiate the function; including: RPA, EXO1, HMGB1, PCNA, and RFC (Zhang *et al.* 2005; Jascur and Boland 2006; Hsieh and Yamane 2008). To initiate the MMR processing, proliferating cell nuclear antigen (PCNA) interacts with MSH2/MSH3 or MSH6 and MLH1/PMS2 via a conserved PCNA interaction motif (Figure 1.20).

Figure 1.20 - The process of eukaryotic MMR (Hsieh and Yamane 2008)**.**

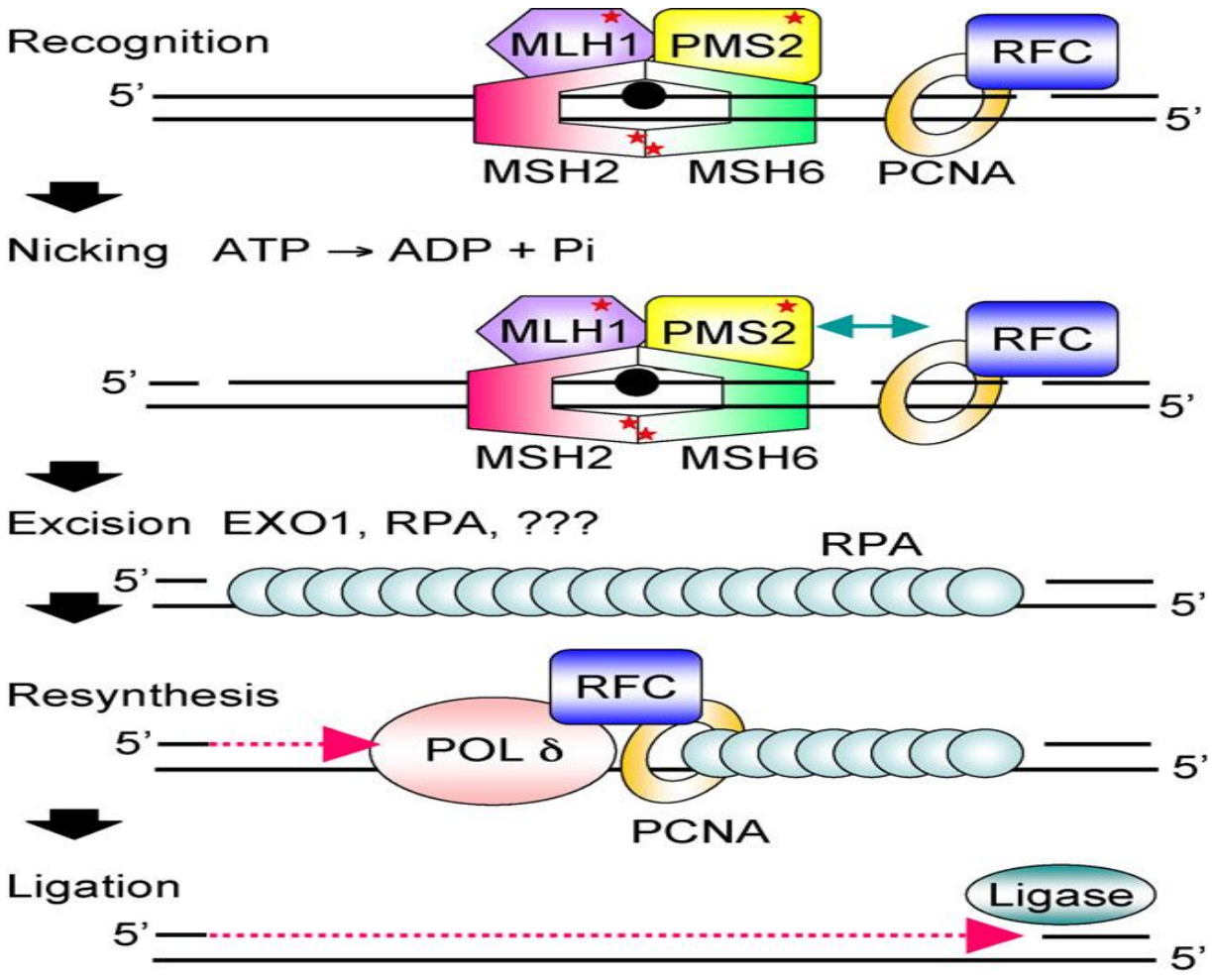

Recognition of a mismatch by MutSα (MSH2–MSH6) or MutSβ (MSH2–MSH3, not shown) and MutLα (MLH1–PMS2) results in the formation of a ternary complex whose protein–protein and protein–DNA interactions are modulated by ATP/ADP cofactors bound by MutSα and MutLα (indicated by red *). PCNA may play an important role in the recruitment of MMR proteins to the vicinity of the replication fork via a PIP motif on MSH6 and MSH3. Nicking by the endonuclease function of PMS2 stimulated by ATP, PCNA, and RFC and relevant protein–protein interactions (indicated by green arrow) may establish strand discrimination targeting repair to the newly synthesised strand. MMR is bi-directional and can be 5'-directed as well; this is not shown. Excision by *EXO1* and possibly other as yet unidentified exonucleases leads to the formation of an RPA-coated single-strand gap. Resynthesis by replicative pol d and ligation restore the integrity of the duplex.

It is proposed that PCNA might be able to help localise MutSα or MutSβ to mismatch errors in the daughter ssDNA. Proper function of this protein is essentially required during mismatch provoked 3'nick-directed excision. However, its existence is not necessary during

5'nick-directed MMR (Abdel-Rahman *et al.* 2006; Jun *et al.* 2006). EXO1 (a 5' to 3' exonuclease) cuts 5'directed mismatches in the presence of MutSα or MutSβ and replication protein A (RPA). RPA, which is a eukaryotic ssDNA binding protein, acts as an excision enhancer. Before MutSα and MutLα, this protein binds to nicked heteroduplex DNA. RPA also acts as stimulator of mismatch-provoked excision and alleviates DNA resynthesis. As soon as DNA polymerase δ is recruited to the gapped DNA substrate, RPA is phosphorylated. It is believed that phosphorylation decline RPA affinity to DNA, indicating that phosphorylated RPA is applied to ease MMR-associated DNA resynthesis more efficiently. Overall, it seems that this protein is involved in all steps of MMR. High mobility group box 1 (HMGB1) protein, a non-histone chromatin protein binding DNA and facilitating protein-protein interactions in MMR processing, is a mismatch binding protein playing a role in DNA unwinding activity. Despite the fact that its function is not fully understood yet, it is believed that HMGB1 may substitute for RPA. For catalysing the 3'nick-directed excision, EXO1 cooperates with MutLα endonuclease. However, MutLα endonuclease should be activated beforehand by PCNA and replication factor C (RFC) interaction. Activation of this complex results in termination of mismatch-provoked excision (Kunkel and Erie 2005; Jun *et al.* 2006).

Defects of the MMR system increase the range of genetic instabilities and accumulation of potential spontaneous mutations, so that damaged cells are predisposed to certain types of malignancy (Guo *et al.* 2004). Defects of MMR genes, particularly *MLH1*, have been reported to have a negative influence of MSI in 10-20% of sporadic tumours (Chew *et al.* 2008). Germline mutation of MMR genes may cause hereditary cancers, such as hereditary non-polyposis colorectal cancer (HNPCC; also called Lynch syndrome), the most prevalent autosomal dominant colorectal cancer (CRC) syndrome (Figure 1.21). HNPCC was discovered in 1913, but it is now called Lynch syndrome because of work by Lynch and

Krush in 1971 (Abdel-Rahman *et al.* 2006). HNPCC patients are normally predisposed to several cancers, particularly CRC, stomach cancer and endometrial adenocarcinoma (Gylling *et al.* 2007; Chew *et al.* 2008; Walsh *et al.* 2008).

Figure 1.21 - Genetic component in colorectal carcinogenesis (Abdel-Rahman *et al.* 2006)**.**

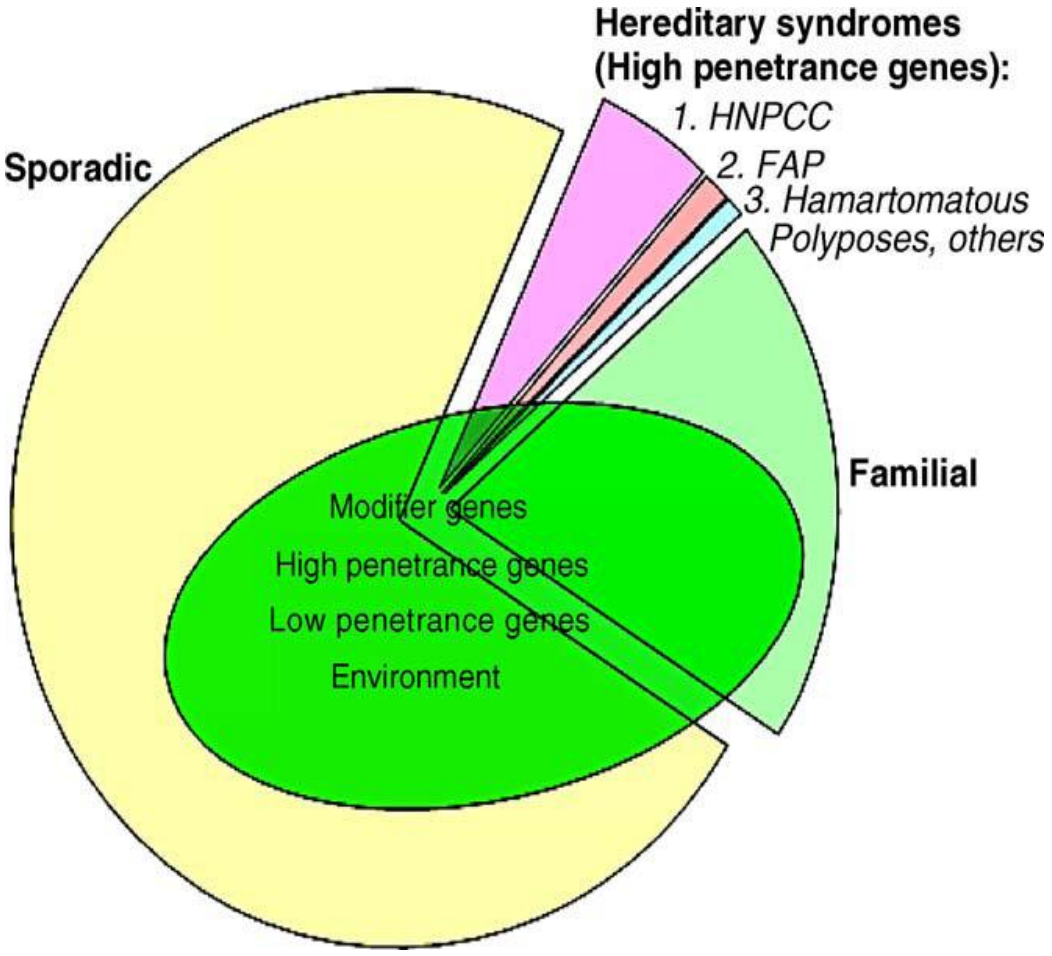

Mutations in high penetrance susceptibility genes underlie the development of hereditary syndromes, such as Lynch syndrome (HNPCC), Familial Adenomatous Polyposis (FAP), or Hamartomatous Polyposis syndromes. Both high and low penetrance susceptibility mutations account for the major share of familial colorectal cancer as well as undetermined fraction of sporadic colorectal cancer. Modifier genes are likely to influence the effects of the predisposition genes while the environment might have a greater role in sporadic cases.

HNPCC is usually caused by germline mutation in one of the *MSH2*, *MSH6* or *MLH1* genes. However, studies indicate that *PMS1*, *PMS2* and *MLH3* mutations can also be affected at

lesser frequencies. Heterozygous germline mutations of *MSH2* and *MLH1* genes are the most prevalent cause of HNPCC (Abdel-Rahman *et al.* 2006; Vasen *et al.* 2007). Interestingly, investigations proved the hypothesis that MSH2 and MLH1 proteins might be disrupted by pre-mRNA splicing (Tournier *et al.* 2008). Microsatellite instability can frequently be found in HNPCC because of MMR gene aberrations. Therefore, it is generally recommended to check for MSI at the initial process of HNPCC molecular diagnosis (Abdel-Rahman *et al.* 2006). Studies reveal that the risks of cancer development (particularly HNPCC) are more prevalent in *MSH2* mutants than *MLH1* mutants (Vasen *et al.* 2001). Finding the role of MMR proteins on MSIs was a good preface to investigating the correlation of MMR proteins and the main molecular cause of many neuromuscular disorders, namely TNR instabilities. Several studies indicate an effect of MMR on CAG and CTG repeat expansions, which may provide an insight into the molecular basis and subsequently therapeutic approaches to treat these disorders (Manley *et al.* 1999). For instance, investigating the effect of prokaryotic MMR proteins on the expanded human *HD* CTG repeats, artificially inserted into *E.coli*, showed that loss of each of MutS, MutL and MutH proteins promoted stability of the expanded CTG repeats. This observation suggested that the presence of MMR proteins could cause TNR repeat expansions and contractions (Jaworski *et al.* 1995).

1.6.1 - *MSH2* gene

MSH2 (MutS homolog 2) is a fundamental MMR gene in eukaryotes. Interest in MSH2 was sparked during investigation of HNPCC because its deficiency was reported as one cause of this hereditary malignancy, resulting in MSI. The critical action of *MSH2* in association with *MSH3* and *MSH6*, as MutSβ and MutSα complexes respectively, is an essential role in the recognition of base-base mismatches and IDLs. Therefore, absence of MSH2 stops the MMR process via disruption of damaged site recognition, and subsequently, no recruitment of the other MMR proteins to follow the repair process. To find out much more about the

consequences of Msh2 deficiency *in vivo*, *Msh2* KO mice were generated. These studies indicated that *Msh2* deficiency leads to a MSI mutator phenotype and tolerance to methylating factors (de Wind *et al.* 1995). *MSH2* may also act as an anti-recombinase during homologous recombination (HR). HR is a crucial intrinsic process in eukaryotic cells that repairs DNA double strand breaks (DSBs) and interstrand crosslinks. HR protects chromosomes against false rearrangements. To achieve that, recombinases, which catalyse natural recombination reactions, should be regulated. Msh2, as an anti-recombinase regulator, prevents unspecific activation of HR. So that, defect of Msh2 results in upregulation of recombinases, and subsequently over-activation of HR. Inaccurate matching of sequences during recombination can itself cause various genomic difficulties, such as Alu-mediated recombination in both somatic and germline cells. Since Alu repeats are the largest multi-genes family in human genome, the risks of HR events are highly estimated. Therefore, any HR between Alu-elements might culminate in duplication, deletion, and translocation (Batzer and Deininger 2002; Maguire and Kmiec 2007; Smith *et al.* 2007). It has also been demonstrated that Msh2 deficiency can contribute to chromosomal abnormality, since the loss of Msh2 activity causes aneuploidy in primary mouse embryonic fibroblasts (MEFs). Furthermore, several model studies have indicated an important role for Msh2 in TNR instability. Investigation of yeast models, containing different tracts of 25-92 CAG repeats, revealed that loss of MSH2 leads to increased instability towards repeat contractions, while these tracts are relatively stable in MSH2-proficient expression (Schweitzer and Livingston 1997).

Subsequently, by comparing transgenic mice carrying exon 1 of the human *HD* gene in the absence or presence of Msh2, Messer and colleagues showed that loss of Msh2 abolishes age-dependent CAG repeat expansions in mouse somatic tissues at 30 weeks of age (Manley *et al.* 1999). Subsequently, by using similar transgenic mouse models, Kovtun and McMurray

demonstrated that Msh2 can also affect germ line cells. Investigation of intergenerational transmission of CAG repeats in these transgenic mice demonstrated that loss of Msh2 leads to total abrogation of germline expansion in the progeny (Kovtun and McMurray 2001). Further studies of the knocked-in Hdh^{Q111} transgenic mice, containing 109 CAG repeats, showed that loss of Msh2 is sufficient to inhibit progression of somatic *HD* CAG expansion in striatum. In contrast, no significant changes were observed in maternal transmission of CAG repeat mutations (including both expansions and contractions) in the absence or presence of Msh2. Paternal germline transmission only showed contractions of CAG repeats in the absence of Msh2, suggesting that Msh2 is required for paternal CAG repeat expansions and protects against CAG repeat contractions (Wheeler *et al.* 2003).

Similar studies have been performed for DM1, another disease caused by TNR expansion, by generating *Msh2*-KO transgenic mice carrying more than 300 CTG repeats in the non-coding region of the human *DMPK* gene. Comparison *DMPK*/$Msh2^{+/+}$ and *DMPK*/$Msh2^{-/-}$ results showed that the overall range of mutability was not changed in both female and male transgenic mice. In this study, loss of Msh2 caused a reduction of CTG repeat expansions and a shift towards contractions in somatic cells. The same situation was also observed in both paternal and maternal intergenerational CTG repeat expansions. To find out the timing effect of the Msh2 defect on intergenerational CTG repeat instability, parental gametes of different Msh2 genotypes were analysed. The results showed that instability of progeny could depend on parental germline instability. Further studies of the somatic instability of various tissues in newborn offspring suggested a second instability event at a very early stage of development, probably just after fertilisation (Savouret *et al.* 2003).

1.6.2 - *MSH3* and *MSH6* genes

MutSα (MSH2-MSH6) binds to base-base mismatches. Both MutSα and MutSβ (MSH2-MSH3) bind to 1-2 nucleotide IDLs, while only MutSβ is able to bind to larger IDLs up to 16 nucleotides long (Kunkel and Erie 2005). The MutSβ complex also contributes to recombination by binding and stabilising nucleotide excision repair (NER) RAD1-RAD10 endonuclease for cleavage of the 3' non-homologous DNA. It has also been shown that MutSβ binds with high affinity to substrates containing double strand (ds)/ single strand (ss) DNA junctions and alters the conformation of such junctions, with a preference for substrates that contain 3' ssDNA (Surtees and Alani 2006).

Connection of the MutSβ complex and PCNA is mediated by the conserved PIP box at the N-terminal of MSH3. Further studies have shown that mutation of the PIP box prevents IDL corrections, particularly IDLs with more than two nucleotides. It is also believed that PCNA helps MutSα to search and recognise the mismatch errors, promoting the mismatch binding specificity of MutSα. PIP box deletion in MSH6 may also lead to partial defects of MutSα activity. Analysis of the N-terminal region (NTR) of Msh6 revealed at least two functions for this polypeptide site, one of which involves in PCNA interaction. Studies in mice have shown that Msh3 and Msh6 NTRs are able to be exchanged, and that the NTR of Msh6 might be functional when placed on Msh2 (Jun *et al.* 2006; Shell *et al.* 2007). Disruption of Msh3 showed susceptibility to malignancies, such as colorectal and endometrial cancers, and elevation of MSI in *Msh3*$^{-/-}$ mouse models. MSH6 deficiency also promotes tumourigenesis, but reduces MSI. It has been demonstrated that combined MSH3 and MSH6 interruption may cause the same adverse effects as *MSH2*$^{-/-}$ (Li 2008). Investigations of the transgenic mice carrying the human *DMPK* gene showed that deficiency of Msh3 blocks the $(CTG)_{84}$ instability, whereas Msh6 deficiency leads to elevation of CTG expansion in somatic cells. Analysis of the CTG repeat expansion in *Msh3*$^{-/-}$ transgenic mice

demonstrated that Msh3 may also play critical role in the expansions of this TNR over generations, while no similar function was observed with lack of Msh6. In other words, Msh6 deficiency causes a decrease of CTG expansions only in maternal transmissions. In this study, Gourdon and colleagues demonstrated that absence of one *Msh3* allele could lead to reduction of CTG repeat expansions (Foiry *et al.* 2006). Since the stability of Msh3 or Msh6 is dependent on their opportunity for binding to Msh2, it seems that the level of Msh2-Msh3 heterodimer in Msh6-deficient cells could be higher than in wild-type cells, resulting in increased TNR instability. In contrast, the presence of only the Msh2-Msh6 complex may result in TNR expansion blockage in somatic cells (van den Broek *et al.* 2002). To investigate the effects of Msh3 and Msh6 on intergenerational and somatic CAG repeat sizes in HD, Wheeler and colleagues cross-bred *HD*-$(CAG)_{101}$ knock-in mice with Msh3-KO or Msh6-KO mice. No significant difference was observed in maternal transmission of CAG repeats by comparing $Hdh^{Q111}/Msh3^{+/+}$, $Hdh^{Q111}/Msh3^{+/-}$ and $Hdh^{Q111}/Msh3^{-/-}$ or $Hdh^{Q111}/Msh6^{+/+}$, $Hdh^{Q111}/Msh6^{+/-}$ and $Hdh^{Q111}/Msh6^{-/-}$ genotypes. Analysis of paternal intergenerational instability showed that loss of Msh3 causes a shift of mutations from expansions towards .no-changes or even contractions, indicating that loss of Msh3 results in reduced CAG repeat expansions. $Msh6^{+/-}$ transgenic mice showed significantly greater CAG repeat contractions in comparison with $Msh6^{+/+}$, suggesting the protective effect of Msh6 against CAG paternal contractions. However, analysing $Msh6^{+/+}$ and $Msh6^{-/-}$ showed no difference in the instabilities of paternal CAG transmission, suggesting that another mechanisms might be involved in promoting male intergenerational CAG contractions in the absence of Msh6 (Dragileva *et al.* 2009). As with DM1, studies of HD transgenic mice carrying CAG expansions showed that Msh3 deficiency may lead to reduced somatic TNR instability in the striatum. However, no obvious effect on somatic instability was observed in the stratum of Hdh^{Q111} CAG knocked-in transgenic mice carrying $Msh6^{-/-}$ (Dragileva *et al.* 2009). Another

study previously showed that absence of Msh6 moderately reduces the CAG expansions in brain tissues, while no effect is observed in many other tissues such as liver and spleen (Owen *et al.* 2005). In contrast to *Msh2*, *Msh3*$^{+/-}$ showed a significant decrease in striatal CAG instabilities suggesting that Msh3 is a limiting factor in somatic instability of CAG, and that CAG striatal instability is probably mediated by Msh2-Msh3 dimers (Dragileva *et al.* 2009). To investigate the potential effects of MutS complex on CAG repeat expansions and related mechanisms, McMurray and colleagues tested the physical and biochemical properties of this heterodimeric enzyme changes while bound to the CAG hairpin. The results showed that MutSβ can recognise the CAG expansion region, blocking the ATPase activity of MutSβ heterodimer proteins (Owen *et al.* 2005).

1.6.3 - *PMS2* gene

Post-meiotic segregation increased 2 (*PMS2*) is one of the four human genes (*PMS1*, *PMS2*, *MLH1* and *MLH3*) encoding proteins similar to *E.coli* MutL. Combination of PMS2 and MLH1 proteins form the MutLα heterodimer, which is the major MutL complex acting in the mismatch repair initiated by the MutS complexes. There are 15 human *PMS2* pseudogenes, which is the main reason why the role of PMS2 has remained enigmatic for 10 years. This number of homologues may decrease the effects of PMS2 deficiency. For instance, *PMS2CL* is recognised as a *PMS2* pseudogene located in chromosome 7p22-23. The similarity of PMS2CL and PMS2 protein structure, particularly in the site where PMS2 binds to MLH1, may generate a false MLH1-PMS2 heterodimer in *PMS2*$^{-/-}$. Loss of PMS2 may cause a defect of MMR, producing somatic instability of microsatellite repeats. Studies have shown that mono-allelic or bi-allelic inactivation of *PMS2* is required to predispose toward cancers, such as Lynch syndrome and Turcot syndrome, a variant of Lynch syndrome. 5% of all Lynch syndrome patients carry some aberration of PMS2 (Niessen *et al.* 2009; Silva *et al.* 2009). Mutations in *PMS2* may lead to dramatic MSI in many cancers (e.g. HNPCC, and Turcot

syndrome). To gain better understanding of the effect of PMS2 on MSI, Monckton and colleagues generated transgenic mice by cross-breeding *Pms2*-deficient mice with mice carrying CTG repeat expansions in the *DMPK* gene. Analysis of somatic tissues showed a consistently lower rate of the expanded CTG repeats in the *Pms2*$^{-/-}$ tissues that usually show high levels of expansion, namely kidney and brain. Pms2 was shown to be required to increase the level of CTG repeat expansions, but was not a critical factor in generating expansion *per se*. Therefore, it was suggested that the level of Pms2 might correlate with the level of CTG repeat expansions. However, compared to *Pms2*$^{-/-}$, no significant differences in repeat expansion rates were observed between *Pms2*$^{+/-}$ and *Pms2*$^{+/+}$ transgenic mice. Thus, it is proposed that even single functional *Pms2* allele could be sufficient to promote CAG repeat expansion levels (Gomes-Pereira *et al.* 2004).

1.6.4 - *MLH1* gene

The human MutL homologue 1 (MLH1) is another essential MMR protein, interacting as MLH1-PMS2, MLH1-MLH3 or MLH1-PMS1 heterodimers with the MutS heterodimer complexes to continue and terminate the MMR process. The MutLα complex (MLH1-PMS2) is able to interact with both MutSα and MutSβ. In contrast, MutLβ (MLH1-MLH3) is only able to interact with MutSβ. It is believed that the presence and proper activity of MLH1 in the MutL heterodimer is necessary to recruit the mammalian EXO1, DNA replication protein A and a component of DNA polymerase δ; PCNA/POL30 (Ellison *et al.* 2004). Thus, lack of MLH1 may result in disruption of MMR complex activity, producing many cellular abnormalities. In addition to the occurrence of somatic point mutations, *MLH1* gene silencing may be caused by loss of heterozygosity (LOH) and hypermethylation of the *MLH1* promoter. Studies have shown that the rate of *MLH1* promoter hypermethylation (83%) is remarkably higher than LOH (24%) and somatic mutations (13%) (Kuismanen *et al.* 2000; Blanco *et al.* 2010). Similar to MSH2, defect of MLH1 often causes hereditary Lynch

syndrome, but it can also cause aggressive and early onset haematological, brain or endometrial tumours, together with increased MSI (Abdel-Rahman *et al.* 2006; Blanco *et al.* 2010).

Few studies have thus far been carried out to understand the effects of MLH1 on TNR instability. In 1999, Hirst and colleagues inserted the normal or pre-mutated (54-200) length of human *FMR1* CGG repeats into the *S. cerevisiae* and investigated the *mlh1* effect on TNR instabilities. The results showed no increase in CGG expansion with the mlh1 defect, while several repeat expansions were seen in the presence of mlh1, indicating that absence of mlh1 reduces the CGG repeat expansion level in yeast (White *et al.* 1999). Later, Lin and Wilson inserted $(CAG)_{95}$ repeats into the inactivated *HPRT* mini gene of the FLAH25 cell line (derived from the human fibrosarcoma cell line: HT1080) and treated it with two siRNAs against *MLH1*. The results showed that CAG repeat expansions are reduced and transcription-induced CAG contractions are increased with loss of MLH1. Further studies showed that simultaneous downregulation of MLH1 and DNMT1 significantly increases repeat instability of CAG towards contractions, suggesting that losses of MLH1 and DNMT1 are involved in a transcription-induced pathway of TNR instability (Lin and Wilson 2009).

1.7 - Aim of the study

FRDA is a fatal neurodegenerative disorder, mainly caused by abnormal expansion of GAA repeats within the first intron of human *FXN* gene. The exact mechanisms that cause FRDA are not yet clear and no effective therapy currently exists. Investigations have shown that different DNA repair genes, including MMR genes, can contribute to many different disorders by destabilising TNR. Therefore, the principle objective of this research was to study the effects of MMR genes (*MSH2*, *MSH3*, *MSH6*, *PMS2* or *MLH1*) on the instability of GAA repeat expansions by two major approaches. Firstly, in chapter 3, the role of each MMR

gene in intergenerational GAA repeat instability was investigated by comparing GAA repeat sizes in *FXN*$^{GAA+}$/ *MMR*$^{-/-}$ and *FXN*$^{GAA+}$/ *MMR*$^{+/+}$ transgenic mice and their offspring. Secondly, in chapter 4, the effect of each MMR gene in somatic GAA repeat instability was investigated by comparing different tissues from *FXN*$^{GAA+}$/*MMR*$^{-/-}$ and *FXN*$^{GAA+}$/*MMR*$^{+/+}$ transgenic mice.

Moreover, it has been demonstrated that GAA repeat expansion is associated with reduced *FXN* transcription (Greene *et al.* 2007; Al-Mahdawi *et al.* 2008). Hence, in chapter 5, to investigate any effect of MMR genes on *FXN* transcription, the *FXN* transcription level was quantified in both *FXN*$^{GAA+}$/*MMR*$^{-/-}$ and *FXN*$^{GAA+}$/*MMR*$^{+/+}$ transgenic mice *in vivo* and human cells *in vitro*.

Furthermore, several investigations have reported a potential role of frataxin deficiency in generating malignant cells. Also, MMR gene aberrations are recognised as the source of various types of cancer, particularly HNPCC. Therefore, the aim of chapter 6 was to investigate the effect of frataxin deficiency on MMR expression levels in human cells and tissues, which may subsequently have an impact on potential cell malignancy.

Chapter 2 - Materials and methods

2.1 - Solutions and reagents

2.1.1 - General solutions

- **Tris/EDTA (TE) buffer:** 10mM Tris-HCl (pH 7.5), 1mM EDTA.
- **Tail digestion buffer:** 100mM Tris-HCl (pH 8.0), 5mM EDTA, 200mM NaCl, 0.2% SDS.
- **DEPC-treated water (0.1%):** 1ml DEPC solution (≥97%), 999ml sterilised water (filtered and then autoclaved twice).
- **Orange G loading dye (6x):** 0.35% Orange G dye, 30% sucrose.
- **TBE (1x):** 90mM Tris, 20mM Boric acid, 2mM EDTA.

2.1.2 - Cell culture media

- **DMEM medium:** 1x DMEM medium, 10% foetal calf serum (FCS), 2% penicillin-streptomycin (Pen-Strep; 5000U/ml penicillin and 500mg/ml of streptomycin, Fisher Scientific Inc.).
- **McCoy's medium:** 1x McCoy's medium, 10% foetal calf serum (FCS), 2% penicillin-streptomycin (Pen-Strep; 5000U/ml penicillin and 500mg/ml of streptomycin, Fisher Scientific).

2.1.3 - NucleoSpin® RNA II reagents

- **Wash buffer RA3 (50 preps):** 12.5ml concentrated RA3, 50ml ethanol.
- **DNase reaction mixture:** 90µl reaction buffer for rDNase, 10µl reconstituted rDNase (used freshly).

2.2 - Genotyping and mRNA quantification primers

Various primers were used for genotyping the FRDA YAC double transgenic mice (*FXN*^{GAA}/*MMR* , Table 2.1) as well as quantification of mRNA expression of different genes in the human and *FXN*$^{GAA+}$ double transgenic mice (Table 2.2). Primer sequences were obtained either from previous studies (as indicated in the Table 2.1 and Table 2.2) or were newly designed by using Primer 3 and BLAST software from NCBI. All primers were purchased from Sigma-Aldrich.

Table 2.1 - Primers used for genotyping genetically altered mice.

Name of the fragment	Primer ID	sequence (5'-3')	Species	Reference
GAA	GAA-F	GGGATTGGTTGCCAGTGCTTAAAAGTTAG	Human	Campuzano et al., 1996
	GAA-R	GATCTAAGGACCATCATGGCCACACTTGCC		
CGG	CGG-F	ATGTCCTAATTCGTATGACAGCTGG	Mouse	Newly designed
	CGG-R	TGCTACAGGAATCACAGGCTTCTA		
CAG	CAG-F	TGTCGCCTCAGCCCTTGTGG	Mouse	Newly designed
	CAG-R	CTGCTCTGCCGTTTGGGGCA		
Msh2 knockout	Msh2-P1	CGGCCTTGAGCTAAGTCTATTATAAGG	Mouse	Toft et al., 1999
	Msh2-P2 (KO specific)	GGTGGGATTAGATAATGCCTGCTCT		
	Msh2-P3 (WT specific)	CCAAGATGACTGGTCGTACATAAG		
Msh3 knockout	Msh3-P1 (WT specific)	CAGGAAGAGGTCACTGGGAAATGG	Mouse	de Wind et al., 1995
	Msh3-P2 (KO specific)	GGTGGGATTAGATAATGCCTGCTCT		
	Msh3-P3	GCTGAGAATACTTAGTCTCTGGCA		
Msh6 knockout	Msh6-P1 (WT specific)	CAAGTCCTAGGATTAGAGGTCTGG	Mouse	de Wind et al., 1995
	Msh6-P2 (KO specific)	CCGGTGGATGTGGAATGTGTGCG		
	Msh6-P3	CCATGCAAATCAGACTCGATACAA		
Pms2 knockout	Pms2-P1	ACAGTTACATTCGGTGACAG	Mouse	Designed by Mark Pook
	Pms2-P2 (KO specific)	TTTACGGAGCCCTGGCGC		
	Pms2-P3 (WT specific)	ACTAATTCCCCTACGGTTTAG		
Mlh1 knokcout	M001	TGTCAATAGGCTGCCCTAGG	Mouse	Edelmann et al., 1999
	M002 (KO specific)	TGGAAGGATTGGAGCTACGG		
	M003 (WT specific)	TTTTCAGTGCAGCCTATGCTC		

Table 2.2 - cDNA primers used for gene expression analysis of genetically altered mice.

Name of the fragment	Primer ID	sequence (5'-3')	Species	Reference
Gapdh	*Gapdh* -m-F	ACCCAGAAGACTGTGGATGG	Mouse	Al-Mahdawi et al., 2008
	Gapdh -m-R	GGATGCAGGGATGATGTTCT		
GAPDH	*GAPDH* -h-F	GAAGGTGAAGGTCGGAGT	Human	Al-Mahdawi et al., 2008
	GAPDH -h-R	GAAGATGGTGATGGGATTTC		
FXN	*FXN* -h-RT-F	CAGAGGAAACGCTGGACTCT	Human	Al-Mahdawi et al., 2008
	FXN -h-RT-R	AGCCAGATTTGCTTGTTTGGC		
MSH2	h-RT-*MSH2*- F	ACAGAAAGCCCTGGAACTTGAGGA	Human	Newly designed
	h-RT-*MSH2* -R	GGCATTTGTTTCACCTTGGACAGG		
MSH3	h-RT-*MSH3*- F	AGGGACGAGCACTCATGATGGA	Human	Newly designed
	h-RT-*MSH3* -R	CCTCACTGACCAAGAATCCCAT		
MSH6	h-RT-*MSH6* -F	TGTGAAGACCCCAGCCAGGAGA	Human	Newly designed
	h-RT-*MSH6* -R	TTCCTCTGGGAGATTAGCAAGCCT		
PMS2	h-RT-*PMS2* -F	GGGGTCATGTGCCGGCCTTC	Human	Newly designed
	h-RT-*PMS2* -R	GGGGACAGTTCCAGGGGTGGT		
MLH1	h-RT-*MLH1* -F	TGGGACGAAGAAAAGGAATG	Human	Newly designed
	h-RT-*MLH1* -R	GATCAGGCAGGTTAGCAAGC		

2.3 - General techniques

2.3.1 - General preparations

Stock solutions and dilutions were prepared in deionised water (18.2 MΩ) unless otherwise specified. Total RNA samples were dissolved in DEPC-treated sterile water and DNase-RNase free water was utilised for polymerase chain reaction (PCR) mastermix preparation. All necessary materials, reagents and deionised water were autoclaved at 121°C, 100 kilo Pascal (kPa) for 20 minutes.

Centrifugation of samples was carried out using different equipment. Samples with large volumes (15-50ml) were centrifuged in a centaur 2 centrifuge (Sanyo/MSE). Depending on the temperature requirement, smaller samples (0.5-1.5ml) were centrifuged at room temperature using a standard bench top micro-centrifuge (16K, BioRad) or at 4°C using a refrigerator micro-centrifuge (5415R, Eppendorf). Very small volume samples (≤ 20µl) were briefly centrifuged by using a mini micro-centrifuge (Heathrow Scientific). 96 well plates were centrifuged at room temperatures using a Legend T centrifuge (Sorvall).

Incubations at 37-60°C were performed in water baths (Grant), whereas a heating block (DB-2A, Techne) was utilised for higher temperatures. The pH of solutions was determined using a pH-meter (Delta 340, Mettler) and pH adjustments were made by adding either concentrated HCl or NaOH.

Genomic DNA solutions were stored at 4°C. PCR products were stored at 4°C for short term or -20°C for long term. Complementary DNA (cDNA) samples were stored frozen at -20°C. All fresh tissues and RNA samples were snap frozen and stored at -80°C. Reagent kits were stored at room temperature, 4°C or -20°C according to manufacturer recommendations, if necessary in the dark. Frozen cells were stored overnight at -80°C in a container with isopropanol and then kept in liquid nitrogen for long term storage.

2.3.2 - Agarose gel electrophoresis

Agarose gel electrophoresis was used to detect and separate DNA, cDNA or RNA based on sequence size. Gels were generally prepared in a 1-2% agarose range using 1x TBE buffer. The agarose mixture in 1x TBE was initially boiled in a standard microwave and allowed to cool. Subsequently, ethidium bromide was added to the gel in a final concentration of 0.5µg/ml and the gel was poured into a casting tray with the required well comb. After adding 6x orange G loading dye (5µl per 25µl of product), samples were loaded into the gels. The small gels were run at 70V for 25-40 minutes in mini gel tanks with the capacity volume

of 50ml (Flowgen Biosciences). In the case of TNR size analyses, PCR products were run overnight in a large volume (300ml) tank, at 60-90V. Finally the gels were visualised and documented using a UV transilluminator imaging system (Alpha Innotech).

2.4 - Cell culture

Two types of adherent human cell lines were used, depending on the objective of experiments: fibroblasts and epithelial cells. Similar procedures were carried out for both fibroblast and epithelial cells, but the culture media was different. To regenerate, grow and cryopreserve fibroblast cells, DMEM culture medium (Gibco) was applied, while McCoy's culture medium (Sigma-Aldrich) was used for epithelial cell lines.

2.4.1 - Culture media

Aliquots of FCS (Gibco) and Pen-Strep (Gibco) were thawed at 37°C for 2 hours or 4°C overnight. Inside a biological safety cabinet, FCS and Pen-Strep were added to 500ml of 1x DMEM or McCoy's medium, which was then mixed gently. The contents were filter sterilised with a 0.22µM pore filter unit (Nalgene) and stored at 4°C until required to use.

2.4.2 - Regeneration of cell lines

Frozen cells were removed from the liquid nitrogen tank and quickly thawed by immersing the vial in a water bath at 37°C. To regenerate the cells, it was critical to thaw the frozen cells as rapidly as possible to minimise the risk of cell damage by ice crystal formation. The cells were then transferred into a 15ml conical tube and 10ml of pre-warmed culture medium was added to the cells, which were mixed gently by pipetting up and down. The cells were collected by centrifugation at 1500 rpm for 5 minutes, then transferred to a flask containing new culture medium. Cells were incubated in a 5% CO_2 incubator at 37°C and 90-95% humidity.

2.4.3 - Passage of cell lines

Both fibroblast and epithelial cells are categorised as adherent cells. Once cells attach to the substratum and spread, they divide, and the cell number increase. Subculture was performed with fresh medium and space to allow continuous growth of the cells. Culture medium, phosphate-buffered saline (PBS) and trypsin/EDTA solutions were pre-warmed at 37°C in water bath. The medium was removed by vacuum suction and cells were washed gently with sterile PBS. Adherent fibroblast or epithelial cells were digested with trypsin/EDTA for 5 minutes at 37°C in the CO_2 incubator to bring them into suspension. The trypsin/EDTA solution was neutralised by adding 10ml of the DMEM culture medium to the fibroblast cell lines or 10ml of the McCoy's culture medium to the epithelial cells. The cells were collected by centrifugation at 1500 rpm for 5 minutes and sub-cultured in 10ml DMEM or McCoy's culture medium at a 1:2 or 1:4 ratio. The cells were then incubated at 37°C, 5% CO_2 with 95% humidity. To compare the growth efficiency of different cell lines within an experiment, the level of population doubling (PDL) was estimated in each passage number of individual cell lines, using the bellow formula:

$$PDL = \frac{\text{Log } (\textit{Dilution factor})}{\text{Log } (2)}$$

In this formula, dilution factor demonstrated fold of confluent culture cell dilutions (Kuranaga *et al.* 2001).

2.4.4 - Cryopreservation of cell lines

To store a back-up for future studies, 1-2 vials of the each cell line were cryopreserved. In contrast to thawing cells, the procedure of cooling cells was performed slowly. Thus, cells were digested with trypsin/EDTA and precipitated by centrifugation at 1500 rpm for

5 minutes. Cells were then resuspended in 1ml of appropriate culture medium (DMEM or McCoy) supplemented with 10% (v/v) DMSO. A good concentration of cells to freeze was considered to be 0.5-1.0 x 10^6 cells/ml. Cell were initially frozen slowly to -80^{o}C using a container containing isopropanol to avoid ice crystallisation damage of cells, then were stored in liquid nitrogen.

2.5 - Husbandry, breeding and genotyping of mice

Mice were housed in conventional open cages with litaspen premium 8/20 bedding, paper wool nesting and standard fun tunnel environmental enrichment. The animal husbandry was carried out at 11 hours dark versus 13 hours light, 20-23°C temperature and 45-60% humidity. The mice were given a diet of SDS RM3 expanded food pellets and standard drinking water. All procedures were performed in accordance with the UK Home Office "Animals (Scientific Procedures) Act 1986".

To yield different types of double genetically modified mice, YG8 and YG22 *FXN* GAA repeat expansion-containing transgenic mice (Al-Mahdawi *et al.* 2004) were cross-bred with each *Msh2*, *Msh3*, *Msh6*, *Pms2* or *Mlh1* heterozygous knockout mice (Baker *et al.* 1995; de Wind *et al.* 1995; Edelmann *et al.* 1996; de Wind *et al.* 1999). All mice were maintained in a predominant C57BL/6J (B6) genetic background. Each double transgenic mouse, containing the *FXN*^{GAA} transgene together with wild type (WT), heterozygous (Het) or homozygous MMR knockout (KO) allele, was then crossed with non-GAA transgenic mice to obtain the necessary offspring for subsequent analyses.

Newborn mice were weaned between 3-4 weeks of age and were processed for initial genotyping of human *FXN* and MMR genes. The ears were clipped for identification and the tip of tail (<5mm) was biopsied by using local anaesthesia with ethyl chloride BP (Cryogesic,

Acorus Therapeutics) for DNA isolation and genotyping, including estimation of GAA repeat sizes and knockout genotypes for the mouse *Msh2*, *Msh3*, *Msh6*, *Pms2* and *Mlh1*. To collect tissues, adult mice were humanely sacrificed, followed by dissection and flash freezing of tissues in liquid nitrogen. Each tissue was subsequently stored at -80°C.

2.6 - Genomic DNA isolation

Genomic DNA was extracted by applying the phenol/chloroform extraction method, to analyse GAA repeat size within different types of mouse tissue, as well as human cell lines. Briefly, 400µl of tail digestion buffer and 10µl of proteinase K (50mg/ml) were added to the collected samples in Eppendorf tubes, followed by brief vortexing and incubation overnight at 55°C. After digestion, 400µl of phenol was added and samples were mixed well by vortexing twice for 15 seconds and then centrifuged at 14000 rpm for 5 minutes at room temperature. Subsequently, 380µl of the supernatant was transferred to a fresh Eppendorf tube and 380µl of chloroform/isoamyl alcohol (24:1, v/v) was added. Samples were briefly vortexed and centrifuged again at 14000 rpm for 5 min at room temperature. Next, 350µl of the resulting supernatant was transferred to a fresh Eppendorf tube and 35µl of 3M Na-acetate (pH 5.2) was added. 700µl of absolute ethanol was then added to the tubes and samples were mixed well by inverting tubes several times. Subsequently, samples were incubated at -80°C for 10 minutes followed by centrifugation at 14000 rpm for 30 minutes at 4°C. The ethanol was removed and the pellets washed with 1ml of 70% ethanol. The samples were again centrifuged at 14000 rpm for 20 minutes at 4°C and then ethanol were carefully drained off and DNA pellets were air dried by inverting the Eppendorf tubes on paper towels for about 10 minutes. The DNA pellets were finally resuspended in 50-100µl of TE buffer and stored at 4°C.

2.7 - Determination of genomic DNA quantity and purity

Genomic DNA samples were quantified by using NanoDrop™ 2000c spectrophotometer (NanoDrop, Thermo Scientific). The concentration of samples was determined by detecting absorption (A) of ultra violet light (UV-light) at 260nm and their purity was verified by analysing $A_{260/280}$ ratio.

2.8 - Polymerase chain reaction (PCR)

Various polymerase chain reaction (PCR) amplification systems were utilised on 200-500ng of bulk genomic DNA samples to identify the different TNR repeat sizes and genotype MMR genes.

2.8.1 -Mycoplasma PCR screening of cell cultures

In order to importance of regularly checking cell lines for any signs of contaminations, mycoplasma PCR was carried out using a Mycosensor™ PCR Assay Kit (Stratagene). Briefly, 100µl of medium supernatant was transferred carefully from a culture flask into a sterile 1.5ml Eppendorf tube and incubated for 5min at 95°C in a water bath. 10µl strataclean was added to the tube and mixed well by flicking the tube followed by the centrifugation. Then, 20-50µl of sample was taken from the supernatant (this was acted as a template) and placed on ice. Mycoplasma PCR mastermix was prepared by adding the following reagents in order: 33µl dH_2O, 5µl of 10x PCR buffer (Qiagen), 1µl Q-buffer (Qiagen), 2.5µl of 10mM dNTP mix, 1µl primer mix, 2µl *Taq* DNA polymerase, 5µl internal control and 5µl test sample. PCR amplification was performed in 250µl tubes using a thermal cycler (PTC-225, MJ Research) and the cycling conditions were as described for "PCR using *Taq* DNA

polymerase" in the Table 2.3. To visualise the results, 10-15µl of PCR products were separated in 1-2% agarose TBE mini-gels along with a $1Kb^{+}$ DNA ladder (Invitrogen) at 75V for approximately 30 minutes.

Table 2.3 - Mycoplasma PCR cycling parameters (adapted from www.stratagene.com)**.**

Cycle(s)	Temperature	PCR using *Taq* DNA polymerase	PCR using *Taq* DNA polymerase with dUTP/UNG decontamination	PCR using the Brilliant Q-PCR mastermix	PCR using the Brilliant Q-PCR mastermix with dUTP/UNG decontamination
1x	37°C	---------	10 minutes	----------	10 minutes
	94°C	---------	10 minutes	10 minutes	10 minutes
35x	94°C	30 seconds	30 seconds	30 seconds	30 seconds
	55°C	1 minute	1 minute	1 minute	1 minute
	72°C	1 minute	1 minute	1 minute	1 minute

2.8.2 - GAA PCR

The conventional PCR amplification of GAA repeat sequences was performed on genomic DNA samples using GAA-F and GAA-R primers (refer to the table 2.1). The reaction was performed in a volume of 25µl containing DNA template, 50µM primers, mastermix ($MgCl_2$, *Taq* DNA polymerase, dNTPs; Qiagen), Q-buffer, and DNase-free water (Table 2.4). Positive and negative controls of PCR were included in each series of samples. PCR amplification was performed in the 250µl tube using a specific program by thermal cycler machine (PTC-225, MJ Research) according to the Table 2.4. PCR reaction tubes were initially heated

at 94°C for 2 minutes. Next, the PCR program was run for 10 cycles followed by another 20 cycles with increment time of extension (20 seconds) per cycle. Finally, the program was terminated by cooling tubes at 68°C for 6 minutes.

Table 2.4 - GAA PCR materials and conditions.

Reaction materials	GAA PCR program	Size of fragment
Materials / **PCR reaction (1x)** 2x Qiagen master mix 12.5µl Q-buffer 5µl 50µM GAA-F primer 1µl 50µM GAA-R primer 1µl dH2O 4.5µl Genomic DNA (200-500ng/µl) 1µl **Total** 25µl	94°C ---------- 2 minutes **Denaturation** 94°C ---------- 10 seconds **Annealing** 60°C ---------- 30 seconds **10x** **Extension** 68°C ---------- 45 seconds **Denaturation** 94°C ---------- 10 seconds **Annealing** 58°C ---------- 30 seconds **20x** **Extension** 68°C ---------- 1 minute* 68°C ---------- 6 minutes	451bp + (GAA)n

*: time increased by 20 second increments per cycle.

To analyse the results, a mixture of 8µl PCR product and 2µl of 6x orange G loading dye was run on a 1% ethidium-bromide stained agarose-TBE mini-gel along with 1Kb^{+} DNA size marker (Invitrogen) at 75V for approximately 30 minutes. Samples, positively identified for presence of the *FXN*^{GAA} transgene, were further analysed to better estimation of the GAA repeat sizes. This was achieved by loading the GAA-PCR products along with two size markers (1Kb^{+} and 100bp ladders; Invitrogen), then running in a 20cm-long 1.5% agarose TBE gel at 60-90V overnight.

2.8.3 - Gradient-TNR-PCR

Further to designing new primers (refer to the tTable 2.1), to investigate the size of other mouse TNR, two gradient-PCR (G-PCR) systems were initially performed for CAG and CGG repeats that are located on chromosomes 19 and 13, respectively. Reaction buffer was

prepared in a total volume of 25µl consisting of DNA template, 50µM primers (forward and reverse), mastermix ($MgCl_2$, *Taq* DNA polymerase, dNTPs, loading dye; Kapabiosystems) and DNase-free water (Table 2.5). PCR amplification was performed in the 250µl tube using a specific program containing 4 different annealing temperatures (58°, 60°, 62° and 64°C). The G-PCR was performed in a 35-cycle program by thermal cycler machine (PTC-225, MJ Research) according to the table 2.5. As the initial and final steps, the program was followed respectively by heating tubes at 94°C for 2 minutes and cooling at 72°C for 10 minutes. To analyse the results, 10-15µl PCR product was run in 1% ethidium bromide stained agarose TBE mini-gel along with $1Kb^+$ DNA size marker at 70V for approximately 30 minutes.

Table 2.5 - Mouse gradient CAG and CGG PCRs.

Reaction materials	Gradient PCR program	Size of fragment
Materials — **PCR reaction (1x)** 2x Kapa mastermix — 12.5µl 50µM forward primer — 0.3µl 50µM revrse primer — 0.3µl dH2O — 10.9µl Genomic DNA (200-500ng/µl) — 1µl **Total** — 25µl	94°C ---------- 2 minutes **Denaturation** 94°C ---------- 45 seconds **Annealing** 58°, 60°, 62° and 64°C ----- 30 seconds **35x** **Extension** 72°C ---------- 45 seconds 72°C ---------- 10 minutes	**CAG fragment size:** 293+(CAG)n **CGG fragment size:** 569+(CGG)n

2.8.4 -TNR-PCR

Following G-PCRs, the optimal annealing temperature was selected to amplify CAG or CGG repeats obtained from mouse genomic DNA. PCR reaction content was the same as for G-PCR systems, in a total volume of 25µl. Negative and positive controls were included into each round of samples. Each PCR reaction was performed in a 250µl tube (Fisher Scientific) using a thermal cycler (PTC-225, MJ Research) in 35 cycles of amplification as shown in the Table 2.6.

Table 2.6 - Mouse CAG and CGG PCRs.

Reaction materials	PCR program	Size of fragment
Materials — **PCR reaction (1x)** 2x Kapa mastermix — 12.5µl 50µM forward primer — 0.3µl 50µM revrse primer — 0.3µl dH2O — 10.9µl Genomic DNA (200-500ng/µl) — 1µl **Total** — 25µl	94°C ---------- 2 minutes **Denaturation** 94°C ---------- 45 seconds **Annealing** 62°C ---------- 30 seconds **Extension** 72°C ---------- 45 seconds **35x** 72°C ---------- 10 minutes	**CAG fragment size:** 293+(CAG)n **CGG fragment size:** 569+(CGG)n

Following on the amplifications, 10µl of PCR products along with 5µl of 1Kb^{+} size marker were run on 1% ethidium-bromide stained mini-agarose-gel with 1x TBE buffer at 70V for 30 minutes, to detect the quality of samples. Subsequently, using two types of size markers (1Kb^{+} and 100bp ladders), the size of relevant TNR for each sample was determined by running on 20cm-long 1.5% agarose gel at 60-90V, overnight.

2.8.5 -MMR-PCRs

A multiplex PCR was carried out on each double genetically altered mouse (*FXN*$^{GAA+}$/*MMR*) genomic DNA sample to detect the MMR genotype. A total volume of 25µl reaction buffer was prepared for each sample containing DNA template, 3 types of the relevant MMR gene primers (refer to the Table 2.1) with concentration of 50µM, mastermix (including: $MgCl_2$, *Taq* DNA polymerase, dNTPs, loading dye; Kapabiosystems) and DNase-free water (Table 2.7). For each experiment a negative control was applied as well as 3 positive controls demonstrating different genotypes of the relevant MMR gene (e.g. *Msh2*-WT, *Msh2*-Het and *Msh2*-KO). PCR reactions were prepared in 250µl tubes using a thermal cycler (PTC-225, MJ Research) and performed in a 35 cycles of amplification, according to the Table 2.7. Each

PCR program was initiated by heating tubes at 94°C for 2 minutes and terminated by cooling samples at 72°C for 10 minutes. Subsequently, analysis of results was carried out by electrophoresis of PCR products, along with a $1Kb^{+}$ size marker, on a 1-2% ethidium bromide stained agarose gel with 1x TBE buffer.

Table 2.7 - Mouse MMR-PCRs.

PCR name	Reaction materials	PCR program	Size of fragment
Msh2 **/*Msh3*** **/** ***Msh6***	**Materials** — **PCR reaction (1x)** 2x Kapa matermix — 12.5µl 50µM primer-1 — 0.3µl 50µM primer-2 — 0.3µl 50µM primer-3 — 0.3µl dH2O — 10.9µl Genomic DNA — 1µl **Total** — 25µl	94°C — 1 minute **Denaturation** 94°C — 30 seconds **Annealing** 60°C — 30 seconds **Extension** 72°C — 1 minute **30x** 72°C — 10 minutes	***Msh2*** **-WT fragement size:** 164bp ***Msh2*** **-KO fragement size:** 194bp ***Msh3*** **-WT fragement size:** 130bp ***Msh3*** **-KO fragement size:** 250bp ***Msh6*** **-WT fragement size:** 220bp ***Msh6*** **-KO fragement size:** 253bp
Pms2	**Materials** — **PCR reaction (1x)** 2x Kapa matermix — 12.5µl 50µM primer-1 — 0.3µl 50µM primer-2 — 0.3µl 50µM primer-3 — 0.3µl dH2O — 10.9µl Genomic DNA — 1µl **Total** — 25µl	94°C — 2 minutes **Denaturation** 94°C — 45 seconds **Annealing** 49°C — 30 seconds **Extension** 72°C — 45 seconds **35x** 72°C — 10 minutes	***Pms2*** **-WT fragment size:** 385bp ***Pms2*** **-KO fragment size:** 189bp
Mlh1	**Materials** — **PCR reaction (1x)** 2x Kapa matermix — 12.5µl 50µM primer-1 — 0.3µl 50µM primer-2 — 0.3µl 50µM primer-3 — 0.3µl dH2O — 10.9µl Genomic DNA — 1µl **Total** — 25µl	94°C — 3 minutes **Denaturation** 94°C — 45 seconds **Annealing** 55°C — 30 seconds **Extension** 72°C — 45 seconds **35x** 72°C — 3 minutes	***Mlh1*** **-WT fragment size:** 350bp ***Mlh1*** **-KO fragment size:** 500bp

2.9 - Isolation of total RNA

Isolation of total RNA was performed using two different methods: column based (NucloSpin® RNA II) and phenol-guanidine isothiocyanate based (TRIzol®) techniques. The former method was only utilised for human cerebellum to yield a better quality of total RNA.

2.9.1 -RNA extraction-NucloSpin® RNA II

Total RNA was extracted from human cerebellum tissues, using NucloSpin® RNA II according to manufacturer instructions (Macherey-Nagel). In this method, 30-50mg cerebellum tissue samples were manually homogenised in 350µl RA1 lysis buffer and 3.5µl β-mercaptoethanol, by passing the lysate several times through a 0.6mm needle fitted to a syringe. After vigorously vortexing, the viscosity of samples was reduced and the lysate was cleaned by using a filter tube (NucloSpin® filter) and centrifugation at 11000 rpm for 1 minute. The NucloSpin® filter tube was then discarded and 350µl ethanol (70%) was added to the cleaned lysate in a fresh Eppendorf tube and mixed well by vortexing. The lysate was loaded to a NucloSpin® RNA II column, placed in a collection tube, and centrifuged at 11000 rpm for 1 minute. The collection tube, containing the aqueous phase, was subsequently discarded and NucloSpin® RNA II column was again placed in a fresh collection tube. Later, 350µl membrane desalting buffer (MDB) was added to this column and the sample was centrifuged in 11000 rpm for 1 minute. Once again, the tube containing aqueous phase was discarded. To digest DNA, 95µl DNase reaction mixture was directly added on to the centre of silica membrane of the column and the sample was incubated at room temperature for 15 minutes. The NucloSpin® RNA II column was then washed by 200µl buffer RA2, to inactive rDNase, followed by centrifugation at 11000 rpm for 30 seconds. Next, the column was washed by 600µl buffer RA3 and centrifuged 11000 rpm for 30 seconds. Once again, the column was washed by adding 250µl buffer RA3 and centrifugation at 11000 rpm

for 2 minutes. Eventually, 30-50µl RNase-free water was added to the column, followed by centrifugation at 11000 rpm for 1 minute. The quality and quantity of RNA samples were determined by performing 1% agarose gel electrophoresis and NanoDrop™ spectrophotometer (see the section 2.7), respectively.

2.9.2 -RNA extraction- TRIzol® method

Total RNA was extracted from human and mouse cell lines and tissues using the TRIzol® method, following supplier guidelines (Invitrogen). About 10^6 cells or 70-100mg tissue was used to extract the total RNA. Each cell pellet was initially loosened by flicking the tube gently and resuspended in 1ml TRIzol®. Individual tissues were likewise homogenised manually in 1ml of Trizol® reagent. Samples were then incubated for 10 minutes at room temperature. 200µl chloroform was added per 1ml TRIzol® to each sample, followed by vigorous shaking for 15 seconds and incubation for further 15 minutes at room temperature. Samples were phase separated by centrifugation at 14000 rpm for 15 minutes at 4°C. The upper aqueous phase (about 500µl) was then transferred to a freshly labelled Eppendorf tube and RNA was precipitated by adding 500µl of isopropyl-alcohol. Samples were incubated for 10 minutes at room temperature and centrifuged at 14000 rpm for 15 minutes at 4°C. The supernatant was carefully removed and the RNA pellet was washed once with 1ml of 75% ethanol (prepared with DEPC-treated water) and centrifuged again at 14000 rpm for 5 minutes at 4°C. The supernatant was subsequently removed carefully and the RNA pellet was briefly dried for a period of 5-10 minutes and resuspended in 20-50µl of double sterile DEPC-treated water, followed by incubation at 60°C for 10 minutes. The quality and quantity of RNA samples were then determined by performing 1% agarose gel electrophoresis and NanoDrop™ spectrophotometry (section 2.7), respectively. Total RNA samples were then stored at -80°C until use.

2.10 - DNase I treatment of RNA

Total RNA samples were treated to prevent DNA contamination by using DNase I (amplification grade, Invitrogen). Essentially, 1µg RNA was added to an RNase-free 200µl microcentrifuge tube on ice, followed by adding 1µl DNase I reaction buffer (10x concentrated) as well as 1µl DNase I (1unit/µl). The total volume of each sample was then made up to 10µl by adding DEPC-treated water. Samples were incubated at room temperature for 15 minutes. Subsequently, DNase I was inactivated by adding 1µl of 25mM EDTA, followed by incubation at 65°C for 10 minutes. The treated RNA samples were then stored at -80°C.

2.11 - Complementary DNA (cDNA) synthesis

Complementary DNA (cDNA) was synthesised by using a cloned AMV first-strand cDNA synthesis kit (Invitrogen). On ice, 2µl RNA (with total concentration of 1µg) was added to 10µl primer component mastermix (7µl DEPC-treated water, 2µl of 10mM dNTP mix and 1µl oligo$(dT)_{20}$ primer). RNA and primer were denatured by keeping the samples at 65°C for 5 minutes and immediately placing the samples on the ice. The following reagents were then added in order: 4µl of 5x cDNA synthesis buffer, 1µl DEPC-treated water, 1µl of 100mM DTT, 1µl RNase-OUT™ (40 units/µl) and 1µl cloned-AMV-RT (15 units/µl). The 20µl reaction mixture was gently mixed by flicking the tube and briefly centrifuged to pull all contents to the bottom of tube. The reaction mixture was incubated at 55°C for 60 minutes, followed by keeping the samples at 85°C for 5 minutes to terminate reverse transcription procedure. The cDNA samples were used immediately or stored at -20°C.

2.12 - Reverse transcriptase PCR (RT-PCR)

Before performing mRNA quantification, different types of reverse transcriptase PCR (RT-PCR) were utilised to investigate the quality of cDNA samples.

2.12.1 - G-RT-PCR for human MMR genes

After designing new primers for each human MMR gene, G-RT-PCRs were performed on cDNA samples to optimise the amplification conditions. Each reaction mixture was prepared in a total volume of 25µl consisting of mastermix buffer (including: $MgCl_2$, *Taq* DNA polymerase, dNTPs, loading dye; Kapabiosystems), 50µM primers (forward and reverse), DNase free water and cDNA sample with concentration of 400-500ng/µl, according to the table 2.8. PCR amplification was performed in 250µl tubes (Fisher Scientific) using a specific program for each MMR gene containing 3 different annealing temperatures (Table 2.8). A negative and a positive control of RT-PCR were applied for each annealing temperature within individual series of samples. The G-RT-PCR programs were carried out in a 35 cycles of amplification by using a thermal cycler machine (PCT-225, MJ Research Co.). As initial and final steps, the programs were followed by heating tubes at 94°C for 2 minutes and cooling at 72°C for 10 minutes. To analyse the results, 10µl of PCR products along with a size marker were run in 1% ethidium bromide stained agarose gel with 1x TBE buffer at 60-70V for approximately 20-30 minutes.

Table 2.8 - G-RT-PCR for human MMR genes.

Gradient RT-PCR name	Reaction materials	Gradient RT-PCR program	Size of fragment
MSH2	**Materials** / **PCR reaction (1x)** 2x Kapa matermix: 12.5µl 50µM h-RT-MSH2-F primer: 0.5µl 50µM h-RT-MSH2-R primer: 0.5µl dH2O: 10.5µl cDNA (400-500ng/µl): 1µl **Total**: 25µl	94°C ---------- 2 minutes **Denaturation** 94°C ---------- 30 seconds **Annealing** 60°, 63° and 65°C ---------- 30 seconds **35x** **Extension** 72°C ---------- 45 seconds 72°C ---------- 10 minutes	**Fragment size:** 151bp
MSH3	**Materials** / **PCR reaction (1x)** 2x Kapa matermix: 12.5µl 50µM h-RT-MSH3-F primer: 0.5µl 50µM h-RT-MSH3-R primer: 0.5µl dH2O: 10.5µl cDNA (400-500ng/µl): 1µl **Total**: 25µl	94°C ---------- 2 minutes **Denaturation** 94°C ---------- 30 seconds **Annealing** 59°, 61° and 63°C --------- 45 seconds **35x** **Extension** 72°C ---------- 30 seconds 72°C ---------- 10 minutes	**Fragment size:** 173bp
MSH6	**Materials** / **PCR reaction (1x)** 2x Kapa matermix: 12.5µl 50µM h-RT-MSH6-F primer: 0.5µl 50µM h-RT-MSH6-R primer: 0.5µl dH2O: 10.5µl cDNA (400-500ng/µl): 1µl **Total**: 25µl	94°C ---------- 2 minutes **Denaturation** 94°C ---------- 30 seconds **Annealing** 63°, 65° and 67°C ---------- 20 seconds **35x** **Extension** 72°C ---------- 35 seconds 72°C ---------- 10 minutes	**Fragment size:** 111bp
PMS2	**Materials** / **PCR reaction (1x)** 2x Kapa matermix: 12.5µl 50µM h-RT-PMS2-F primer: 0.3µl 50µM h-RT-PMS2-R primer: 0.3µl dH2O: 6.9µl cDNA (400-500ng/µl; diluted 1:5): 5µl **Total**: 25µl	94°C ---------- 2 minutes **Denaturation** 94°C ---------- 30 seconds **Annealing** 60°, 63° and 65°C ---------- 30 seconds **35x** **Extension** 72°C ---------- 45 seconds 72°C ---------- 10 minutes	**Fragment size:** 151bp
MLH1	**Materials** / **PCR reaction (1x)** 2x Kapa matermix: 12.5µl 50µM h-RT-MLH1-F primer: 0.5µl 50µM h-RT-MLH1-R primer: 0.5µl dH2O: 10.5µl cDNA (400-500ng/µl): 1µl **Total**: 25µl	94°C ---------- 2 minutes **Denaturation** 94°C ---------- 30 seconds **Annealing** 53°, 55° and 57°C ---------- 30 seconds **35x** **Extension** 72°C ---------- 45 seconds 72°C ---------- 10 minutes	**Fragment size:** 250bp

2.12.2 - RT-PCR

After G-RT-PCR, the optimal annealing temperature was selected to amplify each MMR gene (Table 2.9). In addition, standard RT-PCR was performed for human *FXN*, human *GAPDH* and mouse *Gapdh* genes to determine the cDNA quality (Table 2.10).

Table 2.9 - RT-PCR for the human MMR genes.

RT-PCR name	Reaction materials	RT-PCR program	Size of fragment
MSH2 / ***MSH6*** / ***PMS2***	**Materials** — **PCR reaction (1x)** 2x Qiagen matermix — 12.5µl Q-buffer — 5µl 5µM forward primer — 1µl 5µM revrse primer — 1µl dH2O — 9.5µl cDNA (300-500ng/µl) — 1µl **Total** — 25µl	94°C ---------- 2 minutes **Denaturation** 94°C ---------- 30 seconds **Annealing** 65°C ---------- 30 seconds **Extension** 72°C ---------- 1 minute **35x** 72°C ---------- 10 minutes	***MSH2*** **fragment size:** 151bp ***MSH6*** **fragment size:** 111bp ***PMS2*** **fragment size:** 151bp
MSH3	**Materials** — **PCR reaction (1x)** 2x Qiagen matermix — 12.5µl Q-buffer — 5µl 5µM forward primer — 1µl 5µM revrse primer — 1µl dH2O — 9.5µl cDNA (300-500ng/µl) — 1µl **Total** — 25µl	94°C ---------- 2 minutes **Denaturation** 94°C ---------- 30 seconds **Annealing** 63°C ---------- 30 seconds **Extension** 72°C ---------- 45 seconds **35x** 72°C ---------- 10 minutes	**Fragment size:** 173bp
MLH1	**Materials** — **PCR reaction (1x)** 2x Qiagen matermix — 12.5µl Q-buffer — 5µl 5µM forward primer — 1µl 5µM revrse primer — 1µl dH2O — 9.5µl cDNA (300-500ng/µl) — 1µl **Total** — 25µl	94°C ---------- 2 minutes **Denaturation** 94°C ---------- 30 seconds **Annealing** 57°C ---------- 30 seconds **Extension** 72°C ---------- 45 seconds **35x** 72°C ---------- 10 minutes	**Fragment size:** 250bp

Table 2.10 - RT-PCR for *FXN* and *GAPDH* genes.

RT-PCR name	Reaction materials	RT-PCR program	Size of fragment
Mouse *Gapdh*	**Materials** / **PCR reaction (1x)** 2x Kapa matermix: 12.5µl 5µM forward primer: 1µl 5µM revrse primer: 1µl dH2O: 9.5µl cDNA (300-500ng/µl): 1µl **Total**: 25µl	94°C ---------- 2 minutes **Denaturation** 94°C ---------- 30 seconds **Annealing** 55°C ---------- 30 seconds **Extension** 72°C ---------- 1 minute **35x** 72°C ---------- 10 minutes	**Fragment size:** 81bp
Human *GAPDH*	**Materials** / **PCR reaction (1x)** 2x Kapa matermix: 12.5µl 5µM forward primer: 1µl 5µM revrse primer: 1µl dH2O: 9.5µl cDNA (300-500ng/µl): 1µl **Total**: 25µl	94°C ---------- 2 minutes **Denaturation** 94°C ---------- 30 seconds **Annealing** 55°C ---------- 30 seconds **Extension** 72°C ---------- 1 minute **35x** 72°C ---------- 10 minutes	**Fragment size:** 226bp
Human *FXN*	**Materials** / **PCR reaction (1x)** 2x Kapa matermix: 12.5µl 5µM forward primer: 1µl 5µM revrse primer: 1µl dH2O: 9.5µl cDNA (300-500ng/µl): 1µl **Total**: 25µl	94°C ---------- 2 minutes **Denaturation** 94°C ---------- 30 seconds **Annealing** 55°C ---------- 30 seconds **Extension** 72°C ---------- 1 minute **35x** 72°C ---------- 10 minutes	**Fragment size:** 172bp

As presented in the Table 2.9 and Table 2.10, a total concentration of 25µl reaction buffer was prepared for each sample consisted of mastermix buffer, Q-buffer (if necessary), 50µM primers (forward and reverse) of the relevant gene cDNA, DNase-free water and 300-500ng/µl cDNA template. PCR amplification was performed in 250µl tube using a specific RT-PCR program for each series of samples. All RT-PCR amplifications were carried out in a thermal cycler machine (PCT-225, MJ Research). As initial and final steps, the programs were followed by heating tubes at 94°C for 2 minutes and cooling at 72°C for 10 minutes. Finally, the results were analysed by electrophoresis of 10µl RT-PCR product,

along with size marker ($1Kb^+$ or 100bp), in 1% ethidium bromide stained agarose gel with 1x TBE buffer at 60-70V, for approximately 20-30 minutes.

2.13 - Quantitative real-time RT-PCR (qRT-PCR)

Following cDNA quality analysis, quantitative real-time RT-PCR (qRT-PCR) was carried out using power SYBR® green mastermix (Applied Biosystems) in a real time PCR machine (ABI prism 7900HT, Applied Biosystems). qRT-PCR reactions were performed in 96-well plates (Microamp, Applied Biosystems) in triplicates. A final volume of 20µl mastermix was prepared containing 10µl of 2x power SYBR® green mastermix, 1µl of 5µM optimised respective forward and reverse primers (see the table 2.2 for the applied primers in different gene cDNAs), 5µl of (5x diluted) cDNA and distilled water. Samples were minimised to light exposure. Target and endogenous mastermixes were prepared separately and added to the plate with a repetitive electronic pipette (Rainin) followed by adding the cDNA. Then the plate was sealed with real time plate sealers (MicroAmp, Applied Biosystems) and the contents were mixed gently. The plate was then centrifuged for 1 minute at 1000 rpm to bring all the contents to the bottom of the wells. The cycling conditions varied according to the application and were optimised to amplify the different targets with similar efficiencies. Following qRT-PCR, a dissociation curve run was performed by increasing the temperatures gradually from 60°C to 95°C. Relative quantification values were identified by $2^{-\Delta\Delta Ct}$ method using SDS 2.4 and RQ manager software (Applied Biosystems).

2.14 - Statistical analysis

Statistical analyses such as descriptive measurements and graphical visualisations were performed using Microsoft excel 2007 software. Significant differences of the frequency distributions of the intergenerational transmission of GAA repeat size (including three categories of "GAA repeat expansions", "no changes", and "GAA repeat contractions") between groups of wild type, heterozygous or homozygous MMR knockout parental genotypes were determined by using χ^2 (Chi square) analyses. All other measurements, comparing two groups of sample, were analysed using the student's *t* test to determine statistically significant difference of the values. A *p* value of 0.05 was chosen as the significance threshold.

Chapter 3 - Results: The mismatch repair system protects against intergenerational GAA repeat instability in a FRDA mouse model

3.1 - Introduction

To understand the potential effect of MMR proteins on intergenerational transmission of GAA repeat instability from parent to offspring, an *in vivo* model is considered to be the most useful approach. Since FRDA is a rare autosomal recessive disorder, detecting and comparing intergenerational GAA repeat instabilities of FRDA patients/carriers, carrying different levels of one particular mismatch repair protein (e.g. *MSH2*) is not possible. Precedents from *in vivo* model studies have confirmed the important role of transgenic mouse models to better understand molecular pathogenesis of FRDA disease and develop potential therapies. Thus, the YG8 and YG22 transgenic mice, containing 90 and 190 GAA repeats in the YG8 line and 190 GAA repeats in the YG22 line, are the most efficient models exhibiting intergenerational and somatic instability of GAA repeat expansions. They also show similar molecular and phenotypic pathogenesis to human FRDA, including similar DNA methylation and histone modification epigenetic changes (Al-Mahdawi *et al.* 2004; Al-Mahdawi *et al.* 2008). These models are considered as good systems to test the effect of MMR proteins on the intergenerational instability of GAA repeat expansions, although the GAA repeat sizes are smaller than the average 500-600 GAA repeats found in FRDA patients. Therefore, to develop improved larger GAA repeat models, breeding of transgenic mice was carried out, resulting in increased the number of mutational GAA repeat expansions from 90 and 190 to approximately 140 and 225 repeats in YG8 and from 190 to approximately 250-285 repeats in YG22 (Figure 3.1).

Figure 3.1 - Schematic representation of increasing GAA repeat expansions.

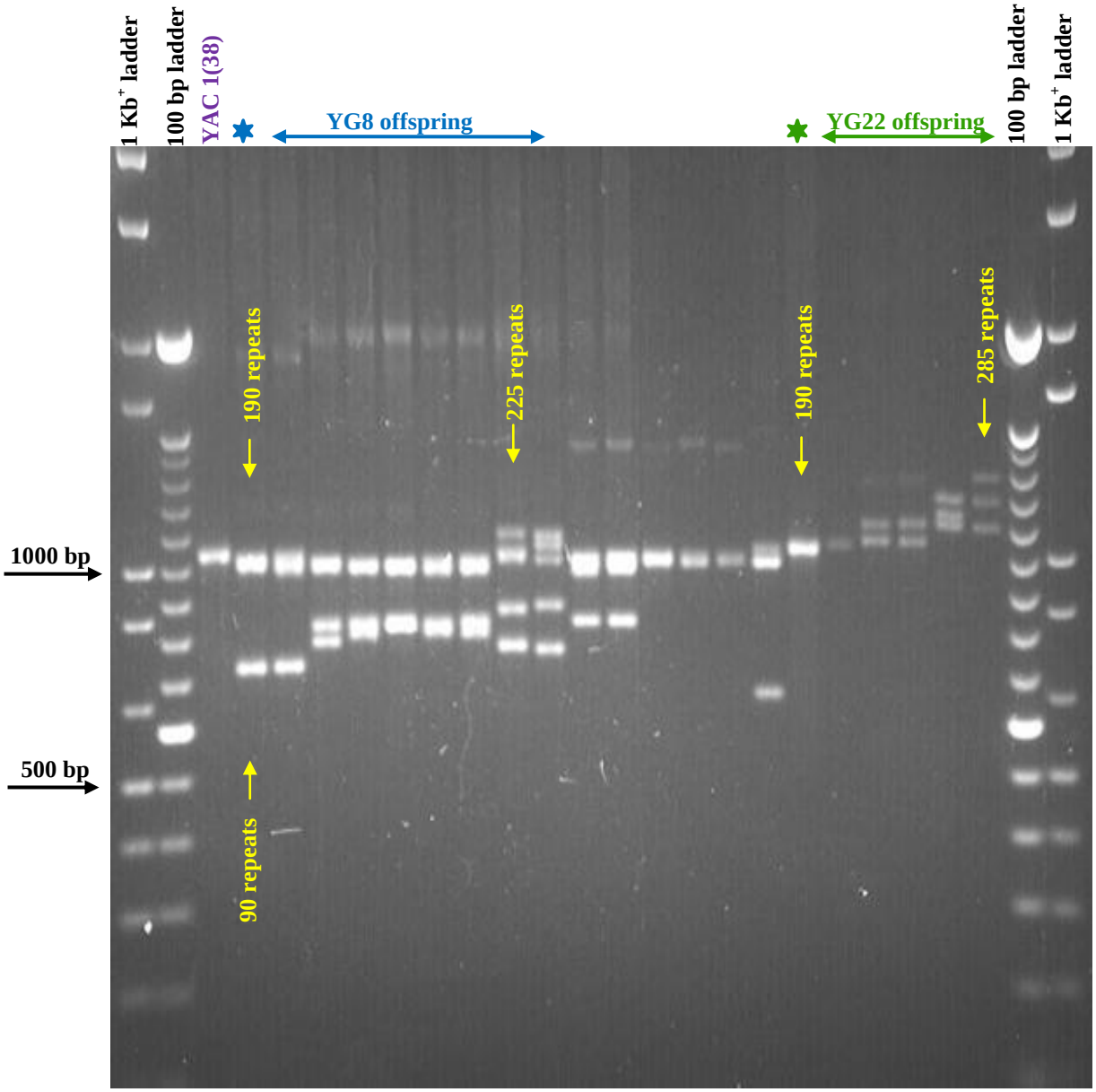

The ethidium bromide-stained agarose gel image illustrates increased GAA expansions up to 225 repeats in YG8 (blue arrow) and 285 repeats in YG22 (green arrow). Each PCR product contains 451bp sequences of flanking non-GAA repeat DNA within *FXN* intron 1. The blue star shows original YG9 parent (90 + 190 repeats) and the green star shows original YG22 parent (190 repeats). YAC 1(38) is initial source of both YG8 and YG22.

3.2 - Establishing genetically modified mice

To find out the role of each MMR gene in intergenerational instability of GAA repeat expansions, it was initially necessary to generate human *FXN* transgenic mice in absence or presence of each MMR protein. To achieve this, *Msh2*, *Msh3* and *Msh6* heterozygous

knockout mice were obtained from H. Te Riele (de Wind *et al.* 1995; de Wind *et al.* 1999), defective *Pms2* mice were obtained from D. Monckton and M. Liskay (Baker *et al.* 1995) and *Mlh1* heterozygous knockout mice, established by Kucherlapati and colleagues, were commercially available from the Jackson laboratory (Edelmann *et al.* 1996).

To generate different double genetically modified mice containing the *FXN* GAA repeat (FXN^{GAA}) transgene together with wild type, heterozygous or homozygous MMR knockout alleles, either YG8 or YG22 FXN^{GAA} hemizygous mice (Al-Mahdawi *et al.* 2004) were cross-bred with one of *Msh2*, *Msh3*, *Msh6*, *Pms2* or *Mlh1* heterozygous knockout mice. Data analysis showed that almost 25% of the first generation (F1) pups simultaneously carried one hemizygous YG8 or YG22 FXN^{GAA} transgene as well as one $MMR^{+/-}$ heterozygous allele. Later, interbreeding between $FXN^{GAA}/MMR^{+/-}$ (e.g. YG8-$FXN^{GAA}/Msh2^{+/-}$ double transgenic mouse) and relevant $MMR^{+/-}$ (e.g. $Msh2^{+/-}$) transgenic mice produced different modifications of transgenic mice for each YG8 and YG22 lines in the second generation (F2); approximately 12.5% $FXN^{GAA}/MMR^{+/+}$ or $FXN^{GAA}/MMR^{-/-}$ and 25% $FXN^{GAA}/MMR^{+/-}$. For the next step, each of the double genetically modified mice was bred, as either a male or a female parent, with non-transgenic mice to obtain the required offspring for subsequent analysis.

3.3 - Mouse genotyping

Following a small tail biopsy collection and genomic DNA isolation from the parent and offspring, two different PCRs were applied for genotyping of all pups in each generation: (i) MMR PCR in the relevant transgenic mouse model (e.g. *Msh2*-PCR was carried out at *Msh2*-transgenic mice) and (ii) GAA PCR. *Msh2* genotyping was performed by using a multiplex PCR system, called *Msh2*-PCR, to discriminate between WT and KO alleles based on the size differences. Compared with a $1Kb^{+}$ DNA size marker (Invitrogen Inc.), the

length of WT and KO fragments were recognised as 164bp and 194bp, respectively. Therefore, a homozygous *Msh2*-WT genotype was revealed by the presence of only a 164bp fragment, a homozygous *Msh2*-KO genotype by the presence of only a 194bp fragment, and a heterozygous *Msh2* genotype by the presence of both fragments. *Msh2* genotyping was performed for each mouse within different generations of *Msh2* double transgenic mouse model generation (Figure 3.2).

Figure 3.2 - *Msh2*-PCR product analysis.

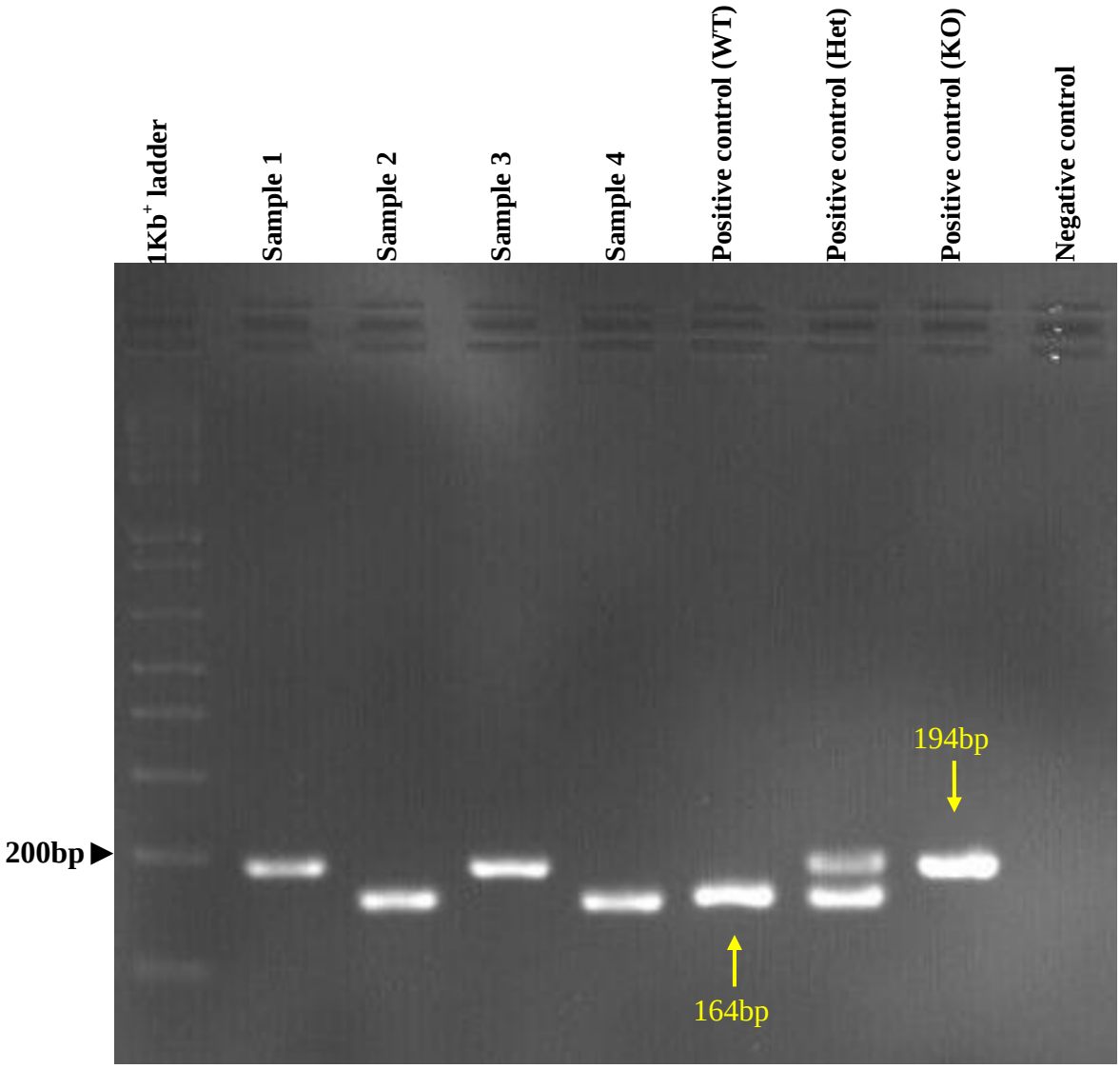

The image illustrates comparative standard PCR analysis of WT, Het and KO genotypes in *Msh2* transgenic mouse samples, in 2% ethidium bromide-stained agarose gel.

Msh3-PCR was also a multiplex PCR system, carried out to analyse the *Msh3* genotype in relevant transgenic mice (*Msh3* double transgenic mouse line). Each specific band was measured against a 1Kb^{+} DNA size marker, showing a single 130bp length of fragment in *Msh3*-WT and a single 250bp length of fragment in *Msh3*-KO mice, while *Msh3*-Het mice showed both 130bp and 250bp fragments (Figure 3.3).

Figure 3.3 - *Msh3*-PCR product analysis.

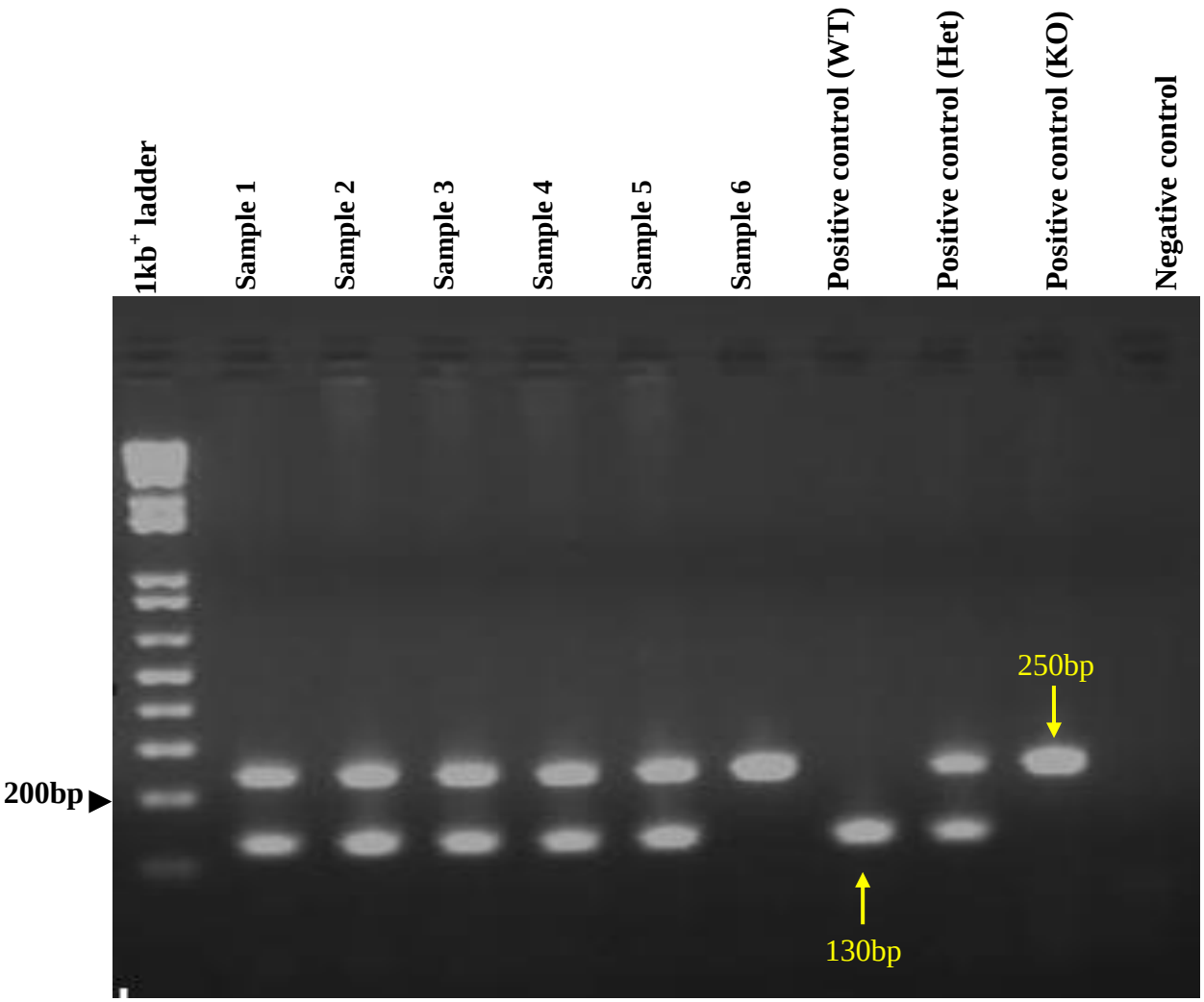

The image illustrates comparative standard PCR analysis of WT, Het and KO genotypes in *Msh3* transgenic mouse samples in 2% ethidium bromide-stained agarose gel.

By using a size marker against PCR products, in agarose gel electrophoresis, analysis of *Msh6* gene, by a system called *Msh6*-PCR, also showed two different fragments presenting

WT, KO or both alleles (Heterozygous; Het) in each *Msh6* double transgenic mouse. In this multiplex PCR analysis, the 220bp band represented WT fragment while KO fragment showed the length of 253bp (Figure 3.4).

Figure 3.4 - *Msh6*-PCR product analysis.

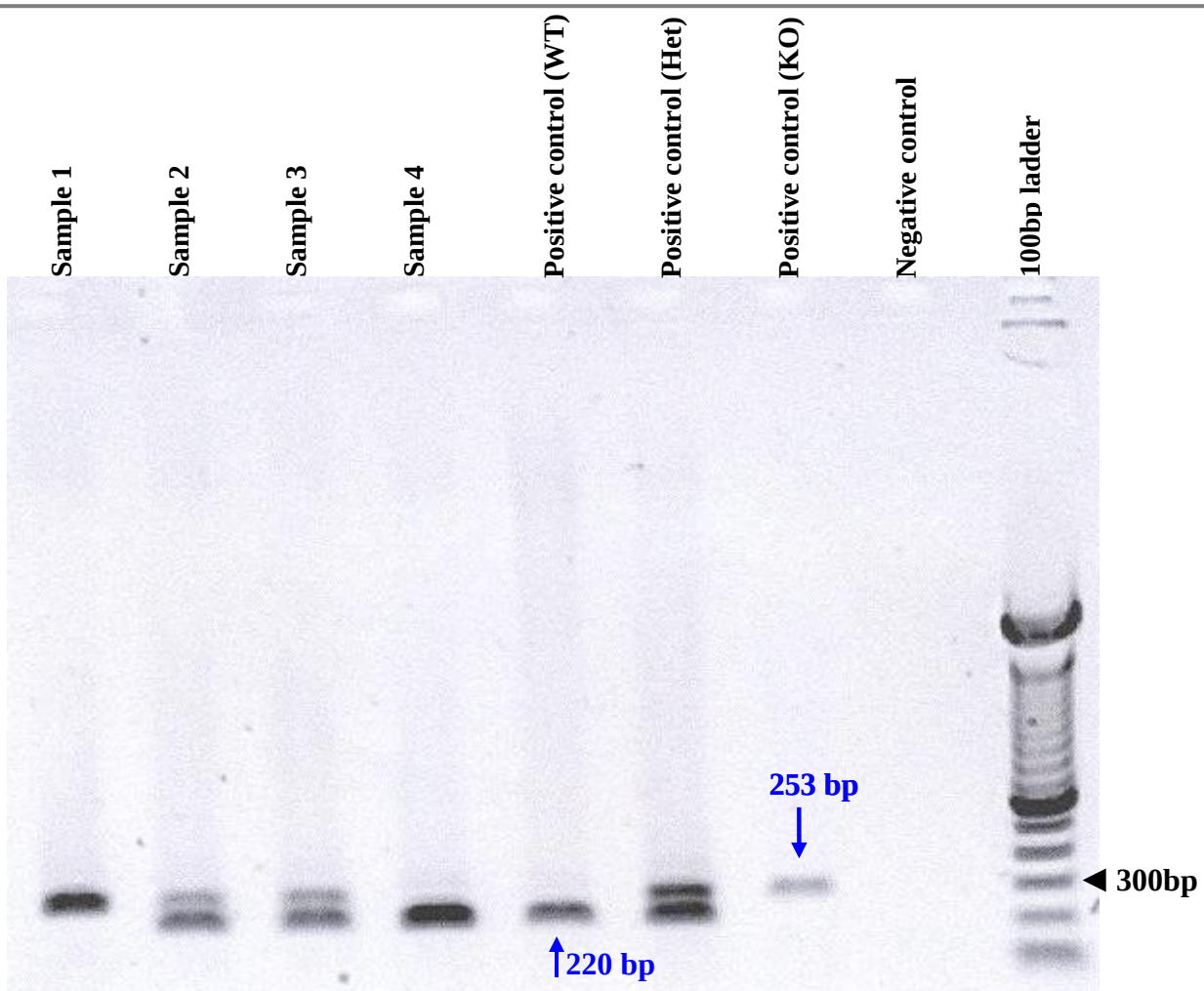

The image illustrates comparative standard PCR analysis of WT, Het and KO genotypes in *Msh6* transgenic mouse samples in 2% ethidium bromide-stained agarose gel.

Similar to the other mentioned MMR lines, another two multiplex PCRs were carried out for *Pms2* and *Mlh1* genes; *Pms2*-PCR and *Mlh1*-PCR. Results of analyses showed two distinct fragments in each PCR, each of which representing an allele. The 385bp and 350bp fragments represented the presence of WT allele in respectively *Pms2* and *Mlh1*, while the

189bp and 450bp fragments represented presence of the KO allele in respectively *Pms2* and *Mlh1* (Figure 3.5).

Figure 3.5 - PCR product analysis for *Pms2* and *Mlh1*.

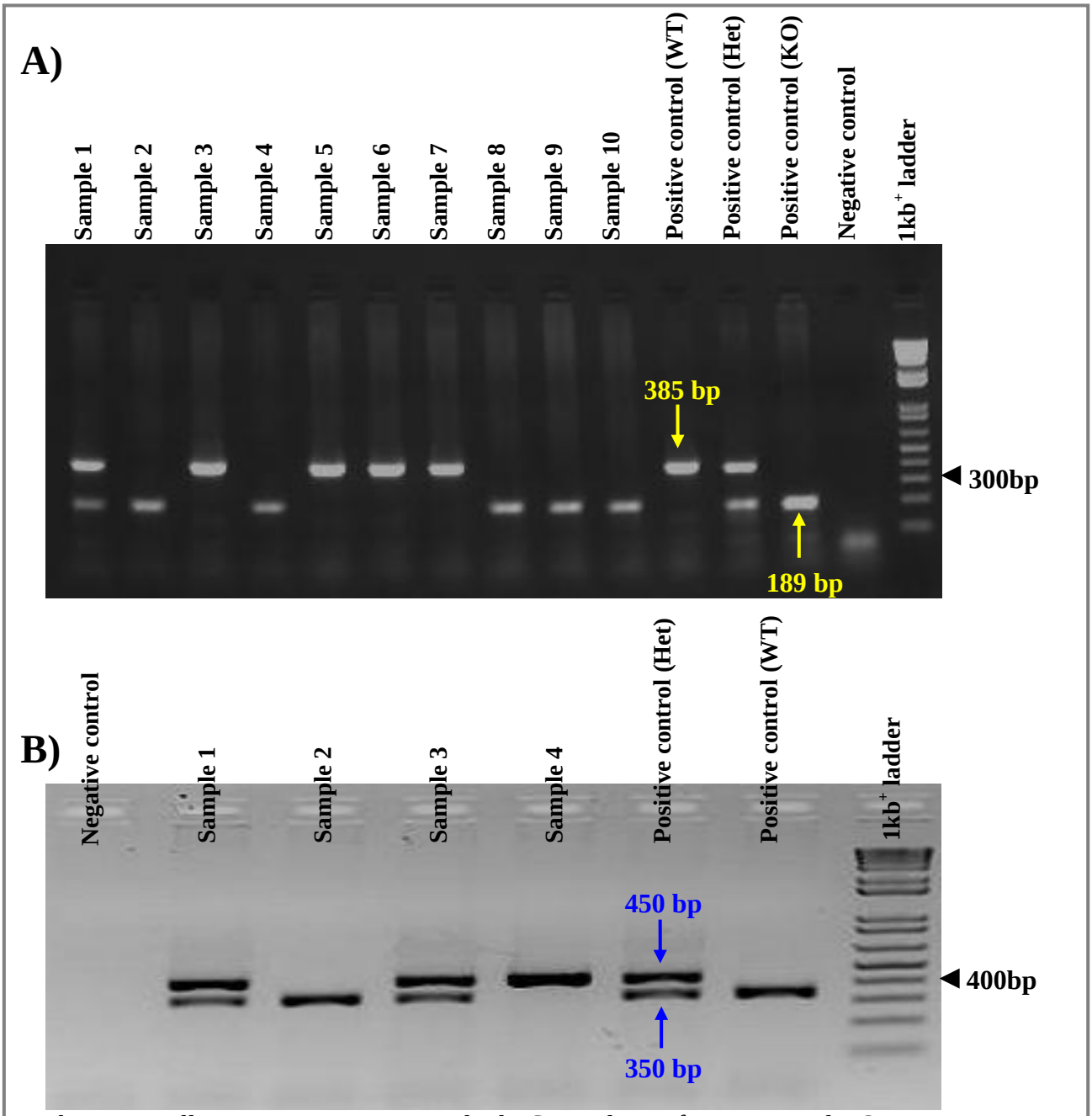

The images illustrate comparative standard PCR analysis of WT, Het and KO genotypes in **(A)** *Pms2* transgenic mouse samples, **(B)** *Mlh1* transgenic mouse samples in 2% ethidium bromide-stained agarose gel.

Further to MMR-PCR, standard GAA-PCR amplification was carried out for all different lines of transgenic mice. Initial analysis of the GAA-PCR products on small agarose gels demonstrated that some mice carried GAA repeats while the others did not carry the *FXN*^{GAA} transgene. Due to the location of the GAA primers, all GAA-PCR products contain 451bp of DNA flanking the GAA repeat region within intron 1, together with the number of GAA repeats (Figure 3.6). All PCRs were confirmed using positive and negative controls, indicating specificity of the fragments in absence of any contamination.

Figure 3.6 - GAA-PCR product analysis.

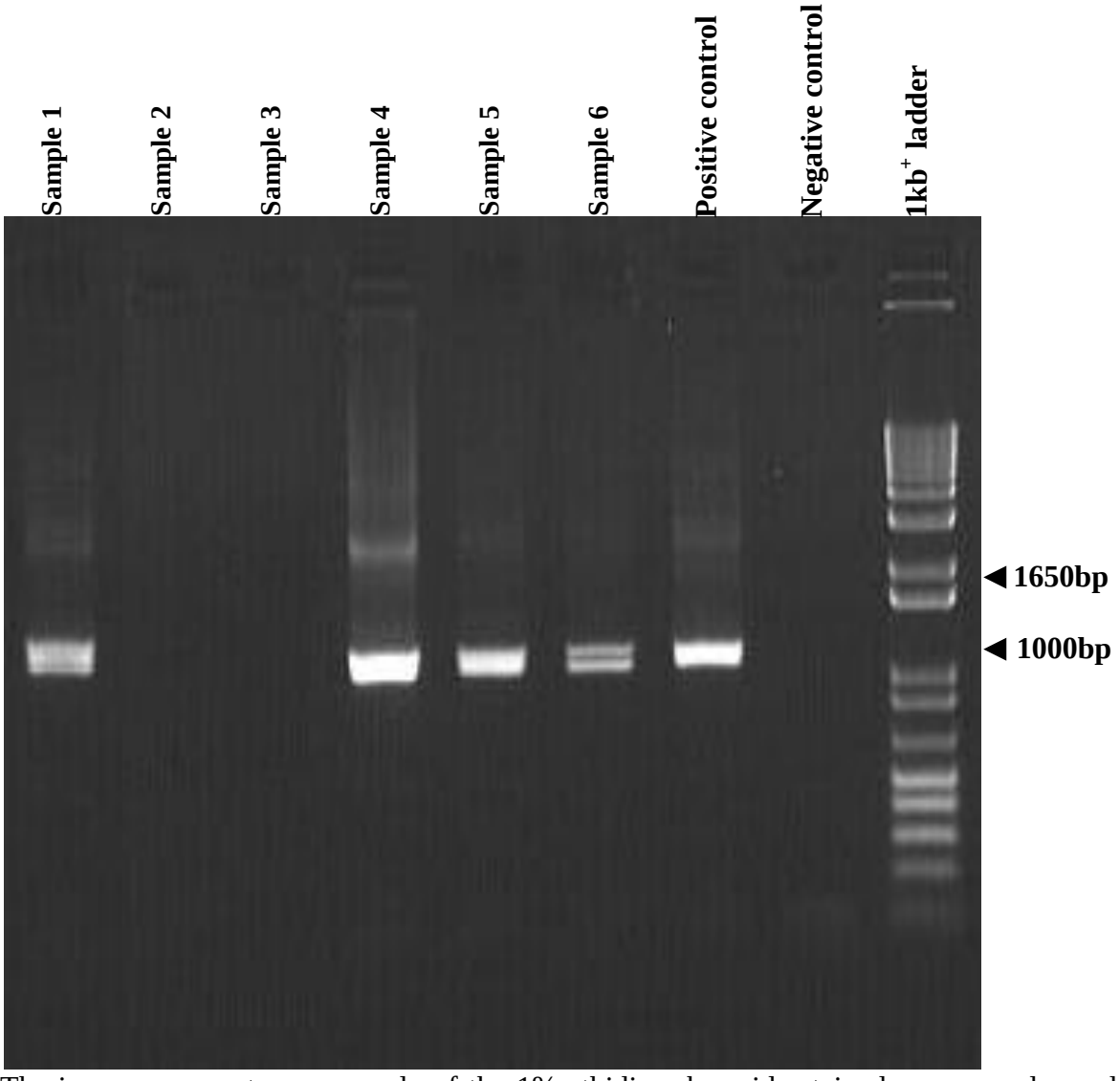

The image represents an example of the 1% ethidium bromide-stained agarose gels used to determine absence or presence of the *FXN* GAA repeat.

3.4 - Intergenerational GAA repeat instability analysis

The effect of each MMR protein on the GAA intergenerational repeat instability was analysed in all GAA^{+} offspring compared to those of FXN^{GAA+} transgenic mouse parent by analysing GAA PCR products obtained from tail genomic DNA at almost 1 month of age. These studies were carried out in both male and female parents of either YG8 or YG22 FXN^{GAA+} lines (except males in $Pms2^{-/-}$ and both males and females in $Mlh1^{-/-}$ which are sterile). In each case, three different parental genotypes were examined, including: $FXN^{GAA+}/MMR^{+/+}$, $FXN^{GAA+}/MMR^{+/-}$ and $FXN^{GAA+}/MMR^{-/-}$. The intergenerational transmitted GAA repeat size differences were classified into 3 different sub-classes for each subset: GAA repeat contractions, no-change and GAA repeat expansions.

3.4.1 - *Msh2* effects on transmission of GAA repeat instability

To determine the effect of *Msh2* on intergenerational transmission, GAA repeat sizes in parents and offspring were compared by long agarose gel electrophoresis (Figure 3.7).

Figure 3.7 - Representative example of intergenerational GAA repeat instability in the *Msh2* transgenic model.

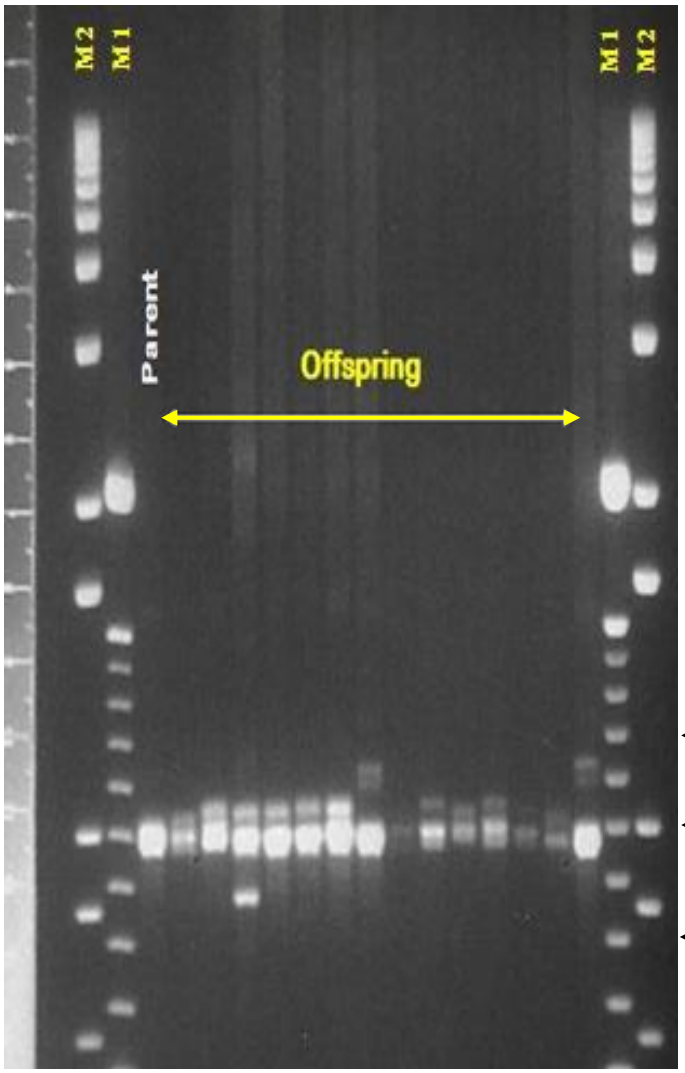

The image illustrates PCR products to determine GAA repeat sizes in a long agarose gel obtained from a YG22 GAA^{+}/*Msh2*$^{+/-}$ parent and 14 GAA^{+} offspring. M1= 100bp DNA size marker; M2= $1Kb^{+}$ DNA size marker.

The sizes of GAA repeat fragments were analysed based on: (i) parental *Msh2* genotypes: *Msh2* homozygous wild type (*Msh2*-WT), *Msh2* heterozygous (*Msh2*-Het) and *Msh2* homozygous knockout (*Msh2*-KO); (ii) *FXN*$^{GAA+}$ transgene status (YG8 or YG22), and (iii) parental gender (paternal or maternal). In this study, the GAA repeat sizes were compared from 4 YG8 parental genotypes against their 54 YG8 offspring as well as from 14 YG22 parental genotypes against their 107 YG22 offspring (Table 3.1).

Table 3.1 - *FXN*$^{GAA+}$/*Msh2* offspring numbers based on different characteristics.

MMR line	MMR genotype	*FXN* line	gender	No. of parents	No. of offspring
Msh2	**WT**	**YG8**	♂	0	0
			♀	2	26
		YG22	♂	2	15
			♀	2	16
	Het	**YG8**	♂	0	0
			♀	1	13
		YG22	♂	3	42
			♀	2	14
	KO	**YG8**	♂	0	0
			♀	1	15
		YG22	♂	3	14
			♀	2	6

Initial analysis of data showed a similar level of GAA repeat mutability (combined expansion and contraction frequencies) of 35-42% for each of YG8 or YG22 *FXN*$^{GAA+}$/*Msh2*$^{+/+}$ transmission profiles. This degree of instability was raised up to almost 60% for both of *FXN*$^{GAA+}$/*Msh2*$^{-/-}$ transmission profiles (Figure 3.8). Although it was determined that the GAA repeat mutation level was increased by absence of Msh2 protein, it was important to understand whether this increase was due to increased GAA expansions or increased GAA contractions. Analysis of the parental YG8 *FXN*$^{GAA+}$/*Msh2*$^{+/+}$ transmissions revealed a similar frequency of expansions and contractions. In contrast, the frequency of no changes in GAA repeat size was notably greater than both expansions and contractions; almost 65% of all GAA repeat sequences. Further investigations demonstrated that loss of both *Msh2* alleles resulted in significantly increased level of GAA contractions compared to expansions. Comparing GAA repeat sizes from *Msh2*$^{+/+}$ intergenerational transmission with *Msh2*$^{-/-}$ showed significantly elevated level of GAA repeat contractions and reduced level of no-changed GAA repeat size. The level of GAA expansions, in this analysis, is slightly

reduced from *Msh2*-WT towards *Msh2*-KO. These findings suggest that lack of Msh2 protein causes increased intergenerational GAA repeat mutability, with a significant bias towards contractions. However, this idea could not be expanded to the absence of *Msh2* in only one allele, due to low levels of expansion and contraction seen in $Msh2^{+/-}$ compared to both $Msh2^{+/+}$ and $Msh2^{-/-}$ (Figure 3.8A). In contrast to YG8 $FXN^{GAA+}/Msh2^{+/+}$, the frequency of GAA expansions was greater than contractions in YG22 $FXN^{GAA+}/Msh2^{+/+}$ offspring, while a similar level of no GAA repeat size change was observed (Figure 3.8).

Figure 3.8 - The effect of Msh2 on intergerational GAA repeat sizes based upon GAA repeat-containing *FXN* transgenic.

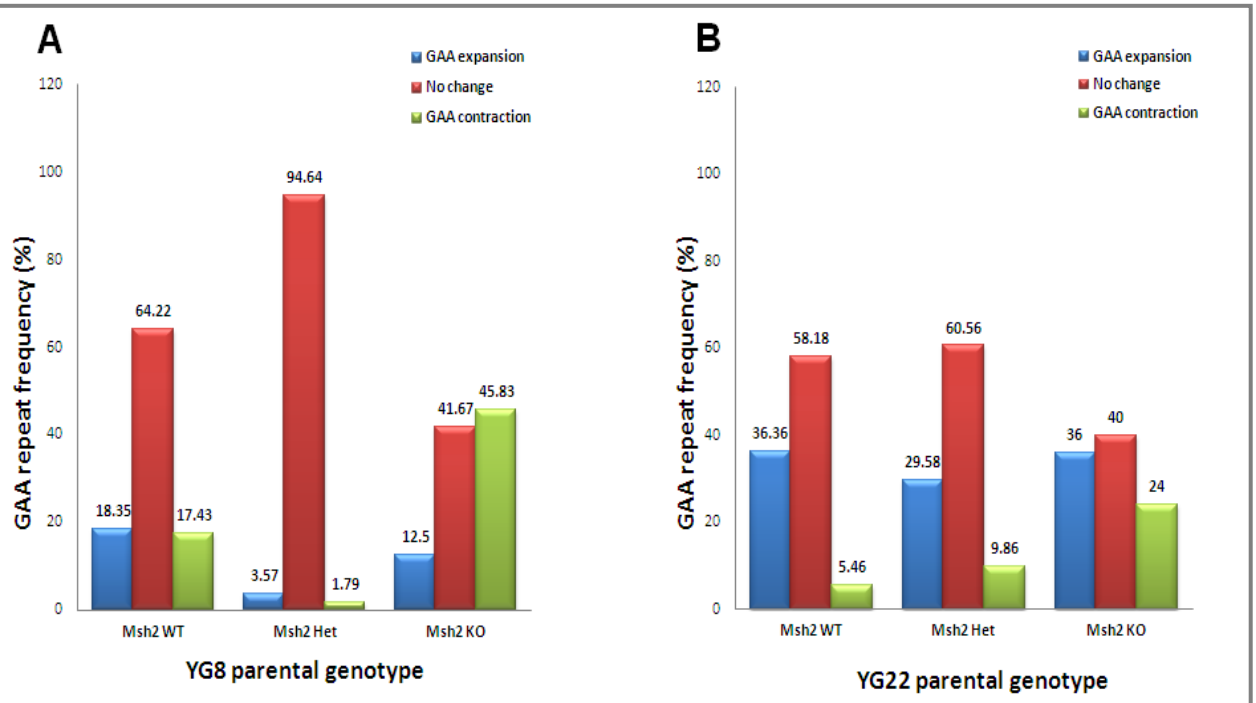

Frequencies of GAA expansions, no chages and GAA contractions transmitted to offspring are presented as percentages of total GAA repat transmission. **(A)** YG8 $GAA^{+}/Msh2$: WT n=109, Het n=56, KO n=48. **(B)** YG22 $GAA^{+}/Msh2$: WT n=55, Het n=142, KO n=50.

Despite observing greater frequency of expansions than contractions from YG22 $GAA^{+}/Msh2^{+/+}$ offspring, significantly increased level of contractions and decreased level of the no-changed GAA repeat size were observed from *Msh2*-KO offspring (Figure 3.8B). Interestingly, *Msh2*-Het showed a higher level of GAA repeat contractions compared to *Msh2*

homozygous WT and a lower level of GAA repeat contractions compared to *Msh2* homozygous KO, suggesting that by reducing the level of Msh2, the incidence of GAA contractions is gradually increased.

Data was then analysed on the basis of difference in parental gender. There were 71 offspring from 8 paternal FXN^{GAA+}/*Msh2* genotypes and 90 offspring from 10 maternal FXN^{GAA+}/*Msh2* genotypes (Table 3.1). Data analysis showed that 54-65% of GAA repeat sizes remained stable with no change and 35-46% of GAA repeat mutability was observed in each of paternal or maternal $FXN^{GAA+}/Msh2^{+/+}$ transmission profiles. The mutability levels were then increased to 56-61% for both paternal and maternal $FXN^{GAA+}/Msh2^{-/-}$ transmission profiles (Figure 3.9).

In paternal $Msh2^{+/+}$ offspring the frequency of intergenerational expansions was significantly greater than contractions. However, more than 50% of offspring did not show any GAA repeat size change (Figure 3.9A). In absence of both *Msh2* alleles, the level of no-changed GAA repeats and expansions were reduced, whilst the frequency of GAA repeat contractions was raised up to the same level of expansions: almost 28%. In comparison with $Msh2^{+/+}$, the range of contractions was notably increased from $Msh2^{-/-}$ mice transmission profiles, while the frequency of expansions was reduced. These results suggest that Msh2 disruption increases mutability level with a trend towards contractions. Further analyses showed that even absence of a single *Msh2* allele slightly increased the level of GAA contractions, implying that progressive reduction of the *Msh2* expression level causes a gradually increased level of GAA repeat contractions.

Maternal $Msh2^{+/+}$ offspring showed less GAA repeat expansion frequency than paternal $Msh2^{+/+}$ offspring. However, this was still greater than frequency of GAA repeat contraction in maternal transmission profiles. Analysing maternal $Msh2^{-/-}$ GAA repeat transmissions showed that the level of contractions was remarkably increased, while the frequency of

no-changed GAA repeat size was remarkably reduced. However, the level of GAA repeat expansions remained almost stable in contrast to maternal *Msh2*$^{+/+}$, indicating that loss of Msh2 protein leads to an increased frequency of transmitting GAA repeat contractions to offspring (Figure 3.9B).

Figure 3.9 - The effect of *Msh2* on intergerational GAA repeat sizes based upon perental genotypes.

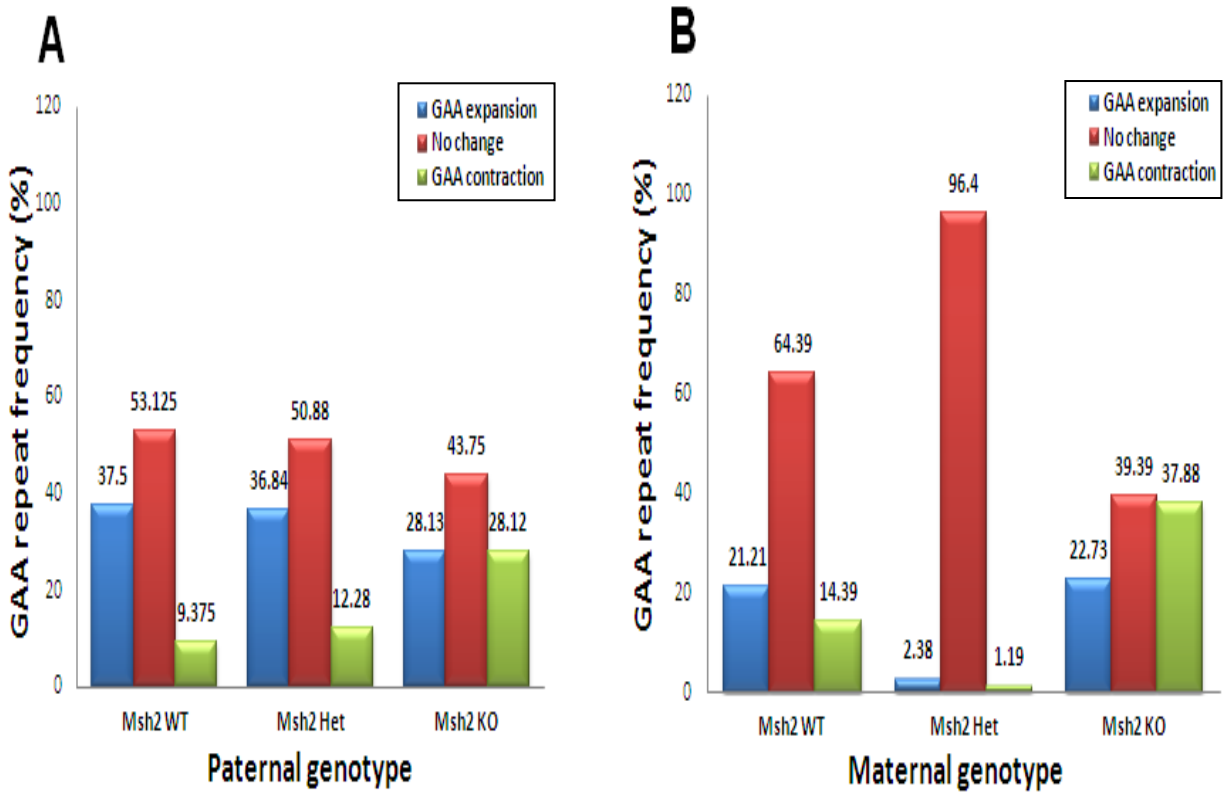

Frequencies of GAA expansions, no chages and GAA contractions transmitted to offspring are presented as percentages of total GAA repat transmission. **(A)** Paternal GAA^{+}/Msh2: WT n=32, Het n=114, KO n=32. **(B)** Maternal GAA^{+}/Msh2: WT n=132, Het n=84, KO n=66.

Ultimately, the combined results of GAA repeat transmission were analysed from 18 *FXN*$^{GAA+}$ parents and 161 offspring based only on *Msh2* genotypes (Table 3.1). Taken together, analysis of the data based only on *Msh2* genotypes showed 38% mutability GAA repeats transmitted from *Msh2* homozygous WT mice, while this level significantly increased to 59% for *Msh2* homozygous KO mice (Figure 3.10, Table 3.2). These findings reveal that

fully disruption of Msh2 causes increased frequency of intergenerational GAA repeat mutability, although a notable frequency of the GAA repeat transmissions remained stable. To further understand the cause of increased mutability with depletion of Msh2, the frequency of each expansion, contraction and no-changed level was analysed in different *Msh2* genotypes. Comparing *Msh2*$^{+/+}$ with *Msh2*$^{-/-}$ GAA repeat sizes showed that the level of expansions remained stable, while GAA repeat contraction frequency was significantly increased in *Msh2*$^{-/-}$ (Figure 3.10, Table 3.2). Moreover, the mean GAA repeat size variations for *Msh2*$^{-/-}$ showed a bias towards contractions, compared with both the *Msh2*$^{+/+}$ and *Msh2*$^{+/-}$ (Table 3.3). Thus, it is proposed that *Msh2* is not the principal cause of intergenerational GAA mutability (both expansions and contractions), but it is involved to some extent in mismatch repair process to protect the expanded GAA repeat from any more instability.

Figure 3.10 - The effect of Msh2 on the intergerational GAA repeat sizes.

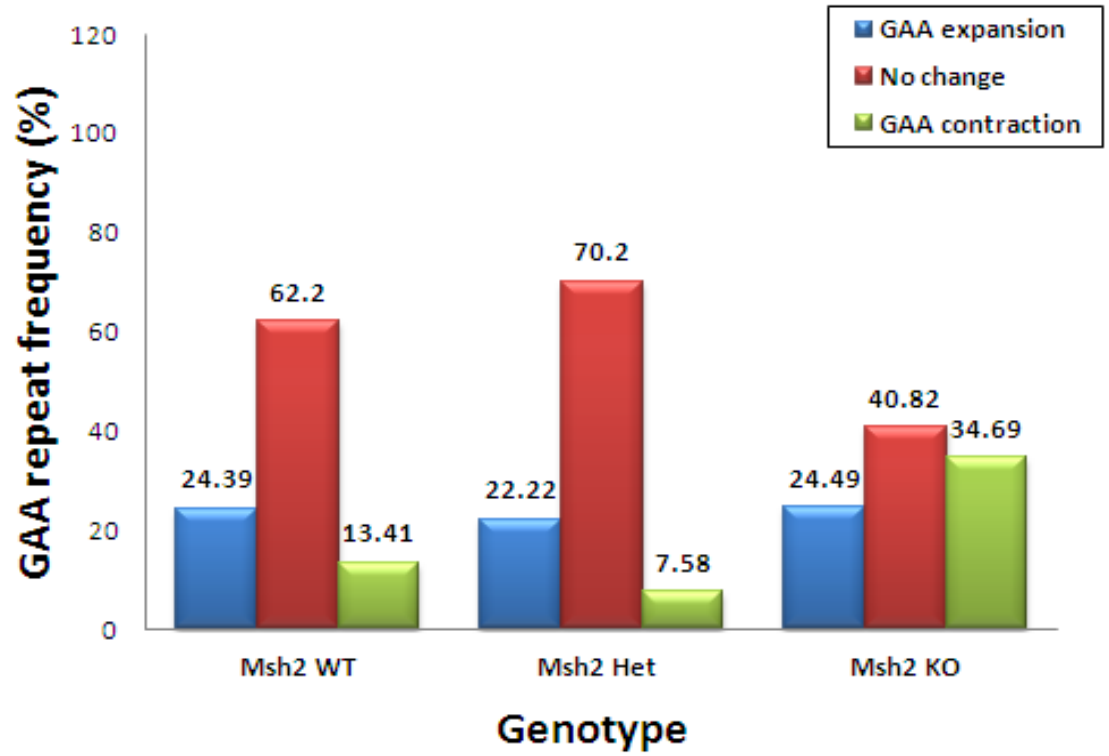

Frequencies of GAA expansions, no chages and GAA contractions transmitted to offspring are presented as percentages of total GAA repat transmission: WT n=164, Het n=198, KO n=98.

Table 3.2 - χ^2 analysis of GAA repeat transmissions in *Msh2* transgenic mice.

Msh2 parental genotype 1	*Msh2* parental genotype 2	χ^2 value	df	*P* value
Msh2$^{+/+}$	***Msh2***$^{+/-}$	4.04	2	0.132
Msh2$^{+/+}$	***Msh2***$^{-/-}$	18.17	2	<0.001
Msh2$^{+/-}$	***Msh2***$^{-/-}$	38.63	2	<0.001

Table 3.3 - Mean transmitted GAA repeat size variations in *Msh2* transgenic mice.

Parent genotype	Mean GAA repeat size increase of expansions	Mean GAA repeat size increase of contractions	Mean GAA repeat size variation of all transmissions
Msh2$^{+/+}$	+ 2.6	-3.3	+ 0.19
Msh2$^{+/-}$	+ 2.6	-17.9	+ 0.42
Msh2$^{-/-}$	+ 2.6	-9.1	-2.54

3.4.2 - *Msh3* effects on transmission of GAA repeat instability

To find out the effect of Msh3 protein on intergenerational transmissions, GAA repeat sizes were initially analysed in agarose gel electrophoresis by comparing *FXN*$^{GAA+}$ offspring with those of the parents (Figure 3.11).

Figure 3.11 - Representative example of intergenerational GAA repeat instability in *Msh3* transgenic model.

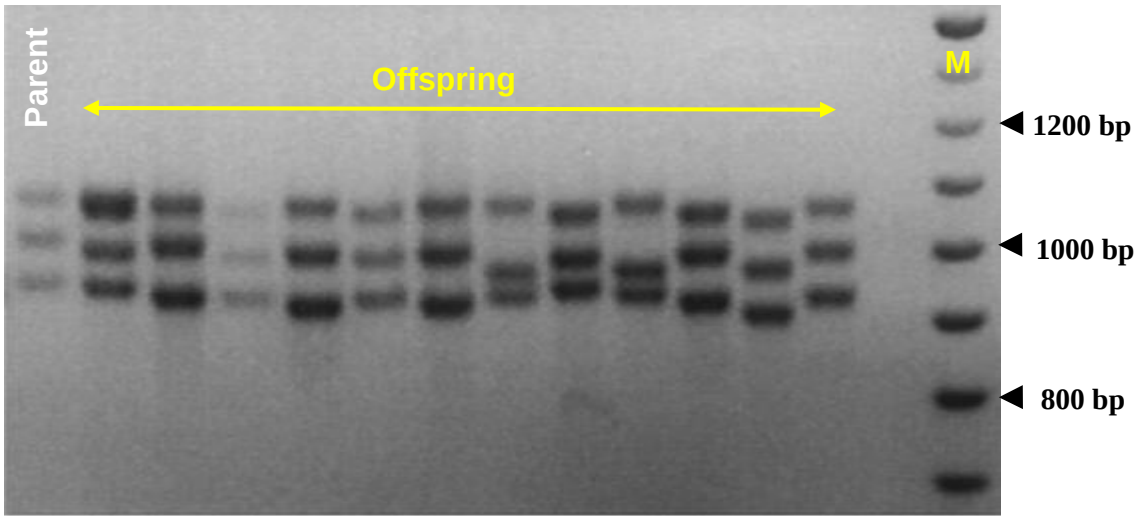

The image illustrates PCR products to determine GAA repeat sizes in a long agarose gel obtained from a YG22 GAA^{+}/*Msh3*$^{-/-}$ parent and 12 GAA^{+} offspring. M= 100bp DNA size marker.

To distinguish any GAA repeat size difference between parent and offspring, based on two different GAA repeat expansion-containing *FXN* transgenes with different *Msh3* genotypes, data from 5 YG8 parents against 43 YG8 offspring and from 15 YG22 parents compared with 129 YG22 offspring were analysed separately (Table 3.4).

Table 3.4 - *FXN*$^{GAA+}$/*Msh3* offspring numbers based on different characteristics.

MMR line	MMR genotype	*FXN* line	gender	No. of parents	No. of offspring
Msh3	WT	YG8	♂	1	5
			♀	1	12
		YG22	♂	1	8
			♀	2	23
	Het	YG8	♂	1	11
			♀	0	0
		YG22	♂	3	21
			♀	2	16
	KO	YG8	♂	1	4
			♀	1	11
		YG22	♂	4	44
			♀	3	17

Initial analysis based on different transgene type showed that more than 60% of each YG8 or YG22 *FXN*$^{GAA+}$/*Msh3*$^{+/+}$ GAA repeat size transmissions remained with no GAA size change. However, this level significantly decreased in both of YG8 and YG22 *FXN*$^{GAA+}$/*Msh3*$^{-/-}$ transmission profiles to less than 30% (Figure 3.12). In parallel the range of mutability level was raised to more than 70% in GAA repeat transmitted from *Msh3*$^{-/-}$ offspring mice, suggesting that presence of Msh3 protein is necessary to protect GAA repeat size against mutability (Figure 3.12).

Figure 3.12 - The effect of *Msh3* on intergerational GAA repeat sizes based upon GAA repeat-containing *FXN* transgenic.

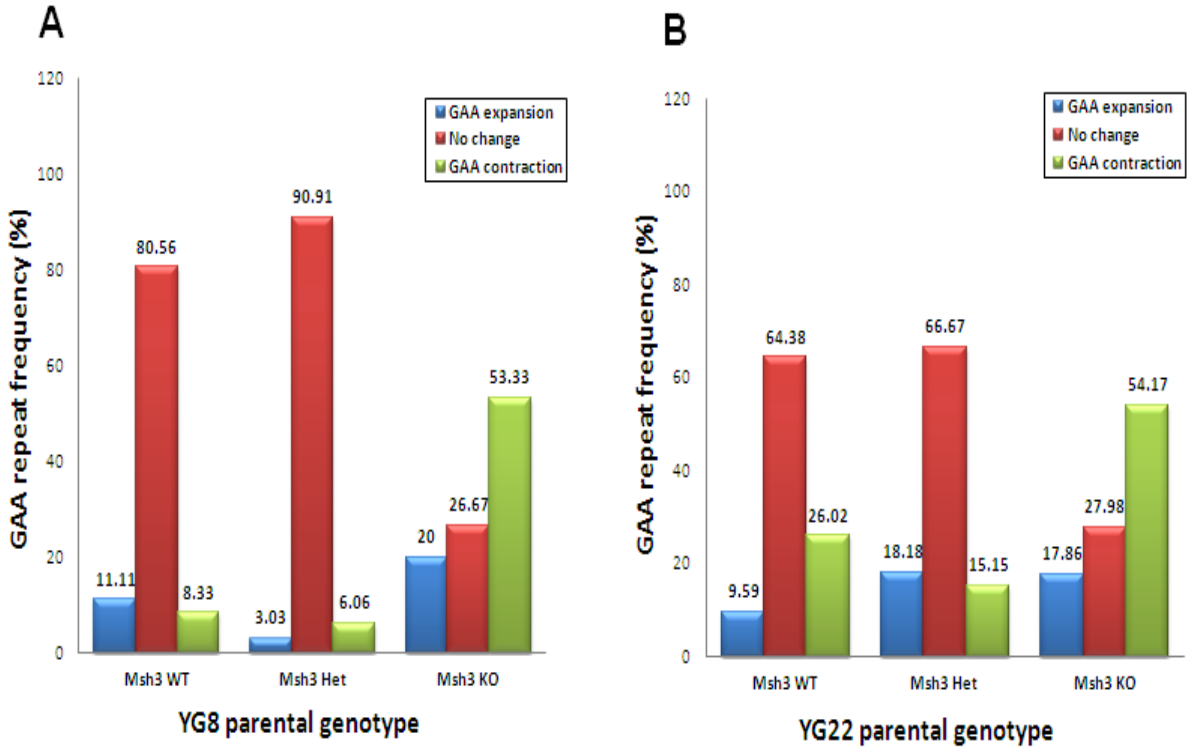

Frequencies of GAA expansions, no chages and GAA contractions transmitted to offspring are presented as percentages of total GAA repat transmission. **(A)** YG8 GAA^{+}/Msh3: WT n=36, Het n=33, KO n=15. **(B)** YG22 GAA^{+}/Msh3: WT n=73, Het n=99, KO n=168.

Analysis of the parental YG8 GAA^{+}/*Msh3*$^{+/+}$ transmissions showed a similar 8-12% frequency of expansions and contractions, while more than 80% of GAA repeat sizes did not

change. A similar profile was observed in *Msh3* heterozygous transgenic mouse offspring GAA repeat sizes. In contrast, YG8 GAA^{+}/*Msh3*$^{-/-}$ analysis showed a sharply increased level of GAA repeat contractions and a reduced level of no-changed GAA repeat size from 80% to 27% (Figure 3.12A). These observations reveal that absence of *Msh3* in YG8 transgenic remarkably increases the GAA repeat instability errors towards contractions.

In the case of YG22 GAA^{+}/*Msh3*$^{+/+}$, the frequency of expansions was almost 3 times more than contractions. However, similar to YG8, the combined level of expansions and contractions was still much less than the no-change GAA repeat size group (Figure 3.12). Compared with YG22 GAA^{+}/*Msh3*$^{+/+}$, *Msh3*$^{+/-}$ transmission did not show any prominent difference in the level of no-change GAA repeat size, while this level was dramatically decreased in YG22 GAA^{+}/*Msh3*$^{-/-}$. Further analysis for *Msh3*$^{-/-}$ transmissions showed a significant trend of mutations towards an increased level of GAA repeat contractions (more than 50%; Figure 3.12), suggesting that fully absence of *Msh3* induces contractions of GAA repeat size. However, even the presence of one *Msh3* allele might be enough to preserve the majority of the YG22 GAA repeat stability.

Further analysis was carried out based on different parental genders, comprising 79 offspring from 11 paternal GAA^{+} genotypes and 129 offspring from 9 maternal GAA^{+} genotypes (Table 3.4). Data analysis showed that the range of mutability in each paternal or maternal *FXN*^{GAA}/*Msh3*$^{+/+}$ transmission profile was less than 50%. The level of mutability then showed a dramatic increase for both *Msh2*$^{-/-}$ parental genders, compared with both wild type and heterozygous states (Figure 3.13). Analysing paternal *Msh3*$^{+/+}$ GAA repeat sizes revealed similar levels of contractions and expansions, with twice as many stable GAA repeat transmissions (Figure 3.13A). In contrast, paternal *Msh3*$^{-/-}$ transmission profiles showed a remarkable increased frequency of contractions, while the level of unchanged GAA repeat sizes significantly decreased and the frequency of GAA expansions remained similar

to *Msh3*$^{+/+}$ (Figure 3.13A). These findings suggest that the absence of Msh3 protein notably increases the intergenerational transmission of GAA repeat contractions. High levels of GAA repeat stability were observed from Msh3$^{+/-}$ transmitting mice, indicating that even the presence of one *Msh3* allele could be sufficient to protect GAA repeat against instability. In other words, even expression from a single allele is sufficient to produce adequate functional Msh3 protein to protect against increased levels of GAA repeat mutability.

Figure 3.13 - The effect of *Msh3* on intergerational GAA repeat sizes based upon perental genotypes.

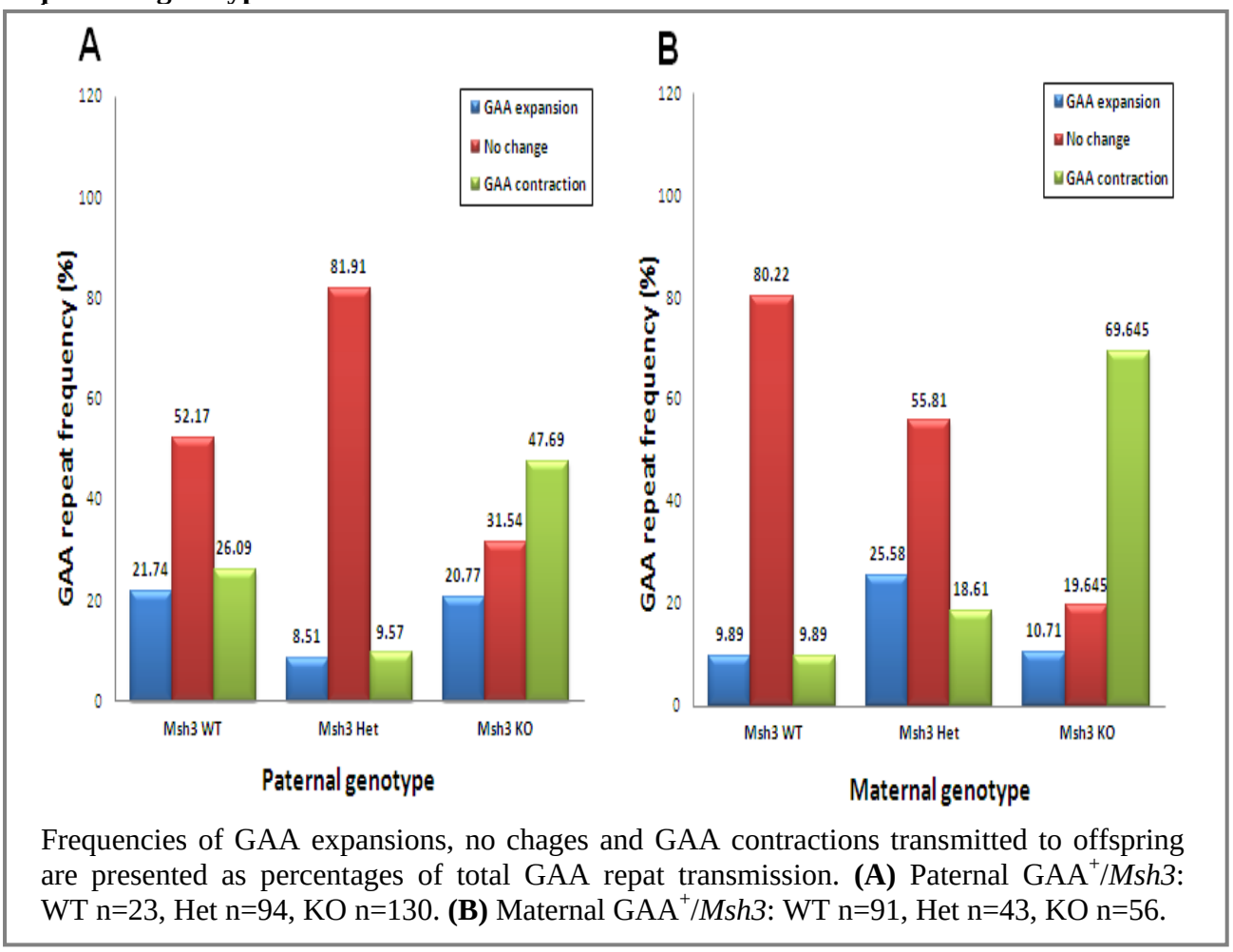

Frequencies of GAA expansions, no chages and GAA contractions transmitted to offspring are presented as percentages of total GAA repat transmission. **(A)** Paternal GAA^{+}/*Msh3*: WT n=23, Het n=94, KO n=130. **(B)** Maternal GAA^{+}/*Msh3*: WT n=91, Het n=43, KO n=56.

Maternal *Msh3*$^{+/+}$ transmission profiles showed that 80% of GAA repeat sizes did not change and the low levels of contractions and expansions were similar. Heterozygous transmission

profiles demonstrated that the frequency of both GAA expansions and contractions were increased with a slight bias towards GAA repeat expansions. In contrast, loss of both *Msh3* alleles led to a dramatically increased level of contractions (Figure 3.13B). These findings suggest that absence of Msh3 protein leads to increase GAA repeat mutability with a notable bias towards greater frequency of GAA repeat contractions.

Overall, analysis based only upon *Msh3* genotype demonstrated that there is no difference between $Msh3^{+/+}$ and $Msh3^{+/-}$ transmission profiles. The level of mutability in both of these profile offspring was almost 25% with similar level of expansions and contractions, while the level of no-changed GAA repeat size was approximately 3 fold higher (Figure 3.14, Table 3.5).

Figure 3.14 - The effect of *Msh3* on the intergerational GAA repeat sizes.

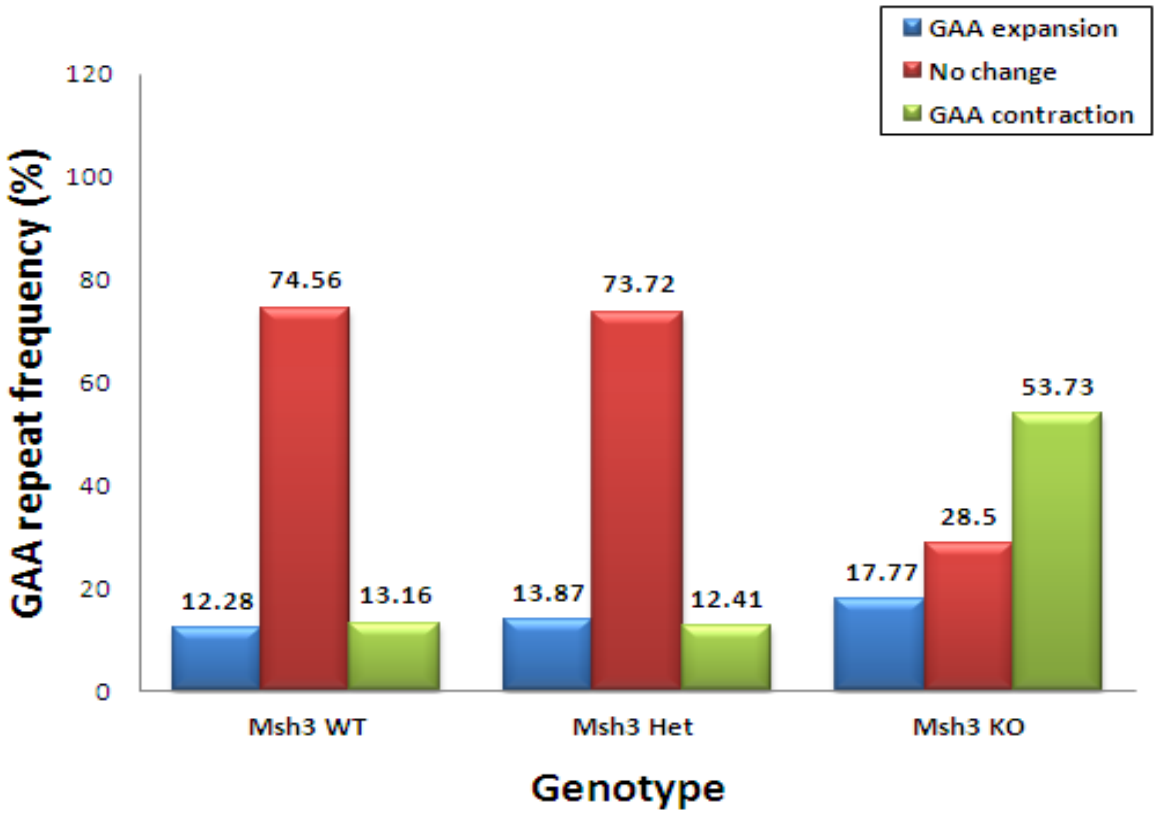

Frequencies of GAA expansions, no chages and GAA contractions transmitted to offspring are presented as percentages of total GAA repat transmission: WT n=114, Het n=137, KO n=186.

Table 3.5 - χ^2 analysis of GAA repeat transmissions in *Msh3* transgenic mice.

***Msh3* parental genotype 1**	***Msh3* parental genotype 2**	**χ^2 value**	**df**	***P* value**
***Msh3*$^{+/+}$**	***Msh3*$^{+/-}$**	0.39	2	0.822
***Msh3*$^{+/+}$**	***Msh3*$^{-/-}$**	64.4	2	<0.001
***Msh3*$^{+/-}$**	***Msh3*$^{-/-}$**	67.5	2	<0.001

In contrast, absence of both *Msh3* alleles caused a significantly increased level of GAA repeat mutability, with a bias towards contractions (54%) rather than expansions (18%) expansions (Figure 3.14, Table 3.5). Furthermore, the mean GAA repeat size variations for *Msh3*$^{-/-}$ showed a bias towards greater contraction size compared with both the *Msh3*$^{+/+}$ and *Msh3*$^{+/-}$ (Table 3.6). These findings indicate that when *Msh3* is fully disrupted, the GAA repeat mutability level is increased with a notable trend towards contractions, while presence of a single *Msh3* allele can produce sufficient Msh3 protein to preserve GAA repeat stability. Since GAA instability persists in the absence of *Msh3*, it can be concluded that Msh3 protein is not the cause of intergenerational GAA repeat instability, but is involved in MMR processes to protect against intergenerational GAA repeat instability.

Table 3.6 - Mean transmitted GAA repeat size variations in *Msh3* transgenic mice.

Parent genotype	**Mean GAA repeat size increase of expansions**	**Mean GAA repeat size increase of contractions**	**Mean GAA repeat size variation of all transmissions**
***Msh3*$^{+/+}$**	+2.2	-3.5	-0.19
***Msh3*$^{+/-}$**	+2.7	-2.9	+0.03
***Msh3*$^{-/-}$**	+3.7	-4.7	-1.88

3.4.3 - *Msh6* effects on transmission of GAA repeat instability

To investigate the effect of Msh6 protein on intergenerational transmission of GAA repeat instability, the GAA PCR products obtained from offspring were initially compared with those of the parent by long agarose gel electrophoresis (Figure 3.15).

Figure 3.15 - Representative example of intergenerational GAA repeat instability in *Msh6* transgenic model.

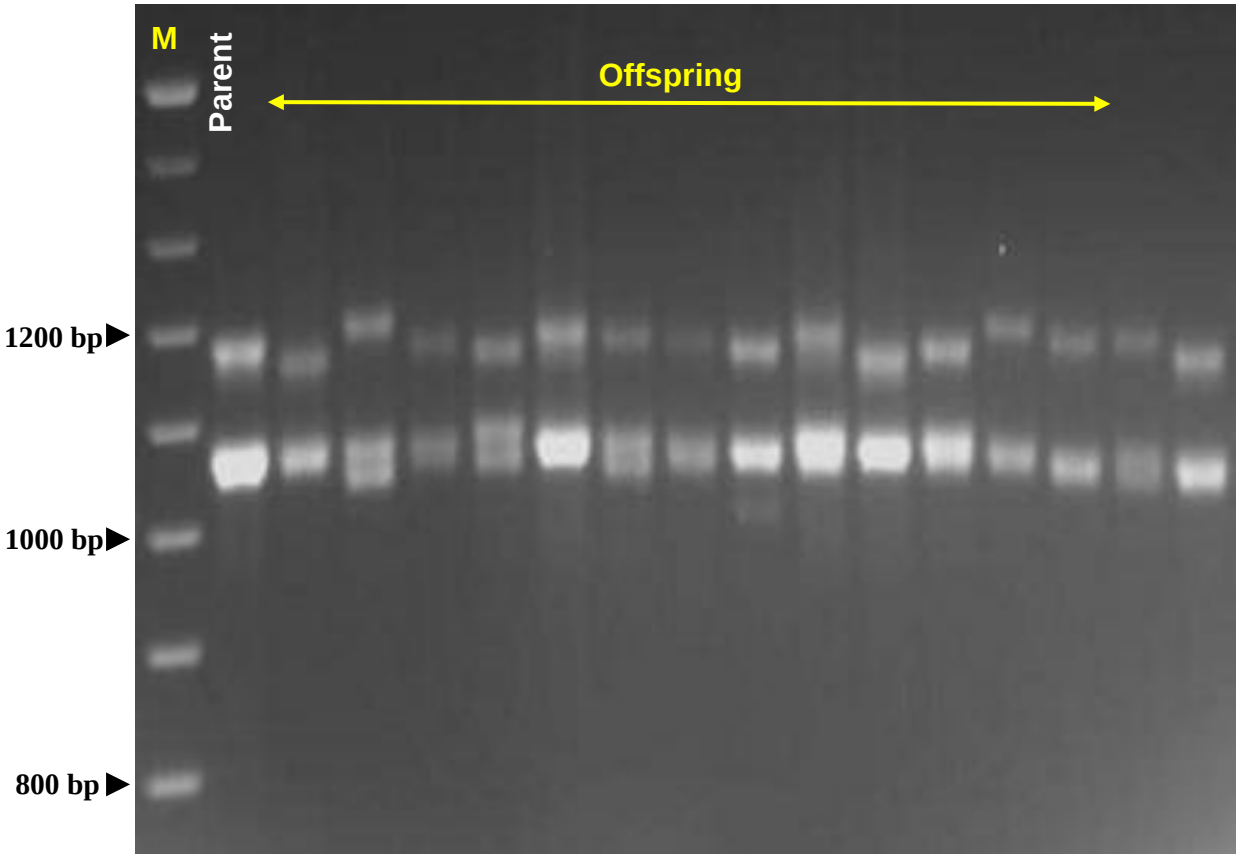

The image illustrates PCR products to determine GAA repeat sizes in a long agarose gel obtained from a YG22 GAA^{+}/$Msh6^{+/-}$ parent and 15 GAA^{+} offspring. M= 100bp DNA size marker.

To determine intergenerational GAA repeat size differences between parent and offspring based upon *Msh6* genotypes, 39 YG8 offspring were compared with 3 YG8 parents and 137 YG22 offspring were compared with 13 YG22 parents (Table 3.7).

Table 3.7 - *FXN*$^{GAA+}$/*Msh6* offspring numbers based on different characteristics.

MMR line	MMR genotype	*FXN* line	gender	No. of parents	No. of offspring
Msh6	WT	YG8	♂	1	9
			♀	0	0
		YG22	♂	1	17
			♀	1	7
	Het	YG8	♂	1	15
			♀	0	0
		YG22	♂	5	55
			♀	2	14
	KO	YG8	♂	0	0
			♀	1	15
		YG22	♂	3	29
			♀	1	15

Similar to *Msh3*, data analysis of the parental YG8 GAA^{+}/*Msh6*$^{+/+}$ transgenic mice transmission showed that more than 80% of GAA repeat sizes did not change (Figure 3.16A). In contrast, analyses of YG8 GAA^{+}/*Msh6*$^{-/-}$ transmission profiles showed that the frequency of no-changed GAA repeat size was reduced to almost half fold (about 44% of no-changed GAA repeat size), indicating a sharply increased level of GAA repeat mutability. The levels of transmitted contractions for *Msh6*-KO were similar to those of *Msh6*-WT and *Msh6*-Het, whilst the level of expansions was dramatically raised to 47%: almost 4 times more than *Msh6*-WT and *Msh6*-Het (Figure 3.16A). These findings suggest that a single *Msh6* allele could be sufficient to the produce sufficient functional Msh6 protein to protect an expanded GAA repeat against further instability. In contrast, complete absence of Msh6 protein dramatically increases the frequency of YG8 GAA repeat instabilities towards expansions.

Figure 3.16 - The effect of *Msh6* on intergerational GAA repeat sizes based upon GAA repeat-containing *FXN* transgenic.

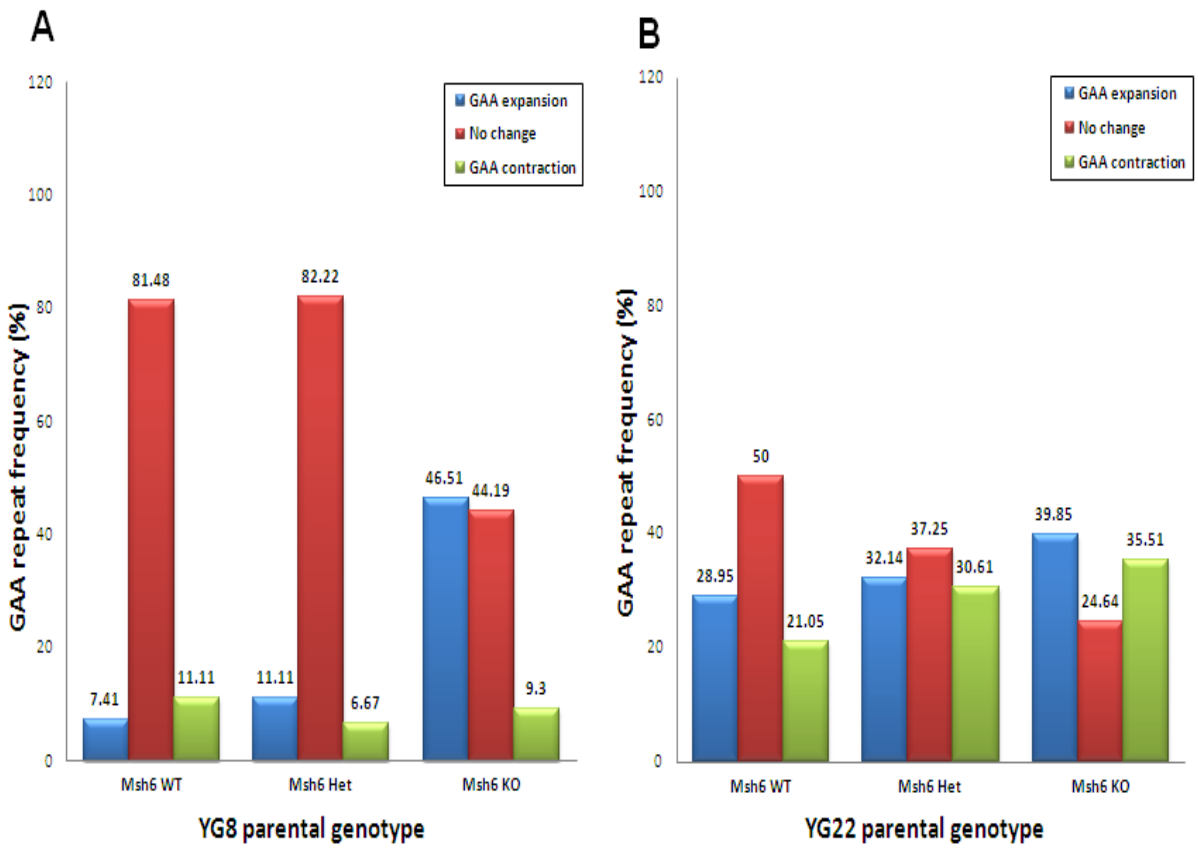

Frequencies of GAA expansions, no chages and GAA contractions transmitted to offspring are presented as percentages of total GAA repat transmission. **(A)** YG8 GAA^{+}/*Msh6*: WT n=27, Het n=45, KO n=43. **(B)** YG22 GAA^{+}/Msh6: WT n=38, Het n=196, KO n=138.

Compared to YG8, the level of mutability was significantly greater in YG22 GAA^{+}/*Msh6*$^{+/+}$. However, the frequency of both expansions and contractions were still remarkably lower than no-changed GAA repeat size. Loss of one *Msh6* allele produced a trend towards a reduced level of no-changed GAA repeat sizes and increased mutability, with equal levels of expansions and contractions. Similar to YG8, loss of both *Msh6* alleles in YG22 transmission profiles showed increased mutability level with a greater bias towards expansions (Figure 3.16B). Although loss of one Msh6 allele showed remarkable difference between YG8 and YG22 mutability, absence of Msh6 consistently increased the size of expanded GAA repeat in both YG8 and YG22.

Further analysis was carried out based on different parental genders, comprising 125 offspring from 11 paternal GAA^+ genotypes and 51 offspring from 5 maternal GAA^+ genotypes (Table 3.7). Analysing paternal *Msh6*$^{+/+}$ transmission of GAA repeats showed that the level of GAA repeat expansions is slightly higher than contractions, while the range of mutability overall was dramatically less than no-changed GAA repeat size (Figure 3.17A). Loss of only one *Msh6* allele resulted in a promoted level of GAA repeat mutability. This trend was towards an increased frequency of GAA repeat expansions, however a slight increase was also observed in contraction frequencies. Loss of both Msh6 alleles resulted in even greater increases of mutability, with a notable bias towards GAA repeat expansions.

Figure 3.17 - The effect of *Msh6* on intergerational GAA repeat sizes based upon parental genotypes.

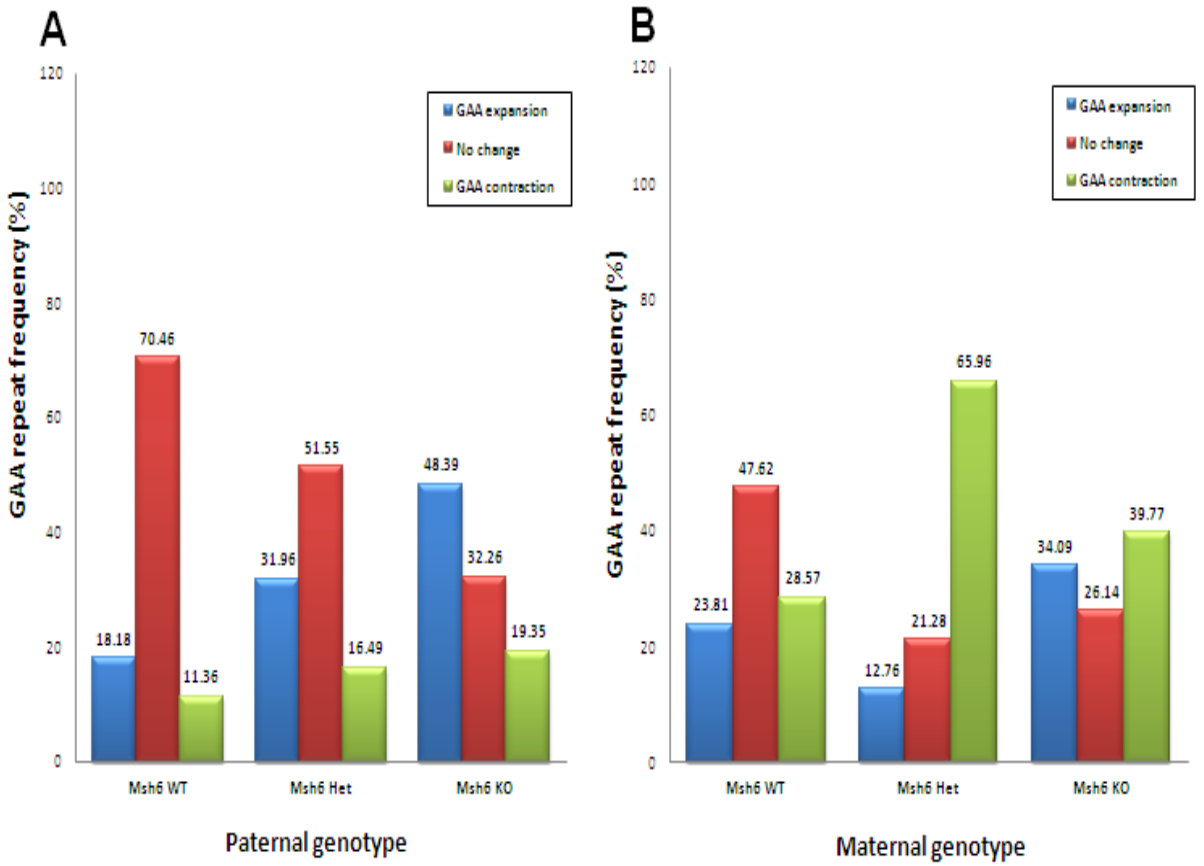

Frequencies of GAA expansions, no chages and GAA contractions transmitted to offspring are presented as percentages of total GAA repat transmission. **(A)** Paternal GAA^+/*Msh6*: WT n=44, Het n=194, KO n=93. **(B)** Maternal GAA^+/*Msh6*: WT n=21, Het n=47, KO n=88.

Analysing the maternal *Msh6*$^{+/+}$ transmission profiles demonstrated that most GAA repeats were stable, but a greater level of mutability was observed in these offspring compared with paternal *Msh6*$^{+/+}$. Analysis of maternal *Msh6*$^{-/-}$ transmission profiles showed that the frequency of both contractions and expansions were increased. Interestingly, paternal and maternal *Msh6*$^{-/-}$ transmission mutability levels showed contrasting results. Thus, paternal *Msh6* deficiency produced an increased frequency of GAA repeat expansions, while maternal *Msh6* deficiency produced increases of both GAA repeat expansions and contractions with a slight bias towards contractions (Figure 3.17B). Although the overall level of mutability was increased in both paternal and maternal GAA repeat transmissions, these results suggest that the trend of GAA repeat mutability frequencies differ towards either contractions or expansions based on the parental gender.

Finally, intergenerational GAA repeat size transmissions were analysed from 16 parents and 176 offspring based only upon *Msh6* genotypes (Table 3.7). This revealed 37% GAA repeat mutability of *Msh6*-WT (*FXN*$^{GAA+}$/*Msh6*$^{+/+}$) transmission profiles, comprising 20% expansions and 17% contractions (Figure 3.18, Table 3.8). In contrast to *Msh2* and *Msh3*, the level of GAA repeat stability was then significantly reduced with loss of only one *Msh6* allele. Mutability frequencies were increased to 54%, with a similar level of expansions and contractions. Loss of both *Msh6* alleles caused further increases in GAA repeat instability. Compared with *Msh6*$^{+/-}$, the level of expansions showed notable increase from *Msh6*$^{-/-}$, while contraction level did not show any prominent change (Figure 3.18, Table 3.8). These findings suggest that a single allele of *Msh6* can partially afford some protection, but both alleles of *Msh6* are required for full protection, against GAA repeat instability.

Figure 3.18 - The effect of *Msh6* on the intergerational GAA repeat sizes.

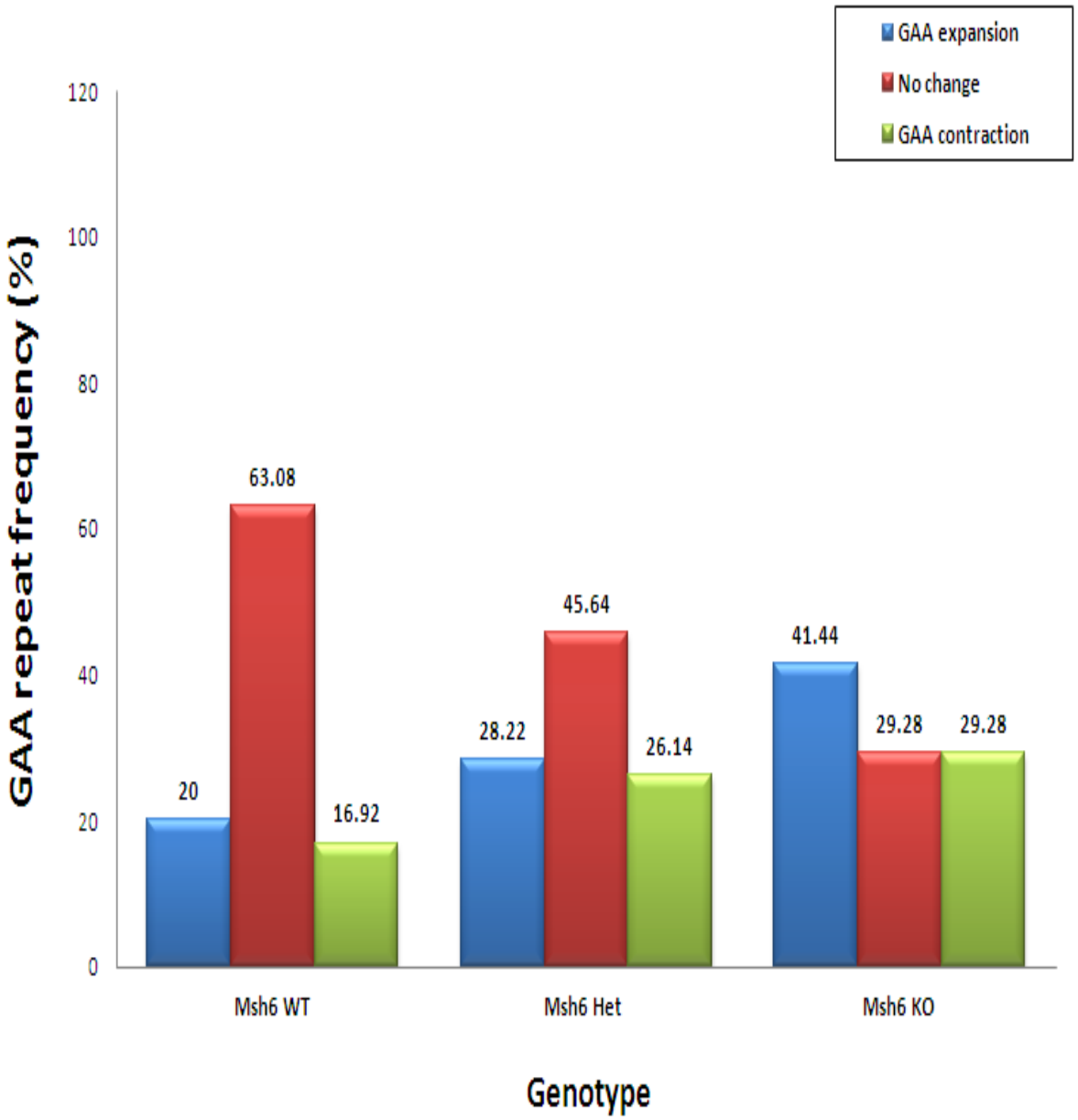

Frequencies of GAA expansions, no chages and GAA contractions transmitted to offspring are presented as percentages of total GAA repat transmission: WT n=65, Het n=241, KO n=181.

Further, to investigate the dynamics of intergenerational GAA repeat transmissions, analysis of the mean GAA repeat size variations for *Msh6*$^{+/-}$ and *Msh6*$^{-/-}$ mice demonstrated a bias towards an increased mean GAA repeat size (Table 3.9).

Table 3.8 - χ^2 analysis of GAA repeat transmissions in *Msh6* transgenic mice.

Msh6 parental genotype 1	*Msh6* parental genotype 2	χ^2 value	df	*P* value
Msh6$^{+/+}$	***Msh6***$^{+/-}$	6.26	2	0.044
Msh6$^{+/+}$	***Msh6***$^{-/-}$	23.25	2	<0.001
Msh6$^{+/-}$	***Msh6***$^{-/-}$	12.87	2	<0.01

Table 3.9 - Mean transmitted GAA repeat size variations in *Msh6* transgenic mice.

Parent genotype	Mean GAA repeat size increase of expansions	Mean GAA repeat size increase of contractions	Mean GAA repeat size variation of all transmissions
Msh6$^{+/+}$	+ 1.8	-3.6	-0.24
Msh6$^{+/-}$	+ 6.2	-5.5	+ 0.31
Msh6$^{-/-}$	+ 3.7	-3.5	+ 0.53

3.4.4 - *Pms2* effects on transmission of GAA repeat instability

To determine the effect of Pms2 protein on intergenerational transmission of GAA repeats, the GAA PCR products obtained from offspring were compared with those of parents by long agarose gel electrophoresis (Figure 3.19). Analysis of paternal *Pms2*$^{-/-}$ GAA repeat frequencies was not feasible, because *Pms2* $^{-/-}$ males are sterile.

Figure 3.19 - Representative example of intergenerational GAA repeat instability in *Pms2* transgenic model.

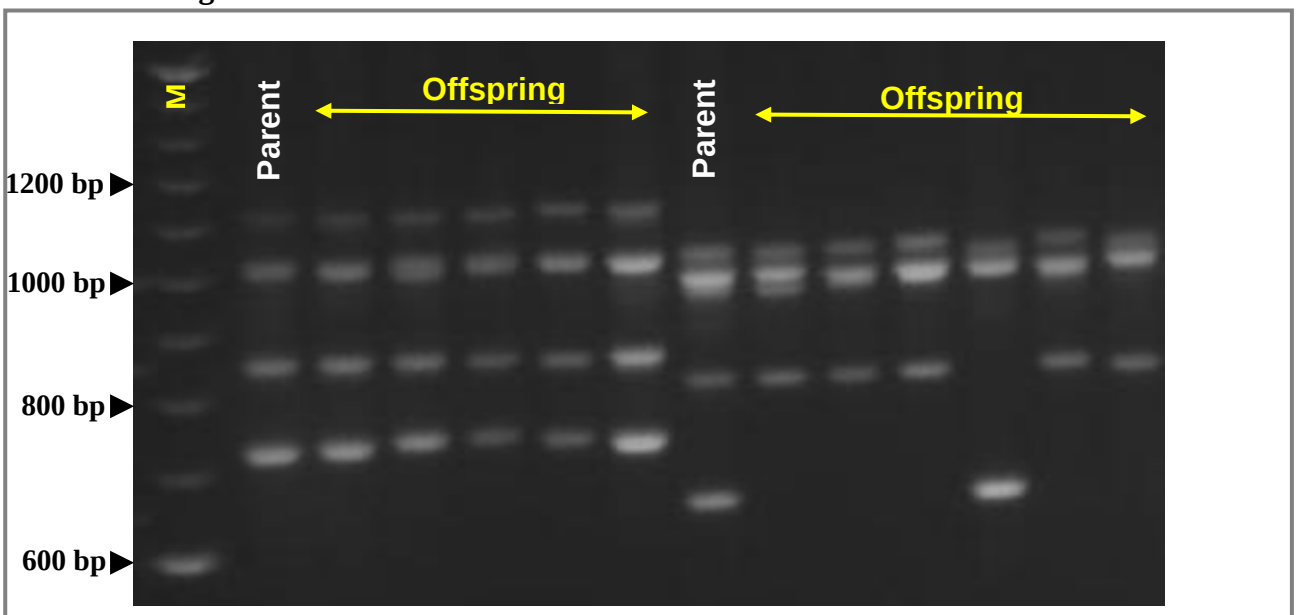

The image illustrates PCR products to determine GAA repeat sizes in a long agarose gel obtained from a YG8 $GAA^{+}/Pms2^{+/+}$ parent and 5 offspring, and from a YG8 $GAA^{+}/Pms2^{+/-}$ parent and 6 GAA^{+} offspring. M= 100bp DNA size marker.

To determine intergenerational GAA repeat size differences between parent and offspring, data were analysed separately from 3 YG8 parental genotypes with 39 offspring and from 13 YG22 parental genotypes with 137 YG22 offspring (Table 3.10).

Table 3.10 - *FXN*$^{GAA+}$/*Pms2* offspring numbers based on different characteristics.

MMR line	MMR genotype	*FXN* line	gender	No. of parents	No. of offspring
Pms2	WT	YG8	♂	3	21
			♀	2	18
		YG22	♂	2	22
			♀	0	0
	Het	YG8	♂	1	23
			♀	2	37
		YG22	♂	3	69
			♀	0	0
	KO	YG8	♂	**Sterile**	0
			♀	1	6
		YG22	♂	**Sterile**	0
			♀	1	14

YG8 GAA^{+}/*Pms2*$^{+/+}$ intergenerational transmission was stable for approximately 68% of GAA repeats, while mutability levels showed a bias towards expansions, with approximately 24% expansions and 9% contractions (Figure 3.20A). Loss of one *Pms2* allele increased the mutability level to 75%. Although the level of contraction was slightly increased, the majority of GAA repeat instability was towards expansions in *Pms2* heterozygous transmission profiles. Transmission of GAA repeat sizes from YG8 *Pms2*$^{-/-}$ showed a similar overall level of mutability to *Pms2*$^{+/-}$, while the frequency of expansions was greater and the level of contraction was notably less than *Pms2*$^{+/-}$ transmission profiles (Figure 3.20A). These findings indicate that similar to *Msh6*, lack of even one *Pms2* allele results in greater instability levels with a bias towards expansions. Curiously, full absence of Pms2 protein not only causes further elevation of GAA repeat expansion, but also reduces the GAA contraction level.

Similar to YG8, the majority (60%) of YG22 GAA^{+}/*Pms2*$^{+/+}$ intergenerational transmission profiles showed no change with GAA repeat size and similar levels of GAA contractions (22%) and expansions (18%) (Figure 3.20). YG22 GAA^{+}/*Pms2*$^{+/-}$ showed a degree of increased mutability level mainly towards expansions, although the frequency of contractions was also slightly increased. Loss of both *Pms2* alleles caused a dramatic increase in mutability level, with expansions up to 99% and contractions down to zero. These findings confirmed the results from YG8, suggesting that absence of Pms2 protein prohibits intergenerational GAA repeat contractions and causes dramatically increased levels of expansions.

Figure 3.20 - The effect of *Pms2* on intergerational GAA repeat sizes based upon transgene

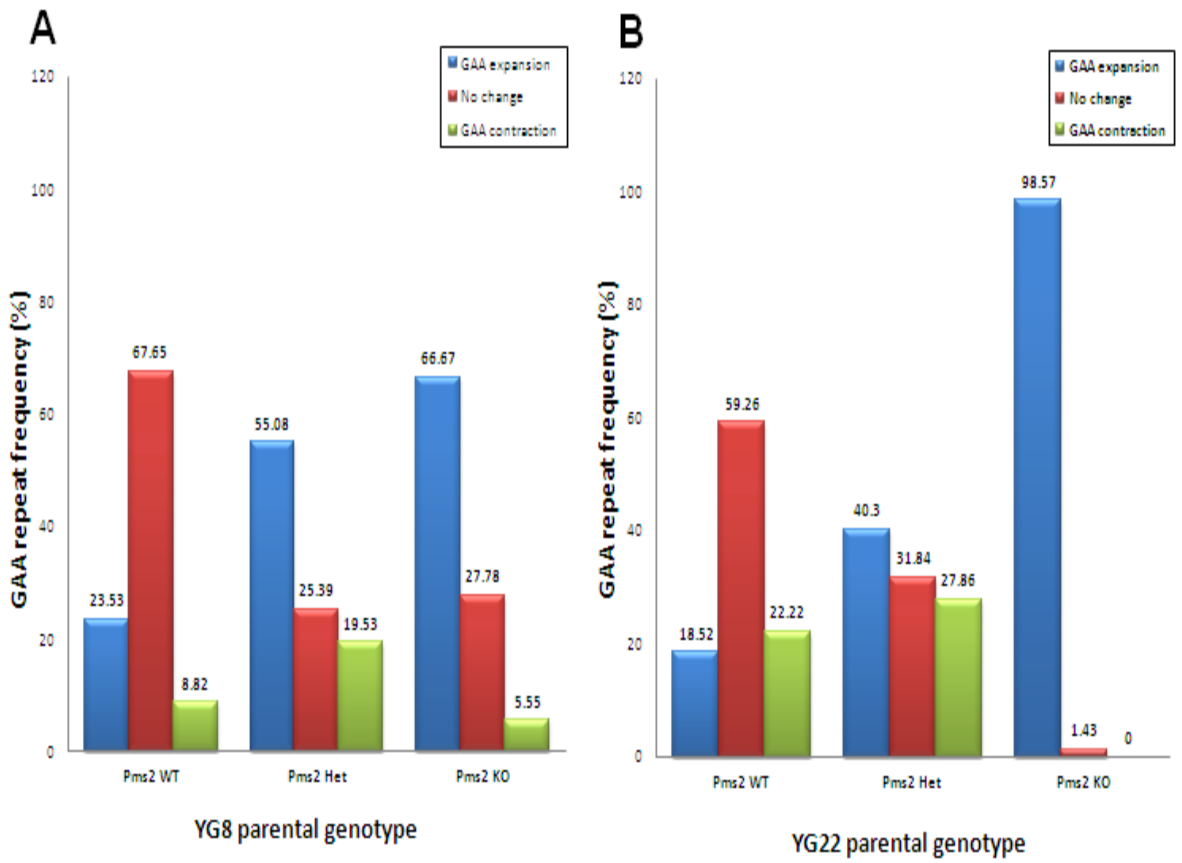

Frequencies of GAA expansions, no chages and GAA contractions transmitted to offspring are presented as percentages of total GAA repat transmission. **(A)** YG8 GAA^{+}/*Pms2*: WT n=102, Het n=256, KO n=18. **(B)** YG22 GAA^{+}/*Pms2*: WT n=54, Het n=201, KO n=70.

Further analysis was carried out based on different parental genders, comprising 135 offspring from 9 paternal GAA^{+} genotypes and 75 offspring from 6 maternal GAA^{+} genotypes (Table 3.10). Investigations of GAA repeat transmission profiles showed that the range of mutability was less than 50% in both paternal and maternal FXN^{GAA+}/$Pms2^{+/+}$ genotypes. This instability level then dramatically increased in parental $Pms2^{+/-}$ and $Pms2^{-/-}$ genotypes. Analysis of paternal $Pms2^{+/+}$ GAA repeat size transmissions showed slightly greater frequency of expansions than contractions, while more than 50% of GAA repeat size transmissions were stable (Figure 3.21A). Since *Pms2* homozygous KO males are sterile, investigation of the paternal $Pms2^{-/-}$ GAA repeat size transmission was not possible.

However, *Pms2*$^{+/-}$ transmissions showed greater levels of GAA expansions and contractions compared to paternal *Pms2*$^{+/+}$ values (Figure 3.21A).

Figure 3.21 - The effect of *Pms2* on intergerational GAA repeat sizes based upon perental genotypes.

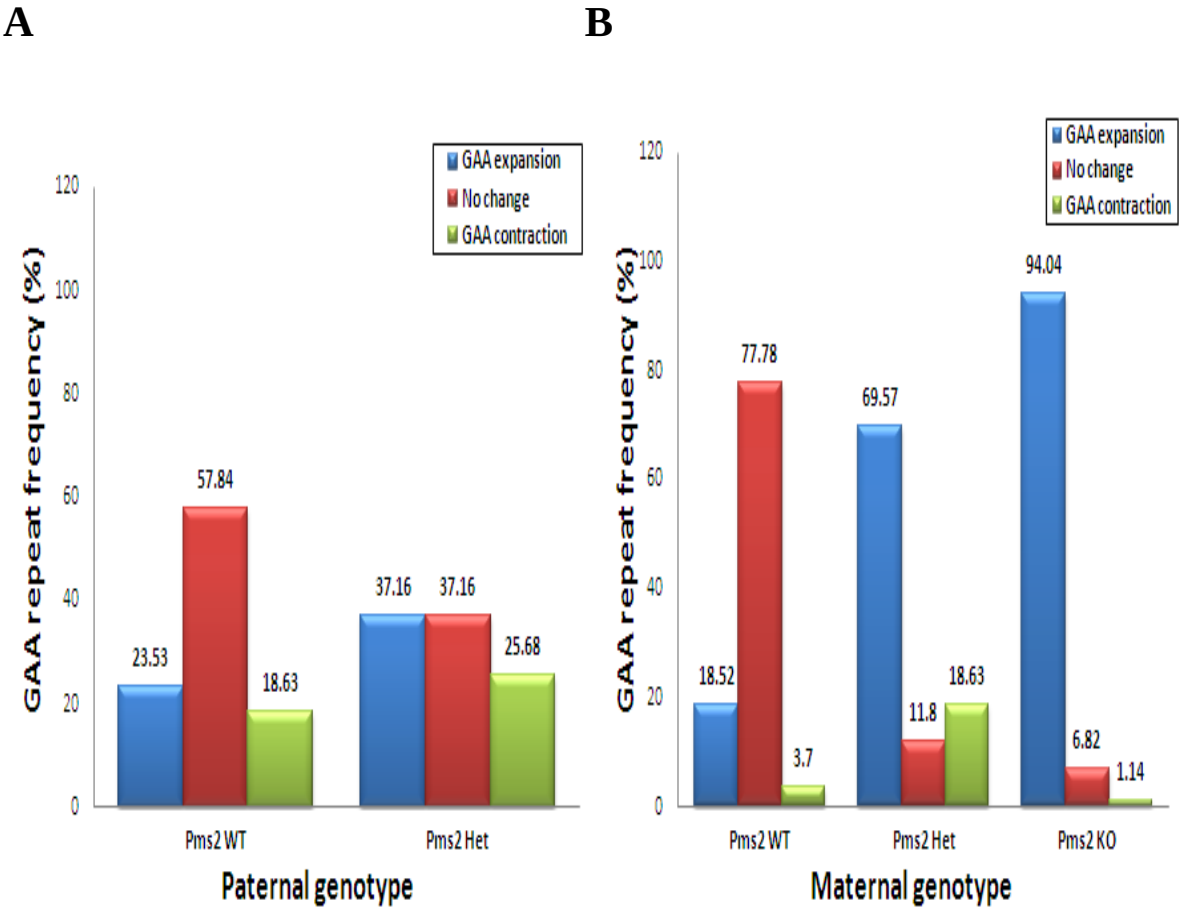

Frequencies of GAA expansions, no chages and GAA contractions transmitted to offspring are presented as percentages of total GAA repat transmission. **(A)** Paternal GAA^{+}/*Pms2*: WT n=102, Het n=296, KO parents are sterile. **(B)** Maternal GAA^{+}/*Pms2*: WT n=54, Het n=161, KO n=88.

Analysing the results of intergenerational transmissions obtained from maternal *Pms2*$^{+/+}$ mice showed that more than 75% of GAA repeats size did not change. Similar to paternal transmissions, the majority of maternal *Pms2*$^{+/+}$ mutability was due to the GAA repeat

expansions (Figure 3.21B). The level of mutability from maternal *Pms2*$^{+/-}$ transmission was significantly increased, showing a strong bias towards GAA repeat expansions. The level of mutability was increased in *Pms2*$^{-/-}$ compared with *Pms2*$^{+/-}$, although the frequency of contractions was reduced to almost 1% (Figure 3.21B). Overall, these findings suggest that loss of a single allele of *Pms2* is similar to lack of both *Pms2* alleles, with insufficient mismatch repair protein being produced to protect against maternal transmission of GAA repeat expansions.

Ultimately, the intergenerational GAA repeat size transmissions were evaluated from 15 parents and 210 offspring, based only upon *Pms2* genotypic states (Table 3.10). Data analysis revealed that almost 35% of all parental *Pms2*-WT transmissions presented GAA repeat mutability, including 22% expansions and 13% contractions (Figure 3.22, Table 3.11). Similar to *Msh6*, with the loss of one *Pms2* allele the level of mutability was significantly increased with a notable bias towards expansions. Interestingly, further analysis showed that lack of both *Pms2* alleles culminated in a sharply increased level of GAA repeat expansions up to 92%, while only 1% GAA repeat contraction was observed in these transmission profiles (Figure 3.22, Table 3.11). These findings suggest that, while one *Pms2* allele exerts some protective effect against GAA repeat expansions, both *Pms2* alleles are required to fully activate mismatch repair protection against GAA repeat expansions and perhaps promote contractions.

Figure 3.22 - The effect of *Pms2* on the intergerational GAA repeat sizes.

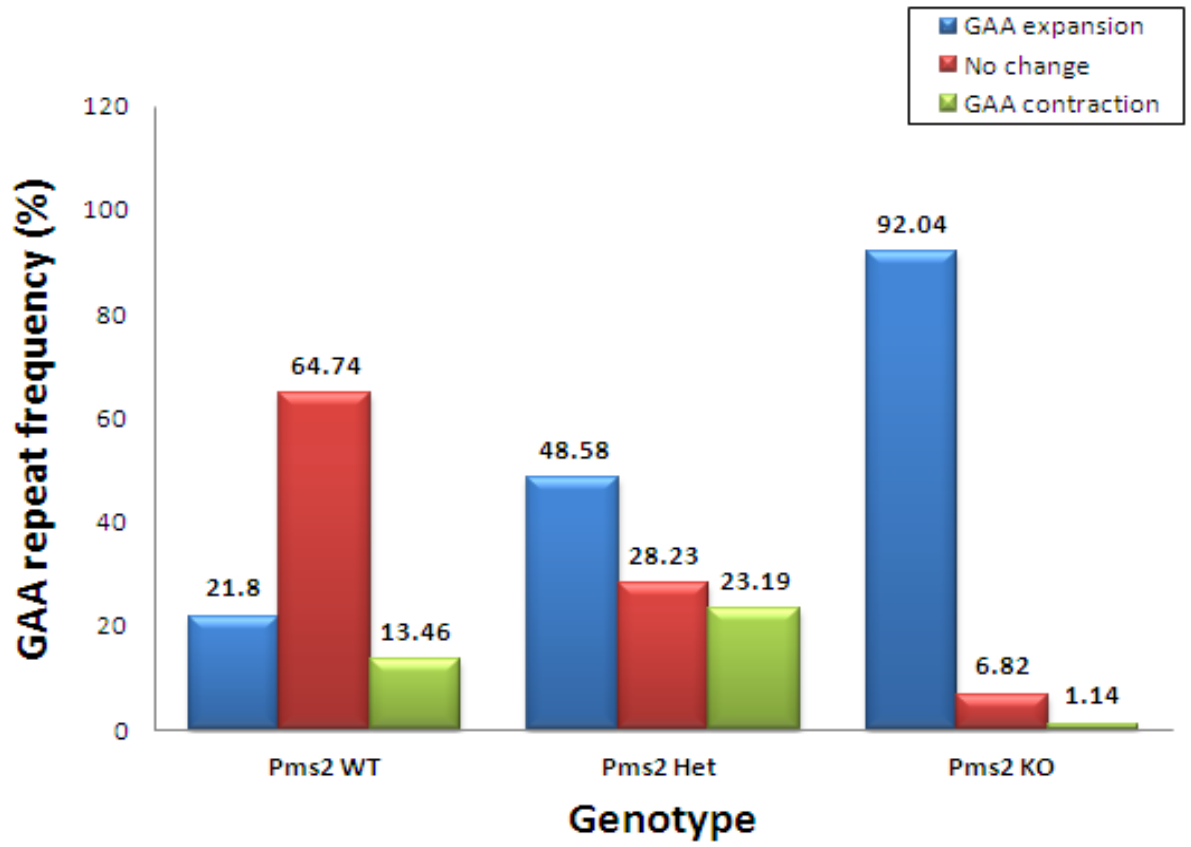

Frequencies of GAA expansions, no chages and GAA contractions transmitted to offspring are presented as percentages of total GAA repat transmission: WT n=156, Het n=457, KO n=88.

Table 3.11 - χ^2 analysis of GAA repeat transmissions in *Pms2* transgenic mice.

***Pms2* parental genotype 1**	***Pms2* parental genotype 2**	**χ^2 value**	**df**	***P* value**
***Pms2*$^{+/+}$**	***Pms2*$^{+/-}$**	66.63	2	<0.001
***Pms2*$^{+/+}$**	***Pms2*$^{-/-}$**	111	2	<0.001
***Pms2*$^{+/-}$**	***Pms2*$^{-/-}$**	57	2	<0.001

Further to analysing frequencies of intergenerational GAA repeat transmission, both *Pms2*$^{+/-}$ and *Pms2*$^{-/-}$ transmissions also showed elevated mean GAA repeat size variations within their offspring in an allele-dose dependent manner (Table 3.12).

Table 3.12 - Mean transmitted GAA repeat size variations in *Pms2* transgenic mice.

Parent genotype	Mean GAA repeat size increase of expansions	Mean GAA repeat size increase of contractions	Mean GAA repeat size variation of all transmissions
Pms2$^{+/+}$	+ 6.4	-8.2	+0.28
Pms2$^{+/-}$	+ 5.7	-4.00	+1.93
Pms2$^{-/-}$	+ 7.6	-1.00	+7.00

3.4.5 - *Mlh1* effects on transmission of GAA repeat instability

To assess the effect of Mlh1 protein on intergenerational transmission of GAA repeat size instability, *FXN*$^{GAA+}$ and *Mlh1* Het mice were developed. Since both male and female *Mlh1*-KO transgenic mice are sterile (Edelmann *et al.* 1996), investigating the intergenerational GAA repeat transmission of these mice could only be done at the heterozygous level. Furthermore, only YG22 mice have thus far been investigated (Figure 3.23, Table 3.13).

Figure 3.23 - Representative example of intergenerational GAA repeat instability in transgenic *Mlh1* model.

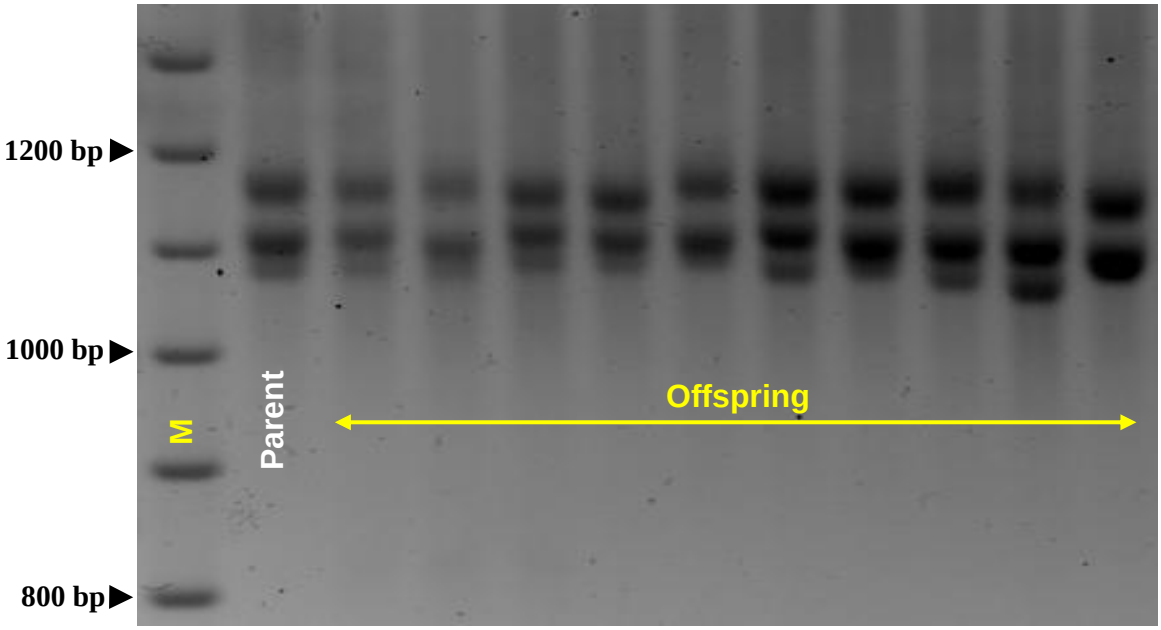

The image illustrates PCR products to determine GAA repeat sizes in a long agarose gel obtained from a YG22 GAA^{+}/$Mlh1^{+/+}$ parent and 10 GAA^{+} offspring. M= 100bp DNA size marker.

Table 3.13 - FXN^{GAA+}/*Mlh1* offspring numbers based on different characteristics.

MMR line	MMR genotype	*FXN* line	gender	No. of parents	No. of offspring
Mlh1	WT	YG22	♂	2	10
			♀	0	0
	Het	YG22	♂	1	4
			♀	3	17
	KO	YG22	♂	**Sterile**	0
			♀	**Sterile**	0

Data analysis revealed that more than 85% of parental *Mlh1*-WT transmission profiles showed mutability with GAA repeat size, including 70% expansion and 17% contractions. This result is contrary to the previous intergenerational transmission results obtained from all $Msh2^{+/+}$, $Msh3^{+/+}$, $Msh6^{+/+}$ and $Pms2^{+/+}$ mice, which showed significantly greater levels

of no-changed GAA repeat sizes (Figure 3.24, Table 3.14). With loss of one *Mlh1* allele, the frequency of contractions sharply increased to almost 75% while the level of expansions decreased to 19%. This was completely opposite to the observed levels of contractions and expansions from *Mlh1*-WT transmission profiles (Figure 3.24, Table 3.14). This suggests that Mlh1 protein could protect against intergenerational GAA repeat contractions and perhaps also promote expansions. However, to clarify this situation, more studies are required on further offspring.

Figure 3.24 - The effect of *Mlh1* on the intergerational GAA repeat sizes.

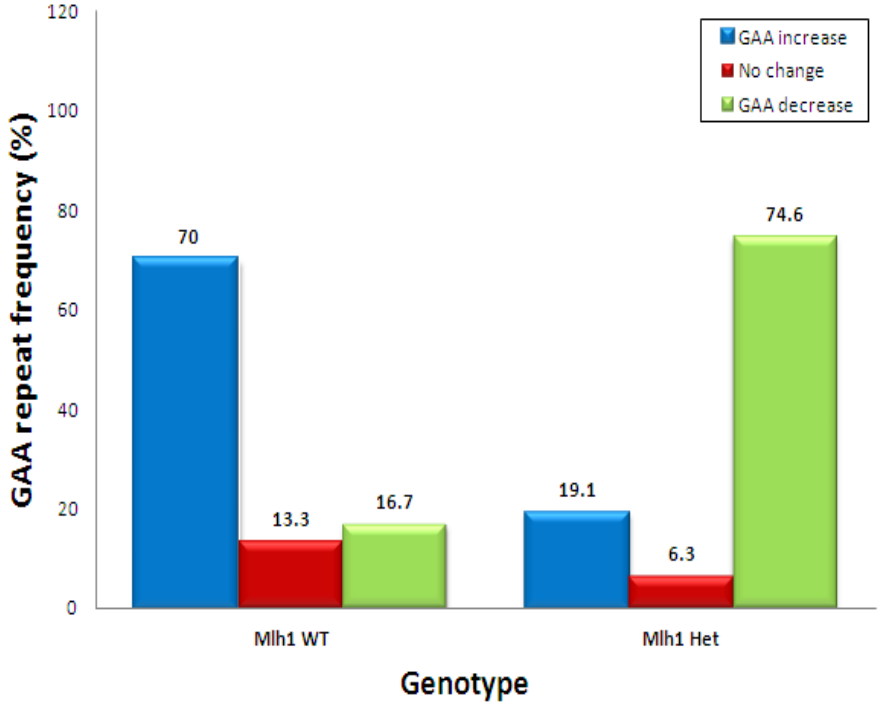

Frequencies of GAA expansions, no chages and GAA contractions transmitted to offspring are presented as percentages of total GAA repat transmission: WT n=30, Het n=63.

Table 3.14 - χ^2 analysis of GAA repeat transmissions in *Mlh1* transgenic mice.

***Mlh1* parental genotype 1**	***Mlh1* parental genotype 2**	**χ^2 value**	**df**	***P* value**
***Mlh1*$^{+/+}$**	***Mlh1*$^{+/-}$**	28.2	2	<0.001

3.5 - Potential effect of the MMR proteins on other TNR instability

To find out whether the increased instability levels induced by defect of MMR proteins are specific for the expanded GAA repeat transgene or a more general effect for the other *in vivo* TNR sequences, transmission of a 12 repeat CGG sequence and a 21 repeat CAG sequences, located on mouse chromosome 19 and 13, respectively, were similarly analysed. After designing PCR primers, the optimal annealing temperature was detected by gradient PCR (G-PCR) for each CAG or CGG fragments, called G-CAG PCR and G-CGG PCR, respectively (Figure 3.25). Based on the PCR product quality, standard PCR systems were then designed with optimal annealing temperatures of 58°C for CAG PCR and 64°C for CGG PCR.

Figure 3.25 - Gradient PCR for CAG and CGG repeats.

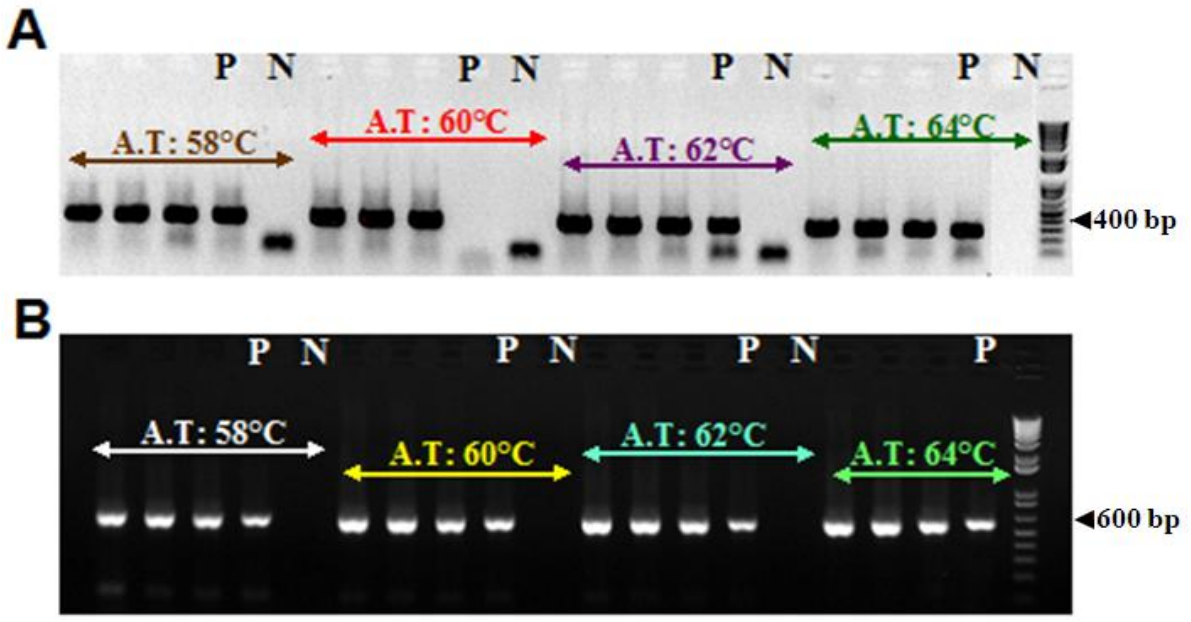

The images show the ethidium bromide-stained agarose gels used to determine gradient mouse **(A)** CGG-PCR and **(B)** CAG-PCR. M: 1Kb^{+} size marker. A.T: Annealing temperature.

Investigating the *Msh2* effect on CGG repeat instabilities showed that lack of this protein increased mutability only towards CGG repeat expansions (Figure 3.26A, Table 3.15). However, Msh2 deficits increased both CAG repeat expansion and CAG repeat contraction frequencies (Figure 3.26B, Table 3.16).

Figure 3.26 - Intergenerational CGG and CAG repeat instabilities in *Msh2* transgenic mice.

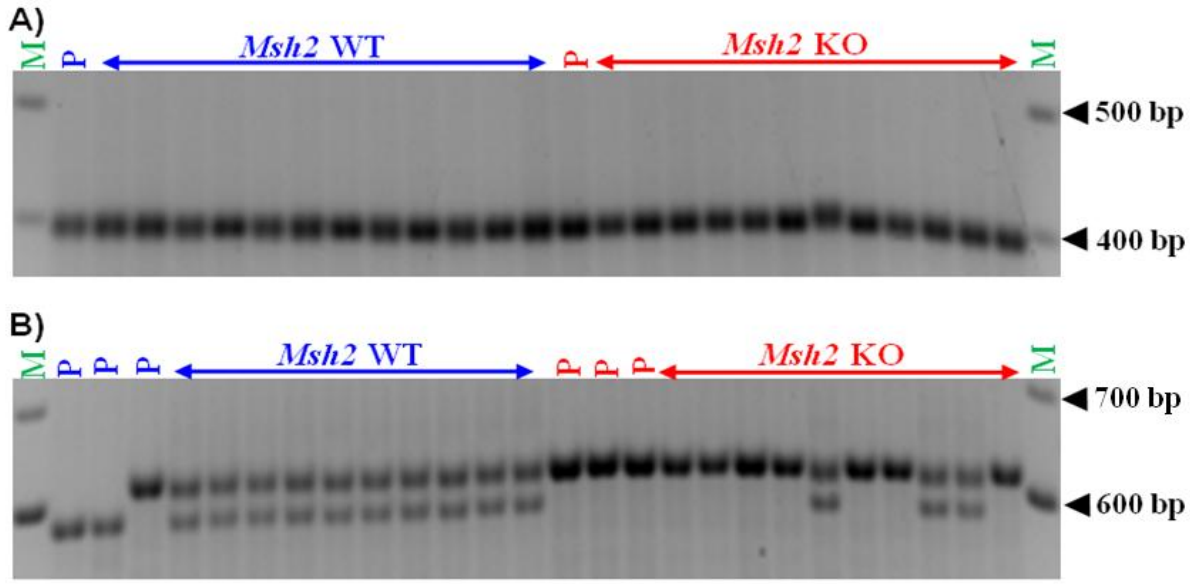

The image illustrates unstable transmission of **(A)** CGG tandem repeat **(B)** CAG tandem repeat from *Msh2*-WT compared with *Msh2*-KO. M: 100bp size marker, P: Parent.

Table 3.15 - Intergenerational CGG repeat instability frequencies in *Msh2* mice.

CGG repeats		Expansions (%)	No change (%)	Contractions (%)
Msh2	**WT**	0	100	0
	KO	33.3	66.7	0

Table 3.16 - Intergenerational CAG repeat instability frequencies in *Msh2* mice.

CAG repeats		Expansions (%)	No change (%)	Contractions (%)
Msh2	**WT**	0	100	0
	KO	10	75	15

Compared with *Msh2*, lack of *Msh3* resulted in reduced mutability level of the CGG repeat observed in *Msh3*$^{+/+}$ mice offspring (Figure 3.27A, Table 3.17). Further analysis showed that *Msh3* deficits did not change the mutability level of CAG repeat compared with *Msh3*$^{+/+}$ mice offspring (Figure 3.27B, Table 3.18).

Figure 3.27 - Intergenerational CGG and CAG repeat instabilities in *Msh3* transgenic mice.

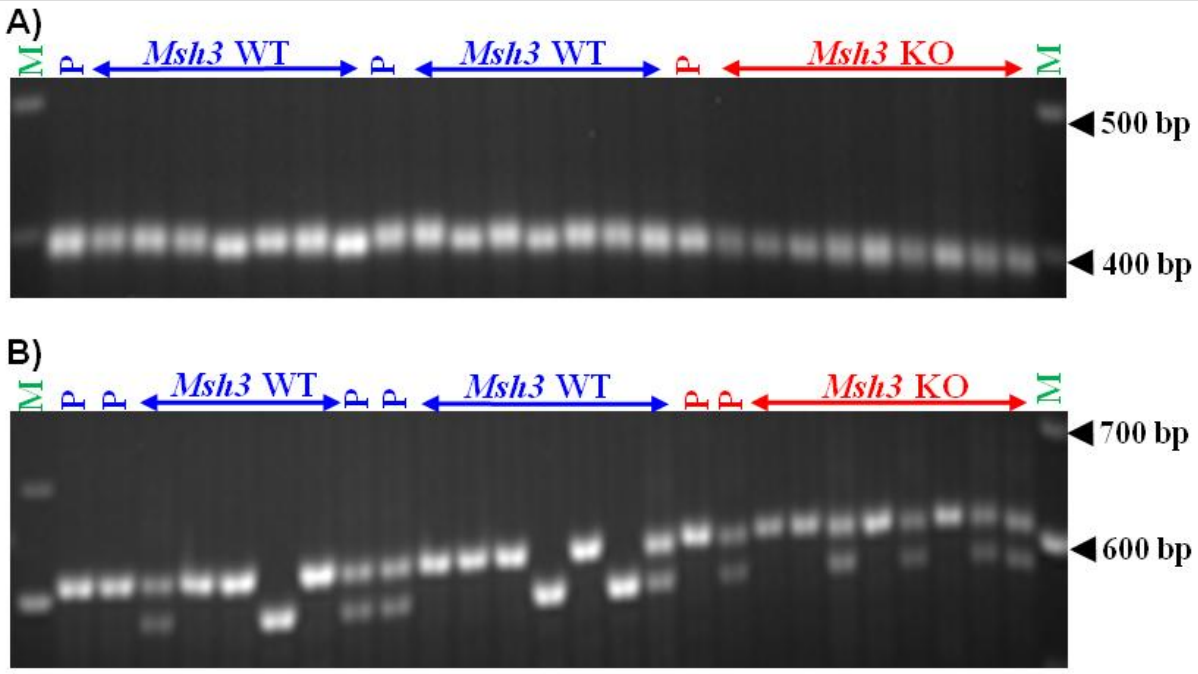

The image illustrates unstable transmission of **(A)** CGG tandem repeat **(B)** CAG tandem repeat from *Msh2*-WT compared with *Msh2*-KO. M: 100bp size marker, P: Parent.

Table 3.17 - Intergenerational CGG repeat instability frequencies in *Msh3* mice.

CGG repeats		Expansions (%)	No change (%)	Contractions (%)
Msh3	**WT**	50	28.6	21.4
	KO	0	100	0

Table 3.18 - Intergenerational CAG repeat instability frequencies in *Msh3* mice.

CAG repeats		Expansions (%)	No change (%)	Contractions (%)
Msh3	**WT**	16.7	62.5	20.8
	KO	33.3	66.7	0

Similar to *Msh3*, the level of CGG repeat mutability was decreased with fully disruption of Msh6 compared to *Msh6*$^{+/+}$ mice transmission (Figure 3.28A, Table 3.19). No CAG repeat mutability was observed neither with *Msh6*$^{+/+}$ nor with *Msh6*$^{-/-}$ transgenic mice. In other words, loss of Msh6 did not effect on the mutability level of CAG repeats (Figure 3.28B, Table 3.20).

Figure 3.28 - Intergenerational CGG and CAG repeat instabilities in *Msh6* transgenic mice.

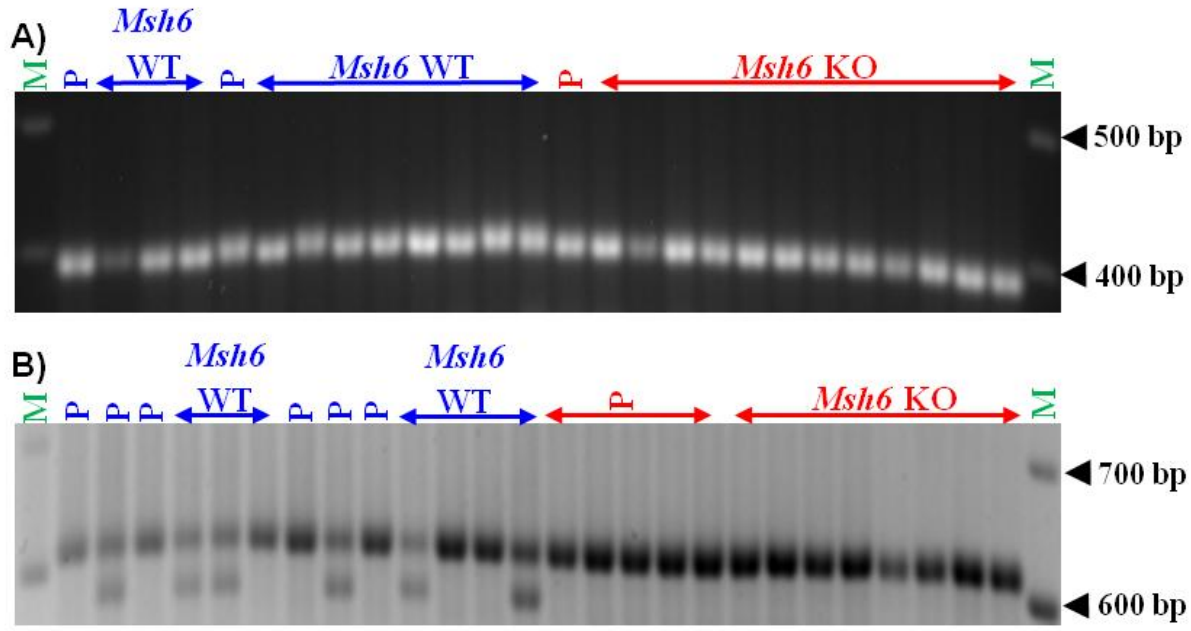

The image illustrates unstable transmission of **(A)** CGG tandem repeat **(B)** CAG tandem repeat from *Msh6*-WT compared with *Msh2*-KO. M: 100bp size marker, P: Parent.

Table 3.19 - Intergenerational CGG repeat instability frequencies in *Msh6* mice.

CGG repeats		Expansions (%)	No change (%)	Contractions (%)
Msh6	**WT**	27.3	63.7	9
	KO	0	100	0

Table 3.20 - Intergenerational CAG repeat instability frequencies in *Msh6* mice.

CAG repeats		Expansions (%)	No change (%)	Contractions (%)
Msh6	**WT**	0	100	0
	KO	0	100	0

Analysing CGG repeat sizes showed greater mutability level with *Pms2*$^{-/-}$ than *Pms2*$^{+/+}$ (Figure 3.29A, Table 3.21), while, similar to *Msh3* and *Msh6*, no CAG repeat mutability was observed with both *Pms2*$^{+/+}$ and *Pms2*$^{-/-}$ states (Figure 3.29B, Table 3.22). No study has been carried out yet to determine the role of *Mlh1* on CAG and CGG repeat instabilities.

Figure 3.29 - Intergenerational CGG and CAG repeat instabilities in *Msh6* transgenic mice.

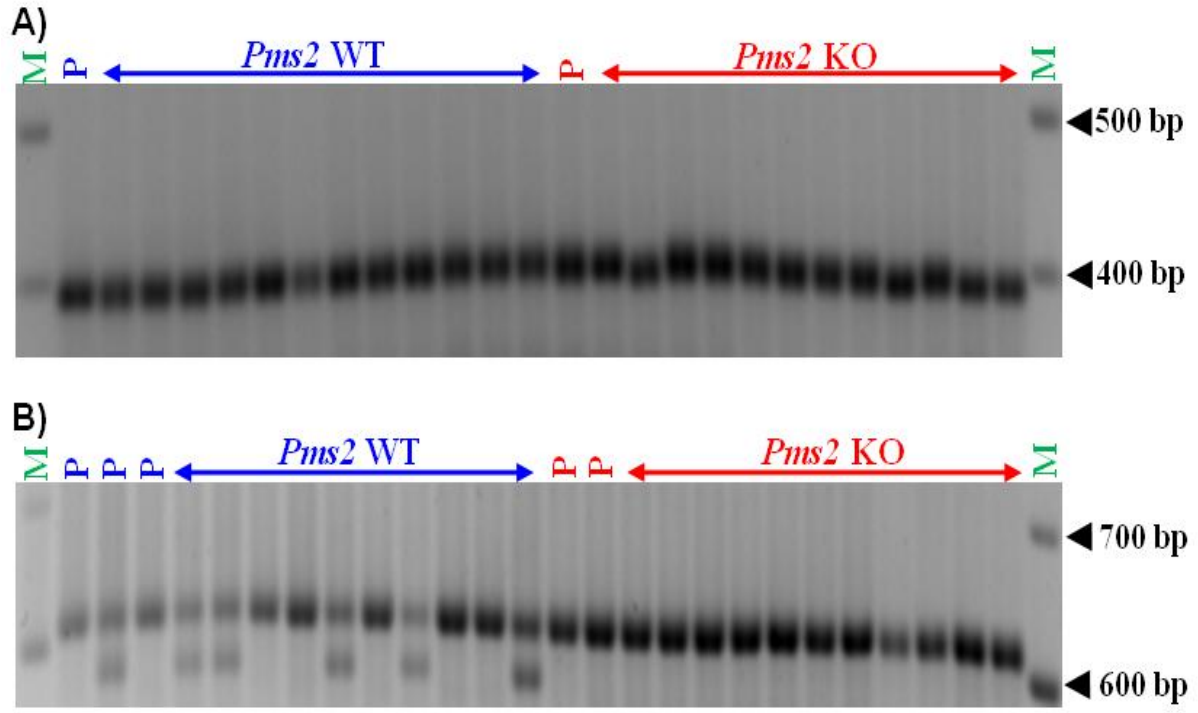

The image illustrates unstable transmission of **(A)** CGG tandem repeat **(B)** CAG tandem repeat from *Msh2*-WT compared with *Msh2*-KO. M= 100bp size marker, P= Parent.

Table 3.21 - Intergenerational CGG repeat instability frequencies in *Pms2* mice.

CGG repeats		Expansions (%)	No change (%)	Contractions (%)
Pms2	**WT**	0	100	0
	KO	25	50	25

Table 3.22 - Intergenerational CAG repeat instability frequencies in *Pms2* mice.

CAG repeats		Expansions (%)	No change (%)	Contractions (%)
Pms2	**WT**	0	100	0
	KO	0	100	0

Taken together, data analysis revealed minor effects of MMR protein deficits on the mutability level of intergenerational CGG or CAG repeat, which are distinguishable from the effects of MMR proteins on intergenerational transmission of the expanded GAA repeat instabilities. Therefore, these findings confirm that is plausible to propose a specific influence of MMR proteins on intergenerational transmission of the expanded GAA repeat within the context of the *FXN* transgene sequence, rather than a general effect on any TNR. In future, it will similarly be necessary to investigate the effect of *Mlh1* on CGG and CAG parental transmissions.

3.6 - Discussion

To investigate potential molecular mechanisms of intergenerational GAA repeat instability in FRDA, the effects of MMR proteins Msh2, Msh3, Msh6, Pms2 and Mlh1 were investigated during parent to offspring transmission of GAA repeats from YG8 and YG22 transgenic mice. Data analysis based upon parental MMR genotypes showed a similar mutability level of 25-37% for each of the *Msh2*-WT, *Msh3*-WT, *Msh6*-WT and *Pms2*-WT transmission profiles. This is consistent with previous findings for YG8 and YG22 transgenic mouse intergenerational instability (Al-Mahdawi et al., 2004). However, the data obtained from YG22 GAA^{+}/$Mlh1^{+/+}$ transmissions was not similar to the previous findings. The reason for

this finding is not clear yet. It is possible that there could be a genetic background difference in the YG22 $GAA^{+}/Mlh1^{+/+}$ mice. There may also be some effect due to the comparatively small number of *Mlh1*-WT intergenerational transmissions analysed compared with the other MMR-WT analyses. Further investigations are required to explain the disparity of these results.

In this chapter, it has been shown that loss of MMR genes results in continued transmission of GAA repeat contractions and expansions over generations, but with a bias towards increased mutability. Thus, it is concluded that, during intergenerational GAA repeat transmissions, Msh2, Msh3, Msh6, Pms2 and Mlh1 are not the main cause of GAA mutability, neither contractions nor expansions, but they rather function in a repair capacity to protect against negative effects of GAA repeat instability. This would agree with the generally accepted functions of the mismatch repair system: (i) to identify and start the repair of small IDLs by Msh2-Msh3 heterodimers, (ii) to identify and start the repair of single base pair mismatches and single base IDLs by Msh2-Msh6 heterodimers, and (iii) the interaction of Mlh1-Pms2 heterodimers with one of Msh2-Msh3 or Msh2-Msh6 heterodimers to continue the repair process during replication and recombination. Despite their similarities, distinct differences were also detected between the effects of Msh2 and Msh3 compared with Msh6, Pms2 and Mlh1. Thus, Msh2 and Msh3 were found to protect against intergenerational GAA repeat contractions, whilst Msh6 was shown to have a minor protective effect against both contractions and expansions. Pms2 was found to significantly protect against expansions but also contribute to the promotion of contractions, whereas Mlh1 protects against intergenerational GAA repeat contractions and promotes expansions. To further investigate the role of MMR proteins on GAA repeats, the occupancy of each MMR protein (except Mlh1) around the expanded GAA repeats was compared with the normal GAA repeats by my colleague, Dr Sahar Al-Mahdawi, who performed ChIP assays at five regions of the YG8 and

YG22 *FXN*$^{GAA+}$ transgenic mice (-1254, promoter, upstream GAA, downstream GAA and intron 2), compared with stable normal-sized GAA repeat-containing Y47 *FXN* transgenic mice. Consistent enrichment of Msh2 occupancy was observed at all 5 regions of the *FXN* locus in both YG8 and YG22 compared with Y47 mice. Although, the most significant level of Msh2 occupancy was detected at downstream GAA and the intron 2 regions. Similarly, Msh3 enrichment was found at downstream GAA and intron 2 regions (Figure 3.30). In contrast, no difference of occupancy was observed at any region of the *FXN* locus for each of Msh6 and Pms2, with one exception of Msh6 enrichment at the downstream GAA region in YG22 mice (Ezzatizadeh *et al.* 2012). These findings suggest that rather than there being a single MMR mechanism in operation, at least two different MMR systems may be involved to identify and start intergenerational FRDA GAA mutability. One mechanism predominantly involves Msh2-Msh3 heterodimers, which play a role in limiting GAA repeat contractions.

Figure 3.30 - MMR occupancy at 5 regions of the *FXN* locus (Ezzatizadeh *et al.* 2012)**.**

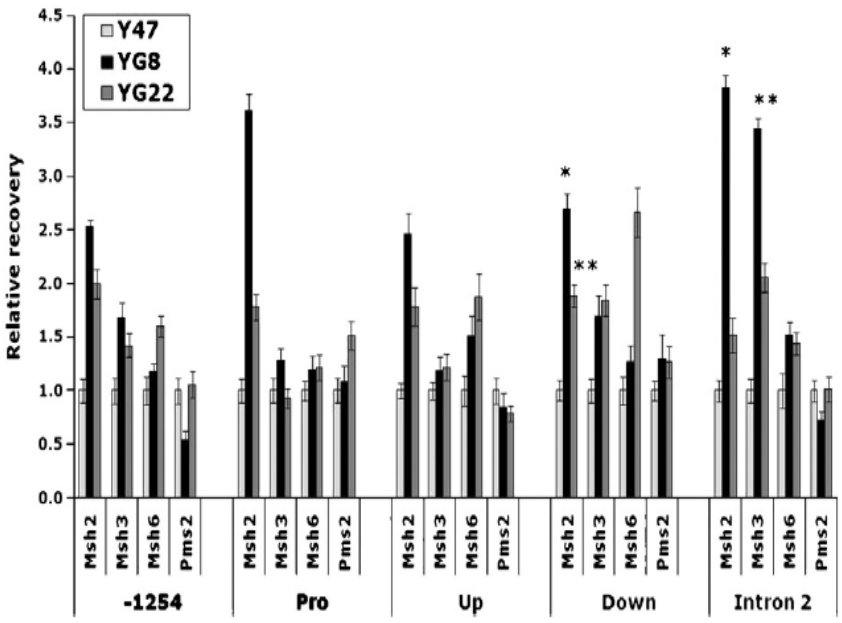

ChIP data showing Msh2, Msh3, Msh6 and Pms2 occupancy at 5 regions of the FXN locus: 1254bp upstream of the transcription start site (−1254), promoter (Pro), upstream GAA (Up), downstream GAA (Down) and 11482bp downstream of the transcription start site (intron 2). Columns represent quantitative PCR data from IP samples relative to input. YG8 and YG22 values are shown as fold changes relative to Y47 set at 1.0. * = P<0.05, ** = P<0.01. Error bars=s.e.m. of independent experiments, n=4.

The second mechanism predominantly involves Msh2-Msh6 heterodimers acting to limit GAA repeat expansions and/or contractions. Loss of Msh3 or Msh6 might cause an alternative MMR system to identify and start repairing expanded GAA repeat mutations. Depending on the loss of either Msh2 or Msh6 protein, GAA repeats might undergo a greater frequency of contractions or both expansions and contractions, respectively.

The results from this study indicate that Pms2 is involved in the continuation of the MMR process to limit GAA repeat expansions. Therefore, Pms2 may be one protein of a MutLα heterodimer that mainly contributes to protecting expanded GAA repeats against further expansion by continuing the MMR processes initiated by MutSα heterodimers. However, the combination of the MutLα with MutSβ may also protect GAA repeats against both expansions and contractions. To find out the exact role of each MMR protein in the repair of GAA repeat expansions, it would be useful to establish triple genetically altered mice, simultaneously having defect of two co-operating heterodimers. Indeed, by generating double KO *FXN*$^{GAA+}$ transgenic mice for both *Msh2* and *Msh3* genes, it may be possible to investigate the role and occupancy of the other MutS protein, Msh6, within expanded GAA repeat region.

The findings of increased frequencies of GAA repeat contractions in the *Msh2*$^{-/-}$ and *Msh3*$^{-/-}$ mice offspring, and to a lesser extent of *Msh6*$^{-/-}$ mice, are in agreement to previous studies of HD and DM1 transgenic mice in which a similar effect of *Msh2*$^{-/-}$ and *Msh3*$^{-/-}$ and *Msh6*$^{-/-}$ deficits on CAG and CTG repeats was respectively observed (Foiry *et al.* 2006; Dragileva *et al.* 2009). This suggests a common MMR system by which all expanded TNR sequences are protected against intergenerational repeat contractions. However, there may be a difference in the way that the MMR system acts on expanded GAA versus CAG or CTG repeats, since there is no GAA repeat expansion loss in *FXN* transgenic mice as observed with CAG and CTG repeat expansions in HD and DM1 transgenic mice, respectively. Therefore, it is

proposed that, unlike MMR effects on CAG and CTG repeat expansions in HD and DM1 disorders, Msh2 and Msh3 proteins are not considered to be essential for intergenerational GAA repeat expansions in FRDA (Savouret *et al.* 2003; Wheeler *et al.* 2003; Foiry *et al.* 2006; Dragileva *et al.* 2009). This is probably due to differences in the secondary structure of GAA repeat expansions compared with CAG and CTG repeat expansions. For example, it is proposed that expanded CAG repeats form hairpin structures, which are recognised by MutSβ heterodimers, but they do not elicit a normal MMR repair function. In this hypothesis, known as "hijacking" of the MMR system, it is believed that instead there may be a non-canonical MutSβ binding DNA segment preventing repair and preserving repeat expansions (McMurray 2008). Another proposal suggests that there might be an alternative, as yet unknown, Msh2-dependent mechanism which induces CAG repeat expansions, independent of Msh3 and Msh6 proteins (Dragileva *et al.* 2009).

Loss of Msh6 or Pms2 was shown to cause an increased frequency and size of GAA repeat expansions in an allele dose dependent condition. Thus, intergenerational GAA repeat expansions may occur when there is insufficient expression of Msh6 or Pms2 protein to produce a normally functioning MMR system. It has previously been observed that defect of Msh6 did not increase intergenerational CAG or CTG repeat expansion frequency in HD or DM1 transgenic mice. These findings are contrary to the increased GAA repeat expansions detected in Msh6-deficient *FXN* mice. However, increased somatic CTG repeat expansion sizes were observed in some tissues from Msh6-deficient DM1 transgenic mice (van den Broek *et al.* 2002). Thus far, our study is the only one to investigate the effect of Pms2 on intergenerational TNR instability. Therefore, it would be interesting to investigate the potential effect of Pms2 on the intergenerational instability of other TNR disorders (Gomes-Pereira and Monckton 2004). Overall, the MMR system would appear to have shown more differences than similarities when comparing its effects on GAA repeat expansions

versus CAG/CTG repeat expansions. This is likely to be due to the different ways that the MMR system recognises and acts upon the secondary structures of different TNRs.

Chapter 4 - Results: The mismatch repair system causes somatic GAA repeat expansions in FRDA mouse models

4.1 - Introduction

In addition to effects on intergenerational GAA repeat transmission, it is also essential to understand the potential effects of MMR proteins on somatic GAA repeat instability. Since FRDA is a tissue-selective disorder, investigation of an *in vivo* model is considered a more useful approach than an *in vitro* model to simultaneously study the effect of these proteins on GAA repeat instability within different tissues. However, this is not possible in humans, because FRDA affects critical organs, such as brain and cerebellum. Precedents from previous *in vivo* studies have shown transgenic mice to be useful models to investigate molecular mechanisms involved in FRDA and subsequently develop potential therapies. Of the currently available FRDA mouse models, YG8 and YG22 transgenic mice are recognised as good models since they exhibit similar somatic GAA instability to FRDA patients (Al-Mahdawi *et al.* 2004). Therefore, these mice were considered as good *in vivo* systems to determine the effect of MMR protein deficits on the somatic instability of GAA repeat expansions.

4.2 - MMR effects on somatic GAA repeat instability

To understand the role of each MMR gene in somatic GAA repeat instability, it was initially important to establish human GAA repeat-containing *FXN* transgenic mice with the presence or absence of each MMR protein. Thus, the same double genetically modified mouse models, as described in chapter 3, were generated by cross-breeding FXN^{GAA+} hemizygous mice together with *MMR* heterozygous knockout mice. Following a small tail biopsy collection, genomic DNA was isolated and two different PCRs were performed (including GAA-PCR and MMR-PCR; refer to the section 3.3), to genotype the mice.

4.2.1 - *Msh2* effects on somatic instability of GAA repeat expansions

Subsequent to initial genotyping, *FXN*$^{GAA+}$/*Msh2*$^{+/+}$ and *FXN*$^{GAA+}$/*Msh2*$^{-/-}$ transgenic mice were selected for both YG8 and YG22 lines and grown to at least 6 months of age. The objective of this study was to understand the dynamics of somatic GAA repeat instability by comparing multiple tissues of *Msh2* proficient and deficient mice. Thus, somatic GAA repeat instability was analysed in two neural tissues (brain and cerebellum) and two non-neural tissues (liver and kidney) from Msh2 proficient and deficient mice of comparable age and gender, after confirming the genotypes. Analysis of tissues from *Msh2*-WT mice showed somatic GAA repeat instability for both YG8 and YG22 lines, with some expansion in the brain and the greatest expansion in the cerebellum. However, liver and kidney tissues showed stable GAA repeats. This result is consistent with previous observations indicating neural somatic tissue selectivity of progressive GAA repeat instability (Al-Mahdawi *et al.* 2004). In contrast, analysis of multiple tissues from *Msh2*-KO *FXN* transgenic mice demonstrated no significant difference in the size of GAA repeats in any tissues (Figure 4.1). Thus, a comparison of *Msh2*-WT mice with *Msh2*-KO showed that progressive somatic GAA repeat expansions were lost in all tissues with the absence of Msh2, even in the cerebellum, which is the most unstable tissue for GAA repeat instability. This finding suggests that lack of Msh2 stabilises expanded GAA repeats and prevents further somatic GAA repeat expansion instability. In other words, the presence of Msh2 is one of the factors necessary for tissue-selective progressive somatic GAA repeat expansion instability in FRDA.

Figure 4.1 - Somatic GAA repeat instability in the *Msh2* transgenic model.

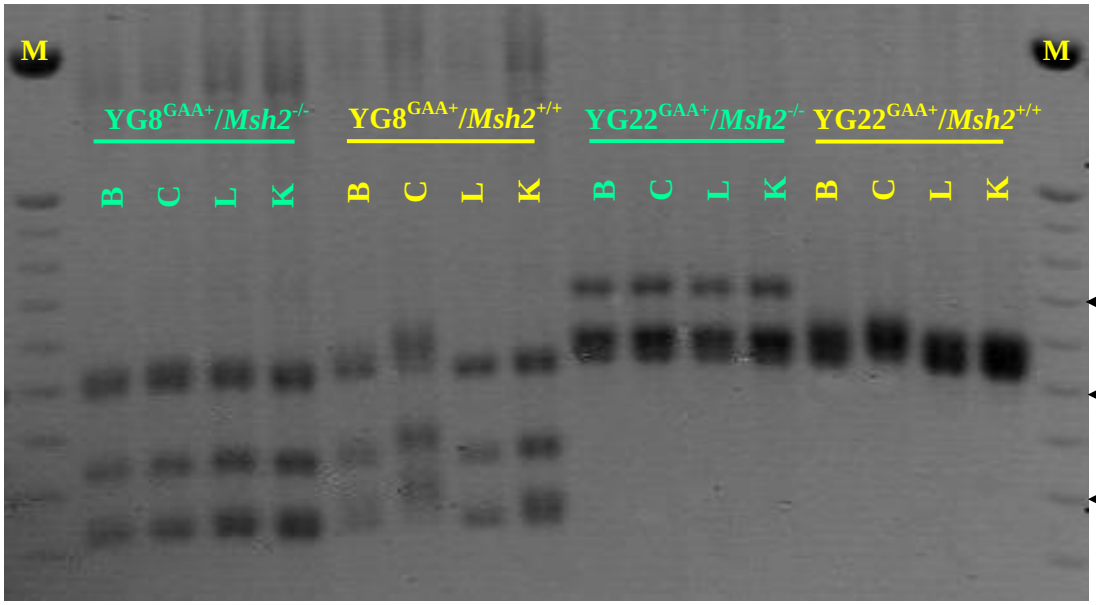

The image illustrates PCR products to determine GAA repeat sizes in 1.5% long agarose gel obtained from YG8 and YG22 multiple tissues in absence or presence of Msh2 protein. M= 100bp size marker, B= brain, C= cerebellum, L= liver, K= kidney.

4.2.2 - *Msh3* effects on somatic instability of GAA repeat expansions

Following initial genotyping, *FXN*$^{GAA+}$/*Msh3*$^{+/+}$ and *FXN*$^{GAA+}$/*Msh3*$^{-/-}$ transgenic mice were selected for YG22 lines and grown to 6 month of age. To investigate the dynamics of somatic GAA repeat instability, multiple tissues of Msh3-WT and Msh3-KO mice were compared. Somatic GAA repeat instability was analysed in two neural tissues (brain and cerebellum) and two non-neural tissues (heart and liver) from Msh3 proficient and deficient mice. As with the *Msh2* mouse model, analysis of *FXN* GAA repeats within different tissues from *Msh3*-WT mice identified somatic GAA repeat instability, with greater expansions particularly in cerebellum, as previously described (Al-Mahdawi *et al.* 2004). Analysis of multiple tissues from *Msh3*-KO mice showed no significant difference in the size of GAA repeats in any tissue (Figure 4.2). This observation suggests that, as with Msh2, loss of Msh3

protects against somatic GAA repeat expansions. Therefore, it is tempting to speculate that Msh3 might be a factor causing tissue selectivity of somatic GAA repeat expansions in FRDA.

Figure 4.2 - Somatic GAA repeat instability in the *Msh3* transgenic model.

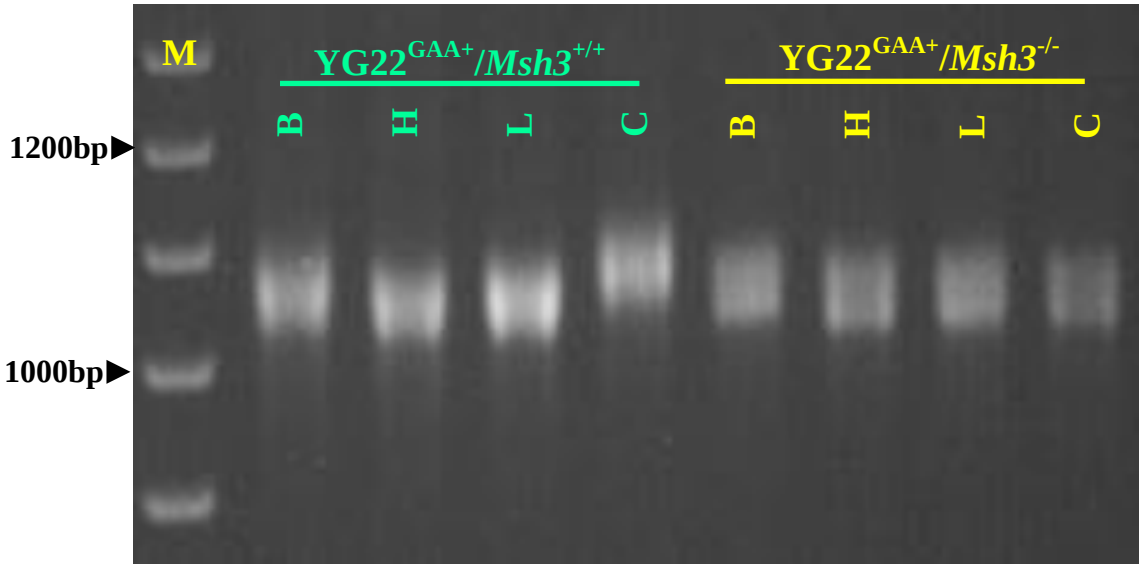

The image illustrates PCR products to determine GAA repeat sizes in 1.5% long agarose gel obtained from YG22 multiple tissues in absence or presence of Msh3 protein. M= 100bp size marker, B= brain, C= cerebellum, L= liver, H= heart.

4.2.3 - *Msh6* effects on somatic instability of GAA repeat expansions

Subsequent to initial genotyping, *FXN*$^{GAA+}$/*Msh6*$^{+/+}$ and *FXN*$^{GAA+}$/*Msh6*$^{-/-}$ transgenic mice were selected for YG22 lines and grown to 4 month of age. The aim of this study was to determine the dynamics of somatic GAA repeat instability by comparing multiple tissues of Msh6 proficient and deficient mice. Thus, somatic GAA repeat instability was assessed in two neural tissues (brain and cerebellum) and two non-neural tissues (heart and liver) from Msh6-WT and Msh6-KO mice of comparable age and gender. Comparing *FXN* GAA repeats

within different tissues of *Msh6*-WT mice showed somatic GAA repeat instability in the YG22 line, with greater expansions particularly in cerebellum (Figure 4.3), as previously described (Al-Mahdawi *et al.* 2004). Investigations showed no difference in the size of the expanded GAA repeats in heart and brain tissues from both *Msh6*-WT and *Msh6*-KO mice. However, the results demonstrated changes in the cerebellum and to a lesser extent in the liver. Analysis of these tissues showed that there is still some residual GAA repeat expansion, but the extent of the expansion is not as great as in the WT mouse (Figure 4.3). Thus, it is proposed that Msh6 promotes further expansions of GAA repeats, while absence of this protein leads to reduced size of expanded GAA repeats, particularly in cerebellum tissue. Therefore, most likely Msh6 promotes somatic GAA repeat expansion to a lesser degree than Msh2 and Msh3.

Figure 4.3 - Somatic GAA repeat instability in the *Msh6* transgenic model.

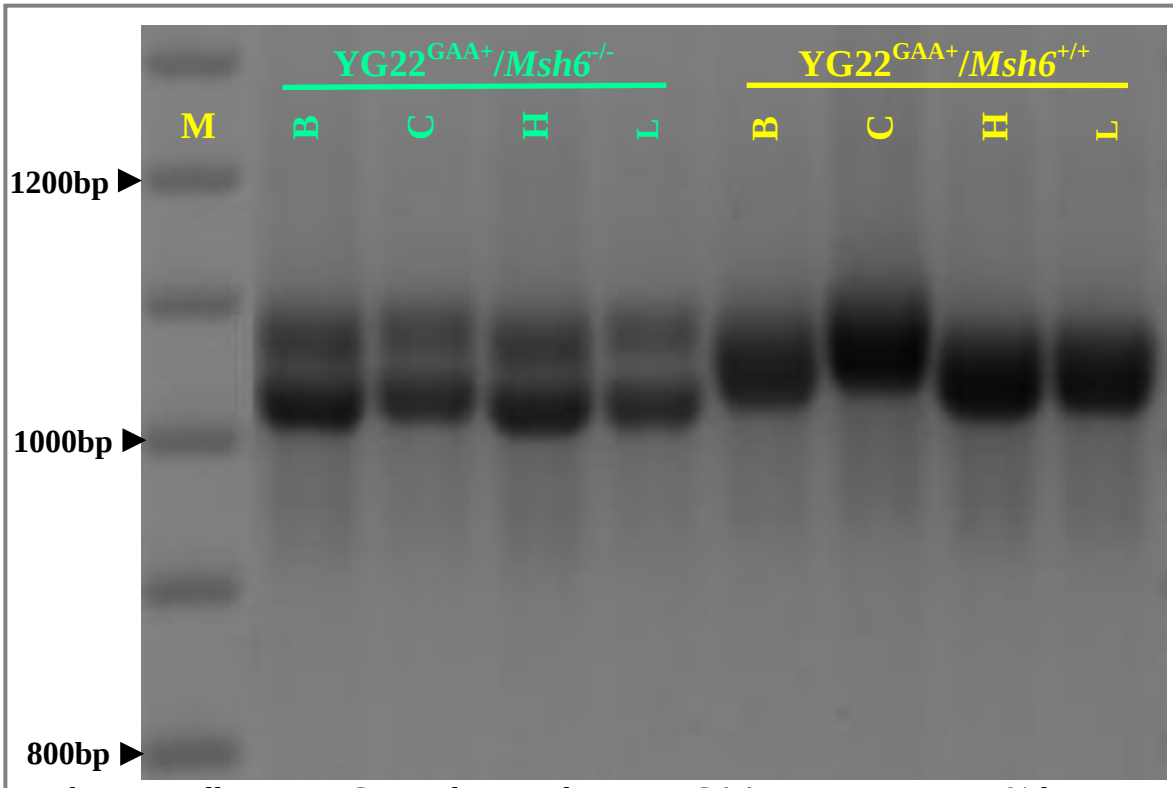

The image illustrates PCR products to determine GAA repeat sizes in 1.5% long agarose gel obtained from YG22 multiple tissues in absence or presence of Msh6 protein. M= 100bp size marker, B= brain, C= cerebellum, H= heart, L= liver.

4.2.4 - *Pms2* effects on somatic instability of GAA repeat expansions

Following initial genotyping, *FXN*$^{GAA+}$/*Pms2*$^{+/+}$ and *FXN*$^{GAA+}$/*Pms2*$^{-/-}$ transgenic mice were selected for YG8 lines and grown to at least 5 month of age. The objective of this experiment was to understand the dynamics of somatic GAA repeat instability by comparing multiple tissues of Pms2 proficient and deficient mice. Thus, somatic GAA repeat instability was analysed in two neural tissues (brain and cerebellum) and two non-neural tissues (heart and liver) from *Pms2*-WT and *Pms2*-KO mice.

Previously Al-Mahdawi and colleagues reported tissue selectivity of somatic GAA repeat expansions, indicating most instability with cerebellum tissue (Al-Mahdawi *et al.* 2004). Similarly, analysing multiple tissues of the *Pms2*-WT mouse showed that the frequency of expanded GAA repeats were increased in brain and particularly cerebellum compared with heart and liver tissues (Figure 4.4). This condition was also observed with *Pms2*-KO mouse. In other words, the tissue-selective progressive GAA repeat expansion was still observed even with the loss of Pms2. In fact, an even greater degree of GAA repeat expansions was observed in brain, and particularly cerebellum, with loss of Pms2 (Figure 4.4). Subsequently, Bourn and colleagues have confirmed these observations by performing small-pool GAA PCR of the same mouse tissues. They have confirmed that loss of Pms2 actually increases the GAA repeat instability towards expansions particularly in cerebellum and DRG tissues (Bourn *et al* 2012). This finding is contrary to the other mismatch repair observations (Msh2, Msh3 or Msh6), suggesting that Pms2 plays a different role in the tissue selectivity of GAA repeat expansions in FRDA. Thus, it is proposed that the presence of Pms2 might protect against further expansion of somatic GAA repeats, particularly in tissues that are highly sensitive to reduced levels of frataxin.

Figure 4.4 - Somatic GAA repeat instability in the *Pms2* transgenic model.

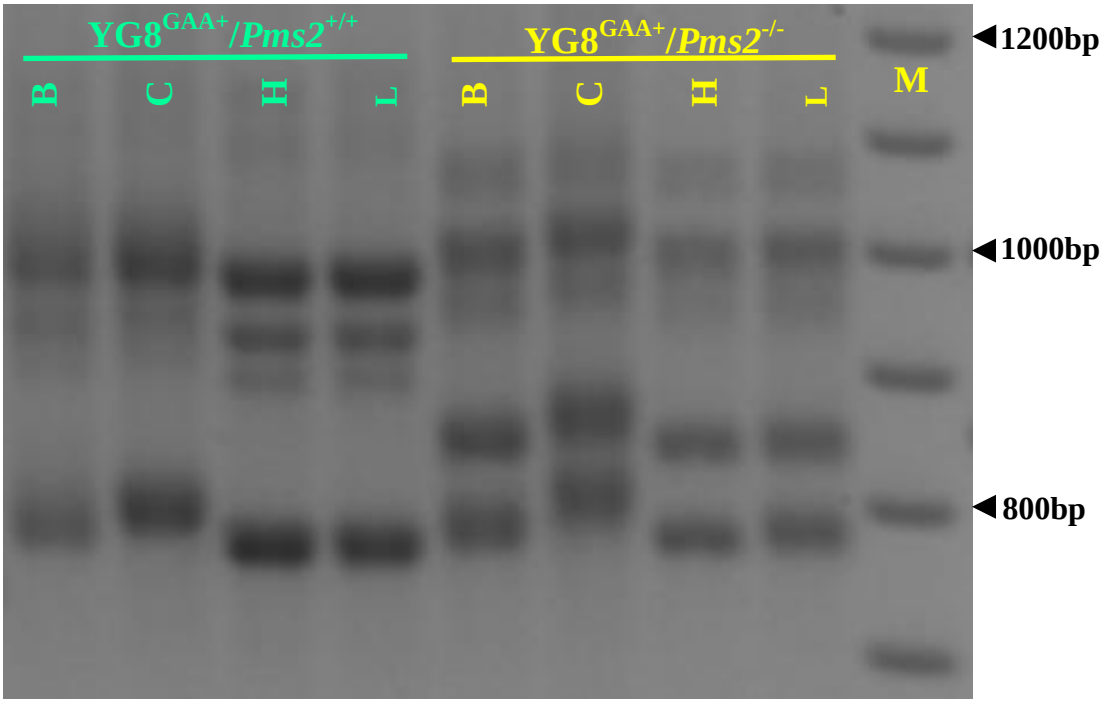

The image illustrates PCR products to determine GAA repeat sizes in 1.5% long agarose gel obtained from YG8 multiple tissues in absence or presence of Pms2 protein. M= 100bp size marker, B= brain, C= cerebellum, H= heart, L= liver.

4.2.5 - *Mlh1* effects on somatic instability of GAA repeat expansions

Subsequent to initial genotyping, *FXN*$^{GAA+}$/*Mlh1*$^{+/+}$ and *FXN*$^{GAA+}$/*Mlh1*$^{-/-}$ transgenic mice were selected for YG22 lines and grown to 3 months of age. Due to the tumour-forming effects caused by disruption of Mlh1 protein, the *Mlh1*-KO transgenic mice did not survive for more than 3 months. After confirming genotypes, to find out the dynamics of somatic GAA repeat instability, multiple tissues of *Mlh1*-WT and *Mlh1*-KO mice were compared together. In this study, somatic GAA repeat instability was analysed in two neural tissues (brain and cerebellum) and two non-neural tissues (heart and liver) from Mlh1 proficient and deficient mice.

Comparing multiple tissues from *Mlh1*-WT mice showed somatic GAA repeat instability, with greater expansions particularly in the cerebellum (Figure 4.5), as previously described (Al-Mahdawi *et al.* 2004). In contrast, tissues from *Mlh1*-KO mice showed no difference in the size of the GAA repeats. Thus, it was determined that the presence of Mlh1 caused somatic GAA repeat expansions, particularly in the cerebellum, while the absence of Mlh1 caused stabilisation of GAA repeats (Figure 4.5). These findings suggest that, as with Msh2 and Msh3, loss of Mlh1 results in stabilisation of GAA repeats. Therefore, it is proposed that Mlh1 protein is a necessary factor for tissue-selective somatic GAA repeat expansion in FRDA.

Figure 4.5 - Somatic GAA repeat instability in the *Mlh1* transgenic model.

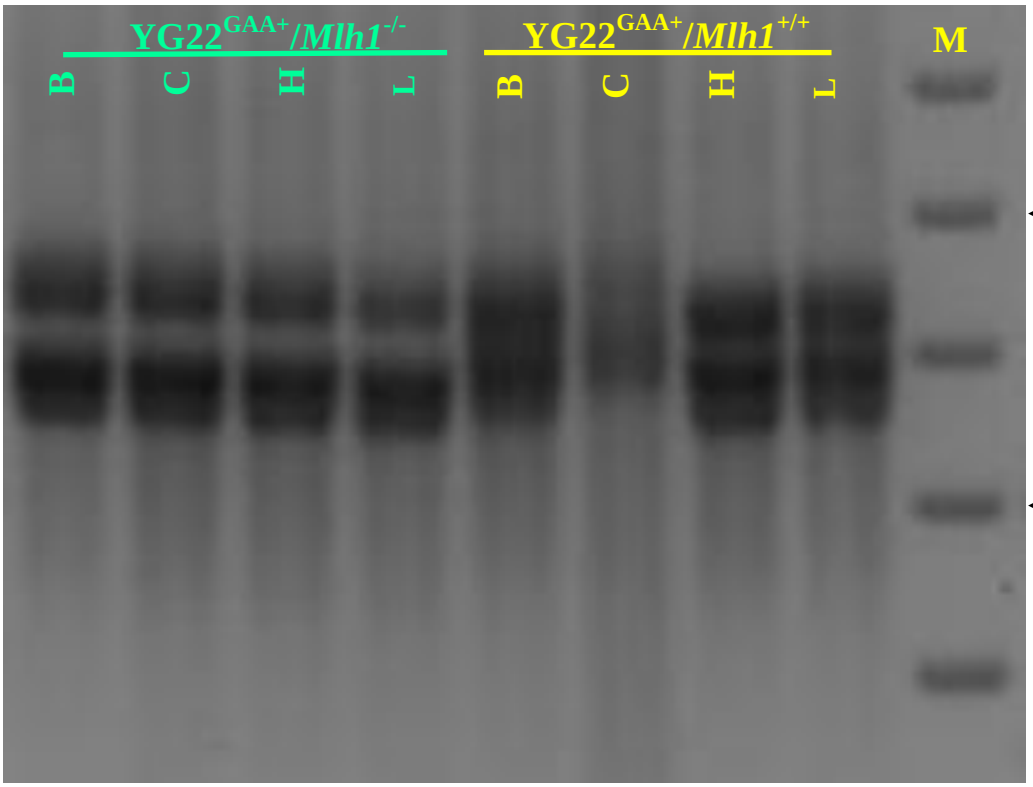

The image illustrates PCR products to determine GAA repeat sizes in 1.5% long agarose gel obtained from YG22 multiple tissues in absence or presence of Pms2 protein. M= 100bp size marker, B= brain, C= cerebellum, H= heart, L= liver.

4.3 - Discussion

To understand the potential molecular mechanisms of somatic GAA repeat expansion instability in FRDA, the role of MMR proteins Msh2, Msh3, Msh6, Pms2 and Mlh1 were investigated in multiple tissues from YG8 and YG22 transgenic mice. In this chapter, the results first revealed GAA repeat instability towards further expansion within neural tissues for each of the *Msh2*-WT, *Msh3*-WT, *Msh6*-WT, *Pms2*-WT and *Mlh1*-WT mice, confirming previously reported tissue selectivity of somatic GAA repeat expansions (Al-Mahdawi *et al.* 2004). The results further showed that deficiency of each of the individual MMR genes could affect somatic GAA repeat expansions within different tissues. However, it seems that the MMR proteins do not all play the same functional role. Lack of Msh2, Msh3, Msh6 or Mlh1 proteins resulted in stabilisation of the expanded GAA repeats in somatic cells. This might be due to either MMR protection against further GAA repeat expansions or induction of GAA repeat contractions in neural tissues, which appear to be the most sensitive tissues to frataxin deficiency. These findings also highlight two points. Firstly, the similar effect of these proteins on somatic GAA repeat expansions suggests that they may cooperate functionally. This would agree with the generally accepted role of the MutS MMR system, which acts as MutSα (Msh2/Msh6) and MutSβ (Msh2/Msh3) heterodimers. Thus, disruption of Msh2, Msh3 or Msh6 proteins may cause dysfunction of one (Msh3 or Msh6) or both (Msh2) MutS heterodimers and subsequently have an effect on the frequency of somatic GAA repeat expansions. However, it is possible that the MutSα and MutSβ complexes interact differently with GAA loops. Provided they have similar functions, then MutSβ (Msh2/Msh3) could compensate for the absence of Msh6 deficits and subsequently cause GAA repeat expansions, and vice versa. However, if the MutS complexes do not act similarly, then each of the Msh3 or Msh6 protein deficits could result in loss of a MutS complex function that prevents further

GAA repeat expansion, which agrees with the results in this thesis. Dysfunction of each MutS complex may prevent binding between the Msh2-ATPase domains of relevant MutS heterodimers to expanded GAA repeat loops. The absence of MutS proteins at the GAA repeat could consequently lead to efficient repair of the expanded GAA repeats by other DNA repair systems. Secondly, the effects of each of the Msh2, Msh3 or Msh6 proteins on GAA repeat stability promotes the idea that, not only are these proteins unable to repair mutations as MutSα or MutSβ heterodimers, leading to further GAA repeat expansions in neural tissues, but also that they may themselves cause increased frequency of the expanded GAA repeats by as yet unknown mechanisms.

The findings of reduced somatic GAA repeat expansions in the *Msh2*$^{-/-}$ and *Msh3*$^{-/-}$ mice are in agreement with recent investigations of GAA repeat-containing human cellular systems (Halabi *et al.* 2012). Previous studies of HD and DM1 transgenic mice also showed similar effects of *Msh2* and *Msh3* deficits on CAG and CTG repeat expansions (van den Broek *et al.* 2002; Savouret *et al.* 2003; Wheeler *et al.* 2003; Tome *et al.* 2009). This suggests a common MMR mechanism by which all expanded TNR sequences undergo further expansions through MutSβ heterodimers function. Therefore, aberration of Msh2 and/or Msh3 could protect TNR against expansions. Moreover, the results also show that Msh6 protein can increase the level of GAA repeat expansions. This finding has been confirmed by small-pool PCR studies carried out by Bidichandani and colleagues, showing a quantitatively significant effect of Msh6 on the expanded GAA repeats in *FXN* transgenic mice (Bourn *et al.* 2012). These findings suggest that interaction of Msh2-Msh6, as MutSα heterodimers, could also affect GAA repeat instability. In contrast, there might be a notable difference in the way that MutSα heterodimers act on the expanded GAA versus CAG or CTG repeats, since the loss of GAA repeat expansions in *FXN*$^{GAA+}$/*Msh6*$^{-/-}$ mice has not been observed with CAG and CTG repeat expansions in HD and DM1, respectively (van den Broek *et al.* 2002; Savouret *et al.*

2003; Wheeler *et al.* 2003; Tome *et al.* 2009). The mechanisms by which MutS complexes affect the GAA repeat expansions are not clear yet. However, it is proposed that non-canonical looped-DNA structures may be a potential mutagenic cause of TNR expansions by binding with the MutS heterodimers and blocking the related ATPase activity. For example, it has been reported that the ATPase domain is a critical part of MSH2, playing a role in the full function of MSH2 protein within MutSβ complexes of MMR system. Thus, absence of this domain might lead to a condition similar to total lack of MSH2, particularly in some TNR diseases (Tome *et al.* 2009). Binding of the MSH2 ATPase domain with a TNR non-canonical loop structure may lead to error-prone instability within expanded TNR sequences, although the exact mechanism of this event are yet to be determined. Investigations have shown that reduced ATPase activity of the MutSβ complex upon binding to CAG hairpins causes blockage of ATPase activity and impaired repair of CAG hairpins, leading to further CAG repeat expansion (Owen *et al.* 2005). Other studies have shown that lack of ATPase activity causes reduced levels of somatic and intergenerational expansions in DM1 CTG repeats, demonstrating the necessity of functional MSH2-ATPase activity within a functional MMR system for TNR expansion (Tome *et al.* 2009).

In the case of somatic GAA repeat expansions, it is proposed that loss of Msh2, Msh3 or Msh6 could result in dysfunction of MutSα and/or MutSβ heterodimers and most likely prevent unusual binding of MutS heterodimers to GAA loops. This event may consequently cause a reduced level of error-prone expansion-biased instability within expanded TNR sequences. On the other hand, recent investigations suggest that MutS complexes might act upon secondary structures caused by GAA repeat expansions via R-loops and DNA-DSBs. Different studies have shown that R-loops can cause further expansions in GAA repeats (Soragni *et al.* 2008; Ditch *et al.* 2009; Rindler and Bidichandani 2011). R-loops could be caused by binding of a nascent mRNA with the transcriptional template strand. However, this

is not a normal event during transcription. Nonetheless, it has been reported that R-loops can occur during transcription of GAA repeats. Several factors may contribute to R-loop formation, such as defective biogenesis of messenger ribonucleoprotein (mRNP) or lack of splicing factors (Aguilera and Gomez-Gonzalez 2008; Bourn *et al.* 2012). It is plausible that GAA repeat expansion sequences may themselves induce abnormal splicing. Furthermore, it is recognised that lack of some splicing factors, such as ASF (also called SF2), can lead to DSB formations (Aguilera and Gomez-Gonzalez 2008). In addition, it is believed that DSBs could occur in neuronal tissues through each of the HR or NHEJ pathways (Merlo *et al.* 2005; Fishel *et al.* 2007; Aguilera and Gomez-Gonzalez 2008). MMR proteins are also involved in DSB repair via the DNA damage response, HR and NEHJ (Zhang *et al.* 2009; Shahi *et al.* 2011). Investigations have shown that a highly error-prone DSB repair system across the GAA repeat sequences that may lead to dramatically increased instability of the repeats (Pollard *et al.* 2008). In summary, it is proposed that the MMR system may be recruited to repair DSBs within GAA repeat R-loops, leading to further GAA expansions. This hypothesis is consistent with the results obtained in this thesis, not only from Msh2, Msh3 and Msh6, but also from Mlh1 proteins.

It has also been shown in this chapter that Pms2 can protect against progressive somatic GAA repeat expansions. Small-pool PCR investigations, carried out by Bidichandani and colleagues, have also confirmed this Pms2 effect (Bourn *et al.* 2012). Curiously, this finding is contrary to the results observed with the other MMR proteins. It is also contrary to the investigations of DM1 transgenic mice, which show depletion Pms2 protein to cause a reduced CTG repeat expansions (Gomes-Pereira *et al.* 2004). The reasons for these differences are not clear. However, it is proposed that Pms2 may not be acting in the usual MMR mechanism to protect GAA repeats against expansions, but may be acting through an Msh2-independent manner (Siehler *et al.* 2009). For instance, it has been reported that Pms2

is able to protect other microsatellites, such as tetramer repeats, against expansions in conditions of non-hairpin-formation (Bourn *et al.* 2012).

As with the intergenerational studies, analysis of somatic tissues has shown that Mlh1 promotes GAA repeat expansions, while Pms2 was found to protect against GAA repeat expansions. To my knowledge, these data are the first to identify a potential role for Mlh1 in somatic TNR instability. The mechanism by which Mlh1 causes greater GAA repeat expansions is unknown. Nonetheless, similar to MutS-complex proteins, it is proposed that Mlh1 causes error-prone instability within expanded GAA repeat sequences either by binding of the ATPase domain with a GAA hairpin or by repairing DSBs caused by R-loops. Mlh1 is an important ATPase member of the MMR system and it is recognised as a regulator of DSB formation. Therefore, Mlh1 could bind via its ATPase domain with secondary structures of GAA repeats, most probably R-loops, and repair DSBs in an error-prone expansion-oriented manner. This hypothesis is consistent with recent investigations that show Mlh1 to play an important role, through its ATPase activity, in DNA end processing and NHEJ error-prone DSB repair (Chahwan *et al.* 2012).

In conclusion, somatic GAA repeat expansions appear to arise from the complex interplay of several different molecular mechanisms, one of which is the MMR system. Further investigations are required to determine the precise mechanisms by which MMR proteins and the other molecular mechanisms are involved in somatic GAA repeat expansions, and thereby to identify potential targets for FRDA therapy.

Chapter 5 - Results: The mismatch repair system affects *FXN* transcription

5.1 - Introduction

Frataxin is a fundamental mitochondrial protein expressed in all cells. Previous studies have shown that there is a link between the greater size of expanded GAA repeats and lower *FXN* transcription level in FRDA human (Greene *et al.* 2007; Al-Mahdawi *et al.* 2008). Further studies have shown similar effects by investigating YG8 FXN^{GAA+} and YG22 FXN^{GAA+} transgenic mice (Figure 5.1).

Figure 5.1 - Analysis of FXN^{GAA+} mouse transcription levels (Al-Mahdawi *et al.* 2008)**.**

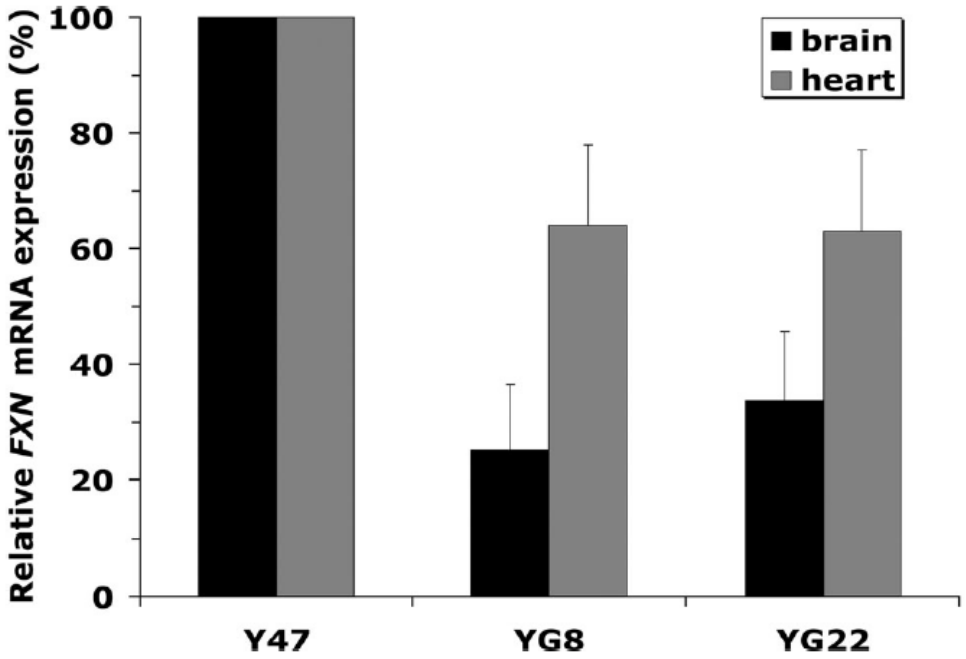

The image represents qRT-PCR analysis of transgenic *FXN* mRNA isolated from Y47 (9 GAA repeats), YG8 (190+90 GAA repeats) and YG22 (190 GAA repeats) mouse brain and heart tissues, normalised to the mean Y47 *FXN* mRNA level taken as 100%.

In the previous chapter, I showed that defects of MMR genes influence somatic GAA repeat expansion instability in different tissues, particularly the cerebellum. However, it is not yet clear whether such instability caused by MMR gene deficits is linked to changes in *FXN* transcriptional levels. To investigate this, YG8 FXN^{GAA+} and YG22 FXN^{GAA+} transgenic mice

were used as *in vivo* systems to determine the effect of MMR protein deficiencies on *FXN* transcription levels. Since prior analysis of *FXN*$^{GAA+}$/*MMR* models had shown brain and cerebellum to be the most sensitive tissues to GAA repeat instability (refer to the chapter 4), the levels of *FXN* transcription were measured in these tissues from different MMR-modified mice by qRT-PCR analysis. The effects of MMR deficiencies on *FXN* transcription were also analysed *in vitro*, using two human epithelial cell lines: HCT-116 (a MMR deficient epithelial cell line causing HNPCC) and NCM-460 (an epithelial unaffected MMR cell line). The use of an *in vitro* model could lead to further understanding of mechanisms by which MMR proteins affect the *FXN* transcription level, in addition to investigating potential differences between the *in vitro* and *in vivo* models.

5.2 - Analysis of cDNA quality

By using the Trizol® method, total RNA was isolated from brain and cerebellum tissues of those YG22 *FXN*$^{GAA+}$/*MMR* transgenic mice which were previously used to study the correlation of MMR proteins with GAA repeat instability (refer to the chapter 4). Similarly, in the case of *in vitro* models, total RNA was isolated from about one million human epithelial cells. Total RNA samples were treated with DNase I enzyme to prevent potential genomic DNA contamination. Following analysis of total RNA quality and quantity, the concentrations were adjusted to 400-500ng/µl and the RNA was converted to cDNA. The quality of cDNA was initially confirmed by performing standard *FXN* RT-PCR and *GAPDH* endogenous control RT-PCR experiments. Analysis of the standard *FXN* RT-PCR products on agarose gels showed a specific *FXN* product of 172bp for all transgenic mice and human epithelial cell line samples (Figure 5.2A). In the case of mouse tissues, analysis of *Gapdh*-RT-PCR products on agarose gels showed a specific 81bp fragment (Figure 5.2B). In

contrast, analysis of human *GAPDH*-RT-PCR products revealed a specific band with length of 226bp in human epithelial samples (Figure 5.2C). In all cases, observation of a specific fragment and no primer-dimer confirmed the adequate quality and quantity of cDNA samples to subsequently use for qRT-PCR.

Figure 5.2 - Standard RT-PCR analysis.

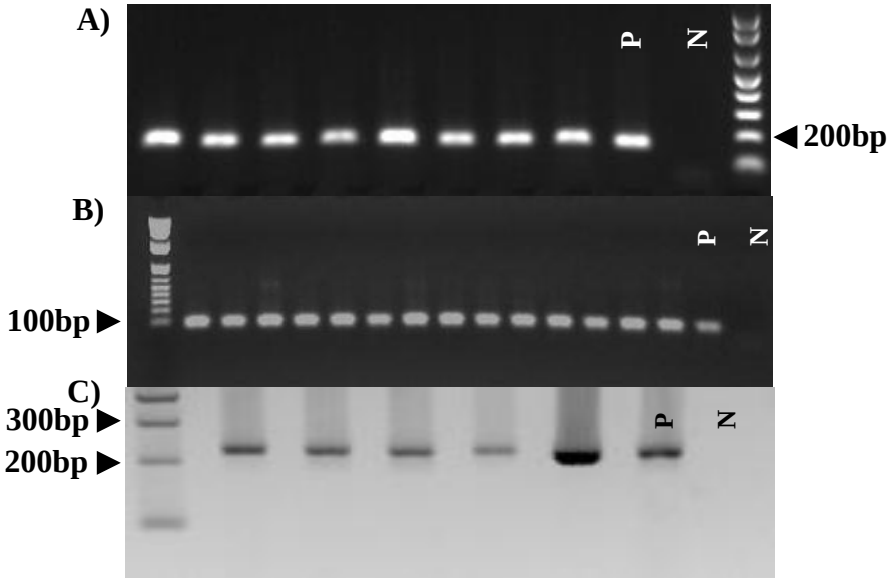

The images show PCR products from **(A)** human *FXN*-RT-PCR, **(B)** mouse *Gapdh*-RT-PCR, and **(C)** human *GAPDH*-RT-PCR run in ethidium bromide-stained 1% agarose gels, together with 1Kb^{+} size markers. P= positive control, N= negative control.

5.3 - Quantification of *FXN* mRNA in mouse tissues

To determine the level of *FXN* transcription, tissues from YG22 *FXN*$^{GAA+}$ transgenic mice with different MMR genotypes (*MMR*-WT and *MMR*-KO) were analysed by qRT-PCR. In as much as some transgenic mice also carried a normal mouse *Fxn* gene, in this experiment, it was essential to use two human *FXN*-transgene specific primers to enable *FXN*-transgene specific qRT-PCR. To quantify the *FXN* expression levels, the Ct values

obtained for *FXN* mRNA were normalised to those for mouse *Gapdh* mRNA, as the endogenous control. Each sample was run in triplicate (Figure 5.3A) and each experiment was performed at least twice. The mean value of each individual triplicate sample was applied for further calculations using the $2^{-\Delta\Delta Ct}$ method to find relative quantification (RQ) values. Later, relative transcription levels of *FXN* from both *MMR*-WT and *MMR*-KO mouse tissues were calibrated by calculating the RQ mean values, followed by setting the *MMR*-WT group arbitrarily as 100%. The mean age of each group of mice was matched throughout all mRNA quantification experiments to prevent any age dependent variability. Following the qRT-PCR amplification program, the quality of the target and endogenous (*FXN* and *Gapdh*) cDNA products, with no primer-dimer formation, were confirmed by performing dissociation curve analysis (Figure 5.3B, Figure 5.3C).

Figure 5.3 - qRT-PCR analysis.

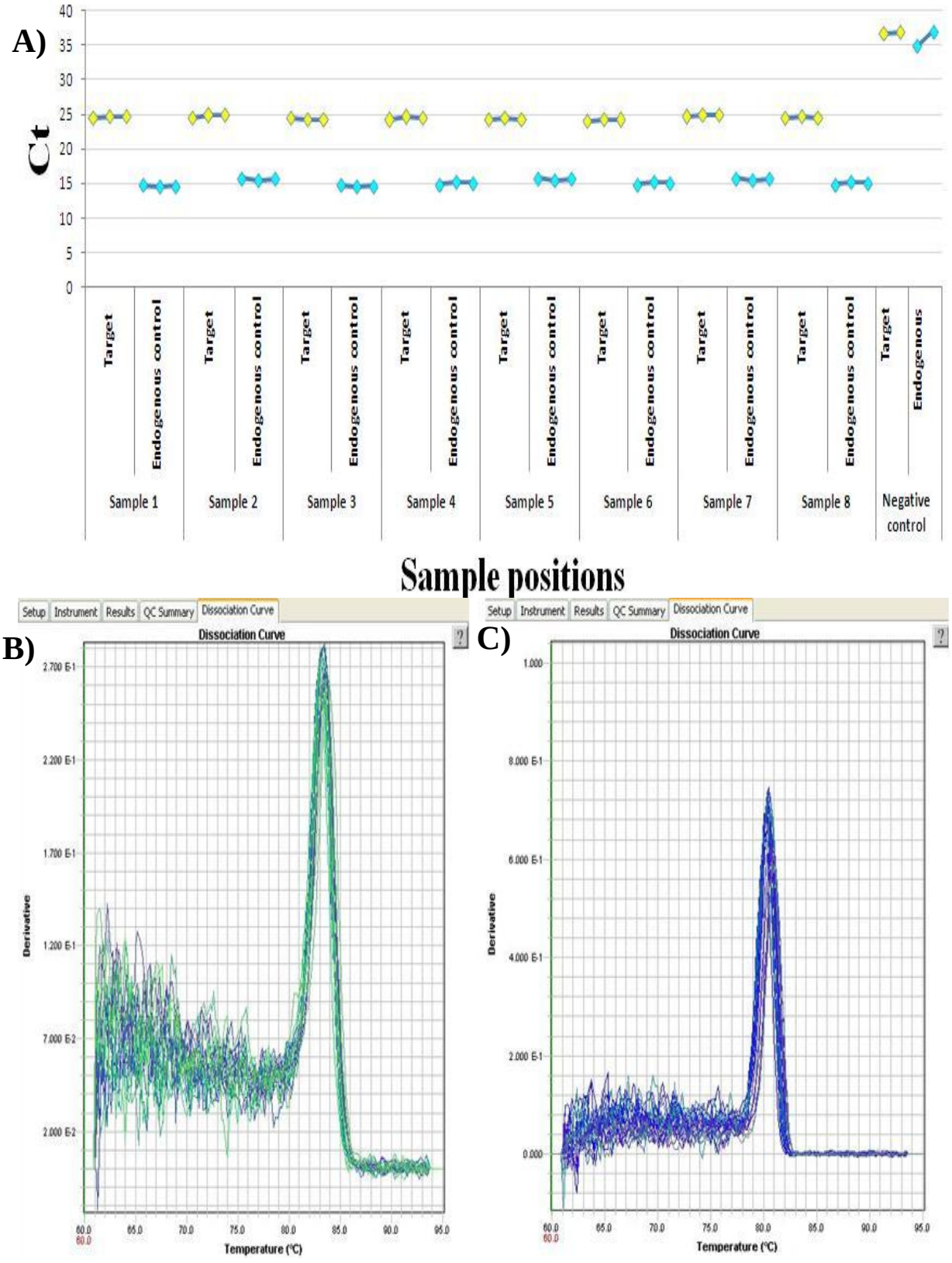

The images show **(A)** Ct of each individual triplicate sample for *FXN* and *Gapdh* cDNAs, **(B)** dissociation curve for RT-*Gapdh* primers, and **(C)** dissociation curve for RT-*FXN* primers.

5.3.1 - Effect of *Msh2* on human transgenic *FXN* transcription

To investigate the effects of Msh2 on *FXN* transcription, 22 *Msh2*-WT with 18 *Msh2*-KO genotypes were analysed. The mean age of each group was approximately 7.5 months. The mRNA level of *FXN* was analysed in brain and cerebellum tissues based on: (i) *Msh2* genotypes: *Msh2*-WT and *Msh2*-KO; (ii) age of genetically modified *Msh2* mice: 6-7 months and 8-9 months; (iii) gender of genetically modified *Msh2* mice: male and female.

- Brain tissue: To assess any possible age effect on *FXN* transcription in brain tissue in the absence or presence of the Msh2 protein, transgenic mice aged 6-7 months (WT n=10, KO n=6) were compared with mice aged 8-9 months (WT n=12, KO n=12). Data analysis showed no statistically significant difference of the *FXN* transcription level between higher age (8-9 months) and lower age (6-7 months) for both *Msh2*-WT and *Msh2*-KO (Figure 5.4).

Figure 5.4 - Effect of Msh2 on the *FXN* transcription level of brain tissues in different age groups.

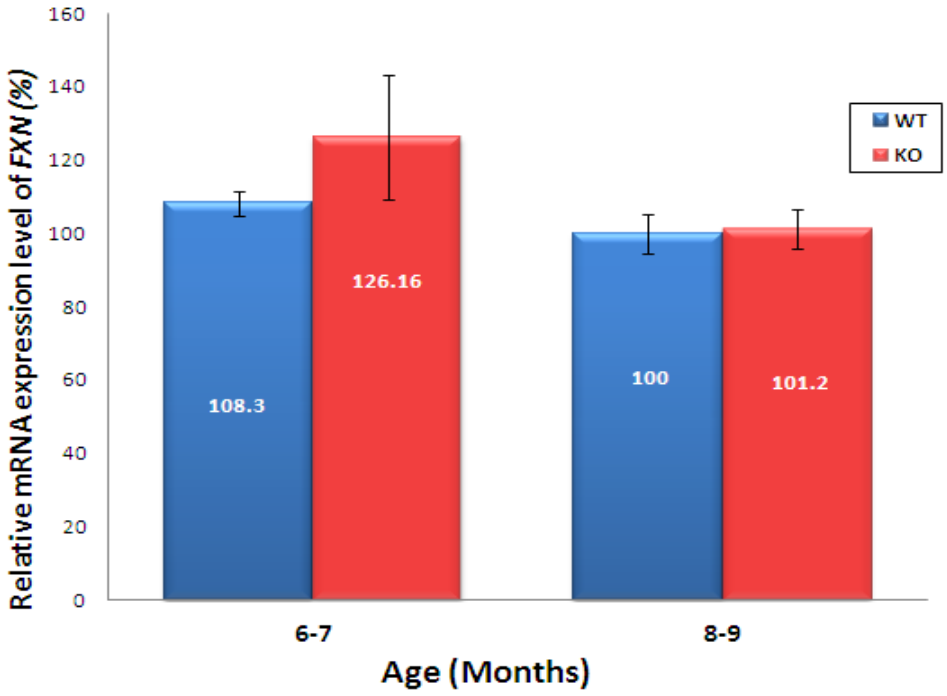

The image represents qRT-PCR analysis of transgenic *FXN* mRNA isolated from brain tissues of 6-7 months (WT n=10, KO n=6) and 8-9 months (WT n=12, KO n=12) mice with different modifications of *Msh2*, normalised to the mean *FXN* mRNA level found in the 8-9 months of age *Msh2*-WT control samples and taken as 100%. Error bars= S.E.M.

To investigate whether the *FXN* transcription level of brain tissue is affected by sex in the absence or presence of Msh2, female samples (WT n=6, KO n=8) were compared with male samples (WT n=16, KO n=10). Curiously, the data showed contrary results in male mice compared with female mice. Thus, the mRNA level of *FXN* was significantly increased with *Msh2*$^{-/-}$ in the male, compared with *Msh2*$^{+/+}$ (Figure 5.5). In contrast, there was a significantly reduced level of *FXN* transcription with *Msh2*$^{-/-}$ in female brain tissue. Comparing *Msh2*-WT brain tissues showed that the *FXN* mRNA level was increased in female (119.5%) compared with male mice (normalised as 100%; $p<0.05$); while analysing *Msh2*-KO mice revealed that the level of *FXN* transcription was increased in male (about 1.5 fold) compared with female mice (86%; $p<0.001$). These findings indicate a modification due to sex of the Msh2 effect on *FXN* transcription in brain tissue, suggesting that absence of Msh2 could increase *FXN* transcription in males, while it decreases *FXN* transcription in females.

Figure 5.5 - Effect of Msh2 on the *FXN* transcription level of brain tissues in different genders.

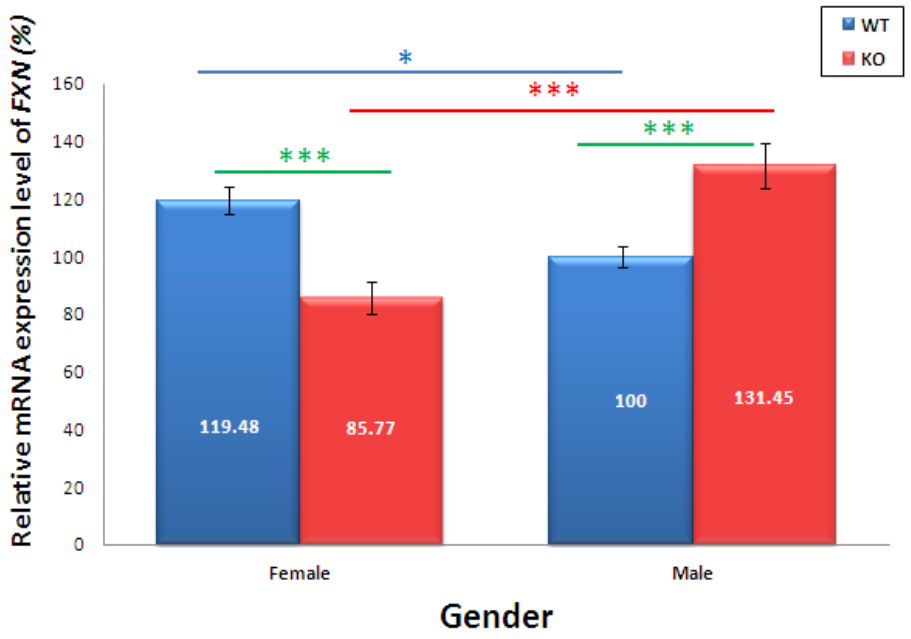

The image represents qRT-PCR analysis of transgenic *FXN* mRNA isolated from brain tissues of female (WT n=6, KO n=8) and male (WT n=16, KO n=10) mice with different modifications of *Msh2*, normalised to the mean *FXN* mRNA level found in the male *Msh2*-WT control samples and taken as 100%. Error bars= S.E.M, *= $p<0.05$, ***= $p<0.001$

Subsequently, the relative quantification of *FXN* transcription in brain tissues, based only upon *Msh2* modifications, was identified by qRT-PCR. Analysing the data showed no difference in the *FXN* transcription with loss of Msh2 protein (Figure 5.6), possibly due to the contrary effects of Msh2 of the different genders cancelling each other out.

Figure 5.6 - Effect of Msh2 on the *FXN* transcription in brain tissue.

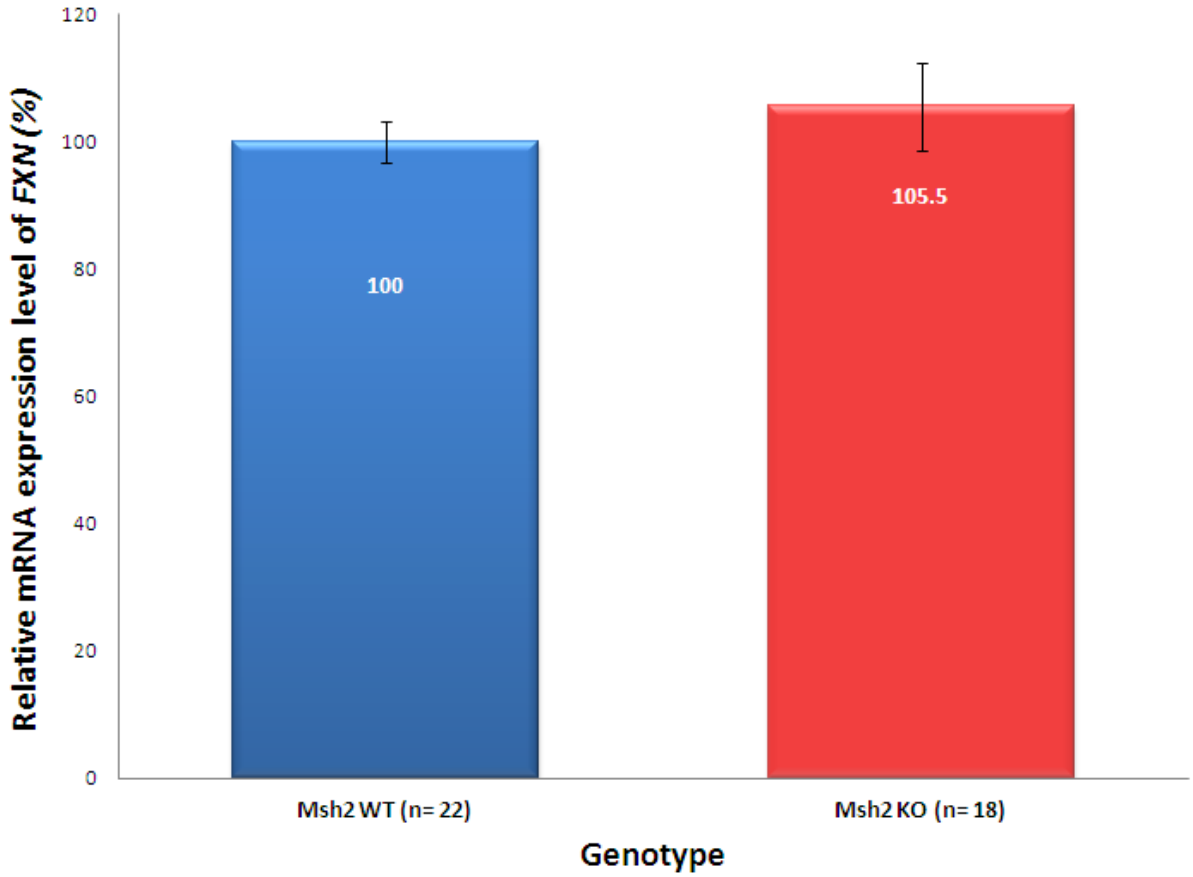

The image represents qRT-PCR analysis of transgenic *FXN* mRNA isolated from brain tissues of *Msh2*-WT and *Msh2*-KO mice, normalised to the mean *FXN* mRNA level found in the *Msh2*-WT control samples and taken as 100%. Error bars= S.E.M.

- Cerebellum tissue: Age effects on the *FXN* transcription level from cerebellum tissues, in the absence or presence of the Msh2 protein, were investigated by comparing samples of 8-9 month-old mice (WT n=10, KO n=12) with 6-7 month-old mice (WT n=12, KO n=6). Data analysis showed that the transcription level of *FXN* was increased in the absence of Msh2 protein with both age groups (Figure 5.7). With regards to previous reports indicating

that larger GAA repeat expansions cause reduced level of *FXN* transcription (Greene *et al.* 2007; Al-Mahdawi *et al.* 2008), the finding here is consistent with my previous results showing that lack of Msh2 reduced somatic GAA repeat expansions (refer to the chapter 4). Further analysis revealed that *FXN* transcription was increased in older *Msh2*$^{-/-}$ (151%) compared with younger *Msh2*$^{-/-}$ mice (128%; p=0.08), while in the presence of Msh2 similar levels of *FXN* transcription were observed. Therefore, comparing brain and cerebellum tissues, it is suggested that any age dependent effect of Msh2 on *FXN* transcription levels is also dependent on the tissue type.

Figure 5.7 - Effect of Msh2 on the *FXN* transcription level of cerebellum tissues in different age groups.

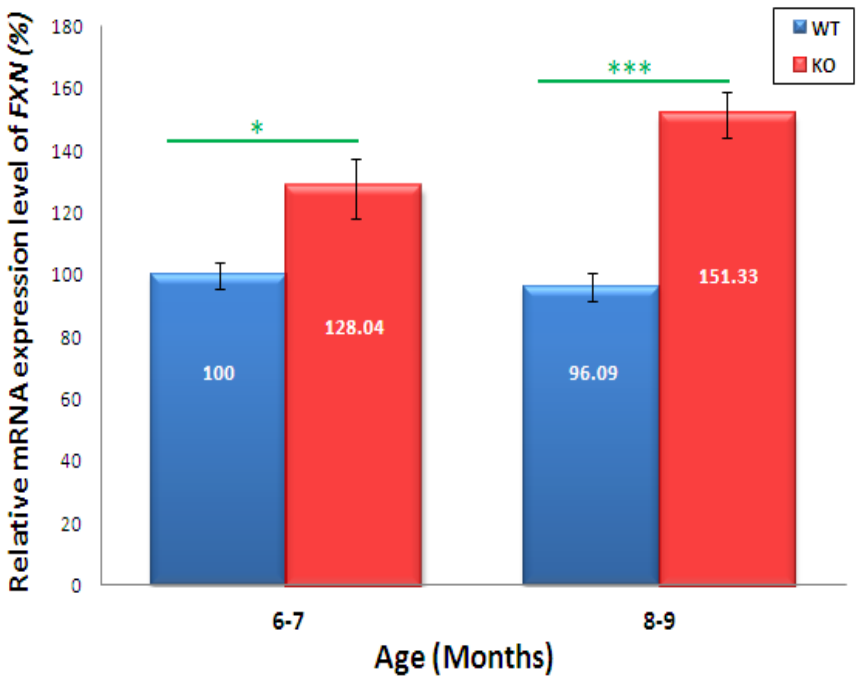

The image represents qRT-PCR analysis of transgenic *FXN* mRNA isolated from cerebellum tissues of 6-7 months (WT n=12, KO n=6) and 8-9 months (WT n=10, KO n=12) mice with different modifications of *Msh2*, normalised to the mean *FXN* mRNA level found in the 6-7 months of age *Msh2*-WT control samples and taken as 100%. Error bars= S.E.M, *= p<0.05, ***= p<0.001

To study whether the *FXN* transcription level of cerebellum tissue is modified by sex in the absence or presence of Msh2, female (WT n=6, KO n=8) were compared with male samples

(WT n=16, KO n=10). Analysing *Msh2*$^{+/+}$ mice showed significantly higher *FXN* transcription in female (161%) compared with male (normalised as 100%, P<0.01) cerebellum tissues (Figure 5.8). As with brain, data analysis showed contrary results in male compared with female mice. Thus, *FXN* transcription was significantly upregulated with lack of Msh2 in males, compared with *Msh2*-WT (P<0.001). In contrast, *FXN* transcription was downregulated with loss of Msh2 in female cerebellum tissue from 161% to 134% (Figure 5.8). Taken together, observations represented similar findings in both brain and cerebellum tissues. These findings indicate a sex-related effect of Msh2 on *FXN* transcription in tissues that are sensitive to the FRDA abnormality, whereby absence of Msh2 increases *FXN* transcription in males, but decreases it in females.

Figure 5.8 - Effect of Msh2 on the *FXN* transcription level of cerebellum tissues in different genders.

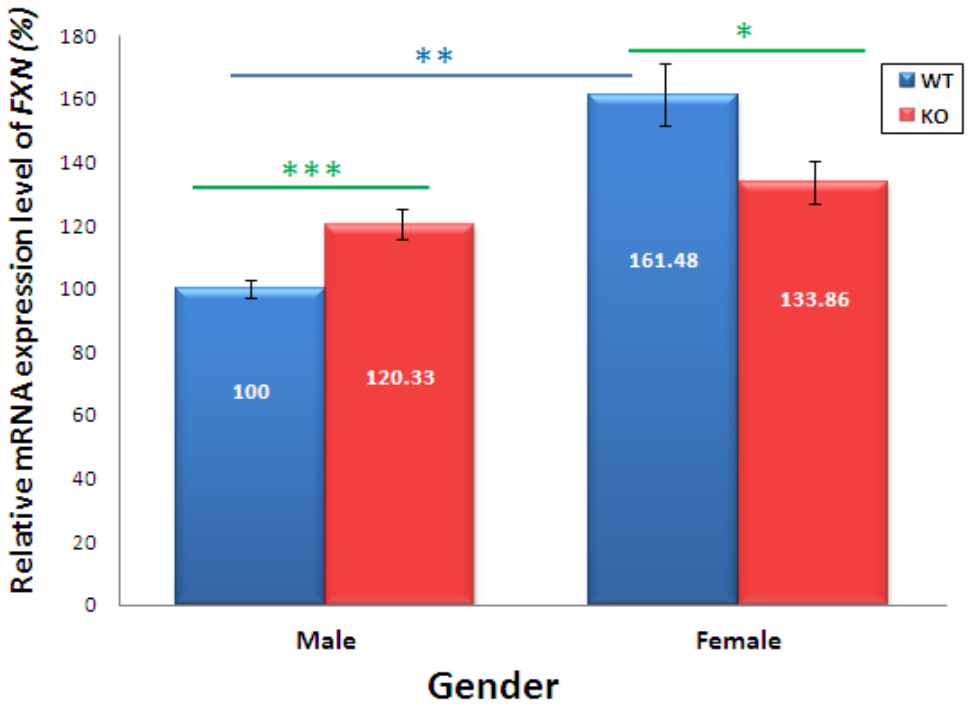

The image represents qRT-PCR analysis of transgenic *FXN* mRNA isolated from cerebellum tissues of female (WT n=6, KO n=8) and male (WT n=16, KO n=10) mice with different modifications of *Msh2*, normalised to the mean mRNA level of *FXN* found in the male *Msh2*-WT control samples and taken as 100%. Error bars= S.E.M, *= p<0.05, **= p<0.01, ***= p<0.001

Finally, the relative quantification of *FXN* transcription in cerebellum tissues, based only upon *Msh2* modifications, was measured by qRT-PCR. A statistically significant increased level of *FXN* transcription was detected with loss of Msh2 protein (Figure 5.9). Comparing these cerebellar findings with the brain tissue results suggest that the overall effect of Msh2 on *FXN* transcription is tissue selective.

Figure 5.9 - Effect of Msh2 on the *FXN* transcription level in cerebellum tissue.

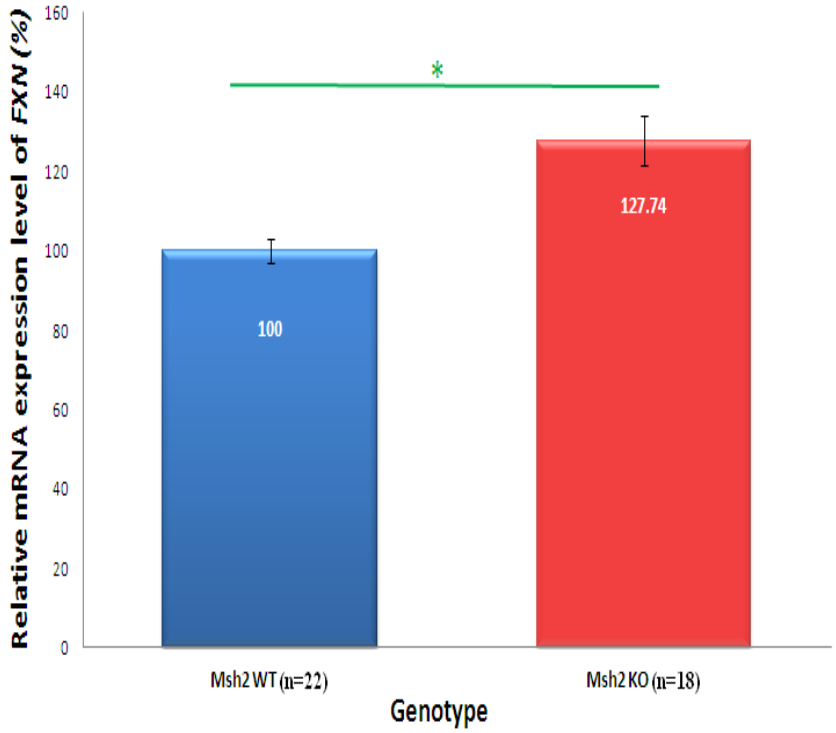

The image represents qRT-PCR analysis of transgenic *FXN* mRNA isolated from cerebellum tissues of *Msh2*-WT and *Msh2*-KO mice, normalised to the mean *FXN* mRNA level found in the *Msh2*-WT control samples and taken as 100%. Error bars= S.E.M, *= $p<0.05$

Taken together, these findings indicate that lack of Msh2 produces increased transcription of *FXN*, particularly in cerebellum tissue. This may possibly be due to comparatively decreased sizes of GAA repeat expansion mutation. However, the Msh2 deficiency effects on *FXN* transcription are modified by the gender of the mice.

5.3.2 - Effect of *Msh3* on human transgenic *FXN* transcription

To examine the effect of Msh3 protein on *FXN* transcription, qRT-PCR was performed on groups of 20 *Msh3*$^{+/+}$ and 13 *Msh3*$^{-/-}$ mice. The *FXN* transcription levels were analysed in either brain or cerebellum tissues based on: (i) *Msh3* genotypes: *Msh3*-WT and *Msh3*-KO; (ii) age of genetically modified *Msh3* mice: 5-7 months and 9-12 months; (iii) gender of genetically modified *Msh3* mice: male and female.

- Brain tissue: To investigate the age effect on *FXN* transcription in brain tissues, in the absence or presence of Msh3 protein, transgenic mice aged 5-7 months (WT n=8, KO n=3) were compared with mice aged 9-12 months (WT n=12, KO n=8). Data analysis showed no statistically significant difference in the *FXN* transcription level between older (9-12 months) and younger (5-7 months) mice for both *Msh3*-WT and *Msh3*-KO (Figure 5.10).

Figure 5.10 - Effect of Msh3 on the *FXN* transcription level of brain tissues in different age groups.

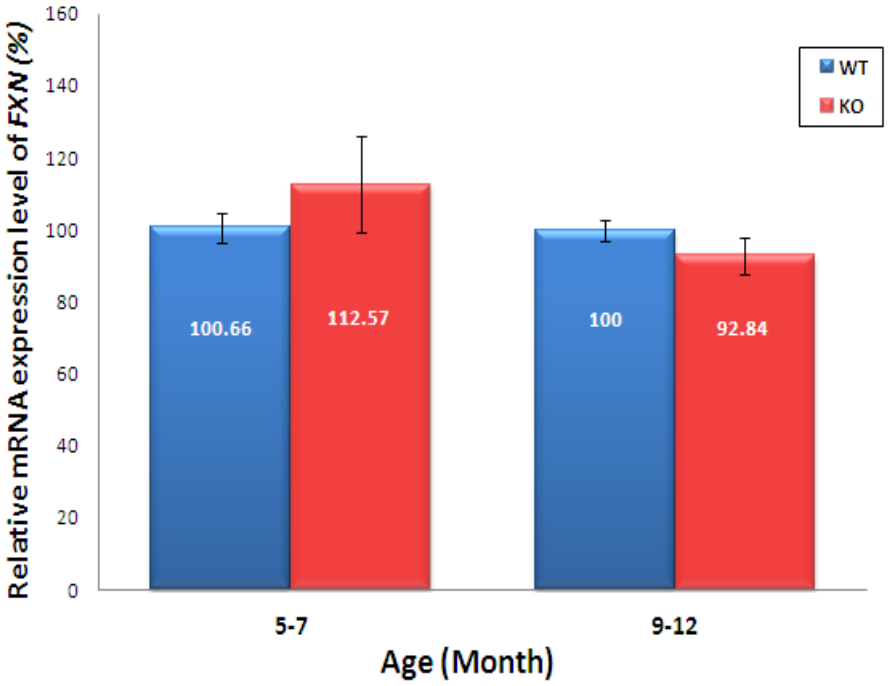

The image represents qRT-PCR analysis of transgenic *FXN* mRNA isolated from brain tissues of 5-7 months (WT n=8, KO n=3) and 9-12 months (WT n=12, KO n=8) mice with different modifications of *Msh3*, normalised to the mean *FXN* mRNA level found in the 9-12 months of age *Msh3*-WT control samples and taken as 100%. Error bars= S.E.M.

To find out whether the *FXN* transcription level of brain tissue was modified by sex in the absence or presence of Msh3, 18 female samples (WT n=10, KO n=8) were compared with 15 male samples (WT n=10, KO n=5). The data analysis demonstrated similar levels of *FXN* transcription in *Msh3*-WT for both males and females, while in *Msh3*$^{-/-}$ mice, *FXN* transcription was significantly higher in males (117%, p<0.001) compared with females (Figure 5.11). Further analysis showed a reduced level of *FXN* transcription in *Msh3*-KO female mice (88%) compared with *Msh3*-WT mice (normalised as 100%).

Figure 5.11 - Effect of Msh3 on the *FXN* transcription level of brain tissues in different genders.

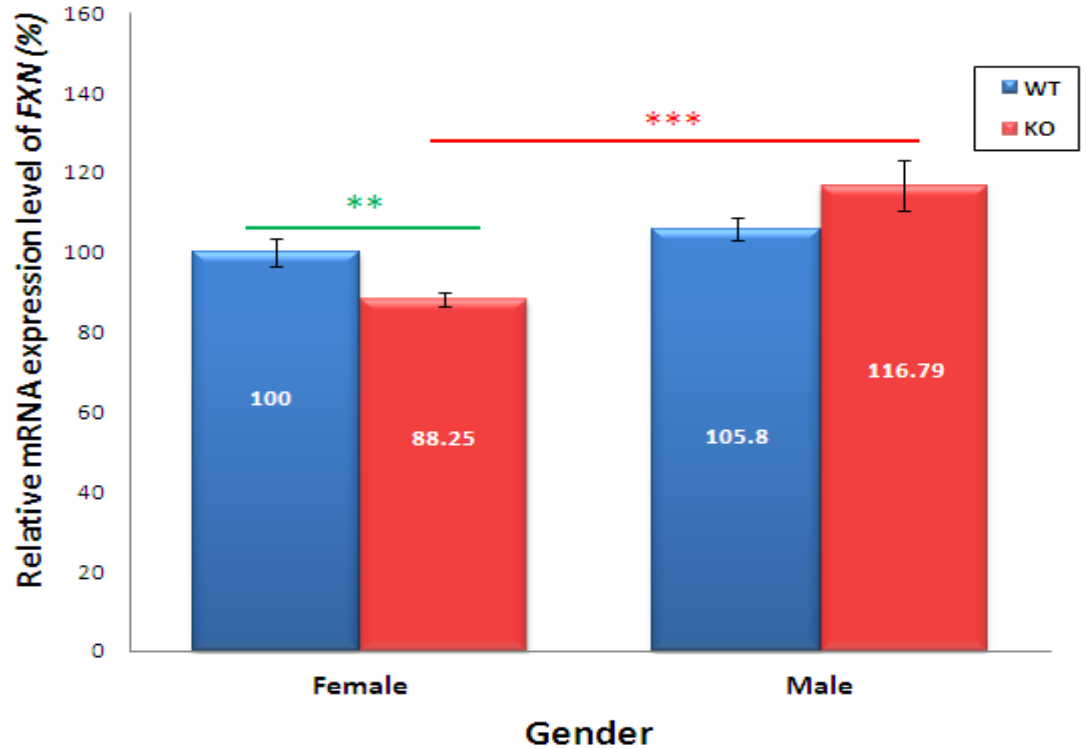

The image represents qRT-PCR analysis of transgenic *FXN* mRNA isolated from brain tissues of female (WT n=10, KO n=8) and male (WT n=10, KO n=5) mice with different modifications of *Msh3*, normalised to the mean *FXN* mRNA level found in the female *Msh3*-WT control samples and taken as 100%. Error bars= S.E.M, **= P<0.01, ***= p<0.001

Subsequently, relative quantification of *FXN* transcription in brain tissues was performed based on *Msh3* modification only. Analysis of data did not reveal any notable difference due

to the loss of Msh3 protein (Figure 5.12). This result suggests that lack of Msh3 does not affect the transcription level of *FXN* in brain tissue.

Figure 5.12 - Effect of Msh3 on the *FXN* transcription level in brain tissue.

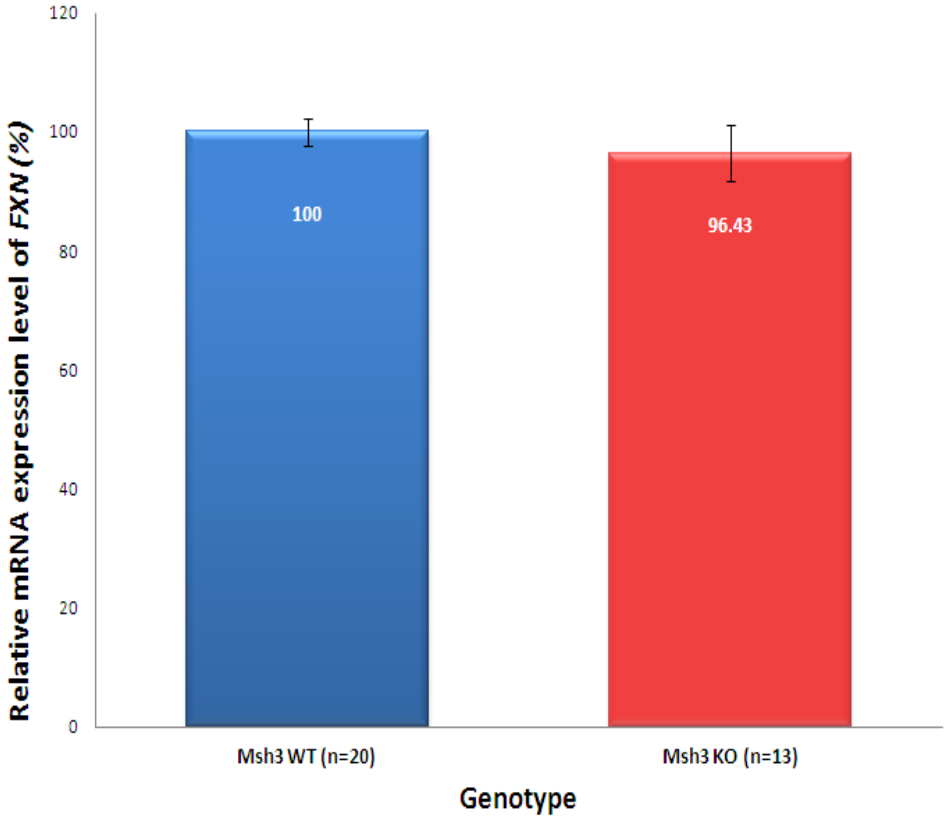

The image represents qRT-PCR analysis of transgenic *FXN* mRNA isolated from brain tissues of *Msh3*-WT and *Msh3*-KO mice, normalised to the mean *FXN* mRNA level found in the *Msh3*-WT control samples and taken as 100%. Error bars= S.E.M.

- Cerebellum tissue: The potential age-modifying effect of Msh3 on *FXN* transcription was assessed in cerebellum tissue samples of the mice aged 5-7 months (WT n=13, KO n=4) and the mice aged 9-12 months (WT n=10, KO n=5). Data analysis did not show any significant difference between *FXN* transcription levels of these differently aged groups (Figure 5.13). In addition, no difference was observed by comparing *Msh3*-WT with *Msh3*-KO in each group. These findings were similar to the results obtained from brain tissue. Thus, it is

proposed that levels of *FXN* transcription in cerebellum are not affected by the absence of Msh3 or modified by different ages of mice.

Figure 5.13 - Effect of Msh3 on the *FXN* transcription level of cerebellum tissues in different age groups.

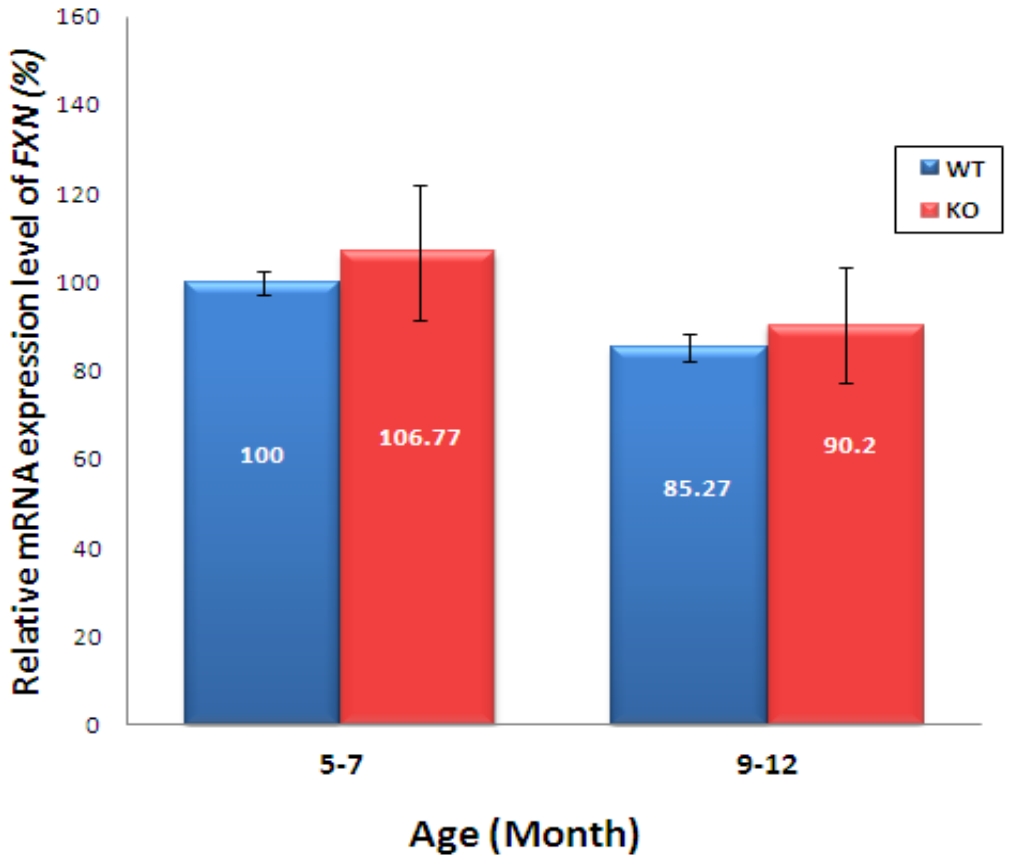

The image represents qRT-PCR analysis of transgenic *FXN* mRNA isolated from brain tissues of 5-7 months (WT n=13, KO n=4) and 9-12 months (WT n= 10, KO n=5) mice with different modifications of *Msh3*, normalised to the mean *FXN* mRNA level found in the 5-7 months of age *Msh3*-WT control samples and taken as 100%. Error bars= S.E.M.

To study whether the *FXN* transcription level of cerebellum tissue is related to the gender in absence or presence of Msh3, female samples (WT n=13, KO n=3) were compared with male samples (WT n=10, KO n=6). Analysis of *Msh3*-WT and *Msh3*-KO males, like in brain tissues, did not show any significant difference in *FXN* transcription (Figure 5.14).

Figure 5.14 - Effect of Msh3 on the *FXN* transcription level of cerebellum tissues in different genders.

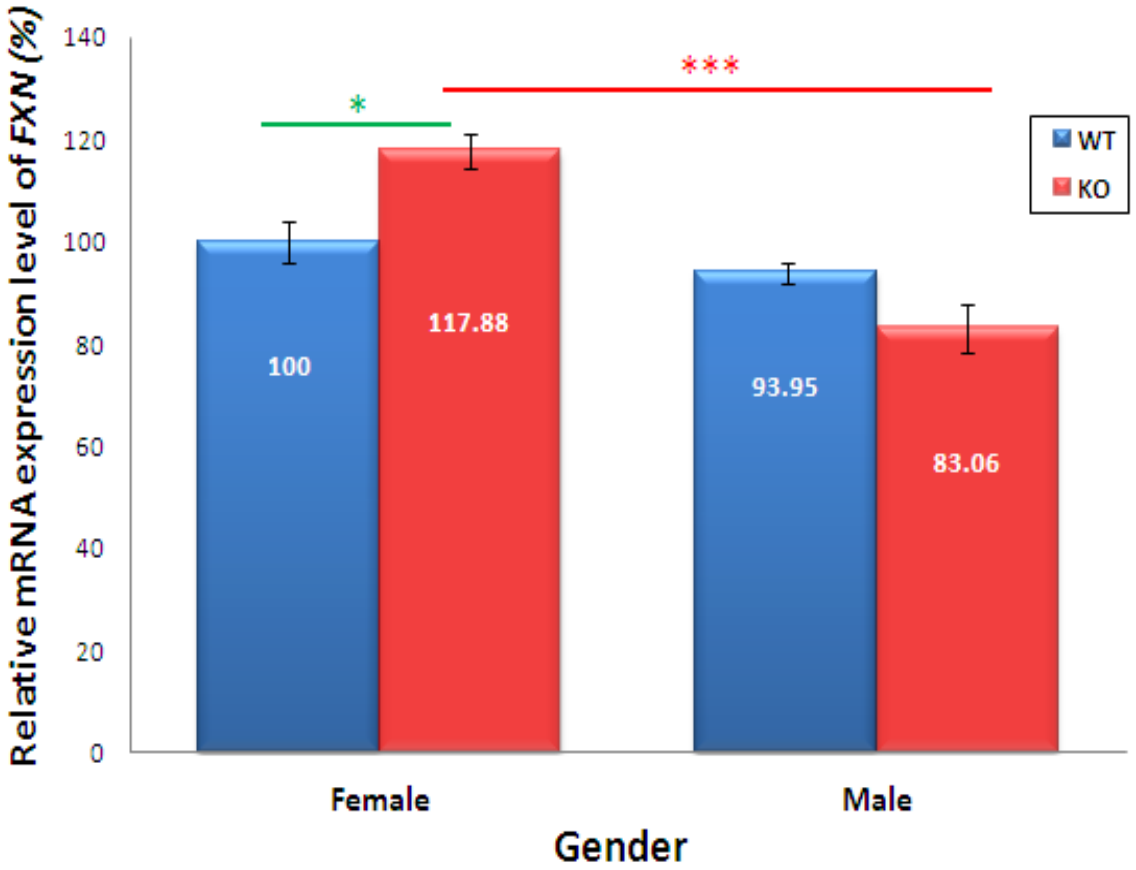

The image represents qRT-PCR analysis of transgenic *FXN* mRNA isolated from cerebellum tissues of female (WT n=13, KO n=3) and male (WT n=10, KO n=6) mice with different modifications of *Msh3*, normalised to the mean *FXN* mRNA level found in the female *Msh3*-WT control samples and taken as 100%. Error bars= S.E.M, *= p<0.05, ***= p<0.001

However, the level of *FXN* transcription was significantly increased in cerebellum tissue of female mice with lack of Msh3 (approximately 1.5 fold, P<0.05). This is consistent with observations obtained from brain tissue showing a significant difference of *FXN* transcription levels in females, and not males, when comparing *Msh3*-WT and *Msh3*-KO mice. Nonetheless, it is important to say that level of *FXN* transcription in the brain tissue of *Msh3*-KO was reduced compared with *Msh3*-WT (refer to the figure 5.11), while this situation was reversed in cerebellum tissues. These findings indicate that *FXN* transcription exhibits a degree of tissue selectivity in *Msh3*-female transgenic mice. Finally, the levels of

FXN transcription in cerebellum tissues were analysed based only upon *Msh3* genotype. Analysis of data did not show any notable difference in *Msh3*-KO compared with *Msh3*-WT (Figure 5.15). This result suggests that lack of Msh3 does not affect the *FXN* transcription level in cerebellum tissue. Taken together, the findings obtained from this study indicate that Msh3 defect does not have any significant influence on the *FXN* transcription, other than female mice showing a tissue selective effect.

Figure 5.15 - Effect of Msh3 on the *FXN* transcription level in cerebellum tissue.

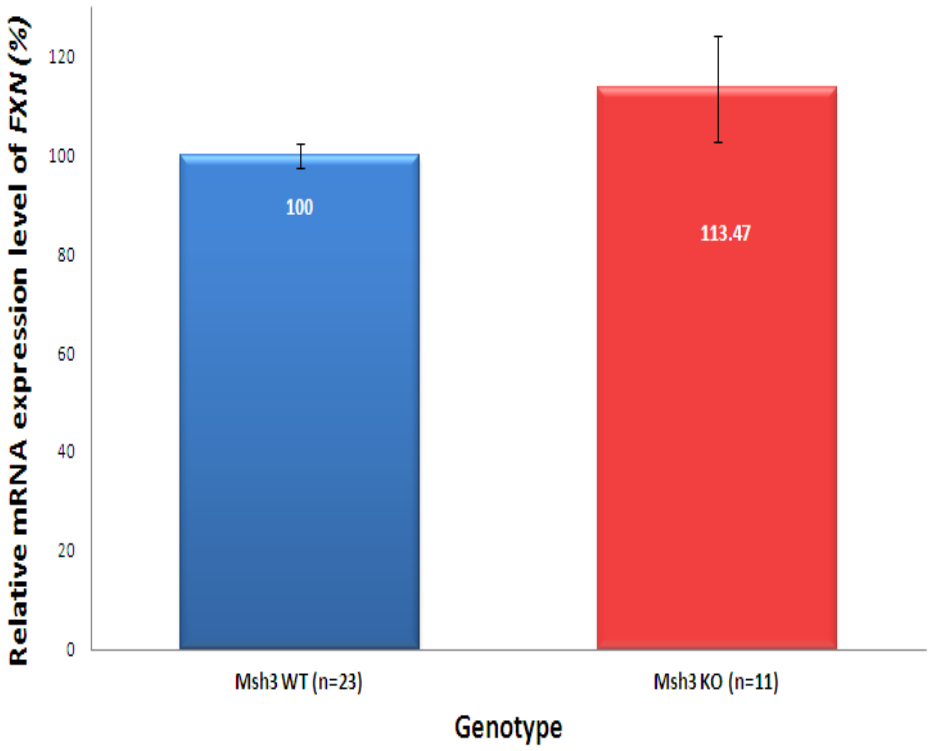

The image represents qRT-PCR analysis of transgenic *FXN* mRNA isolated from cerebellum tissues of *Msh3*-WT and *Msh3*-KO mice, normalised to the mean *FXN* mRNA level found in the *Msh3*-WT control samples and taken as 100%. Error bars= S.E.M.

5.3.3 - Effect of *Msh6* on human transgenic *FXN* transcription

To understand the effect of Msh6 on *FXN* transcription, qRT-PCR was utilised to compare the *FXN* transcription levels of 12 *Msh6*-WT (both male and female mice) with 3 *Msh6*-KO

samples (female mice only). In this experiment, the age of each individual mouse was 9 months. The *FXN* transcription level in both brain and cerebellum tissues was analysed based on: (i) *Msh6* genotypes: *Msh6*-WT and *MSh6*-KO; (ii) gender of genetically modified mice: female.

- Brain tissue: To understand whether the *FXN* transcription level of brain tissue is modified by sex in the absence or presence of Msh6, 9 samples from *Msh6*$^{+/+}$ females were compared with 3 samples from *Msh6*$^{-/-}$ females. Since no *Msh6*-KO male sample was available, *FXN* transcriptional analysis in males was not feasible. Data analysis from brain tissues of female mice showed that the level of *FXN* transcription was significantly reduced (1.8 fold; $p<0.001$) in the absence of Msh6 compared with the presence of Msh6 (Figure 5.16).

Figure 5.16 - Effect of Msh6 on the *FXN* transcription level of brain tissues in different genders.

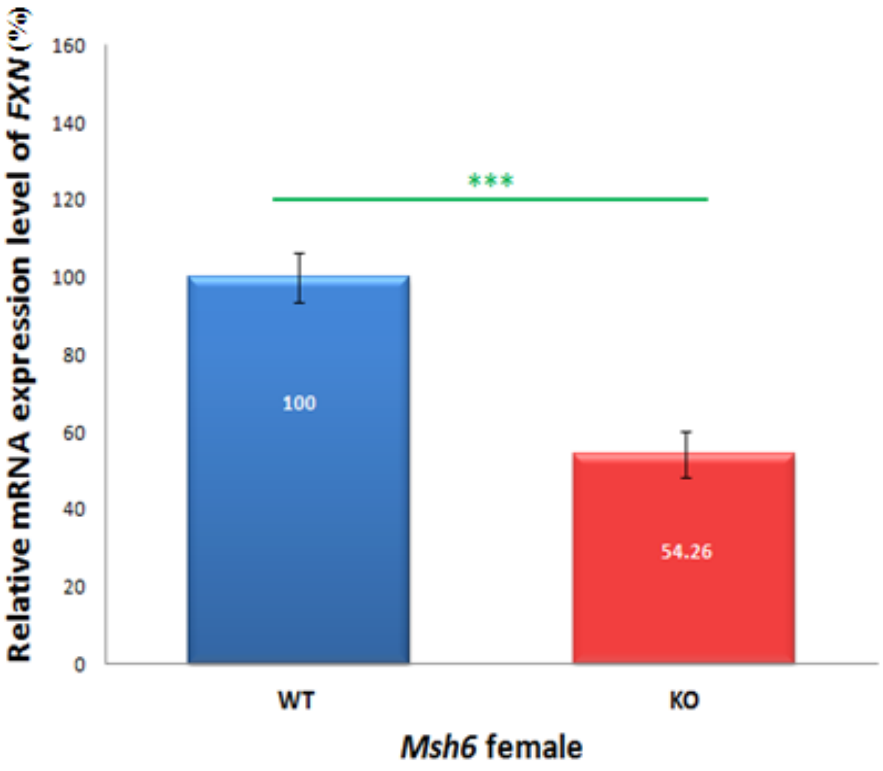

The image represents qRT-PCR analysis of transgenic *FXN* mRNA isolated from brain tissues of female mice with different modifications of *Msh6* (WT n=9; KO n=3), normalised to the mean *FXN* mRNA level found in the male *Msh6*-WT control samples and taken as 100%. Error bars= S.E.M, ***= $p<0.001$

Moreover, relative quantification of the transcription level of *FXN* in brain tissues was performed only based upon *Msh6* genotype only. The data analysis showed remarkably reduced levels of *FXN* transcription (less than 56%; $p<0.01$) with loss of Msh6 (Figure 5.17), suggesting that lack of Msh6 causes downregulation of *FXN* transcription. Although this latter finding was based on analysis of both male and female samples, it showed similar effect to those findings of only based on female mice. This comparison suggests that the effect of Msh6 deficiency on *FXN* transcription level would not be modified by gender in brain tissue.

Figure 5.17 - Effect of Msh6 on the *FXN* transcription level in brain tissue.

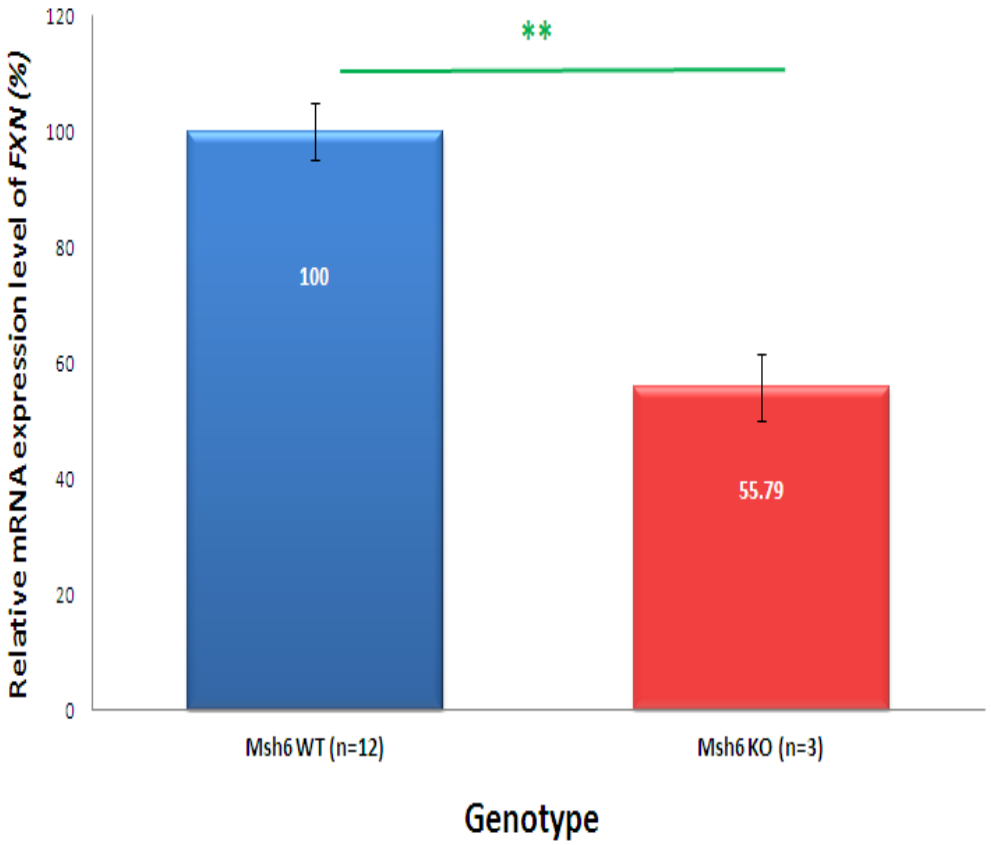

The image represents qRT-PCR analysis of transgenic *FXN* mRNA isolated from brain tissues of *Msh6*-WT and *Msh6*-KO mice, normalised to the mean *FXN* mRNA level found in the *Msh6*-WT control samples and taken as 100%. Error bars= S.E.M, **= $p<0.01$

- Cerebellum tissue: To investigate whether *FXN* transcription of cerebellum tissue was related to the gender of mice in the absence or presence of Msh6, nine samples from female

Msh6$^{+/+}$ genotype were compared with three samples from *Msh6*$^{-/-}$. Since *Msh6*-KO male mice were not available, *FXN* transcriptional analysis in males was not feasible. Analysing the data from cerebellum tissues of female mice showed that the level of *FXN* transcription was significantly reduced (1.6 fold; $p<0.001$) in the absence of Msh6 compared with the presence of Msh6 (Figure 5.18).

Figure 5.18 - Effect of Msh6 on the *FXN* transcription level of cerebellum tissues in different genders.

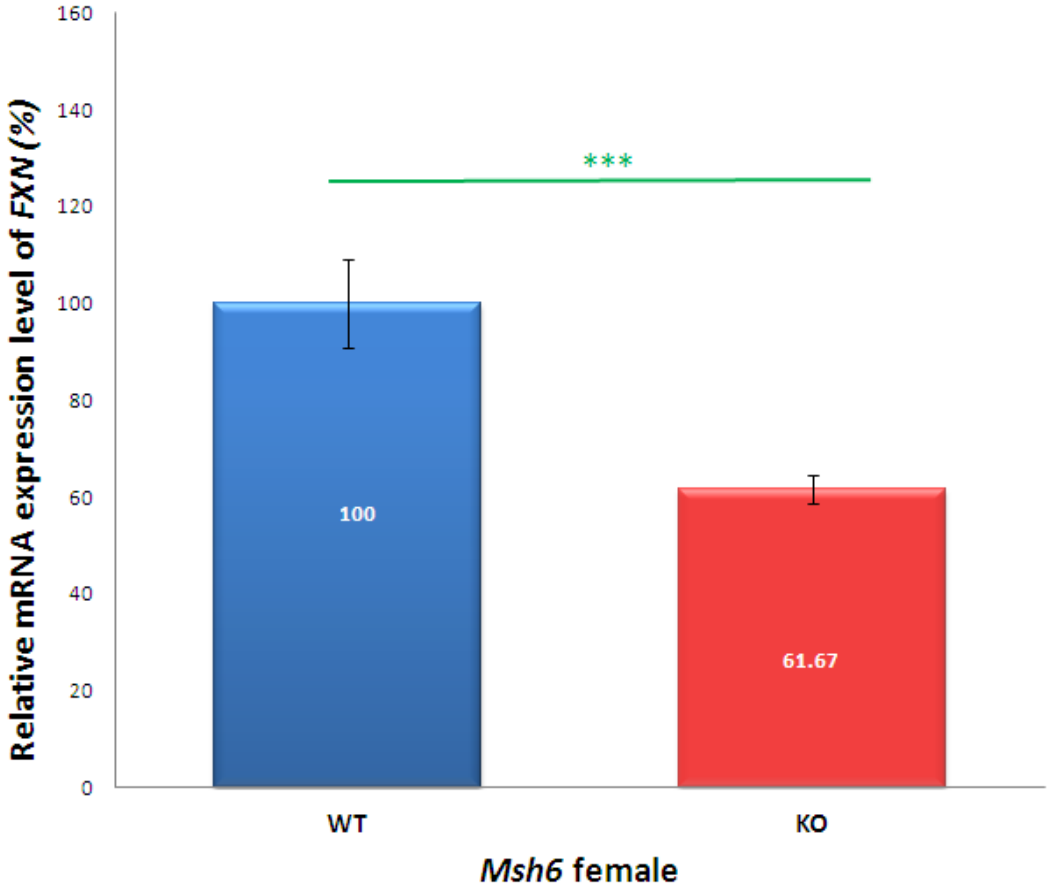

The image represents qRT-PCR analysis of transgenic *FXN* mRNA isolated from cerebellum tissues of female mice with different modifications of *Msh6* (WT n=9, KO n=3), normalised to the mean *FXN* mRNA level found in the male *Msh6*-WT control samples and taken as 100%. Error bars= S.E.M, ***= $p<0.001$

Furthermore, relative quantification of the *FXN* transcription in cerebellum tissues was performed based only upon Msh6 genotype. The data analysis showed remarkably reduced

levels of *FXN* transcription (60%; p<0.001) in the absence of Msh6 compared with the presence of Msh6 (Figure 5.19), indicating that, similar to brain tissue, lack of Msh6 causes downregulation of *FXN* transcription in cerebellum tissue, which again is unmodified by gender.

Figure 5.19 - Effect of Msh6 on the *FXN* transcription level in cerebellum tissue.

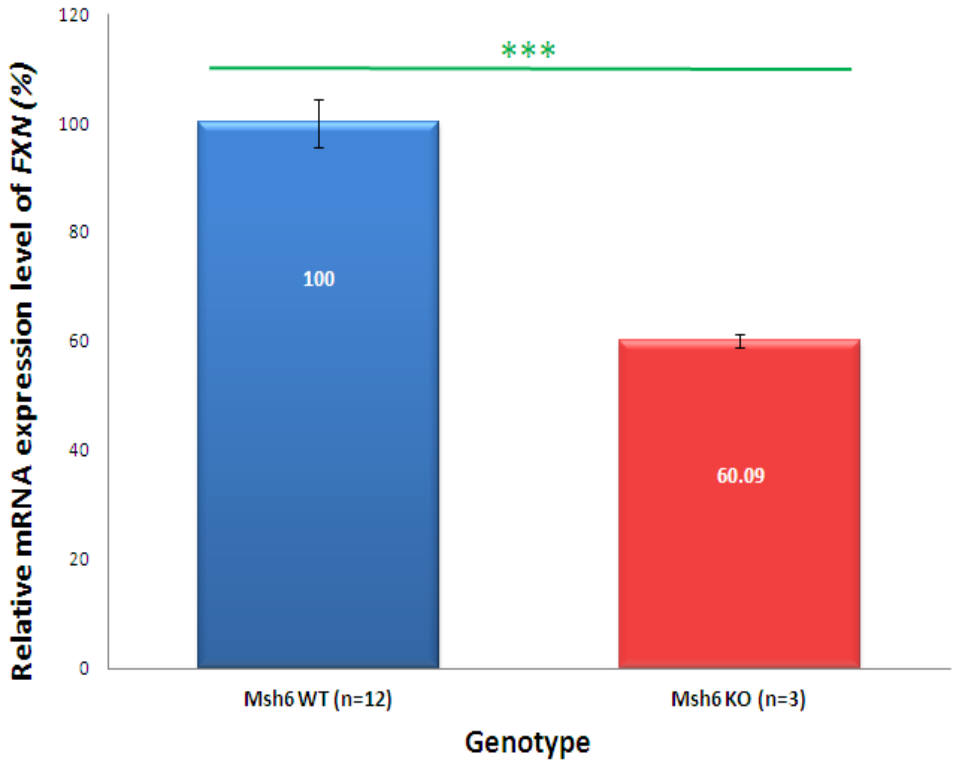

The image represents qRT-PCR analysis of transgenic *FXN* mRNA isolated from cerebellum tissues of *Msh6*-WT and *Msh6*-KO mice, normalised to the mean *FXN* mRNA level found in the *Msh6*-WT control samples and taken as 100%. Error bars= S.E.M, ***= p<0.001

Taken together, these findings reveal that Msh6 deficits result in a general downregulation of *FXN* transcription.

5.3.4 - Effect of *Pms2* on human transgenic *FXN* transcription

To understand the effect of Pms2 protein on *FXN* transcription, qRT-PCR was performed to compare the *FXN* transcription level of 9 *Pms2*-WT samples with that of 17 *Pms2*-KO

samples (from both male and female mice). In this study, *FXN* transcription was analysed in both brain and cerebellum tissues based on: (i) *Pms2* genotypes: *Pms2*-WT and *Pms2*-KO; (ii) gender of genetically modified mice: male and female.

- Brain tissue: To find out whether the *FXN* transcription levels of brain tissue were modified by sex in the absence or presence of Pms2, samples from female mice (WT n=3, KO n=6) were compared with those of male mice (WT n=6, KO n=11). The data analysis demonstrated that the *FXN* transcription level was reduced from 128% in *Pms2*-WT females to less than 91% in Pms2-KO females. A similar trend, although not statistically significant, was also observed between *Pms2*-WT and *Pms2*-KO males (Figure 5.20).

Figure 5.20 - Effect of Pms2 on the *FXN* transcription level of brain tissues in different genders.

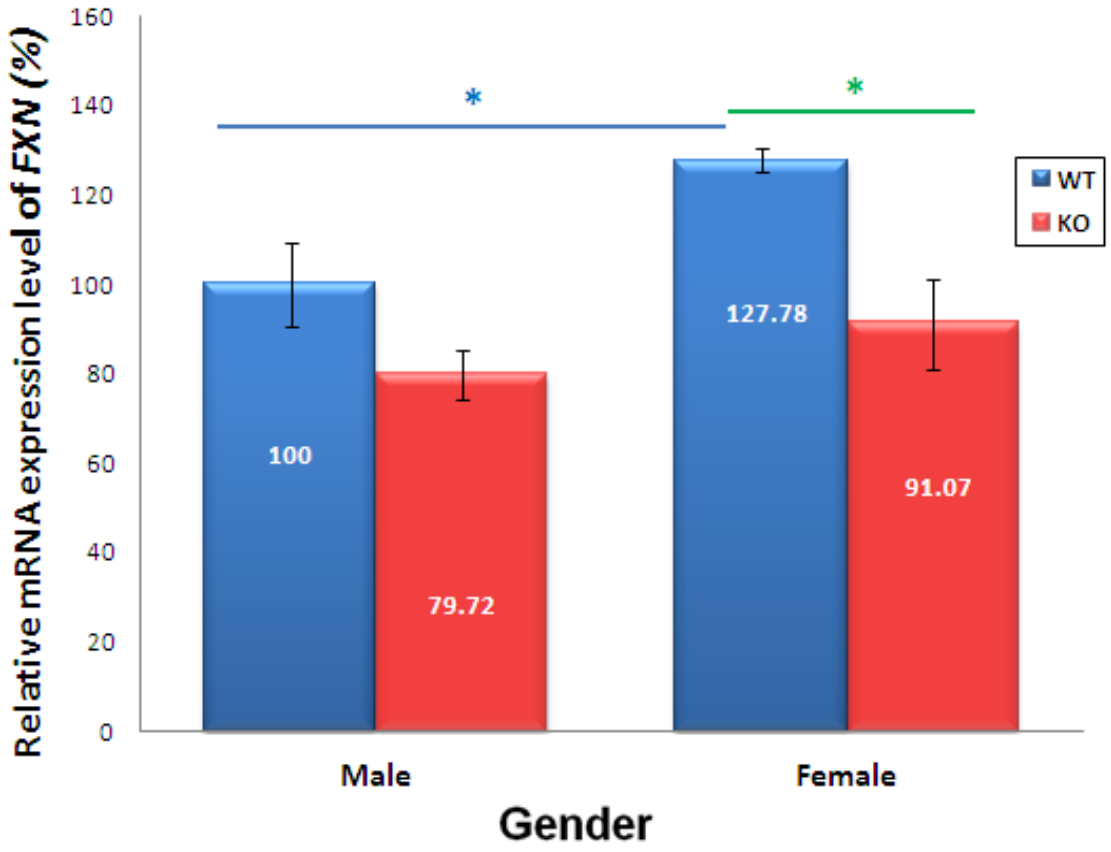

The image represents qRT-PCR analysis of transgenic *FXN* mRNA isolated from brain tissues of female (WT n=3, KO n=6) and male (WT n=6, KO n=11) mice with different modifications of *Pms2*, normalised to the mean *FXN* mRNA level found in the male *Pms2*-WT control samples and taken as 100%. Error bars= S.E.M, *= $p<0.05$

Subsequently, relative quantification of *FXN* transcription in brain tissues was performed based upon *Pms2* genotype only. Data analysis showed that the level of *FXN* transcription was significantly reduced with loss of Pms2 (Figure 5.21; $p<0.05$).

Figure 5.21 - Effect of Pms2 on *FXN* transcription level in brain tissue.

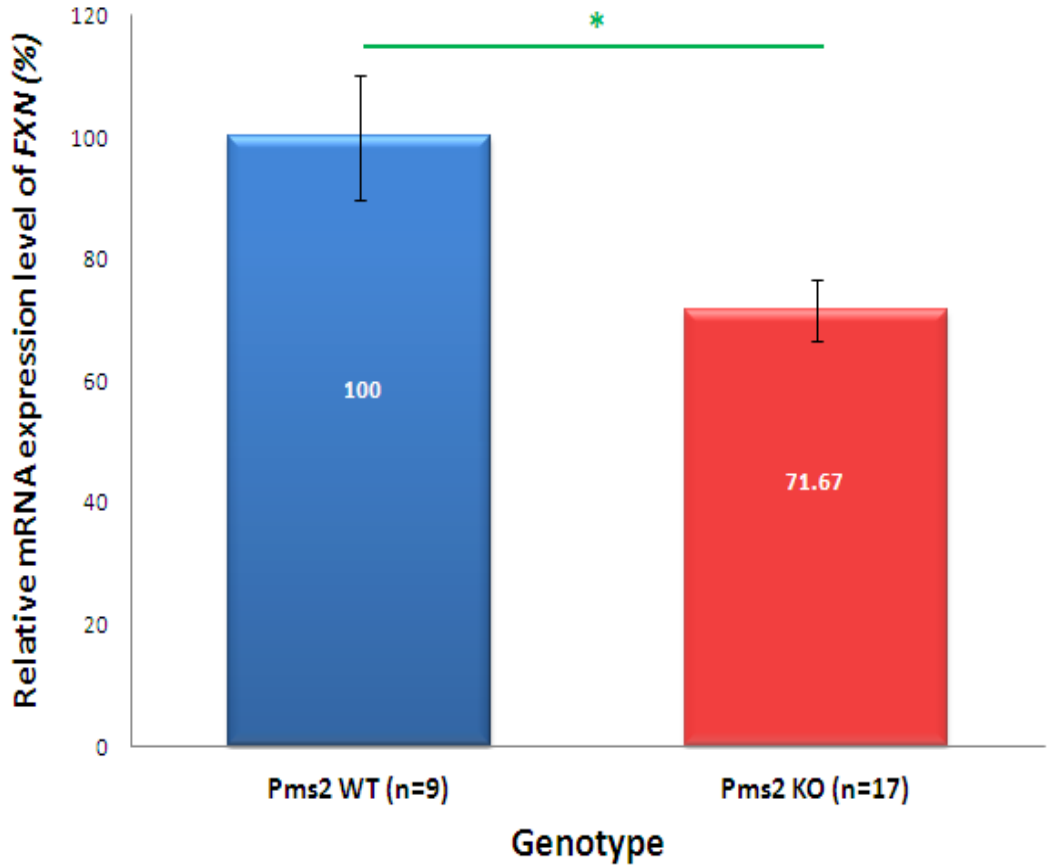

The image represents qRT-PCR analysis of transgenic *FXN* mRNA isolated from brain tissues of *Pms2*-WT and *Pms2*-KO mice, normalised to the mean *FXN* mRNA level found in the *Pms2*-WT control samples and taken as 100%. Error bars= S.E.M, *= $p<0.05$

- Cerebellum tissue: To study whether *FXN* transcription in cerebellum was modified by gender in the absence or presence of Pms2, female samples (WT n=8, KO n=5) were compared with male samples (WT n=6, KO n=5). Analysis of data from male cerebellum tissue demonstrated that loss of Pms2 culminated in reduced *FXN* transcription compared

with *Pms2*-WT (Figure 5.22). A similar trend, but not statistically significant, was observed by comparing *Pms2*-KO and *Pms2*-WT females.

Figure 5.22 - Effect of Pms2 on the *FXN* transcription level of cerebellum tissues in different genders.

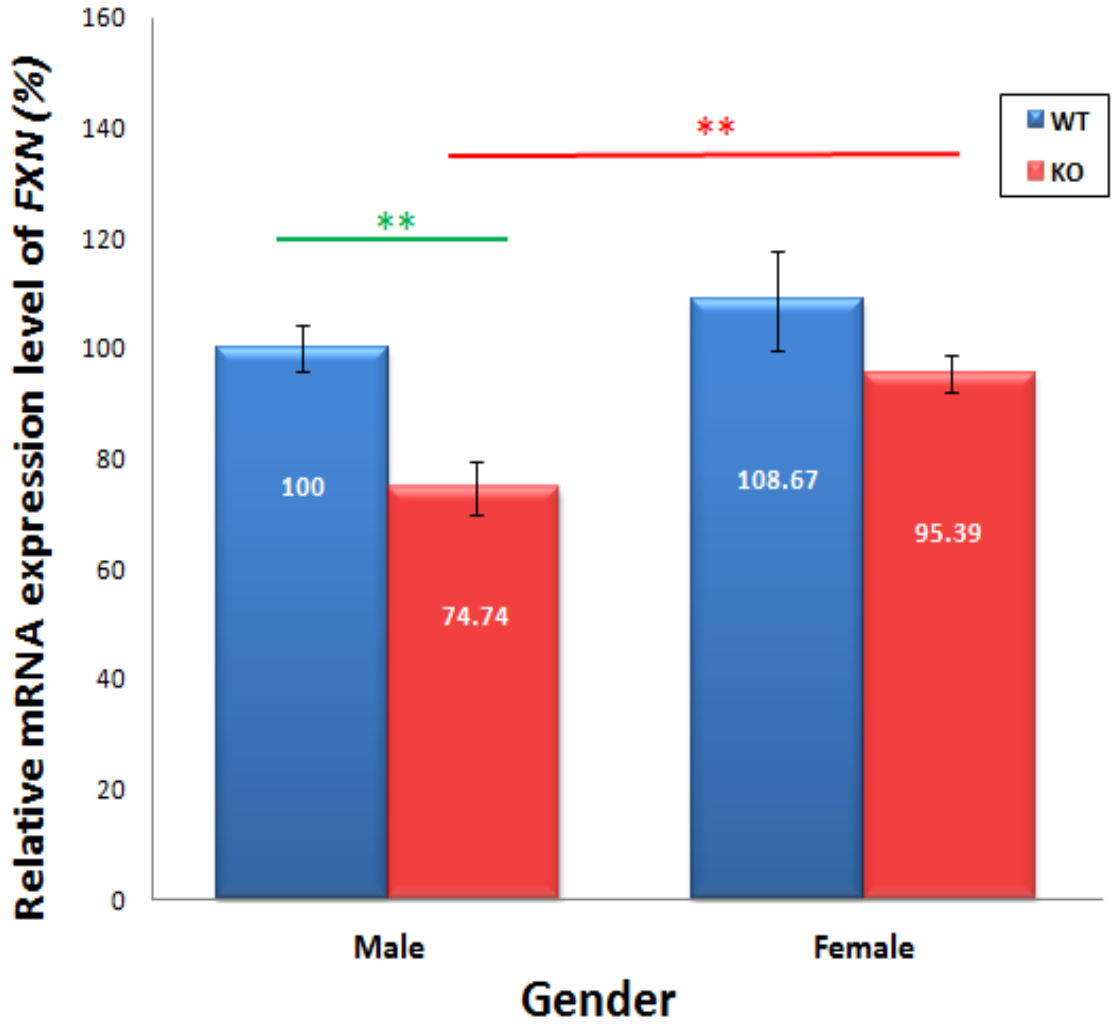

The image represents qRT-PCR analysis of transgenic *FXN* mRNA isolated from cerebellum tissues of female (WT n=8, KO n=5) and male (WT n=6, KO n=5) mice with different modifications of *Pms2*, normalised to the mean *FXN* mRNA level found in the male *Pms2*-WT control samples and taken as 100%. Error bars= S.E.M, **= $p<0.01$

Finally, the relative quantification of *FXN* transcription in cerebellum tissues was measured based on *Pms2* genotype only. As with brain, data analysis showed that the *FXN* mRNA level of cerebellum tissues was significantly reduced with loss of Pms2 (Figure 5.23; $p<0.05$).

Figure 5.23 - Effect of Pms2 on *FXN* transcription level in cerebellum tissue.

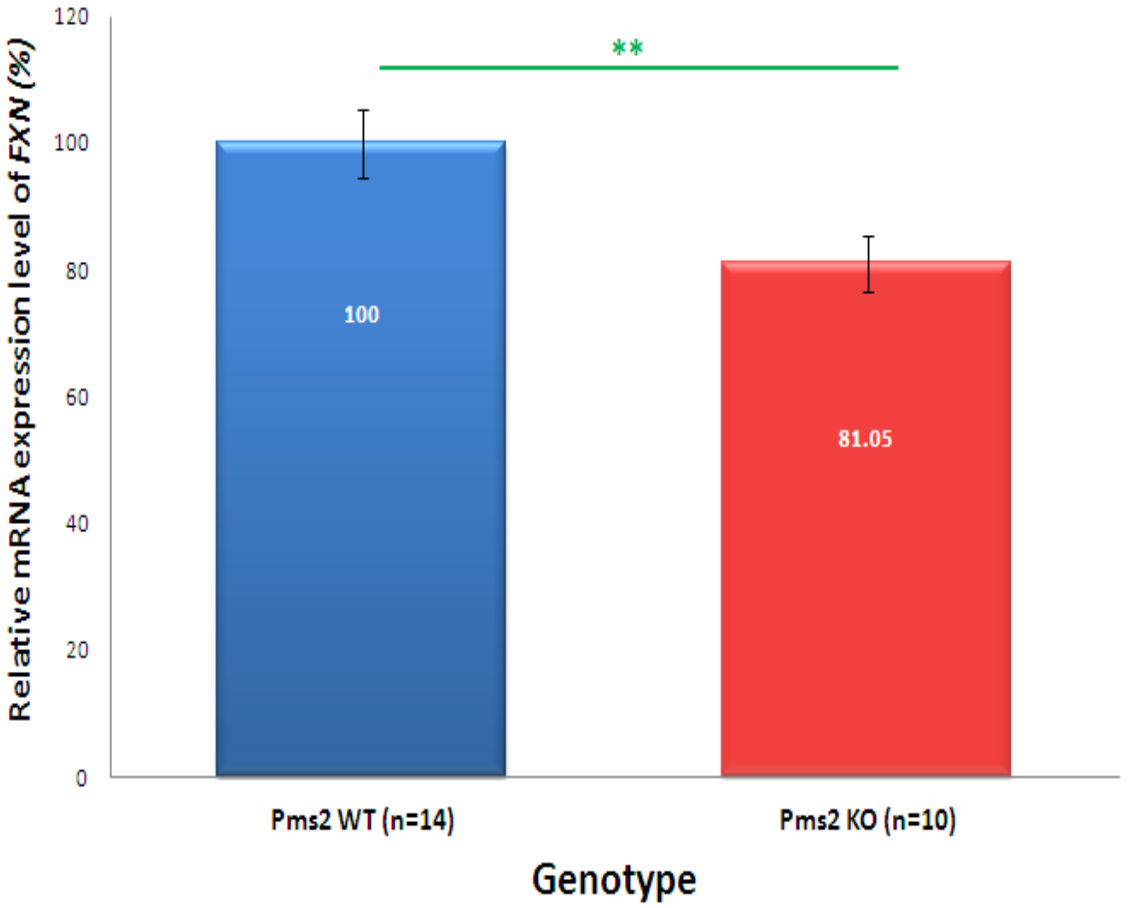

The image represents qRT-PCR analysis of transgenic *FXN* mRNA isolated from cerebellum tissues of *Pms2*-WT and *Pms2*-KO mice, normalised to the mean *FXN* mRNA level found in the *Pms2*-WT control samples and taken as 100%. Error bars= S.E.M, **= $p<0.01$

Taken together, these findings indicate that loss of Pms2 causes reduced levels of *FXN* transcription, which might be due to comparatively increased sizes of GAA repeat expansion, as described in the chapter 4.

5.3.5 - Effect of *Mlh1* on human transgenic *FXN* transcription

To assess the effect of Mlh1 protein on *FXN* transcription, qRT-PCR analysis was performed for brain and cerebellum tissues based only upon *Mlh1* genotypes in male transgenic mice. Since *Mlh1*-KO mice did not survive beyond more than 3 months, data analysis based on age was not feasible. Analysing data from brain tissues of 2 samples of *Mlh1*-WT mice compared with 3 samples of *Mlh1*-KO revealed that, with loss of Mlh1, the level of *FXN* transcription was decreased to approximately half that of *Mlh1*-WT (Figure 5.24).

Figure 5.24 - Effect of Mlh1 on the *FXN* transcription level in brain tissue.

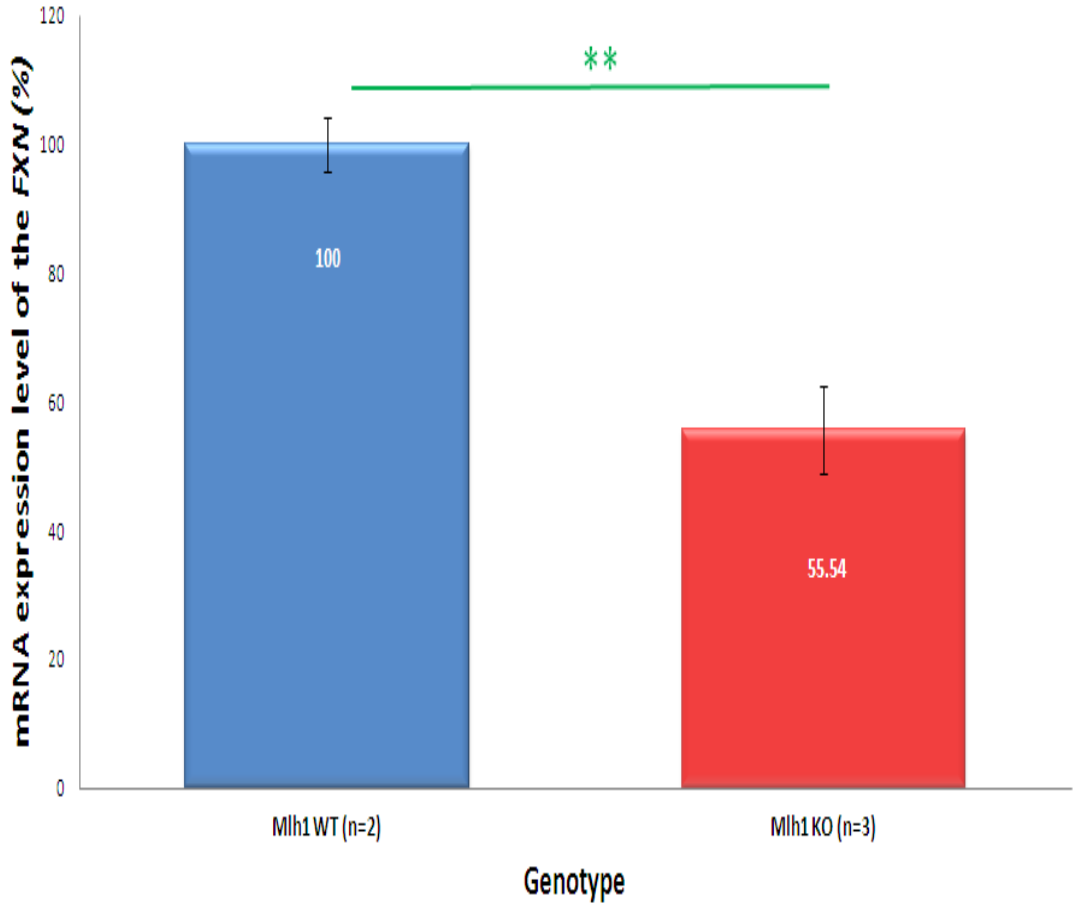

The image represents qRT-PCR analysis of transgenic *FXN* mRNA isolated from brain tissues of *Mlh1*-WT and *Mlh1*-KO mice, normalised to the mean *FXN* mRNA level found in the *Pms2*-WT control samples and taken as 100%. Error bars= S.E.M, *= $p<0.05$

Data analysis of cerebellum tissue from 4 *Mlh1*-WT mice compared with 12 *Mlh1*-KO mice demonstrated that, as with brain tissue, the level of *FXN* transcription decreased dramatically with loss of Mlh1 (about 5.5 fold, Figure 5.25).

Figure 5.25 - Effect of Mlh1 on the *FXN* transcription level in cerebellum tissue.

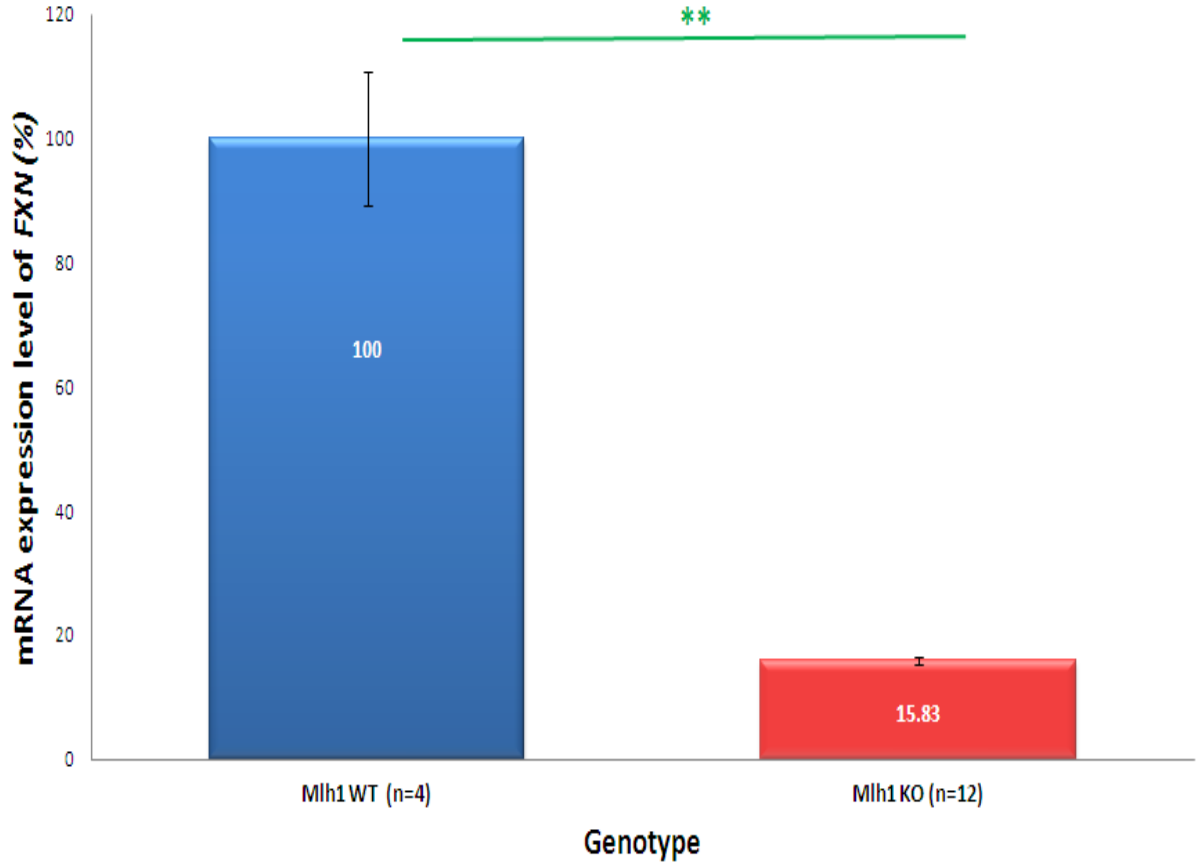

The image represents qRT-PCR analysis of transgenic *FXN* mRNA isolated from cerebellum tissues of *Mlh1*-WT and *Mlh1*-KO mice, normalised to the mean *FXN* mRNA level found in the *Mlh1*-WT control samples and taken as 100%. Error bars= S.E.M, **= $p<0.01$

Taken together, these findings indicate that deficits of Mlh1 lead to remarkable downregulation of *FXN* transcription in both brain and cerebellum tissues.

5.4 - Quantification of *FXN* mRNA in human cell lines

Following on from the previous section, the effects of MMR genes on *FXN* transcription were also investigated in human epithelial cell lines. This strategy was designed to establish whether a human *in vitro* cell model could be considered as a valid system to study the effects of MMR proteins on *FXN* transcription, compared with the mouse *in vivo* model system. Hence, the aim of this experiment was to investigate the effect of MMR proteins on *FXN* transcription *in vitro*. Since MMR deficiencies are particularly observed in HNPCC malignancy, a human epithelial colorectal cell line was considered as the most efficient cell type to use. In this study, a human MMR-proficient epithelial cell line, named NCM-460, was selected as the control (Moyer *et al.* 1996), and this was compared with a human MMR-deficient epithelial colorectal adenocarcinoma cell line, HCT-116. Observations have shown that HCT-116 contains a mutation within *MLH1* causing dysfunction of the related protein (Davis *et al.* 1998). This mutation could prevent binding of MLH1 to PMS2 *in vitro* subsequently causing MutLα heterodimer dysfunction (Belvederesi *et al.* 2006). Further studies have shown that PMS2 protein function is also disrupted in HCT-116 cells (Shimodaira *et al.* 2003), due to degradation of PMS2 in the absence of MLH1 (Chang *et al.* 2000). Thus, it is proposed that HCT-116 cell lines could be an efficient model to investigate the effect of dysfunction of MutLα, the critical secondary complex that continues and completes the MMR process.

To investigate the effect of MLH1 and PMS2 on *FXN* transcription in unaffected human MMR epithelial colorectal cells and HNPCC cells, the cells were initially sub-cultured for 10 passages (from passage 30 to 40). In addition to comparing NCM-460 with HCT-116 from compatible passages, to further understand the potential variability of *FXN* transcription

within different cell passages, *FXN* expression levels were analysed at three passage numbers: 30, 35 and 40. Briefly, total RNA was extracted from about one million cells by the Trizol® method and was converted into cDNA, followed by relative quantification of *FXN* transcription using qRT-PCR. To assess differences in gene expression efficiency, the Ct values from *FXN* cDNA were normalised to human *GAPDH*, as an endogenous control. Each sample was run in triplicate and each experiment was carried out at least two times. The mean value of each sample was applied for further calculations to obtain RQ values by using the $2^{-\Delta\Delta Ct}$ formula. Later, relative levels of *FXN* transcription from multiple passages of both NCM-460 and HCT-116 cell lines were determined by calculating the RQ mean values, followed by designating the value from passage number 30 of the NCM-460 cell line arbitrarily as 100%.

5.4.1 - The effects of *PMS2* and *MLH1* on *FXN* transcription

Analysis of data showed that the mean value of *FXN* transcription was significantly higher in the MMR-proficient NCM-460 control cells compared with the lack of MLH1 and PMS2 proteins in HCT-116 cell lines (Figure 5.26), indicating that lack of MLH1 and/or PMS2 protein(s) cause(s) reduced *FXN* transcription. This result is consistent with previous finding in mouse models with lack of each individual Pms2 (refer to the figure 5.22) or Mlh1 (refer to the figure 5.23) protein, suggesting the same mechanism of action for PMS2 and MLH1 in both *in vivo* mouse cells and *in vitro* human cells.

Figure 5.26 - *FXN* transcription level analysis in human epithelial cell lines.

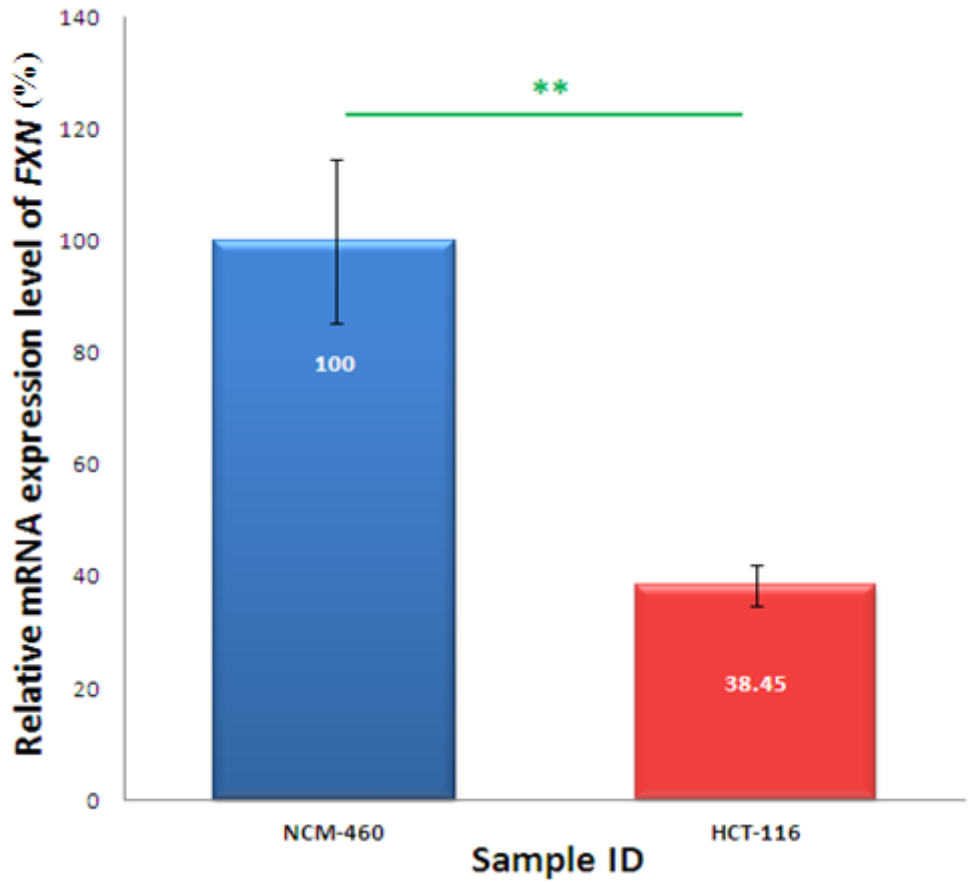

The image represents qRT-PCR analysis of the mean *FXN* transcription level (passage numbers 30, 35 and 40) isolated from MMR proficient cell line, NCM-460, and MutLα heterodimers deficient cell line, HCT-116, normalised to the mean *FXN* mRNA level found in the NCM-460 control sample and taken as 100%. Error bars= S.E.M, **= p<0.01

Further data, based on the number of passages, likewise showed less *FXN* transcription in HCT-116 cells compared with NCM-460 cells. Curiously, analysis showed that the trend of *FXN* mRNA expression was downwards in HCT-116 passage number 30 to 40, indicating that *FXN* transcription was gradually reducing with increasing passage number (Figure 5.27). The principle cause of *FXN* transcription level variation within different passages of HCT-116 cells was not clear.

Figure 5.27 - *FXN* transcription analysis in different passages of human epithelial cell lines.

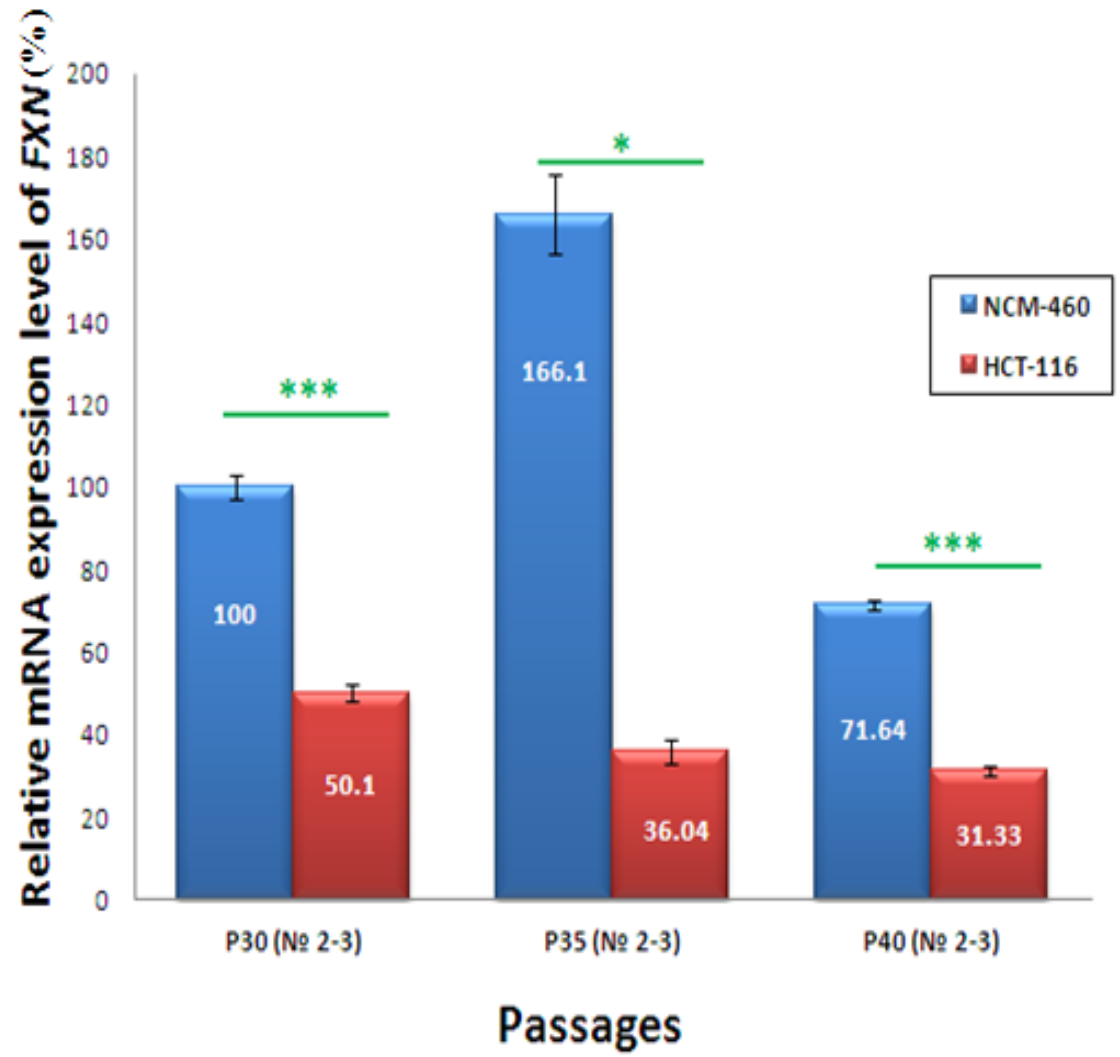

The image represents qRT-PCR analysis of the *FXN* transcription level with different passage numbers (30, 35 and 40) of MMR proficient cell line, NCM-460, and MutLα heterodimers deficient cell line, HCT-116, normalised to the mean *FXN* mRNA level found in the passage number 30 of NCM-460 control sample and taken as 100%. Error bars= S.E.M, *= $p<0.05$, ***=$p<0.001$.

To determine whether or not GAA repeat instability could be the cause of progressive *FXN* transcription reduction in HCT-116 cells, GAA repeat sizes were assessed in different passages of HCT-116 and NCM-460 cells. However, all passages of both cell types gave GAA PCR products of about 485bp, indicating approximately 11 GAA repeats, and no instability was observed (Figure 5.28). This shows that PMS2 and MLH1 deficiencies caused

reduced *FXN* transcription without affecting the size of normal GAA repeats, suggesting a different mechanism of action.

Figure 5.28 - GAA-PCR in human epithelial cell lines.

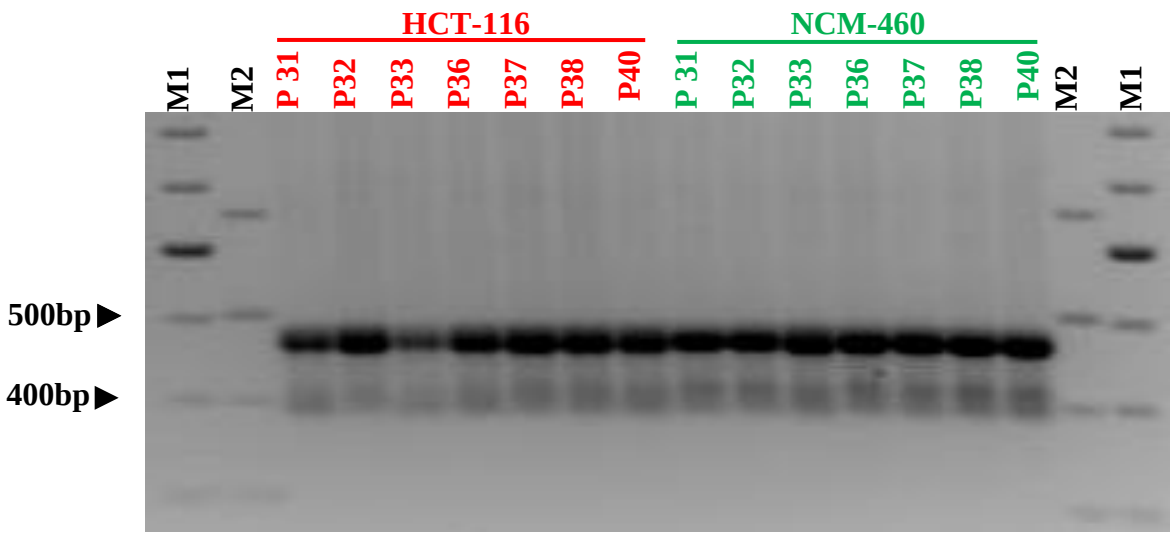

The image illustrates GAA-PCR analysis of samples serial-passages of HCT-116 and NCM460 cell lines in 1.5% ethidium bromide-stained agarose gel electrophoresis. P= Passage, M1= 100bp ladder, M2= $1Kb^{+}$ ladder.

5.5 - Discussion

The aim of this chapter was to investigate the effect of MMR proteins on *FXN* transcription *in vivo* and *in vitro*. Analysis of the *in vivo* results, taken together with the somatic GAA repeat instability findings of the chapter 4, addresses the relationships between MMR proteins, GAA repeat expansions and *FXN* transcription. In addition, categorisation of the data based on age and gender, helps to further understand potential modifier effects.

Analysis of the data from FXN^{GAA+} MMR-WT mice based on age did not reveal any significant difference between the *FXN* transcription levels of older versus younger mice. Likewise, findings indicated no age-related effect on *FXN* transcription in $Msh3^{-/-}$ transgenic mice. In contrast, a higher level of *FXN* transcription was identified in older $Msh2^{-/-}$

transgenic mice, compared with younger mice, suggesting an age-related effect. Further investigations are required to understand how age could affect *FXN* transcription in the absence of Msh2. No study has yet been carried out on Msh6, Pms2 and Mlh1 deficient mice in terms of age modification. Therefore, it would be noteworthy to investigate the effect of these proteins on *FXN* transcription based on age.

In the case of gender, the data revealed that the level of *FXN* transcription is generally modified by sex in FXN^{GAA+} MMR-WT mice. Thus, the *FXN* mRNA levels in female brain and cerebellum tissues were shown to be higher than those in males. In contrast, loss of Msh2 or Msh3 resulted in upregulation of *FXN* transcription in males compared with females. Curiously, no significant difference was observed between males and females with loss of Pms2. Further studies are required to determine how sex could modify the MMR-affected changes of *FXN* transcription. In addition, the investigation of any sex-modifying effects of Msh6 and Mlh1 proteins on *FXN* transcription levels would be useful future studies.

Data analysis based only upon *MMR* genotypes showed no significant difference in *FXN* transcription levels by comparing *Msh3*-KO with *Msh3*-WT mice, while loss of Msh2 resulted in increased *FXN* transcription in the cerebellum. The latter finding was consistent with previous observations of somatic GAA repeat instability (refer to the chapter 4), whereby a loss of GAA repeat expansion, and hence likely increased *FXN* expression, was demonstrated in *Msh2*-KO cerebellar tissues. In contrast, loss of Pms2 causes further increased somatic GAA repeat expansions (refer to the chapter 4) and a corresponding reduction in the level of *FXN* transcription. A similar decrease in *FXN* expression was seen in the PMS2-deficient human cell models, but without any accompanying GAA repeat expansion. This suggests a comparable non-GAA repeat-related mechanism of PMS2/Pms2 action, not only within *in vitro* and *in vivo* models, but also within mice and humans. In addition, loss of Msh6 or Mlh1 proteins led to reduced levels of *FXN* transcription, despite

corresponding losses of somatic GAA repeat expansions. The reasons for these conflicting results are not known. However, it is proposed that another mechanism, which does not involve GAA repeat expansions, may cause reduced levels of *FXN* transcription in Msh6 or Mlh1 deficient cells. In addition to repairing base mismatches or short IDLs resulting from replication errors, MMR proteins are also able to cooperate with the nucleotide excision repair (NER) system to amend genomic errors with bulky helix loops (Kobayashi *et al.* 2005; Denver *et al.* 2006). Generally, the NER system contributes to DNA repair through two sub-pathways; global genome NER (GG-NER) and transcription-coupled NER (TC-NER). Within TC-NER, the NER system is recruited to repair genomic errors, caused by preferentially binding transcription and RNA polymerase II to the transcribed DNA strand in expressed genes (Mellon and Hanawalt 1989; Kobayashi *et al.* 2005). Several investigations of different organisms have implicated MMR proteins in TC-NER. Thus, studies of *E.coli* have shown that lack of MutS and MutL proteins leads to dysfunction of TC-NER in the *Lac* operon (Mellon and Champe 1996). Moreover, it is reported that all yeast MMR proteins are involved in TC-NER of oxidative damage, while no effect was observed on TC-NER of ultraviolet (UV) light damage (Sweder *et al.* 1996; Leadon and Avrutskaya 1997; Kathe *et al.* 2004). In comparison with lower organisms, the role of MMR on mammalian TC-NER is still controversial. Nonetheless, several studies have indicated involvement of MMR proteins in TC-NER within particular expressed genes. Interestingly, defect of MSH2/MSH6 heterodimers in LOVO cells (a human colon defected MMR adenocarcinoma cell line) resulted in hypersensitivity of this epithelial cell type to UV due to loss of TC-NER function (Mellon *et al.* 1996; Kobayashi *et al.* 2005). Since MMR-defective mouse fibroblasts showed no effect of *Msh2* loss on sensitivity of UV damage (Sonneveld *et al.* 2001), it is proposed that MSH6 is the principal MMR protein contributing to TC-NER in LOVO cells. Studies of HCT-116 human epithelial *MLH1*-defective cells have also shown hypersensitivity to UV

light, due to the lack of TC-NER, while artificially introducing *MLH1* gene to this cell line culminated in TC-NER and a reduced sensitivity to UV light (Mellon *et al.* 1996; Kobayashi *et al.* 2005). These studies have all implicated MSH6 and MLH1 in TC-NER. Interestingly, this is consistent with the findings described in this chapter, regarding the effect of Msh6 or Mlh1 on transcription level of *FXN*. However, it has also been reported that defects of TC-NER result in reduced levels of transcription of particular genes (Michalowski *et al.* 2001). Taken together, these observations suggest a similar mechanism of action of Msh6 and Mlh1 on *FXN* transcription. Thus, it is proposed that transcribed *FXN* mRNA sequences and RNA polymerase II perhaps bind to an opened GAA/TTC repeat expansion within the first intron of the *FXN* gene to form an R-loop. In this case, the presence of Msh6 and Mlh1 may recruit the TC-NER system to correct the blockage and allow transcription to proceed. However, with a loss of Msh6 or Mlh1, TC-NER cannot proceed appropriately, the *FXN* mRNA fragment and RNA polymerase II are not released and *FXN* transcription is reduced.

In summary, this thesis has identified an important role of the MMR system in *FXN* transcription. Comparing individual MMR genes suggests that they have similar effects on *FXN* transcription, except for Msh2. Thus, analysis of Msh6, Pms2 and Mlh1 deficient mice demonstrated lower *FXN* transcription compared with $FXN^{GAA+}/MMR^{+/+}$ transgenic mice, while Msh2 deficient mice showed increased *FXN* transcription. Taken together, the findings obtained from chapters 4 and 5 suggest that there might be a direct link between GAA repeat expansions and *FXN* transcription with loss of Msh2 or Pms2. In contrast, no direct link was determined between GAA repeat expansions and *FXN* transcription level with lack of Msh6 or Mlh1. Loss of Msh6 or Mlh1 protein caused reduced levels of GAA repeat expansions, while the levels of *FXN* transcription were also reduced. The mechanisms by which Msh6 and Mlh1 proteins are involved in *FXN* transcription are not clear yet. Nevertheless, it is proposed these MMR proteins may be able to increase the levels of *FXN* transcription by

activating the TC-NER system. However, further investigations are now required to confirm this hypothesis.

Chapter 6 - Results: The effects of frataxin deficiency on MMR gene expression and potential malignant cell transformation

6.1 - Introduction

Various types of cancer have been detected in the FRDA patients (Barr *et al.* 1986; Ackroyd *et al.* 1996; De Pas *et al.* 1999; Kidd *et al.* 2001), although, the prevalence of the simultaneous occurrence of both FRDA and cancer is very low. It has been proposed that due to the cardiomyopathy at the early onset of the disease, FRDA patients do not generally live long enough to develop cancers, such as breast cancers (Kidd *et al.* 2001). Further investigations have also revealed that deficiency of frataxin is associated with multiple types of cell malignancy (Schulz *et al.* 2006; Guccini *et al.* 2011; Kirches *et al.* 2011).

Dysfunction of DNA repair genes might cause gene aberrations, resulting in disorders such as FRDA and cancer. An investigation of cultured FRDA cells has shown increased *MSH2* mRNA levels and increased GAA repeat expansions in induced pluripotent stem cells (iPSCs) compared to the donor FRDA fibroblasts. In contrast, no significant difference was observed in the *MSH3* mRNA expression level by comparing FRDA iPSC with donor fibroblasts (Ku *et al.* 2010). These findings suggested that expansion of GAA repeats, and subsequently *FXN* deficits, are associated with increased MMR gene expression in iPSCs. Considering the involvement of frataxin in cell malignancy and the relationship between GAA repeat expansions and MMR expression levels, it was considered relevant to investigate the potential role of frataxin deficiency in the formation of malignant cells via the MMR pathway. Therefore, the aim of this study was to understand whether a reduced level of frataxin could affect the mRNA expression level of different MMR genes. To reach this objective, the transcription levels of MMR genes were quantified both *in vitro*, using FRDA and unaffected human fibroblast cells, and *in vivo*, using FRDA and unaffected human autopsy tissues.

6.2 - Analysis of cDNA quality

To investigate the effect of *FXN* on the mRNA expression levels of MMR genes *in vitro*, total RNA was isolated using Trizol® from about 1 million human FRDA and human unaffected primary fibroblast cells. For the human *in vivo* study, total RNA was isolated from cerebellar tissue of FRDA patients and unaffected individuals using a NucloSpin® RNA II column based method. All RNA samples were treated with DNase I enzyme to prevent potential false positive results caused by MMR pseudogenes in contaminating DNA. Following quantity and quality analysis, 300-400ng/µl RNA was converted into cDNA. Then PCR primers were designed and reactions were optimised for each MMR gene by performing G-RT-PCR (Figure 6.1).

Figure 6.1 - Analysis of G-RT-PCR for MMR genes.

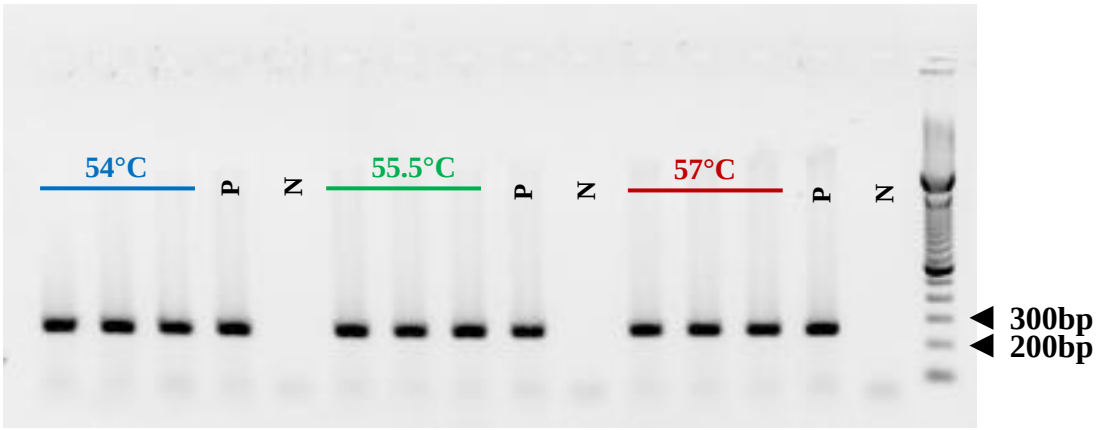

An example of G-RT-PCR for human MMR genes showing *MLH1* PCR products obtained by using different annealing temperatures run in ethidium bromide-stained 1% agarose gels, together with 1Kb+ size markers. P= positive control, N= negative control.

Subsequently, the quality of cDNA samples was confirmed by performing standard RT-PCR of the relevant MMR genes or human *GAPDH* endogenous control (refer to the figure 5.2C). In all cases, no primer-dimers were observed and only the specific PCR products were obtained, confirming a suitable quality of cDNA samples to use for qRT-PCR.

6.3 - Quantification of human MMR gene transcription *in vitro*

In this study, three different FRDA patient primary fibroblast cell cultures, containing different sizes of GAA repeat expansion, were compared with two to three control fibroblast cell cultures containing normal-sized GAA repeat sequences. These fibroblast cell lines originated from skin biopsies of FRDA and unaffected individuals (Table 6.1).

Table 6.1 - Details of the human primary fibroblasts.

	ID	Sex	Age (Yrs)	Number of GAA repeats	References
Control	**H. Normal**	Male	27	Normal	Kindly provided by Ian Kill
	GM07492	Male	17	Normal	Coriell cell repositories Inc.
	GM04503	Female	31	Normal	Coriell cell repositories Inc.
FRDA	**GM03816**	Female	36	330/380	Coriell cell repositories Inc.
	GM04078	Male	30	420/541	Coriell cell repositories Inc.
	GM03665	Female	13	445/740	Coriell cell repositories Inc.

Despite previous observations showing that the level of *FXN* transcription is reduced in expanded GAA repeats of FRDA patients (Greene *et al.* 2007; Al-Mahdawi *et al.* 2008), in this study, quantifying *FXN* transcription was considered to be useful to investigate the potential link between GAA repeat size, *FXN* transcription and *MMR* gene transcription. Therefore, *FXN* and *MMR* transcription levels were determined in each fibroblast cell line by qRT-PCR.

To analyse mRNA expression levels of *MMR* and *FXN* genes, the Ct value for each gene was normalised to human endogenous *GAPDH*. Each sample was run in triplicate and each experiment was carried out at least twice. The mean value of each individual triplicate sample was applied for further calculations using the $2^{-\Delta\Delta Ct}$ method to find RQ values. Next, the

relative transcription level of each gene, from both FRDA and unaffected cell lines, was calibrated against one of the unaffected *FXN* controls, 'H.Normal', which was arbitrarily assigned as 100%. All cell lines were matched in terms of passage number to prevent any potential passage-based variability. Analysis of the dissociation curve showed specificity of each set of primers (*GAPDH* and each MMR gene) without any non-specific PCR products, in the condition of optimised primer concentration (Figure 6.2).

Figure 6.2 - qRT-PCR analysis.

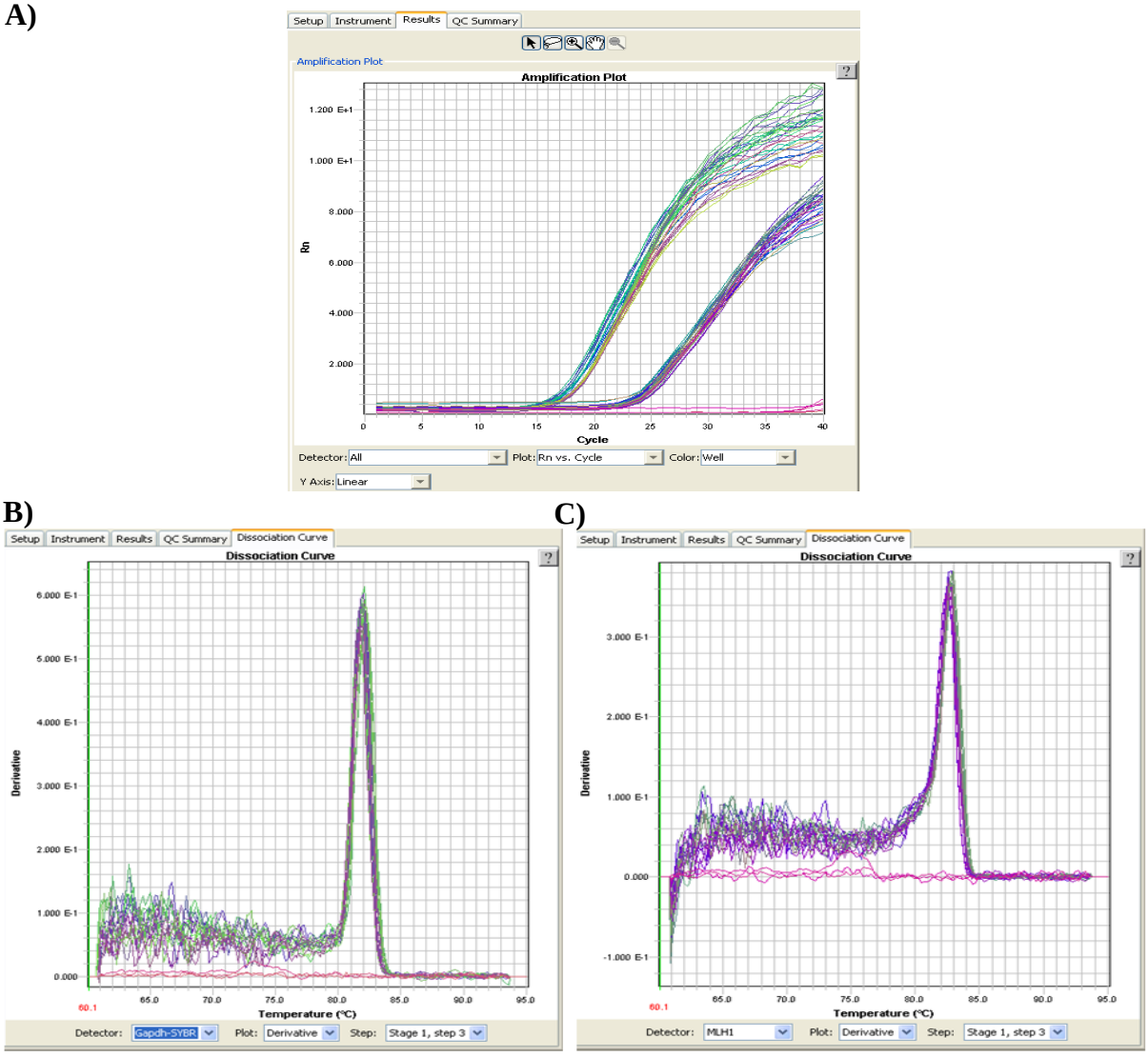

The images show schematic example of **(A)** Ct of each individual triplicate sample for target gene and *GAPDH* cDNAs, **(B)** dissociation curve for RT-*GAPDH* primers, and **(C)** dissociation curve for RT-*FXN* primers.

Quantification of the unaffected primary fibroblast cells demonstrated comparable levels of *FXN* transcription, while the sizes of GAA sequences were 9 to 16 repeats (Table 6.1, Figure 6.3).

Figure 6.3 - Quantification of *FXN* mRNA in human primary fibroblasts.

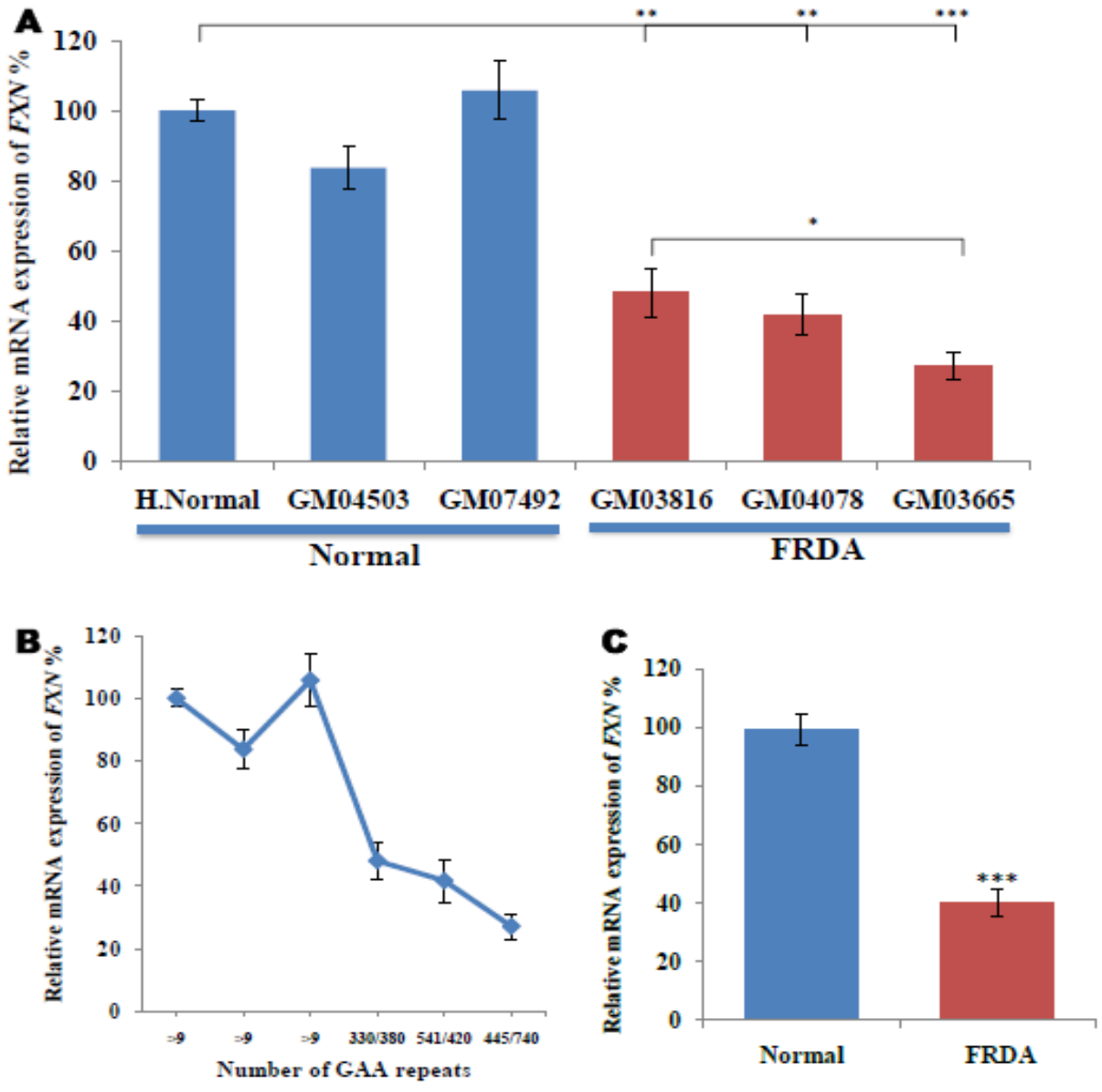

qRT-PCR measurement of *FXN* mRNA expression in **A-B**) individual fibroblast cell lines, and **C**) average expression between the unaffected and FRDA primary fibroblasts. *FXN* expression values were first normalised to *GAPDH* and then calibrated to unaffected fibroblasts expression. Each result is the mean of two independent experiments. Error bars = S.E.M, *= $p<0.05$, **= $p<0.01$, ***= $p<0.001$ (Chiranjeevi Sandi, personal discussions).

In contrast, comparing different FRDA fibroblast cell lines presented statistically significant differences in *FXN* transcription between the cells with greatest and least GAA repeat expansions. Thus, FRDA cells with less GAA repeat expansions (GM03816) showed a higher level of *FXN* transcription. Moreover, further analyses showed reduced levels of *FXN* transcription in all three FRDA fibroblast cells, GM04078, GM03816 and GM03665, compared with the unaffected fibroblast cell lines (Figure 6.3). The mean level of *FXN* transcription in FRDA cells was confirmed as 40% that of unaffected fibroblasts ($p<0.001$). This finding would agree with generally accepted view of the effect of GAA repeat expansion on the *FXN* transcription (Pianese *et al.* 2004; Greene *et al.* 2007; Al-Mahdawi *et al.* 2008).

6.3.1 - The effect of reduced *FXN* on *MSH2* transcription

The effect of frataxin deficiency on *MSH2* transcription was analysed by comparing *MSH2* mRNA expression in two unaffected *FXN* primary fibroblasts with three FRDA primary fibroblast lines. qRT-PCR results clearly showed an increased value of *MSH2* mRNA expression in human FRDA fibroblasts (more than 2.5 fold; $p<0.001$), suggesting upregulation of the mRNA expression level of this MMR gene with defects of frataxin (Figure 6.4A). This finding suggests that MSH2 is not likely to play a role in tumourigenesis of defective *FXN* fibroblast cells, since MSH2 upregulation is a natural intrinsic response to mutations, while downregulation of MSH2 has been recognised to cause various types of cell malignancy, such as HNPCC. I propose that upregulation of *MSH2* transcription leads to the increased level of MSH2 protein, which is consequently recruited to repair the GAA repeat expansion mutations and other DNA damage in FRDA fibroblast cells.

Since different sizes of GAA repeat expansions were observed in the three FRDA fibroblast cell lines, to study whether the increased *MSH2* mRNA expression level was directly related to GAA repeat expansions, *MSH2* transcription levels were determined individually in each cell line and statistical differences were assessed by the student t-test (Figure 6.4B-C).

Figure 6.4 - Analysis of *MSH2* mRNA expression level in fibroblast cells.

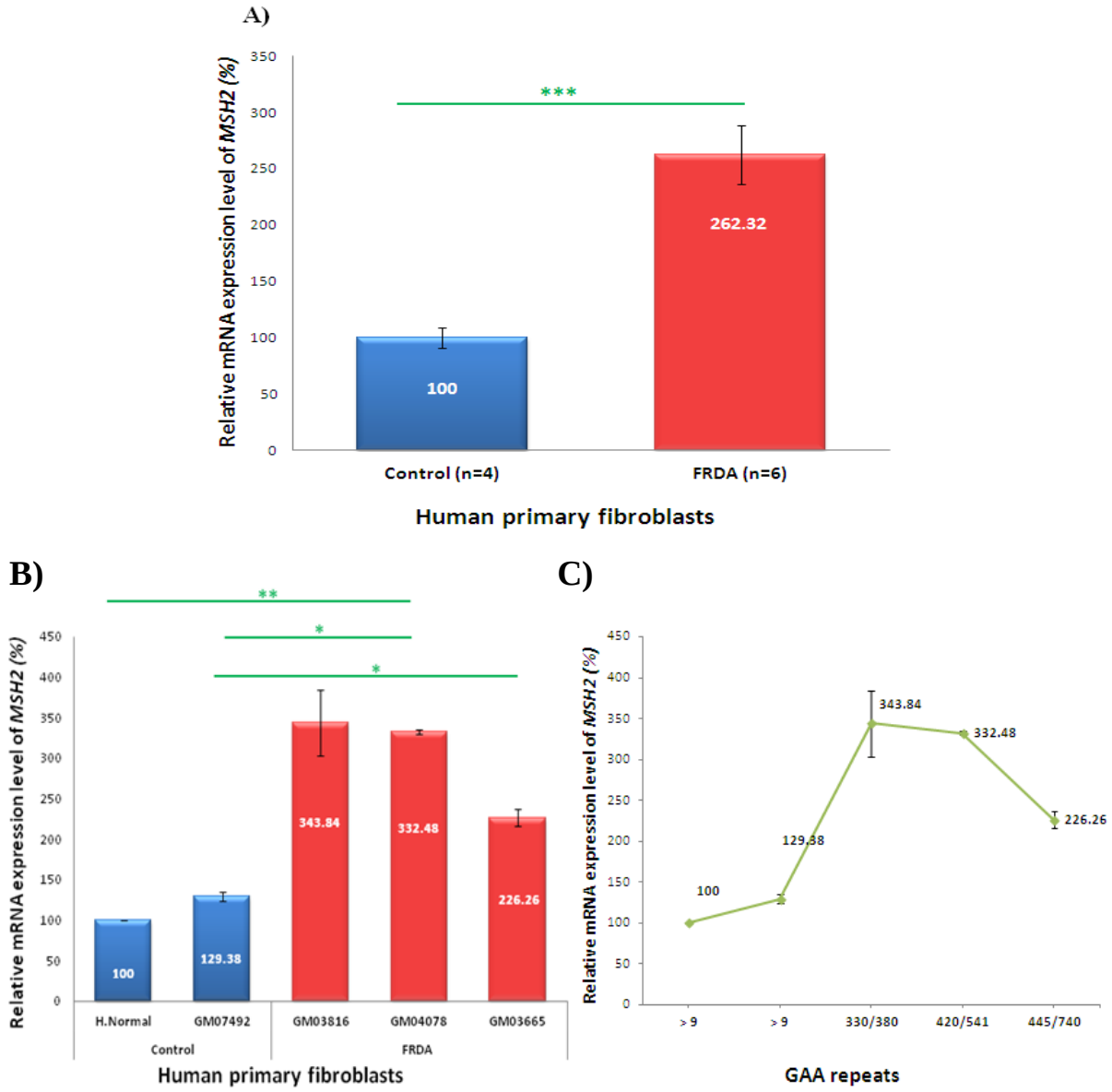

The graphs represent *MSH2* mRNA level in **(A)** average expression between unaffected and FRDA primary fibroblasts, **(B)** individual fibroblast cells, and **(C)** comparison with GAA repeat sizes. Error bars = S.E.M, *=P<0.05, **= P<0.01, ***= P<0.001

Table 6.2 - Student t-test *p*-values of frataxin deficiency effect on the *MSH2* mRNA expression level during individual cell line analyses.

		Control		FRDA		
		H. Normal	**GM07492**	**GM03816**	**GM04078**	**GM03665**
Control	**H. Normal**		0.12	0.11	0.007	0.05
	GM07492	0.12		0.12	0.019	0.015
FRDA	**GM03816**	0.11	0.12		0.83	0.221
	GM04078	0.007	0.019	0.83		0.064
	GM03665	0.05	0.015	0.221	0.064	

Although increased mRNA levels of *MSH2* were observed in the GM03816 and GM04078 FRDA cell lines compared with GM03665, the differences were not statistically significant (Figure 6.4B-C, Table 6.2). This finding suggests that there is no obvious relationship between sizes of expanded GAA repeats and levels of *MSH2* mRNA. Thus, GAA repeat expansion is not the principle cause of MSH2 upregulation in FRDA fibroblasts. Therefore, other mechanisms that result from frataxin deficiency are more likely to be involved in the upregulation of *MSH2*. In other words, these findings suggest a mechanistic pathway between upregulation of *MSH2* transcription, GAA repeat expansions and decreased frataxin levels in FRDA fibroblasts.

6.3.2 - The effect of reduced *FXN* on *MSH3* transcription

To investigate the effect of frataxin deficiency on *MSH3* expression, *MSH3* mRNA was analysed in two cell lines of primary fibroblasts compared with three FRDA primary fibroblast cells. qRT-PCR data analysis demonstrated upregulation of *MSH3* mRNA expression in FRDA cell lines compared with controls (Figure 6.5A). This is in contrast with the hypothesis that frataxin deficiency may form malignant cells by reducing *MSH3* expression. Therefore, I suggest that, as with *MSH2*, upregulation of *MSH3* results in increased level of MSH3 protein to repair expanded GAA repeat mutations and other DNA damage in FRDA fibroblast cells.

With regards to the different sizes of GAA repeat expansions in FRDA fibroblasts, analysis of data showed slight fluctuations in the *MSH3* mRNA expression level within the three individual FRDA fibroblast cells; however, no statistically significant differences were observed (Figure 6.5B-C, Table 6.3). This observation indicates that there is not any direct link between GAA repeat expansion sizes and levels of *MSH3* mRNA expression. Therefore, other mechanism(s) are likely to be involved in upregulation of *MSH3* transcription within FRDA fibroblasts.

Figure 6.5 - Analysis of *MSH3* mRNA expression level in fibroblast cells.

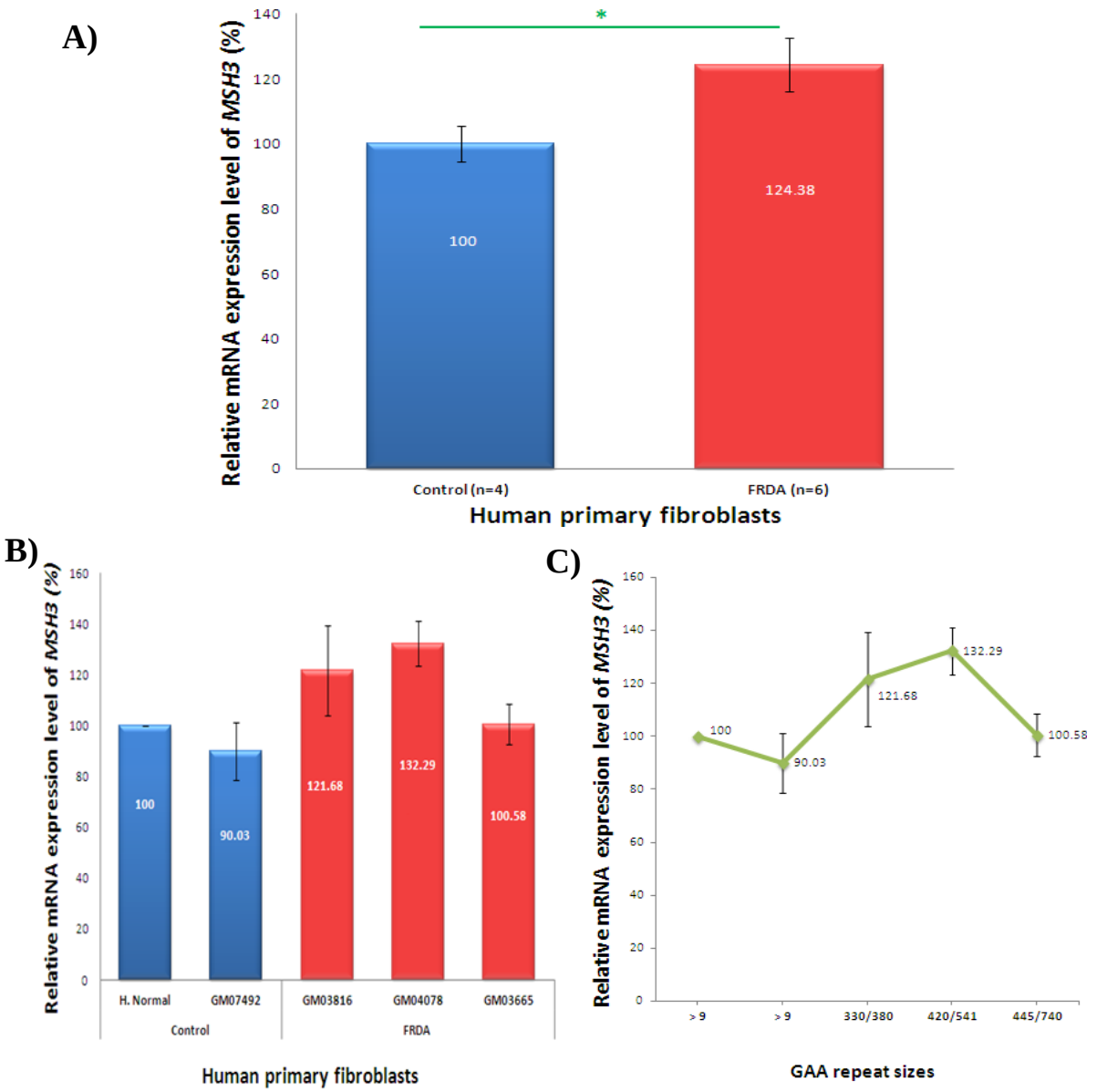

The graphs represent *MSH3* mRNA level in **(A)** average expression between unaffected and FRDA primary fibroblasts, **(B)** individual fibroblast cells, and **(C)** comparison with GAA repeat sizes. Error bars = S.E.M, *=P<0.05

Table 6.3 - Student t-test *p*-values of frataxin deficiency effect on the *MSH3* mRNA expression level during individual cell line analyses.

		Control		FRDA		
		H. Normal	**GM07492**	**GM03816**	**GM04078**	**GM03665**
Control	**H. Normal**		0.54	0.44	0.17	0.95
	GM07492	0.54		0.27	0.1	0.52
FRDA	**GM03816**	0.44	0.27		0.92	0.475
	GM04078	0.17	0.1	0.92		0.12
	GM03665	0.95	0.52	0.475	0.12	

6.3.3 - The effect of reduced *FXN* on *MSH6* transcription

To examine the effect of frataxin deficiency on *MSH6* expression, *MSH6* mRNA expression was analysed in three FRDA primary fibroblast cell lines compared with two unaffected *FXN* fibroblasts. qRT-PCR analysis clearly demonstrated an increase of *MSH6* mRNA expression in FRDA cells, approximately 1.5-fold that of control cells ($p<0.001$; Figure 6.6A), indicating that frataxin deficiency results in upregulation of *MSH6* mRNA expression. Therefore, it is proposed that defects of frataxin do not lead to cell malignant transformation through affecting the level of *MSH6* expression. Rather, it is proposed that, as with *MSH2* and *MSH3*, upregulation of *MSH6* mRNA expression causes an increased level of MSH6 protein required to repair expanded GAA repeat mutations and general DNA damage in FRDA fibroblast cells. Analysing individual cell lines demonstrated no significant difference of the *MSH6* mRNA expression level in the unaffected *FXN* primary fibroblasts. Likewise, by comparing the *MSH6* transcription level in each FRDA cell line, no statistically significant variability was observed, while they showed different sizes of GAA repeat expansion (Figure 6.6B-C, Table 6.4). This finding suggests no direct link between sizes of expended GAA repeats and mRNA levels of *MSH6*. Thus, GAA repeat expansion is not the main cause of MSH6 upregulation in FRDA fibroblasts. Therefore, it is proposed that other mechanisms might also be involved in this upregulation.

Figure 6.6 - Analysis of *MSH6* mRNA expression level in fibroblast cells.

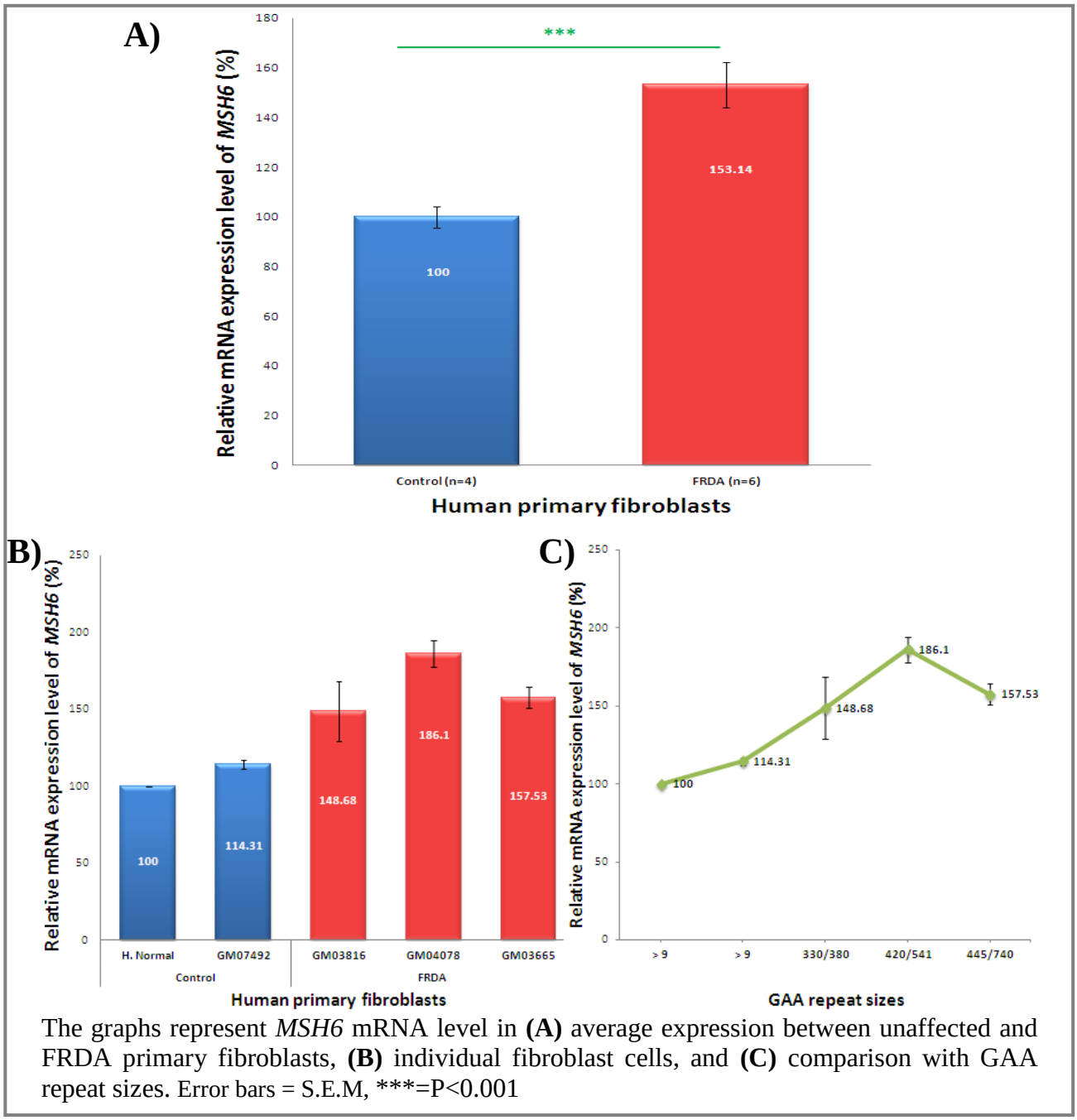

The graphs represent *MSH6* mRNA level in **(A)** average expression between unaffected and FRDA primary fibroblasts, **(B)** individual fibroblast cells, and **(C)** comparison with GAA repeat sizes. Error bars = S.E.M, ***=P<0.001

Table 6.4 - Student t-test *p*-values of frataxin deficiency effect on the *MSH6* mRNA expression level during individual cell line analyses.

		Control		FRDA		
		H. Normal	**GM07492**	**GM03816**	**GM04078**	**GM03665**
Control	**H. Normal**		0.12	0.24	0.06	0.075
	GM07492	0.12		0.33	0.08	0.11
FRDA	**GM03816**	0.24	0.33		0.33	0.74
	GM04078	0.06	0.08	0.33		0.12
	GM03665	0.075	0.11	0.74	0.12	

6.3.4 - The effect of reduced *FXN* on *PMS2* transcription

To determine if *PMS2* expression was affected by frataxin deficiency, *PMS2* mRNA transcription was quantified in three primary FRDA fibroblast cell lines compared with two unaffected fibroblast cell lines. Analysis of the results showed increased *PMS2* mRNA expression in FRDA cell lines (127%) compared with controls (normalised as 100%); however, the results were not statistically significant (p=0.14, Figure 6.7). To accurately quantify the *PMS2* mRNA levels individually in each cell line, further experiments would be needed.

Figure 6.7 - Analysis of *PMS2* mRNA expression level in fibroblast cells.

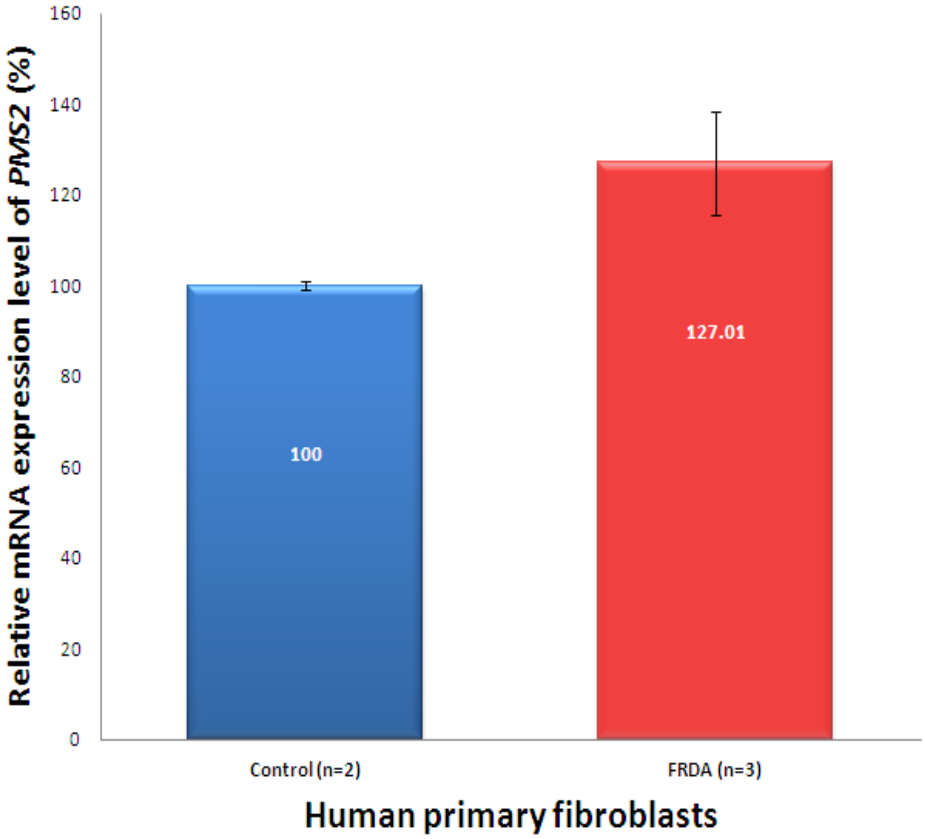

The graph illustrates mean value of the *PMS2* mRNA level in unaffected and FRDA primary fibroblasts. Error bars =S.E.M.

6.3.5 - The effect of reduced *FXN* on *MLH1* transcription

In this experiment, the *MLH1* mRNA level was quantified by qRT-PCR to examine the effect of frataxin deficiency. Data obtained from three FRDA and two unaffected primary fibroblast cell lines demonstrated that the value of *MLH1* mRNA was significantly higher in FRDA cells (approximately 1.5-fold; $p<0.05$), suggesting that the *MLH1* mRNA level is upregulated as a result of defects of *FXN* in human fibroblasts (Figure 6.8A). Considering that downregulation of MLH1 has been reported to cause various types of cell malignancies, this result indicates that *MLH1* expression level is not involved in tumourigenesis in defective *FXN* fibroblast cells. It is proposed that, as with the other MMR proteins, upregulation of the *MLH1* mRNA expression level might be a natural cellular mechanism to repair GAA repeat expansion mutations and other general DNA damage in FRDA fibroblasts. To determine if sizes of GAA repeat expansions are directly linked to MLH1, the mRNA level of this MMR gene was analysed within individual FRDA primary fibroblasts. Although, the data analysis showed fluctuations in the level of *MLH1* transcription within these three cell lines, no statistically significant difference was observed (Figure 6.8B-C, Table 6.5). This finding suggests that expanded GAA repeat sizes do not directly affect the transcription level of *MLH1* gene. In other words, expansion of GAA repeats is not the direct cause of *MLH1* mRNA upregulation in FRDA fibroblasts. Therefore, it is also proposed that other mechanism(s) might also be involved in this upregulation. Further investigations are required to clarify the exact mechanism(s) involved in this event.

Figure 6.8 - Analysis of *MLH1* mRNA expression level in fibroblast cells.

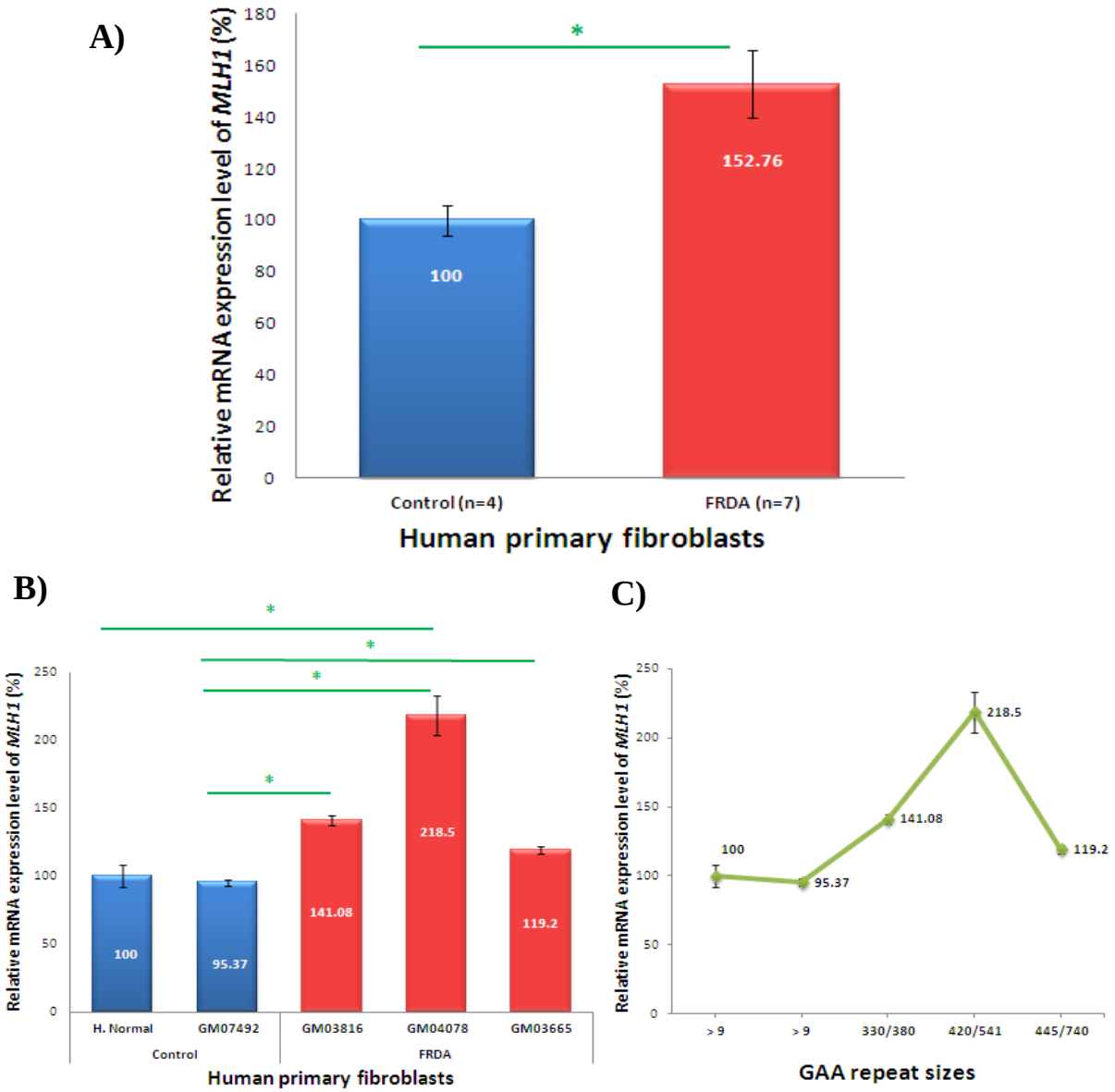

The graphs represent *MLH1* mRNA level in **(A)** average expression between unaffected and FRDA primary fibroblasts, **(B)** individual fibroblast cells, and **(C)** comparison with GAA repeat sizes. Error bars =S.E.M, *=P<0.05

Table 6.5 - Student t-test *p*-values of frataxin deficiency effect on the *MLH1* mRNA expression level during individual cell line analyses.

		Control		FRDA		
		H. Normal	**GM07492**	**GM03816**	**GM04078**	**GM03665**
Control	**H. Normal**		0.31	0.26	0.03	0.8
	GM07492	0.31		0.015	0.03	0.04
FRDA	**GM03816**	0.26	0.015		0.09	0.06
	GM04078	0.03	0.03	0.09		0.051
	GM03665	0.8	0.04	0.06	0.051	

6.4 - Quantification of MMR transcription in human FRDA tissues

Following on from the FRDA cell culture studies, the effects of frataxin deficiency on MMR mRNA expression levels (excluding *MSH3* mRNA expression level) were investigated in human FRDA tissues. In this study, cerebellum tissues were obtained from 4 FRDA patients compared with 4 unaffected individuals. Initial analysis of FRDA patient blood DNA samples showed different sizes of GAA repeat expansions (Table 6.6), while analysis of unaffected individuals showed normal-sized (<16) GAA repeats within brain and cerebellum tissues (Figure 6.9)

Table 6.6 - Details of the human cerebellum tissues.

	ID	Sex	Age (Yrs)	Number of GAA repeats
FRDA patients	**22/CA**	M	24	550/750
	44/HK	M	17	630/750
	58/CR	M	40	570/930
	80/JT	M	25	780/780
unaffected individuals	**3/HN**	M	80	<16
	8/HN	F	82	<16
	13/HN	M	81	<16
	16/HN	M	64	<16

Figure 6.9 - Analyses of GAA repeat size in the unaffected individuals.

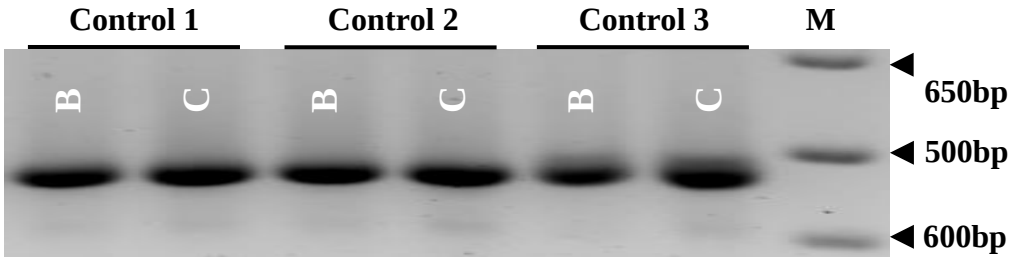

The image represents example of the ethidium bromide-stained agarose gel used to determine GAA repeat sizes, showing an inverted image of PCR products obtained from two tissues of three unaffected individuals (controls 1-3). B= brain tissue, C= cerebellum tissue, M= 1Kb^{+} size marker.

Prior to quantifying *MMR* gene transcription, the quality of cDNA samples was analysed by performing a standard RT-PCR for the human *GAPDH* gene (Figure 6.10). The results demonstrated a specific PCR product for all FRDA and control samples, with an absence of any non-specific products, indicating a good enough quality of samples to perform qRT-PCR. To verify the specificity of MMR gene PCR products, conventional RT-PCRs were also performed for each MMR gene. The results confirmed the specificity of all MMR genes, with the exception of *MSH3*, which showed only a non-specific PCR product. Therefore, *MSH3* RT-PCR was not performed as part of this study, but will require further optimisation in it is to be performed in the future.

Figure 6.10 - *GAPDH*-RT-PCR analysis.

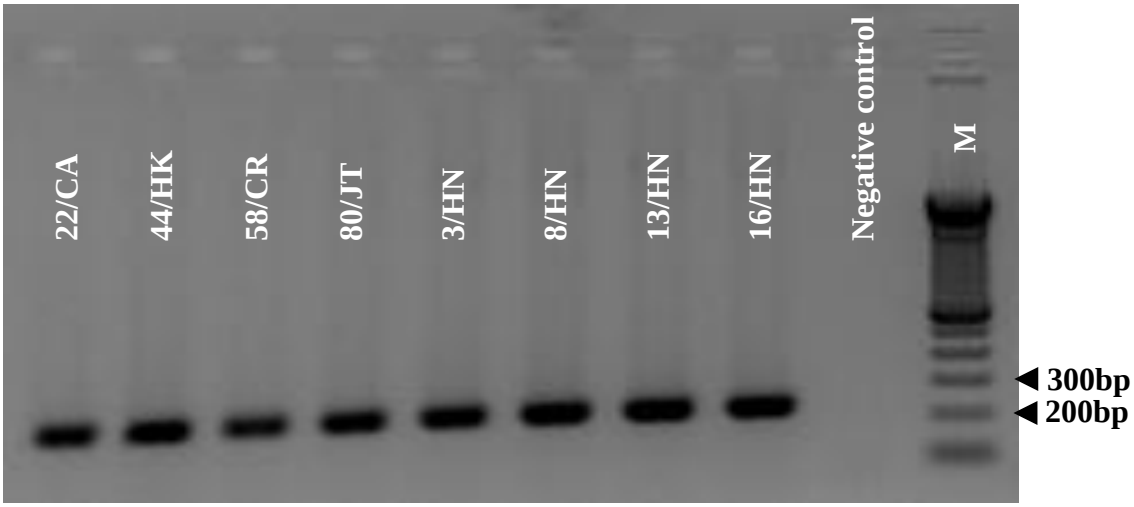

The image represents quality of cDNA obtained from human cerebellum tissues of four FRDA patients compared with four unaffected individuals by analysing human *GAPDH*-RT-PCR products in 1% ethidium bromide-stained agarose gel electrophoresis. M= 1kb size marker.

To quantify the mRNA expression, the Ct value for each target gene was normalised to the human endogenous *GAPDH*. In this study, each sample was run in triplicate and each experiment was performed at least twice. The mean value of each individual triplicate sample was calculated for further analysis using the $2^{-\Delta\Delta Ct}$ formula to find the RQ value. Subsequently, the relative level of transcription of each gene was determined for all FRDA and unaffected samples by calculating the RQ mean values, followed by setting one of the human unaffected cerebellum samples arbitrarily as 100%.

To understand the potential link between *FXN* deficiency and transcription levels of MMR genes, *FXN* mRNA expression levels were first verified. Standard *FXN* RT-PCR did not produce any products in any of the FRDA patients, whilst the control samples obtained from human unaffected cerebellum tissues gave specific RT-PCR products (Figure 6.11).

Figure 6.11 - Human *FXN*-RT-PCR analysis.

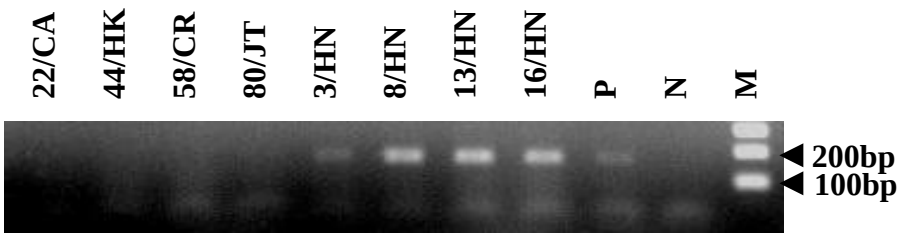

The image illustrates human *FXN*-RT-PCR analyses of samples in 1% ethidium bromide-stained agarose gel electrophoresis. M= $1Kb^{+}$ size marker, P= positive control, N= negative control. n.b. this was a preliminary result to confirm the quality of cDNAs, before optimising primers for qRT-PCR.

As shown earlier (Figure 6.10), analysing RT-PCR products for *GAPDH* confirmed the quality of cDNA in all FRDA and unaffected individuals. Since the FRDA patients had very large GAA repeat expansions, and since frataxin is poorly expressed in cerebellum, I would propose that not observing a *FXN* RT-PCR product in the FRDA samples indicates very low levels of *FXN* expression in these samples.

6.4.1 - The effect of *FXN* deficiency on *MSH2* transcription

To understand the effect of *FXN* on *MSH2* transcription, the *MSH2* mRNA expression level was analysed by comparing cerebellum tissues of four FRDA patients with four unaffected individuals. Analysis of mean values demonstrated a remarkably reduced level of the *MSH2* mRNA in FRDA patients (approximately 23%) in comparison with unaffected individuals (Figure 6.12A), indicating that *MSH2* mRNA expression is downregulated in FRDA cerebellum tissue.

Since the GAA repeat expansion sizes were variable within the four different FRDA patients, a comparison was made between GAA repeat expansions and *MSH2* cerebellum mRNA expression levels. Quantification of the individual tissue samples by qRT-PCR clearly

showed reduced levels of *MSH2* mRNA expression in all four FRDA patients: 22/CA, 44/HK, 58/CR and 80/JT showed levels of 25%, 23%, 23% and 10%, respectively, compared to the reference unaffected control, 8/HN. Further analyses did not show any significant differences in the level of *MSH2* transcription with increasing magnitude of GAA repeat expansions in FRDA samples, except in the 80/JT (Figure 6.12B-C, Table 6.7). In this experiment, quantification of unaffected tissues showed slight fluctuation in *MSH2* mRNA expression levels; however, no statistically significant differences were observed.

Taken together, findings obtained from this experiment demonstrated that defects of *FXN* expression, most likely caused by GAA repeat expansions, led to downregulation of *MSH2* transcription in FRDA cerebellum tissues. That means frataxin deficiency might be able to contribute to cell malignancies by reducing *MSH2* expression in the cerebellum. However, finding no direct link between expanded GAA repeat size and levels of *MSH2* expression indicates that GAA repeat expansions do not by themselves downregulate *MSH2* mRNA expression in the human cerebellum tissue. It is proposed that other mechanisms, such as epigenetic modifications, might be involved in this downregulation. In other words, these findings suggest an interactive pathway between GAA repeat expansion, frataxin deficiency and downregulation of *MSH2* transcription in FRDA cerebellum.

Figure 6.12 - Analysis of *MSH2* mRNA expression levels in human cerebellum tissues.

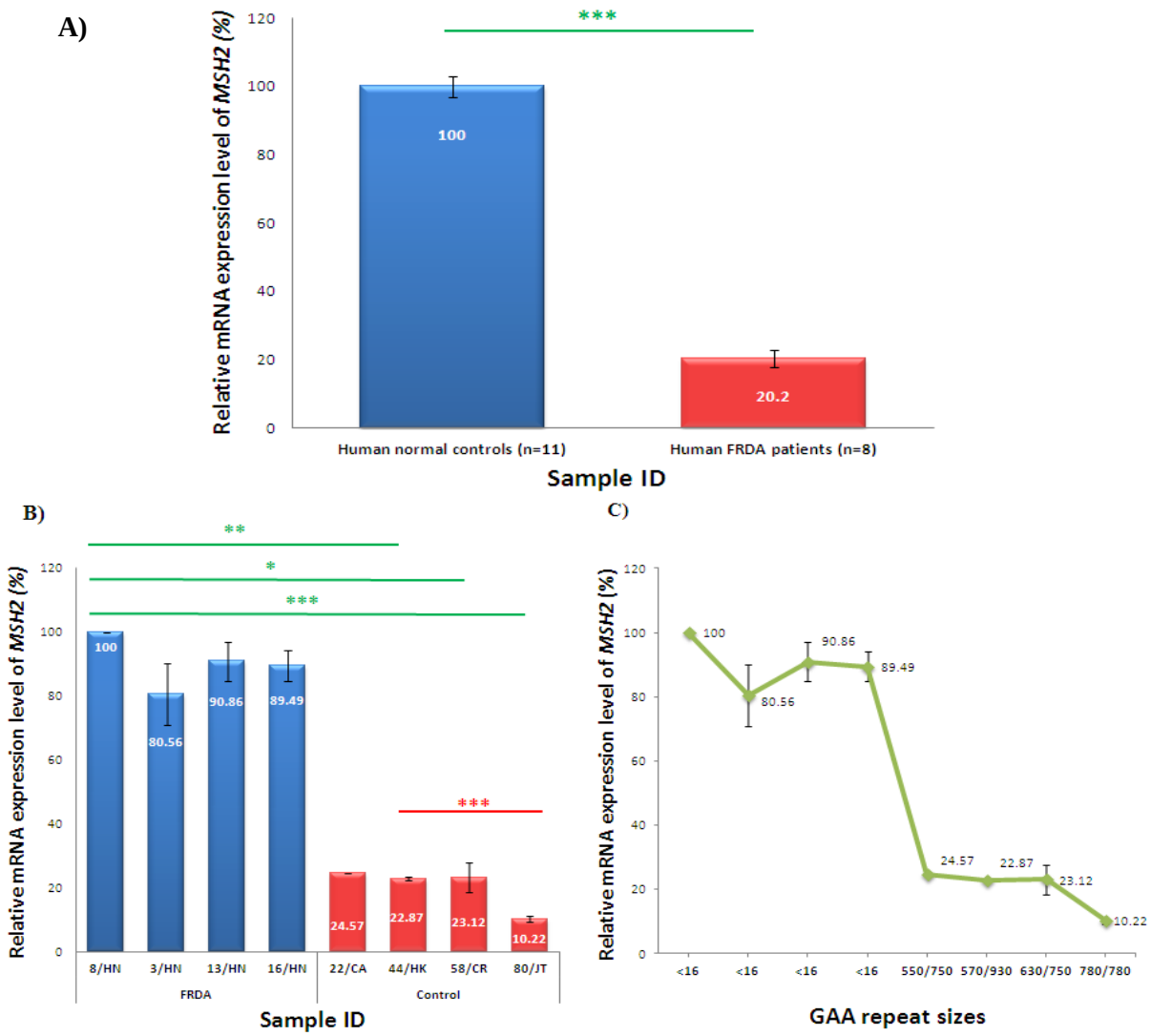

The graphs represent *MSH2* mRNA level in **(A)** average expression between unaffected and FRDA cerebellum tissues, **(B)** individual cerebellum tissues, and **(C)** comparison with GAA repeat sizes. Error bars= S.E.M, *=P<0.05, **= P<0.01, ***= P<0.001

Table 6.7 - Student t-test *p*-values of frataxin deficiency effect on the *MSH2* mRNA expression level during individual cerebellum tissue analyses.

	44/HK	58/CR	80/JT	8/HN	3/HN	13/HN	16/HN
44/HK		0.97	0.0009	0.003	0.195	0.08	0.06
58/CR	0.97		0.22	0.04	0.17	0.06	0.014
80/JT	0.0009	0.22		0.0001	0.09	0.07	0.053
8/HN	0.003	0.04	0.0001		0.29	0.27	0.15
3/HN	0.105	0.17	0.09	0.29		0.46	0.43
13/HN	0.08	0.06	0.07	0.27	0.46		0.9
16/HN	0.06	0.014	0.053	0.15	0.43	0.9	

6.4.2 - The effect of *FXN* deficiency on *MSH6* transcription

To investigate effects of frataxin deficiency on *MSH6* transcription, the level of *MSH6* mRNA was quantified in cerebellum tissue of three different FRDA patients and three unaffected individuals. Analysis of mean values demonstrated a 46% level of *MSH6* mRNA in FRDA patient cerebellum tissues compared with unaffected controls ($p<0.001$; Figure 6.13A). This finding suggests that deficit of frataxin in cerebellum tissue causes downregulation of *MSH6* mRNA expression level. Individual sample analysis demonstrated a reduced level of *MSH6* mRNA expression in all FRDA samples compared with unaffected controls, but a statically significant difference was only observed with one of the FRDA samples (80/JT) (Figure 6.13B, Table 6.8). Further analyses showed that, while there were fluctuations in the mRNA expression levels of *MSH6*, no statistically significant differences were observed within all three FRDA cerebellum tissues (Figure 6.13B-C, Table 6.8).

Taken together, these findings reveal that frataxin deficiency caused downregulation of *MSH6* transcription in cerebellum tissue, suggesting a possible effect of frataxin defects on cerebellum tissue tumourigenesis through MSH6 aberrations. Moreover, finding no direct link between expanded GAA repeat size and levels of *MSH6* mRNA indicates that GAA repeat expansions are sufficient, but not necessary to downregulate *MSH6* expression. Therefore, it is proposed that there is interplay of GAA repeat expansion, frataxin deficiency and reduced expression of both *MSH6* and *MSH2* in FRDA cerebellum tissues.

Figure 6.13 - Analysis of *MSH6* mRNA expression levels in human cerebellum tissues.

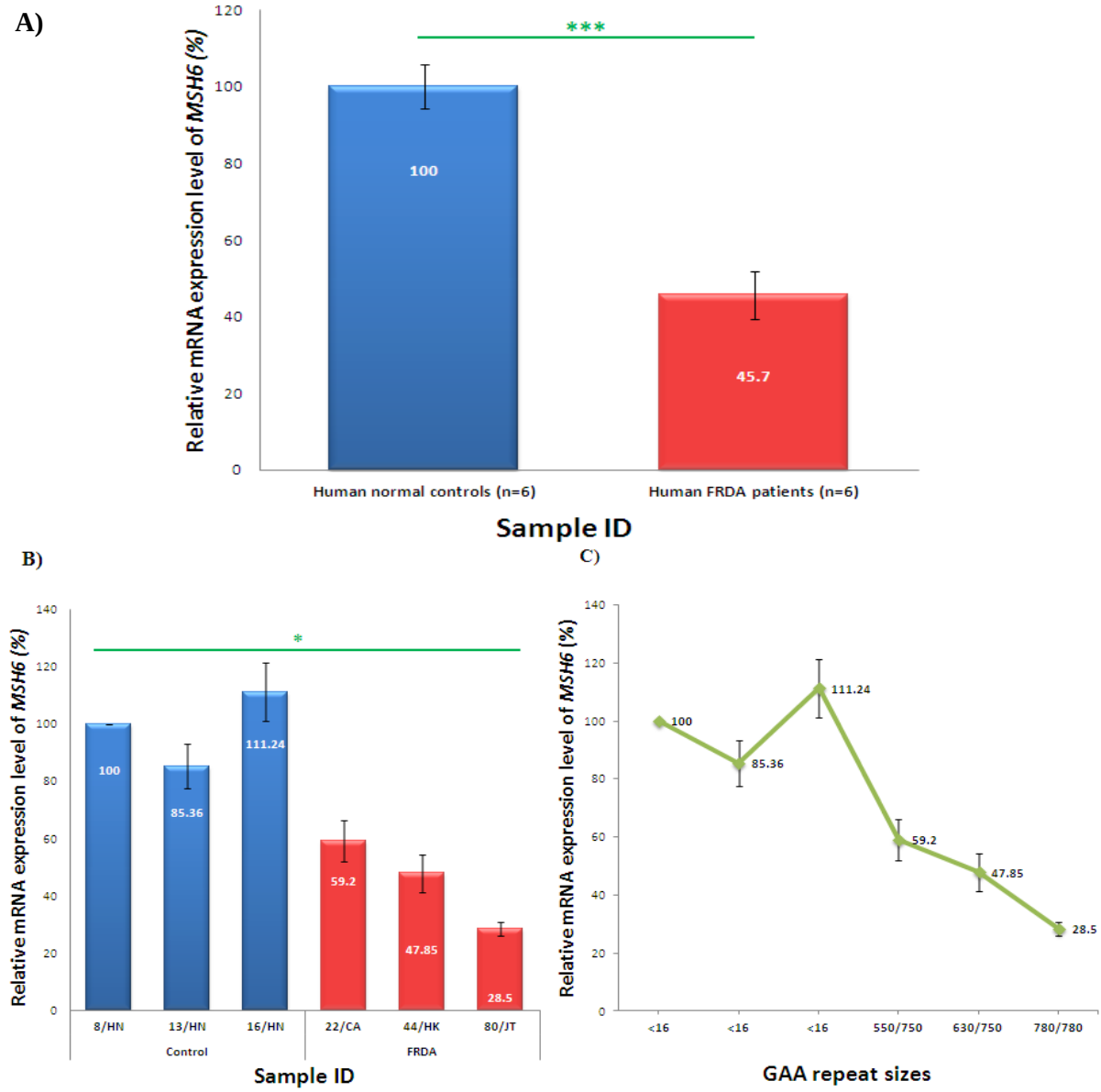

The graphs represent *MSH6* mRNA level in **(A)** average expression between unaffected and FRDA cerebellum tissues, **(B)** individual cerebellum tissues, and **(C)** comparison with GAA repeat sizes. Error bars= S.E.M, *=P<0.05, ***= P<0.001

Table 6.8 - Student t-test *p*-values of frataxin deficiency effect on the *MSH6* mRNA expression level during individual cerebellum tissue analyses.

	8/HN	13/HN	16/HN	22/CA	44/HK	80/JT
8/HN		0.32	0.47	0.11	0.08	0.021
13/HN	0.32		0.18	0.13	0.069	0.092
16/HN	0.47	0.18		0.053	0.035	0.08
22/CA	0.11	0.13	0.053		0.36	0.15
44/HK	0.08	0.069	0.035	0.36		0.22
80/JT	0.021	0.092	0.08	0.15	0.22	

6.4.3 - The effect of *FXN* deficiency on *PMS2* transcription

The *PMS2* mRNA expression levels were quantified in cerebellum tissues of four FRDA patients and four unaffected individuals. Analysis of mean values demonstrated significant downregulation of the *PMS2* mRNA in FRDA patients compared with unaffected individuals ($p<0.05$: Figure 6.14A), indicating that the level of *PMS2* expression is remarkably reduced in FRDA cerebellum tissues. Analysis of individual samples revealed fluctuation of *PMS2* mRNA expression levels, although no statistically difference was observed (Figure 6.14B-C, Table 6.9).

Taken together, these observations showed that frataxin deficiency resulted in downregulation of *PMS2* transcription in FRDA cerebellum tissues, but in a manner that was not related to GAA repeat size. Therefore, it is proposed that there may be interplay between GAA repeat expansion, frataxin deficiency and downregulation of *MSH2*, *MSH6* and *PMS2* in FRDA cerebellum tissue.

Figure 6.14 - Analysis of *PMS2* mRNA expression levels in human cerebellum tissues.

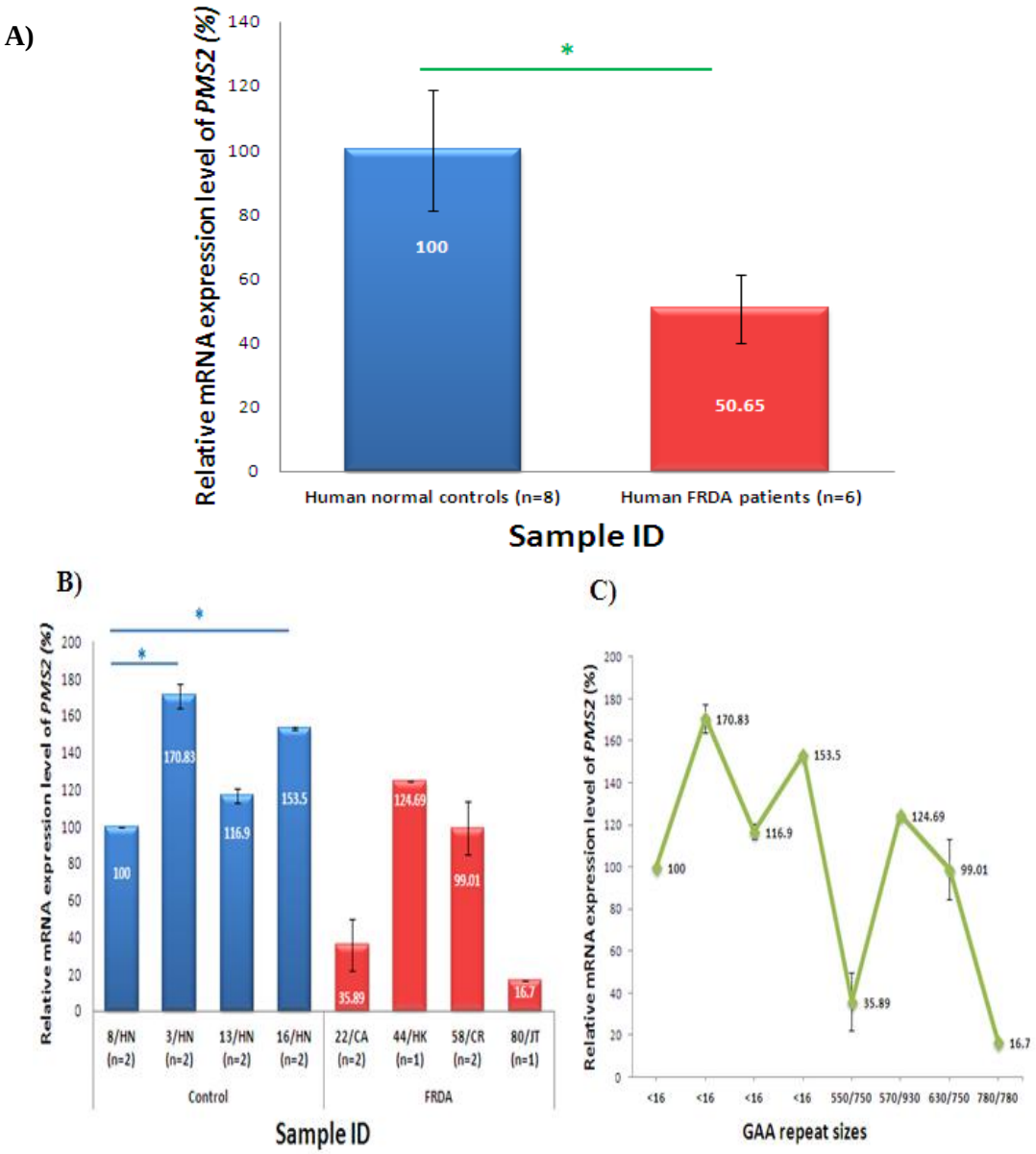

The graphs represent *PMS2* mRNA level in **(A)** average expression between unaffected and FRDA cerebellum tissues, **(B)** individual cerebellum tissues, and **(C)** comparison with GAA repeat sizes. Error bars= S.E.M, *=P<0.05

Table 6.9 - Student t-test *p*-values of frataxin deficiency effect on the *PMS2* mRNA expression level during individual cerebellum tissue analyses.

	22/CA	58/CR	8/HN	3/HN	13/HN	16/HN
8/HN	0.14	0.96		0.06	0.14	0.009
3/HN	0.07	0.14	0.06		0.02	0.24
13/HN	0.11	0.44	0.14	0.02		0.07
16/HN	0.07	0.16	0.009	0.24	0.07	
22/CA		0.09	0.14	0.07	0.11	0.07
58/CR	0.09		0.96	0.14	0.44	0.16

6.4.4 - The effect of *FXN* deficiency on *MLH1* transcription

To determine if *MLH1* expression was affected by frataxin deficiency, the *MLH1* mRNA levels were quantified in cerebellum tissues of four FRDA patients and four unaffected individuals. Analysis of mean values demonstrated a remarkably reduced level of *MLH1* mRNA expression in FRDA patients, at approximately 20% of the level in unaffected cerebellum tissues ($p<0.001$; Figure 6.15A). This finding indicates that defects of frataxin caused by GAA repeat expansions induce downregulation of *MLH1* expression in cerebellum. Quantification of individual samples by qRT-PCR clearly demonstrated reduced levels of *MLH1* mRNA expression in all four FRDA patients: 22/CA (38%), 44/HK (32%), 58/CR (29%), and 80/JT (29%), compared with controls (Figure 6.15B). The data showed no statistically significant differences between *MLH1* expression in the four FRDA cerebellum tissues (Figure 6.15B-C, Table 6.10). Further analyses did not suggest any direct link between the level of *MLH1* transcription and size of expanded GAA repeats in the FRDA cerebellum tissues.

Taken together, the observations obtained from this experiment demonstrated that frataxin deficiency downregulates the *MLH1* transcription level in cerebellum tissue, suggesting a possible effect of frataxin defects on cerebellum tissue tumourigenesis through MLH1 aberrations. Furthermore, finding no direct link between sizes of expanded GAA repeats and levels of *MLH1* mRNA indicates that GAA repeat expansions are sufficient, but not necessary, to downregulate *MLH1* expression. Therefore, other mechanisms might be involved in this downregulation. Further investigations are required to clarify the exact mechanisms involved in this interaction, which now appears to involve GAA repeat expansion, frataxin deficiency and downregulation of all four MMR genes so far investigated, namely *MSH2*, *MSH6*, *PMS2* and *MLH1*.

Figure 6.15 - Analysis of *MLH1* mRNA expression levels in human cerebellum tissues.

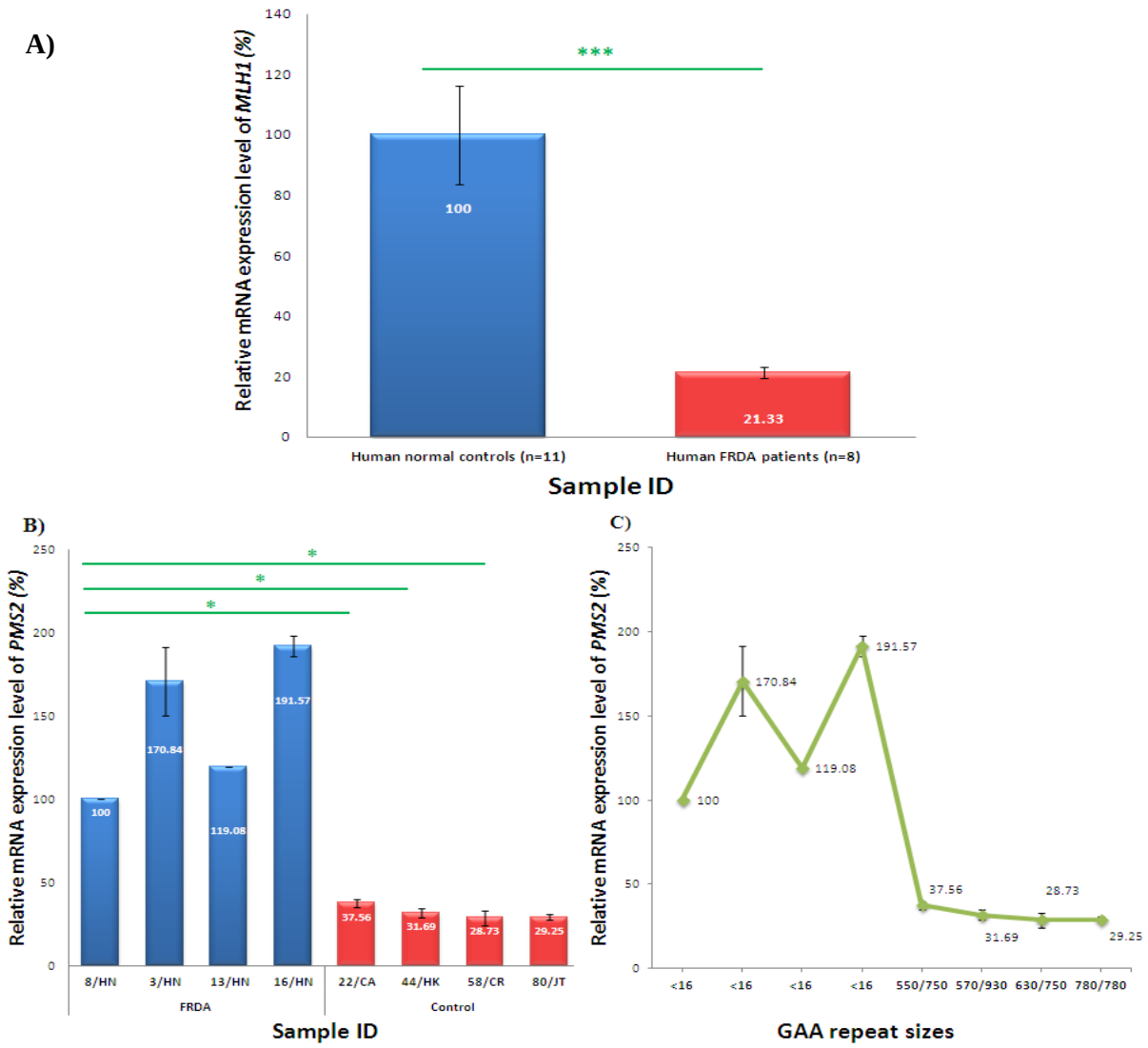

The graphs represent *MLH1* mRNA level in **(A)** average expression between unaffected and FRDA cerebellum tissues, **(B)** individual cerebellum tissues, and **(C)** comparison with GAA repeat sizes. Error bars= S.E.M,*=P<0.05, **= P<0.01, ***= P<0.001

Table 6.10 - Student t-test *p*-values of frataxin deficiency effect on the *PMS2* mRNA expression level during individual cerebellum tissue analyses.

	22/CA	44/HK	58/CR	80/JT	8/HN	3/HN	16/HN
22/CA		0.27	0.34	0.1	0.02	0.1	0.03
44/HK	0.27		0.64	0.55	0.03	0.09	0.03
58/CR	0.34	0.64		0.93	0.04	0.09	0.002
80/JT	0.1	0.55	0.93		0.93	0.09	0.025
8/HN	0.02	0.03	0.04	0.93		0.18	0.043
3/HN	0.1	0.09	0.09	0.09	0.18		0.51
16/HN	0.03	0.03	0.002	0.025	0.43	0.51	

6.5 - Discussion

To understand the molecular mechanisms that could potentially contribute to malignant cell transformation of frataxin-deficient cells, the mRNA expression levels of human MMR genes were investigated using *in vitro* and *in vivo* FRDA model systems. *In vitro* analysis demonstrated upregulation of *MSH2*, *MSH3*, *MSH6* and *MLH1* gene expression in FRDA fibroblasts compared to unaffected fibroblasts. *PMS2* also showed a non-statistically significant trend towards upregulation in FRDA fibroblasts. Therefore, it is proposed that MMR expression is upregulated in FRDA fibroblasts as a natural intrinsic response to DNA errors, perhaps including GAA repeat expansion mutation itself. These findings are compatible with the known role of the MMR system, which involves recruitment of MMR proteins to repair damaged DNA. Since frataxin deficiency is mainly caused by GAA repeat expansion, it is possible that expansion of this repeat may be involved in upregulation of MMR expression. To investigate this, GAA repeat sizes were compared with the level of MMR expression in individual FRDA fibroblast cells. However, no correlation was observed, suggesting that GAA repeat expansion is not directly involved in upregulation of different MMR expression.

In contrast to the human fibroblast results, studies of human cerebellum tissues identified significantly reduced levels of MMR transcription in FRDA patients compared with unaffected individuals, which was once again not related to GAA repeat size. This indicates that frataxin deficiency may cause reduced MMR gene expression in the cerebellum. The discrepancy between the results from human cerebellum tissues (*in vivo*) compared with human fibroblast cell lines (*in vitro*) could be explained in two ways. Firstly, it may be due to the use of different cell systems: *in vivo* versus *in vitro*. Secondly, since FRDA is known to be a tissue selective disorder, different cell types may respond differently to frataxin

deficiency. Indeed, further investigations have been performed on the *FXN*$^{GAA+}$ transgenic mouse cell lines in the Pook laboratory showing that the levels of *Msh2*, *Msh3*, *Msh6*, and *Pms2* mRNA expression are all significantly reduced in GAA repeat-containing YG8 and YG22 differentiated neural stem cells (NSCs), compared with Y47 transgenic mice that carry the normal human *FXN* gene (C. Sandi, personal communication). This is consistent with the observations of human cerebellum tissues, suggesting comparable effects in human cerebellum tissue and mouse differentiated NSC cell lines. Moreover, investigation of transgenic mouse kidney fibroblast cell lines showed that *Msh2*, *Msh3*, *Msh6*, and *Pms2* mRNA expression levels were either not significantly changed (YG8) or increased (YG22) compared with Y47 fibroblasts (C. Sandi, personal communication). This finding is also comparable with data obtained from analysis of human FRDA fibroblasts, suggesting similar effects in both human FRDA and *FXN*$^{GAA+}$ transgenic mouse fibroblast cell lines. These findings support the notion that different cell types respond differently to frataxin deficiency. Thus, tissues that have higher sensitivity to frataxin deficiency, such as cerebellum, show reduced levels of MMR expression, while tissues that are less-sensitive (e.g. skin, the source of human fibroblasts) show increased levels of MMR expression.

The principle cause of downregulation of MMR gene expression in tissues that are highly sensitive to frataxin deficiency is not yet clear. Studies have shown that non-cytotoxic levels of H_2O_2, which is an important source of oxidative stress, can inactivate MMR functions in a dose dependent manner (Chang *et al.* 2002). Other studies have also reported that oxidative stress can lead to the induction of frameshift mutations within MMR genes in human colorectal epithelial cell lines, subsequently inactivating MMR functions (Gasche *et al.* 2001). It is not exactly clear how oxidative stress could inhibit MMR gene transcription. However, studies have indicated that oxidative stress can affect *Mlh1* mRNA expression in malignant cells in a histone deacetylase-dependent manner. Thus, induction of oxidative

stress overactivates histone deacetylation, consequently leading to downregulation of *Mlh1* mRNA expression. Treatment of these cells with HDACi agents, such as TSA, restored the normal levels of *Mlh1* mRNA expression, confirming the role of oxidative stress on downregulation of *Mlh1* transcription (Mihaylova *et al.* 2003).

Since oxidative stress is one of the consequences of frataxin deficiency, it is proposed that reduced MMR transcription in tissues that are highly sensitive to frataxin deficiency might be due to increased levels of oxidative stress. This may then lead to the induction of epigenetic changes, particularly deacetylation of histones, within the MMR genes. Future investigations of such epigenetic changes within the MMR genes may provide valuable insights into the possible mechanisms involved in downregulation of MMR gene expression in the frataxin deficient cells.

Chapter 7 - General discussion

7.1 - General discussion

This thesis aimed to investigate the relationships between MMR genes, GAA repeat instability and *FXN* gene expression in the inherited neurodegenerative disorder FRDA. The reasoning was that MMR proteins are known to play a critical role in correcting DNA replication errors, while investigations of the other TNR disorders (e.g. CAG and CTG repeats in HD and DM1, respectively) have previously demonstrated an important role of MMR proteins in the stability of these microsatellite repeats. Furthermore, frataxin deficiency has also been associated with malignant cell transformation, which may be due to modulation of DNA repair gene expression (in the case of this project, MMR gene expression).

The novel findings of this thesis have been categorised into four sections. Firstly, observations from genetically altered mouse studies demonstrated the importance of MMR proteins in intergenerational GAA repeat instability. Thus, the mutability frequency of GAA repeats was shown to generally increase in the offspring of mice that lack MMR proteins. Furthermore, the results indicated that neither Msh2 nor Msh3 is involved in causing GAA expansions, but rather they appear to protect against contraction of GAA repeats. In contrast, Pms2 acts by a different mechanism to Msh2 and Msh3, promoting GAA repeat contractions and preventing GAA repeat expansions. Msh6 confers some protection against both GAA repeat expansions and contractions, but it has a less obvious role to play in intergenerational GAA repeat dynamics. Mlh1 appears to protect against contractions and promote expansions, but further investigations are required to confirm the exact role of this protein.

Secondly, investigations of the same genetically altered mice showed that MMR proteins also play an important role in somatic GAA repeat instability. Thus, loss of Msh2, Msh3, Msh6 or Mlh1 was shown to cause a reduction of progressive GAA repeat expansion within CNS tissues, particularly the cerebellum. Conversely, Pms2 deficiency produced even larger GAA repeat expansions. Comparing intergenerational and somatic GAA repeat instability systems

revealed different effects of Msh2, Msh3, Msh6 or Mlh1 proteins, while the effects of Pms2 were similar for both systems.

Thirdly, MMR proteins were found to have an effect on *FXN* transcription in CNS tissues. Thus, Msh6-, Pms2- and Mlh1-deficient brain and cerebellum tissues showed downregulation of *FXN* transcription, while Msh2-deficient tissues showed increased *FXN* transcription and Msh3-deficient cells showed no change. The Msh2- and Pms2-deficient *FXN* transcription changes could be accounted for by corresponding changes in GAA repeat sizes. However, analysis of Msh6- or Mlh1-defective brain and cerebellum tissues did not reveal a direct link between GAA repeat sizes and *FXN* transcription levels, suggesting that regulation of *FXN* transcription occurs through mechanisms that do not involve GAA repeat instability.

Finally, investigations showed that frataxin deficiency has varying effects on MMR mRNA expression depending on the type of cell or tissue. Thus, cells that are less sensitive to frataxin deficiency (e.g. fibroblast cells isolated from skin) show upregulation of MMR expression, perhaps in response to DNA replication errors, while tissues that contain non-dividing cells that are highly sensitive to frataxin deficiency (e.g. CNS tissues) show reduced MMR expression. Overall, these findings suggest that various mechanisms may contribute to the interaction of MMR proteins and GAA repeat instability, and in turn, to the level of frataxin and MMR transcription. These mechanisms will now be discussed further by proposing models that may explain the relationships between GAA repeat expansion, *FXN* transcription and MMR gene transcription.

7.2 - How might MMR proteins affect GAA repeat instability?

Data from this thesis and other *in vitro* and *in vivo* studies (Bourn *et al.* 2012; Du *et al.* 2012; Ezzatizadeh *et al.* 2012; Halabi *et al.* 2012) have put emphasis on a critical role of MMR proteins in GAA repeat instability and *FXN* gene expression. Although the exact mechanisms of action are unknown, observations would suggest a complicated system of interactions. Since dsDNA is only normally opened up during replication or transcription, two models are proposed to explain the effect of MMR proteins on GAA repeat expansions.

7.2.1 - How could the MMR system induce GAA repeat expansion during DNA replication?

It is generally accepted that repeat expansions can adopt different types of non-B DNA structures during DNA replication. Investigations have shown that GAA repeat expansions may form triplexes between intermolecular GAA.GAA.TTC (R.R.Y) sequences (Vetcher *et al.* 2002) or a more complicated form of sticky DNA by the binding of two separate GAA repeat runs in naked supercoiled DNA (Sakamoto *et al.* 1999; Chandok *et al.* 2012). Such sequences may lead to inefficient DNA replication. Therefore, it is proposed that the MMR system could be recruited to attempt the repair such non-canonical DNA structural errors. In the initial stage of repair, a small loop that is produced as a result of GAA triplex formation (Figure 7.1B-C) could be recognised by the MutSα or the MutSβ complex (Figure 7.1D). Interestingly, ChIP assays have demonstrated that both of the MutSβ complex proteins, Msh2 and Msh3, and to a lesser extent Msh6, show increased occupancy in the downstream region of expanded GAA repeat sequences, which could indicate binding to the

GAA repeat itself (Du *et al.* 2012; Ezzatizadeh *et al.* 2012). However, the results shown in chapter 4 of this thesis, together with the results from another study (Bourn *et al.* 2012), suggest that Msh2, Msh3 and Msh6 all have roles to play in somatic GAA repeat instability. Therefore, it is proposed that MutSβ (Msh2-Msh3) most likely plays the more important role in binding to a triplex DNA loop, while MutSα (Msh2-Msh6) plays a somewhat lesser role. Following binding of the MutS complex to the triplex DNA loop, a MMR-directed excision may be made by endonuclease activity within the single-strand of DNA that occurs opposite the loop (Figure 7.1D). This event may then recruit the MutLα complex and other coordinating proteins to proceed with MMR system (Figure 7.1E). Providing both Mlh1 and Pms2 are present, the MutLα complex is recruited to continue and terminate the MMR procedure. Simultaneously, an alternative enzyme (most likely a helicase) may open up the triplex sequences, creating a gap in the nicked opposing single strand of DNA, which is then filled with additional sequence by a DNA polymerase (Figure 7.1E). Hence, this event not only resolves the GAA repeat triplex structure, but at the same time causes further GAA repeat expansions. However, this mechanism does not account for how loss of Pms2 can cause the observed increased expansion of GAA repeats. Therefore, it is proposed that Pms2 can induce GAA repeat contractions by a separate mechanism.

Figure 7.1 - MMR proteins may act on DNA triplex structures to cause GAA expansions.

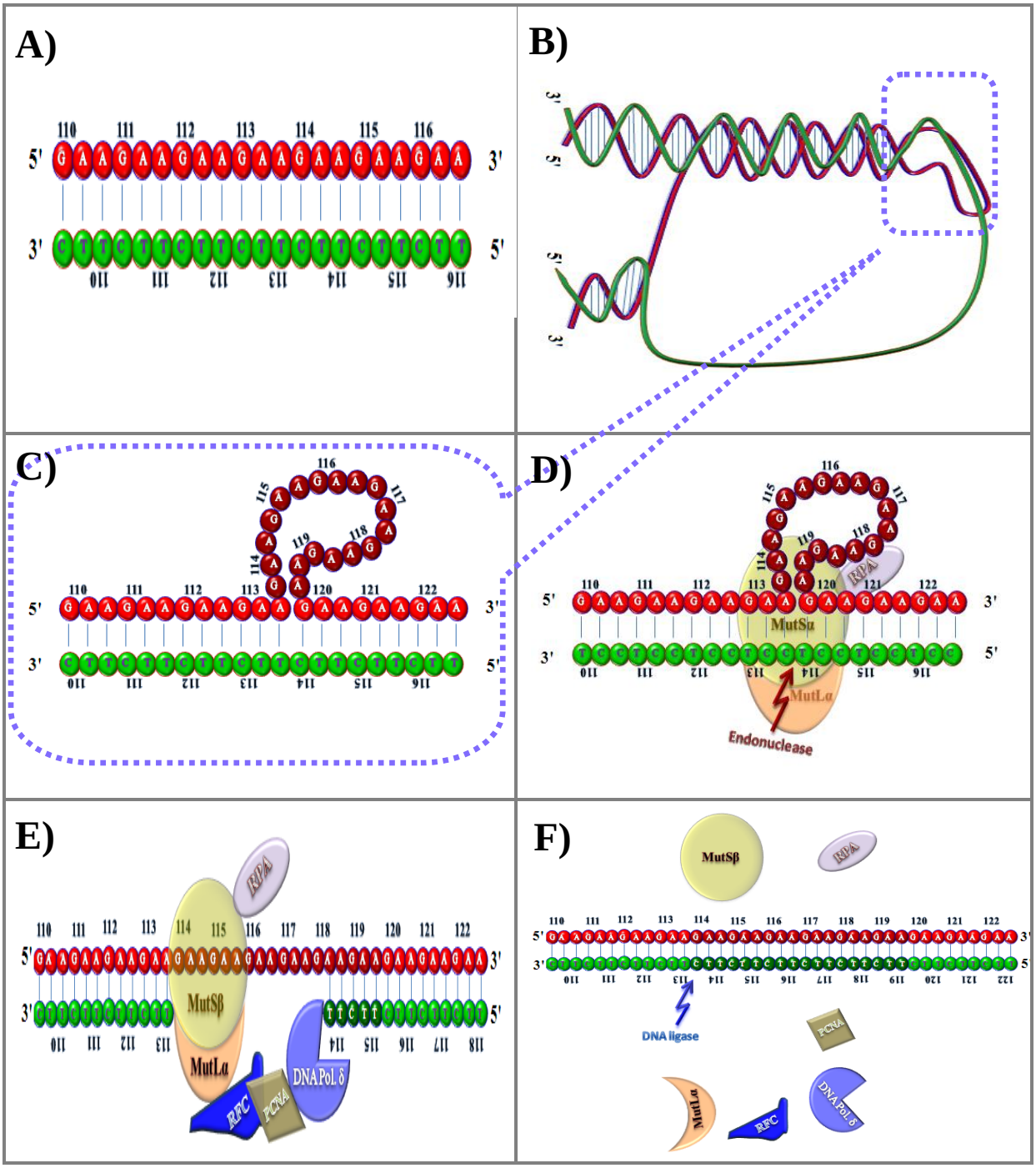

Schematic images representing: **(A)** normal GAA repeat structure, **(B)** triplex Y.R.R structure of the expanded GAA repeats, **(C)** focus on the small loop caused by triplex DNA structure **(D)** recognition of the loop by MutSβ/MutLα and cleavage with endonuclease, **(E)** opening of the loop, recruiting MMR complexes and synthesis of DNA by DNA polymerase δ, and **(F)** ending repair by ligation of the further expanded strand and release of MMR proteins and protein assemblies (e.g. RFC, PCNA and RPA).

7.2.2 - How could the MMR system induce GAA repeat expansion during transcription?

Another hypothesis that could explain the formation of progressive GAA repeat expansions is the involvement of MMR proteins during *FXN* transcription. Previous studies have shown that there is a direct link between GAA repeat expansion and transcription (Greene *et al.* 2007; Al-Mahdawi *et al.* 2008; Ditch *et al.* 2009). Furthermore, evidence suggests that transcription of GAA repeats can produce unusual RNA.DNA hybrid sequences *in vitro* (Grabczyk and Usdin 2000; Grabczyk *et al.* 2007) and in bacteria (Grabczyk *et al.* 2007), resulting in RNA polymerase II stalling. Non-canonical DNA/RNA hybrid structures may be created during transcription by the binding of single-stranded template TTC repeat sequences to premature transcribed GAA mRNA sequences forming loop outs of the single-stranded non-template GAA repeats (Figure 7.2B-D). These loop outs may then be recognised by one of the MutS complexes (Figure 7.2E). As part of the resolution process, a MMR-directed excision may be made in the TTC template strand of DNA (Figure 7.2E) and the mRNA may be released from the template strand by helicase enzyme activity. Subsequently, the MutS complex may recruit MutLα and other MMR system proteins to repair the cut TTC strand of DNA, but with the introduction of expanded repeat sequences (Figure 7.2F). Since somatic GAA repeat expansions occur predominantly in tissues that contain mainly non-dividing cells, such as brain and cerebellum, a transcription-based mechanism is indeed the most pertinent model to explain the role of the MMR system in somatic GAA repeat expansions.

Figure 7.2 - MMR proteins may act on RNA/DNA triplex structures to cause GAA expansions.

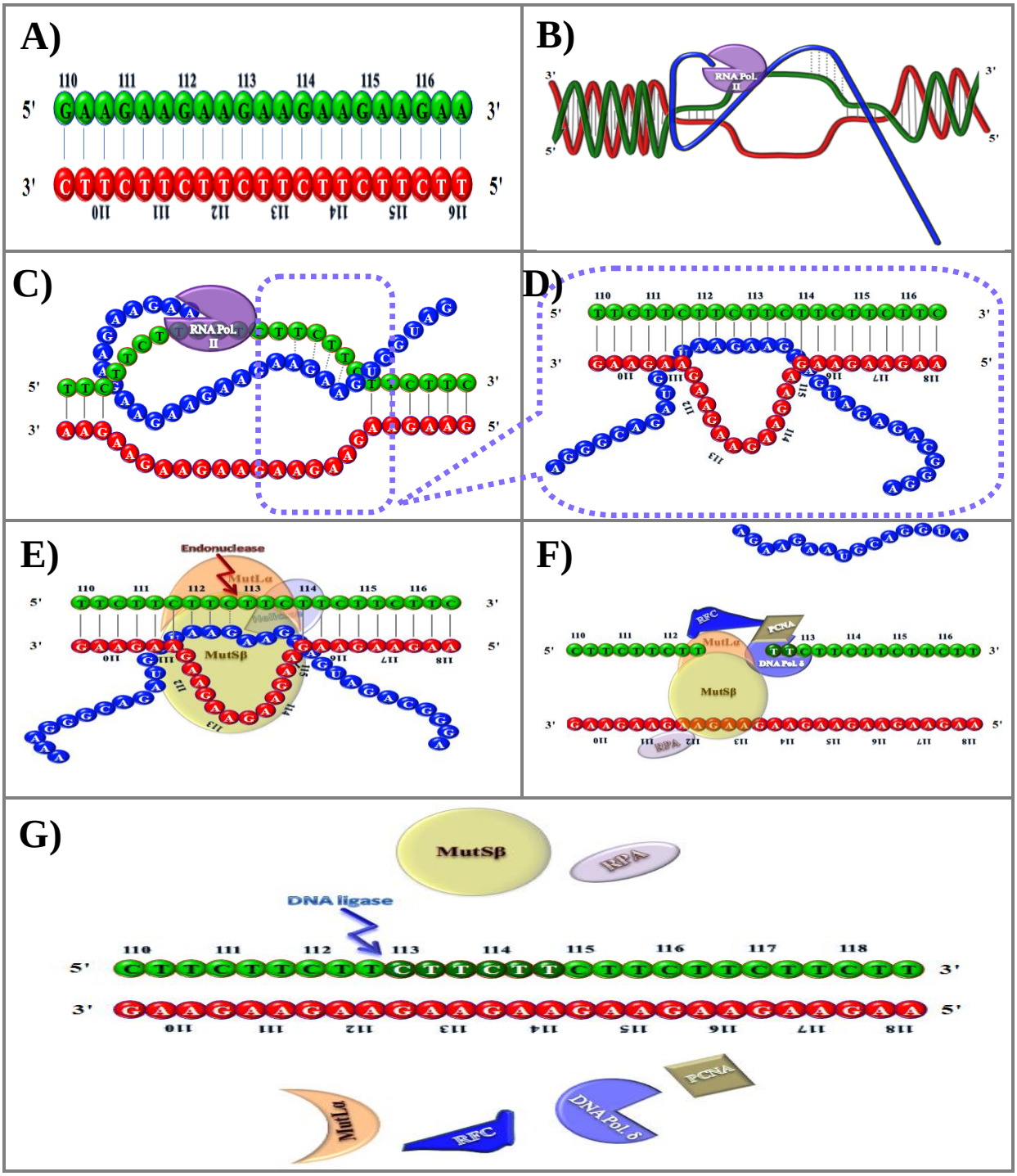

Images illustrating: **(A)** normal structure of expanded GAA repeats, **(B)** a small triplex DNA.RNA structure formed within GAA repeats, **(C)** focus on the unwound region during transcription **(D)** focus on the small loop caused by DNA.RNA binding, **(E)** recognition of the loop by MutS heterodimers and cleavage of the opposite DNA strand with an endonuclease, **(F)** release of the RNA and synthesis of expanded DNA by DNA polymerase δ and **(G)** ending repair by ligation of the expanded strand and release of MMR proteins as well as protein assemblies (e.g. PCNA, RFC and RPA).

7.3 - How could MMR proteins affect *FXN* transcription?

The previous hypotheses may explain how somatic GAA repeat expansions could arise due to MMR activity. However, they do not explain why the level of *FXN* mRNA expression is not increased to correspond with the reduced size of GAA repeats in Msh6- or Mlh1-deficient genetically altered mouse tissues, as previously reported for FRDA cells and tissues that are MMR proficient (Greene *et al.* 2007; Al-Mahdawi *et al.* 2008; Ditch *et al.* 2009). Therefore, it is proposed that another mechanism, separate from the canonical MMR system, might be in operation, whereby defects of *Msh6* or *Mlh1* cause both a reduction of *FXN* mRNA expression as well as a reduced level of expanded GAA repeats. Previous studies have highlighted the importance of MSH6 and MLH1 proteins in TC-NER (Mellon *et al.* 1996; Kobayashi *et al.* 2005) and defects of TC-NER can result in reduced gene transcription (Michalowski *et al.* 2001). Therefore, it is proposed that deficiencies of MSH6 or MLH1 may have dual effects, reducing GAA repeat expansions via the MMR system and reducing *FXN* transcription via the TC-NER system.

In this model, a complex of primary *FXN* mRNA sequences and RNA polymerase II may bind to form an unusual RNA/DNA triplex structure (Figure 7.3A). This abnormal structure may be able to cause further GAA expansions, on the one hand, and block transcription of the *FXN* gene, on the other. It is not certain how MSH6 or MLH1 may participate in *FXN* transcription via the TC-NER system. However, the findings presented in chapter 5 of this thesis would suggest that MSH6 and MLH1 can act, perhaps as a complex with other proteins, to enhance *FXN* transcription. MSH6 and MLH1 proteins may bind to the abnormal DNA/RNA hybrid structure and, by acting through the TC-NER system, they may assist in the release of stalled RNA polymerase II enzyme (Figure 7.3B), resulting in the resumption of *FXN* transcription (Figure 7.3C). In contrast, in the absence of MSH6 or MLH1 proteins,

RNA polymerase II would not be released due to the failure of the TC-NER system (Figure 7.3D) and blockage of *FXN* transcription would persist.

Figure 7.3 - The effect of MSH6 and MLH1 on *FXN* transcription via TC-NER.

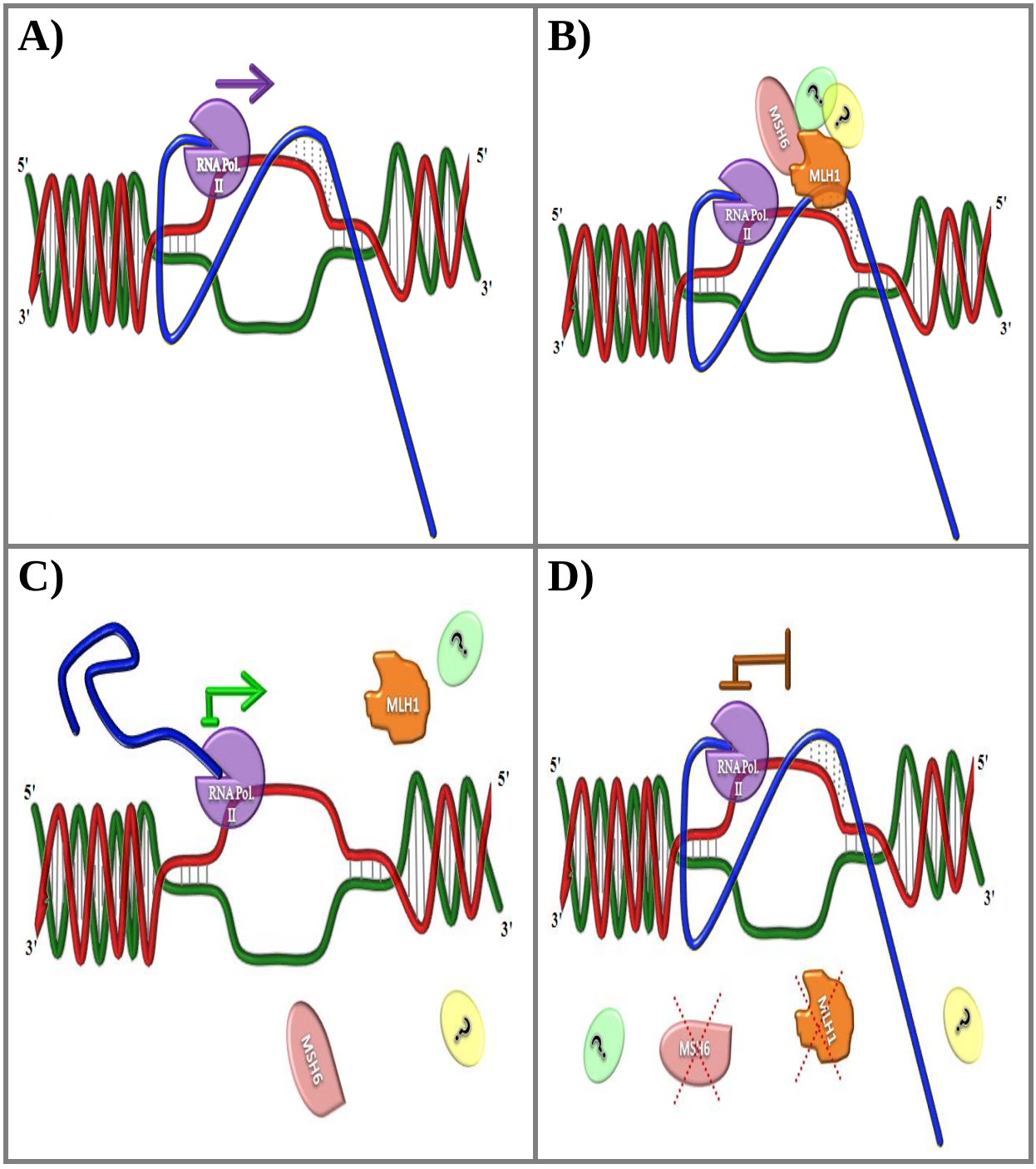

Images showing: **(A)** inhibition of transcription by stalling RNA polymerase II activity due to RNA.DNA triplex formation, **(B)** binding of MLH1 and MSH6 to the triplex, **(C)** release of premature mRNA and continuation of transcription, and **(D)** inhibition of transcription in the absence of MSH6 or MLH1.

7.4 - How could frataxin deficiency cause downregulation of MMR gene transcription?

The mechanism that causes downregulation of MMR gene transcription in FRDA cerebellum tissue is not yet clear. However, it is proposed that frataxin deficiency may downregulate mRNA expression of MMR genes due to induction of oxidative stress. It is known that frataxin deficiency increases the levels of iron and H_2O_2 through two mechanisms. Firstly, there is impairment of the ISC synthesis pathway, which leads to increased levels of Fe^{3+}, causing iron accumulation. Secondly, there is impairment of ISC-containing MRC I, II and III activities, resulting in an increase of the ROS superoxide (O_2^-) and consequently accumulation of H_2O_2. Under normal physiological conditions, H_2O_2 is generated from dismutation of O_2^-, which is catalysed in mitochondria by SOD2 (Pandolfo 2009). H_2O_2 is then converted into H_2O in the mitochondria by glutathione peroxidase (GPX) (Figure 7.4) (Tozzi *et al.* 2002).

It is known that defects of frataxin hinder GPX activity, which then leads to an accumulation of H_2O_2 and subsequent hypoxia (i.e. a reduced level of O_2) of the cell. Investigations of frataxin deficiency in eukaryotic cells have revealed a high sensitivity to the accumulation of H_2O_2 (Babcock *et al.* 1997; Wong *et al.* 1999), with the generation of highly toxic hydroxyl radicals ($OH^{\bullet}$) in the presence of Fe^{2+} (Tozzi *et al.* 2002). This eventually culminates in the induction of oxidative stress (Tozzi *et al.* 2002; Guccini *et al.* 2011).

Furthermore, other studies have demonstrated a role for H_2O_2 in dysfunction of the MMR system by the induction of hypoxia (Chang *et al.* 2002). Hypoxia is recognised as a characteristic feature of most solid tumours, causing either an adaptive response to cell malignancy or cell death through apoptosis and/or necrosis.

Figure 7.4 - ROS generation in mitochondria.

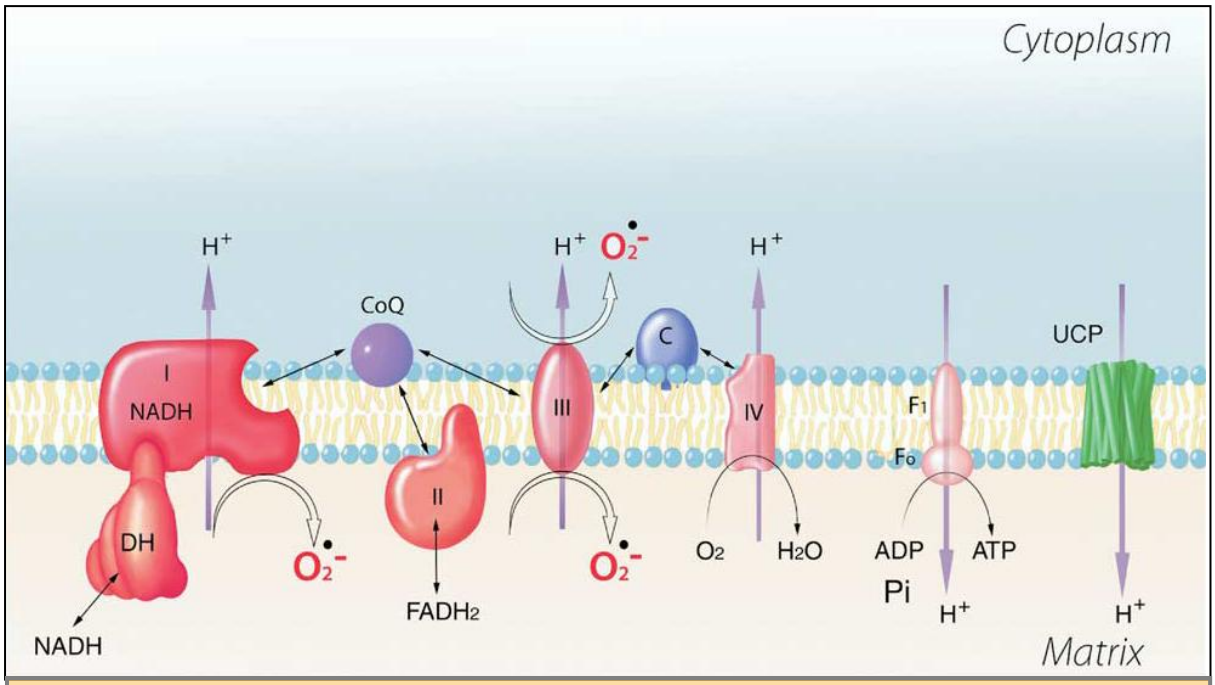

ROS antioxidant scavenger reaction:

$$O_2^{\bullet -} \xrightarrow{SOD2} H_2O_2 \xrightarrow{GPX} H_2O + O_2$$

An image representing the major production sites of superoxide anions ($O_2^{\bullet -}$) at MRC complexes I and III along with one of the major ROS scavenging pathways, in normal cells. Antioxidant enzymes include mitochondrial superoxide dismutase (SOD2) and glutathione peroxidase (GPX). Image adapted from (Balaban *et al.* 2005).

The responsibility for maintaining the balance between adaptation and cell death in response to hypoxia is mainly performed by the hypoxia-inducible factor (HIF) family of molecules (Guccini *et al.* 2011). HIF complexes contain two subunits, HIF-1α and HIF-2α, which form a heterodimer by binding with HIF-β. In normal physiological conditions, both HIF-α subunits are degraded by the proteasome. However, hypoxia inhibits degradation of HIF-α subunits, leading to the hypoxic adaptation response. It is reported that HIFs can regulate the expression of several genes containing a conserved hypoxia-responsive element (HRE) (Guccini *et al.* 2011). Interestingly, several studies have shown that protection of HIF-1α

from degradation causes downregulation of MMR gene transcription, possibly by affecting the relevant HREs (Mihaylova *et al.* 2003; Koshiji *et al.* 2005; Lehtonen *et al.* 2007; Rodriguez-Jimenez *et al.* 2008). These investigations suggest an interesting potential pathway in which defects of frataxin may cause downregulation of MMR mRNA expression in tissues that are highly sensitive to frataxin deficiency and subsequent hypoxia, such as brain. Therefore a model is proposed whereby defects of frataxin may inhibit GPX function, causing an accumulation of H_2O_2, which then leads to oxidative stress and the induction of hypoxia (Figure 7.5). Hypoxia may then induce stabilisation of HIF-1α protein, leading to HIF complex hyperactivation and subsequent binding to HRE sequences within individual MMR genes, leading to transcription inhibition (Figure 7.5). To confirm this hypothesis, several experimental studies would be required to determine the activity of SOD2, GPX and HIF-1α proteins and the levels of oxidative stress and hypoxia in the brain cells.

Figure 7.5 – Downregulation of MMR expression due to frataxin deficiency.

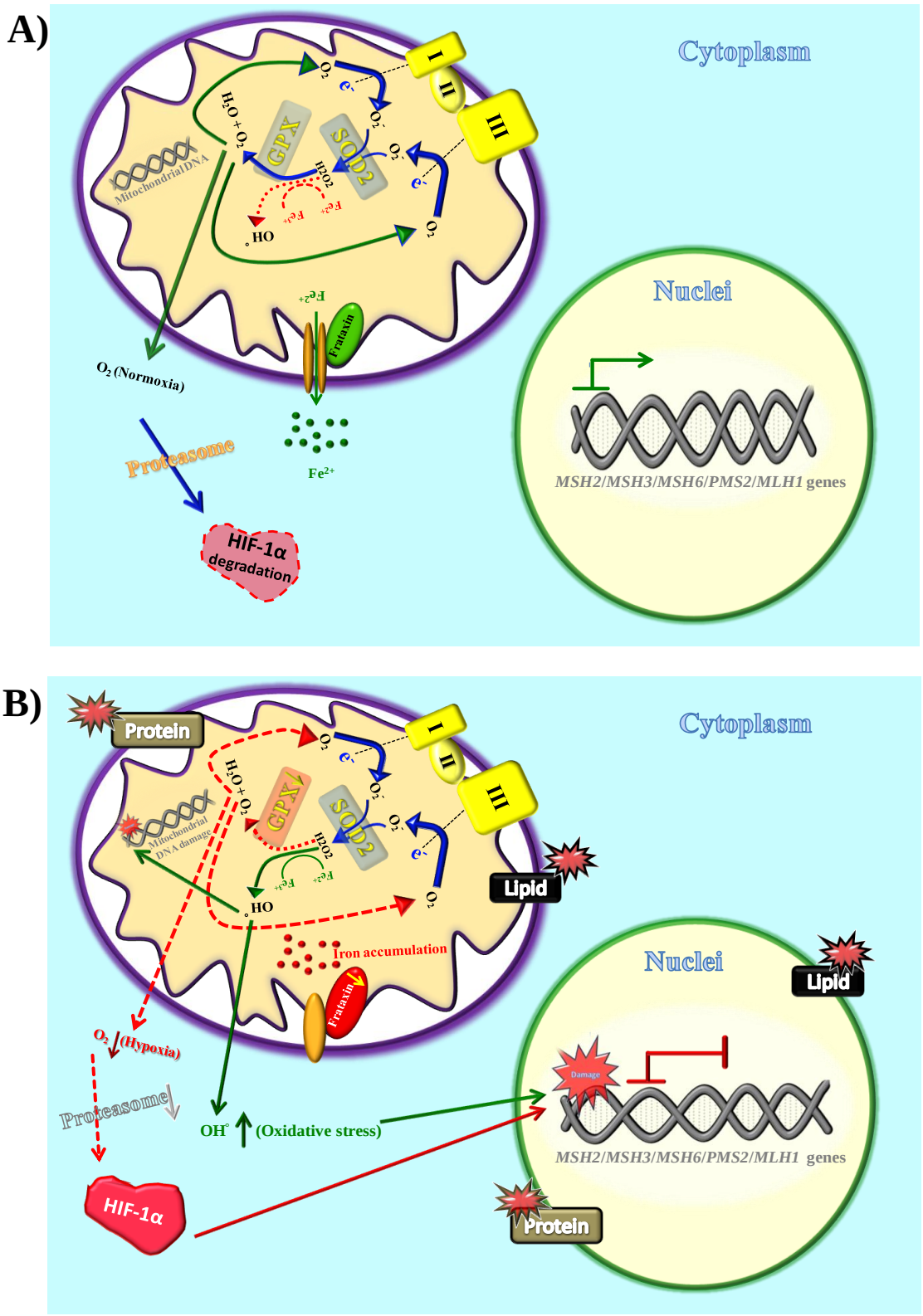

Images representing potential mechanism of MMR protein downregulation in FRDA brain tissues. **(A)** Shows the mechanisms in a brain cell with normal frataxin expression, and **(B)** shows the mechanisms in a brain cell with defective frataxin expression. SOD2= superoxide dismutase, GPX= glutathione peroxidase, HIF-1α= hypoxia-inducible factor-1α.

7.5 - Future investigations

The results presented in this thesis open new avenues for further studies. For example, data has now been generated using FRDA mouse model tissues, human cells and human tissues that reveal some similarities, but also some differences, between the different model systems. Therefore, further studies would be useful to more fully understand the compatibility of different FRDA model systems and to determine which models are most representative of FRDA disease. This may reveal insights into which are the most efficient models to study the interaction between MMR, GAA repeat instability and frataxin expression. Thus, mouse models may be the most effective way to investigate tissue-specific mechanisms and therapies for FRDA. Alternatively, human or mouse cell models may, under certain circumstances, be able to replace the use of mouse models for the investigation of other aspects of FRDA pathogenesis and therapy.

Some of the data in this thesis also indicates that Mlh1 may have a significant role to play in FRDA disease progression, but further investigations are now required. For example, further mouse model genomic DNA studies would be useful to determine the effect of Mlh1 on the dynamics of intergenerational transmission of GAA repeats. In addition, applying advanced techniques, such as SP-PCR, may be able to more accurately quantify the effects of Mlh1 on somatic GAA repeat expansions.

Other useful studies could include the detection of MMR protein occupancy at the *FXN* locus using ChIP assays and identification of the epigenetic status of MMR genes in FRDA compared with non-FRDA cells and tissues. These studies would be useful to unravel the mechanisms by which MMR proteins may affect GAA repeat expansions and *FXN* transcription, or in turn, by which frataxin may contribute to MMR gene regulation. The investigation of MMR protein expression levels and enzyme activities would also result in a broader understanding of MMR effects on GAA repeat instability and *FXN* gene

expression, or in turn, frataxin effects on the regulation of MMR proteins. Furthermore, investigating the role of other relevant molecules or mechanisms, such as SOD2 and GPX proteins or oxidative stress and hypoxia, could gain further insights into the exact relationship between MMR and *FXN* gene regulation.

Since mutation of the MSH3 does not cause tumour formation, unlike mutations of the other MMR proteins (MSH2, MSH6, PMS2 and MLH1), it has previously been suggested that targeting MSH3 to reduce somatic instability of the GAA repeats could be considered as a potential FRDA therapy (Halabi *et al.* 2012). However, my results did not reveal any significant change in *FXN* transcription in CNS tissues upon loss of Msh3, despite the decrease of somatic GAA repeat expansions. Therefore, further studies are required to clarify the potential role of MSH3 as a therapeutic target for FRDA. Ultimately, combining the findings of this thesis with other studies may lead to the identification of novel mechanisms and therapeutic approaches for FRDA.

List of references

Abdel-Rahman W. M., Mecklin J. P. and Peltomaki P. (2006). "The genetics of HNPCC: application to diagnosis and screening." Crit Rev Oncol Hematol **58**(3): 208-220.

Abel T. and Zukin R. S. (2008). "Epigenetic targets of HDAC inhibition in neurodegenerative and psychiatric disorders." Curr Opin Pharmacol **8**(1): 57-64.

Ackroyd R., Shorthouse A. J. and Stephenson T. J. (1996). "Gastric carcinoma in siblings with Friedreich's ataxia." Eur J Surg Oncol **22**(3): 301-303.

Adinolfi S., Iannuzzi C., Prischi F., *et al.* (2009). "Bacterial frataxin CyaY is the gatekeeper of iron-sulfur cluster formation catalyzed by IscS." Nat Struct Mol Biol **16**(4): 390-396.

Aguilera A. and Gomez-Gonzalez B. (2008). "Genome instability: a mechanistic view of its causes and consequences." Nat Rev Genet **9**(3): 204-217.

Al-Mahdawi S., Pinto R. M., Ismail O., *et al.* (2008). "The Friedreich ataxia GAA repeat expansion mutation induces comparable epigenetic changes in human and transgenic mouse brain and heart tissues." Hum Mol Genet **17**(5): 735-746.

Al-Mahdawi S., Pinto R. M., Ruddle P., *et al.* (2004). "GAA repeat instability in Friedreich ataxia YAC transgenic mice." Genomics **84**(2): 301-310.

Al-Mahdawi S., Pinto R. M., Varshney D., *et al.* (2006). "GAA repeat expansion mutation mouse models of Friedreich ataxia exhibit oxidative stress leading to progressive neuronal and cardiac pathology." Genomics **88**(5): 580-590.

Alper G. and Narayanan V. (2003). "Friedreich's ataxia." Pediatr Neurol **28**(5): 335-341.

Anderson P. R., Kirby K., Hilliker A. J., *et al.* (2005). "RNAi-mediated suppression of the mitochondrial iron chaperone, frataxin, in Drosophila." Hum Mol Genet **14**(22): 3397-3405.

Auer R. L., Dighiero G., Goldin L. R., *et al.* (2007). "Trinucleotide repeat dynamic mutation identifying susceptibility in familial and sporadic chronic lymphocytic leukaemia." Br J Haematol **136**(1): 73-79.

Babcock M., de Silva D., Oaks R., *et al.* (1997). "Regulation of mitochondrial iron accumulation by Yfh1p, a putative homolog of frataxin." Science **276**(5319): 1709-1712.

Baker S. M., Bronner C. E., Zhang L., *et al.* (1995). "Male mice defective in the DNA mismatch repair gene PMS2 exhibit abnormal chromosome synapsis in meiosis." Cell **82**(2): 309-319.

Balaban R. S., Nemoto S. and Finkel T. (2005). "Mitochondria, oxidants, and aging." Cell **120**(4): 483-495.

Barr H., Page R. and Taylor W. (1986). "Primary small bowel ganglioneuroblastoma and Friedreich's ataxia." J R Soc Med **79**(10): 612-613.

Batzer M. A. and Deininger P. L. (2002). "Alu repeats and human genomic diversity." Nat Rev Genet **3**(5): 370-379.

Becker E. and Richardson D. R. (2001). "Frataxin: its role in iron metabolism and the pathogenesis of Friedreich's ataxia." Int J Biochem Cell Biol **33**(1): 1-10.

Beckman J. S. and Weber J. L. (1992). "Survey of human and rat microsatellites." Genomics **12**(4): 627-631.

Bedalov A., Gatbonton T., Irvine W. P., *et al.* (2001). "Identification of a small molecule inhibitor of Sir2p." Proc Natl Acad Sci U S A **98**(26): 15113-15118.

Belvederesi L., Bianchi F., Loretelli C., *et al.* (2006). "Assessing the pathogenicity of MLH1 missense mutations in patients with suspected hereditary nonpolyposis colorectal cancer: correlation with clinical, genetic and functional features." Eur J Hum Genet **14**(7): 853-859.

Berciano J., Infante J., Garcia A., *et al.* (2005). "Very late-onset Friedreich's ataxia with minimal GAA1 expansion mimicking multiple system atrophy of cerebellar type." Mov Disord **20**(12): 1643-1645.

Berciano J., Mateo I., De Pablos C., *et al.* (2002). "Friedreich ataxia with minimal GAA expansion presenting as adult-onset spastic ataxia." J Neurol Sci **194**(1): 75-82.

Bhidayasiri R., Perlman S. L., Pulst S. M., *et al.* (2005). "Late-onset Friedreich ataxia: phenotypic analysis, magnetic resonance imaging findings, and review of the literature." Arch Neurol **62**(12): 1865-1869.

Biacsi R., Kumari D. and Usdin K. (2008). "SIRT1 inhibition alleviates gene silencing in Fragile X mental retardation syndrome." PLoS Genet **4**(3): e1000017.

Bidichandani S. I., Garcia C. A., Patel P. I., *et al.* (2000). "Very late-onset Friedreich ataxia despite large GAA triplet repeat expansions." Arch Neurol **57**(2): 246-251.

Blanco A. M., Chen Y., Grenert J. P., *et al.* (2010). "Heritable epigenetic mutation of MLHI in a mother and daughter with Lynch syndrome." Hereditary Cancer in Clinical Practice **8**: 3-4.

Bourn R. L., De Biase I., Pinto R. M., *et al.* (2012). "Pms2 Suppresses Large Expansions of the (GAA.TTC)(n) Sequence in Neuronal Tissues." PLoS One **7**(10): e47085.

Bradley J. L., Blake J. C., Chamberlain S., *et al.* (2000). "Clinical, biochemical and molecular genetic correlations in Friedreich's ataxia." Hum Mol Genet **9**(2): 275-282.

Branda S. S., Yang Z. Y., Chew A., *et al.* (1999). "Mitochondrial intermediate peptidase and the yeast frataxin homolog together maintain mitochondrial iron homeostasis in Saccharomyces cerevisiae." Hum Mol Genet **8**(6): 1099-1110.

Bulteau A. L., O'Neill H. A., Kennedy M. C., *et al.* (2004). "Frataxin acts as an iron chaperone protein to modulate mitochondrial aconitase activity." Science **305**(5681): 242-245.

Calabrese V., Lodi R., Tonon C., *et al.* (2005). "Oxidative stress, mitochondrial dysfunction and cellular stress response in Friedreich's ataxia." J Neurol Sci **233**(1-2): 145-162.

Campuzano V., Montermini L., Molto M. D., *et al.* (1996). "Friedreich's ataxia: autosomal recessive disease caused by an intronic GAA triplet repeat expansion." Science **271**(5254): 1423-1427.

Carey N. and La Thangue N. B. (2006). "Histone deacetylase inhibitors: gathering pace." Curr Opin Pharmacol **6**(4): 369-375.

Castaldo I., Pinelli M., Monticelli A., *et al.* (2008). "DNA methylation in intron 1 of the frataxin gene is related to GAA repeat length and age of onset in Friedreich ataxia patients." J Med Genet **45**(12): 808-812.

Cavadini P., Gellera C., Patel P. I., *et al.* (2000). "Human frataxin maintains mitochondrial iron homeostasis in Saccharomyces cerevisiae." Hum Mol Genet **9**(17): 2523-2530.

Cellini E., Forleo P., Nacmias B., *et al.* (2001). "Clinical and genetic analysis of hereditary and sporadic ataxia in central Italy." Brain Res Bull **56**(3-4): 363-366.

Chahwan R., van Oers J. M., Avdievich E., *et al.* (2012). "The ATPase activity of MLH1 is required to orchestrate DNA double-strand breaks and end processing during class switch recombination." J Exp Med **209**(4): 671-678.

Chamberlain, S., Shaw, J., Rowland, A., *et al.* (1988). "Mapping of mutation causing Friedreich's ataxia to human chromosome 9." Nature **334**(6179): 248-249.

Chandok G. S., Patel M. P., Mirkin S. M., *et al.* (2012). "Effects of Friedreich's ataxia GAA repeats on DNA replication in mammalian cells." Nucleic Acids Res **40**(9): 3964-3974.

Chang C. L., Marra G., Chauhan D. P., *et al.* (2002). "Oxidative stress inactivates the human DNA mismatch repair system." Am J Physiol Cell Physiol **283**(1): C148-154.

Chang D. K., Ricciardiello L., Goel A., *et al.* (2000). "Steady-state regulation of the human DNA mismatch repair system." J Biol Chem **275**(37): 29178.

Chen O. S., Hemenway S. and Kaplan J. (2002). "Inhibition of Fe-S cluster biosynthesis decreases mitochondrial iron export: evidence that Yfh1p affects Fe-S cluster synthesis." Proc Natl Acad Sci U S A **99**(19): 12321-12326.

Chew M. H., Koh P. K., Ng K. H., *et al.* (2008). "Phenotypic characteristics of hereditary non-polyposis colorectal cancer by the Amsterdam criteria: an Asian perspective." ANZ J Surg **78**(7): 556-560.

Clark R. M., De Biase I., Malykhina A. P., *et al.* (2007). "The GAA triplet-repeat is unstable in the context of the human FXN locus and displays age-dependent expansions in cerebellum and DRG in a transgenic mouse model." Hum Genet **120**(5): 633-640.

Condo I., Malisan F., Guccini I., *et al.* (2010). "Molecular control of the cytosolic aconitase/IRP1 switch by extramitochondrial frataxin." Hum Mol Genet **19**(7): 1221-1229.

Condo I., Ventura N., Malisan F., *et al.* (2007). "In vivo maturation of human frataxin." Hum Mol Genet **16**(13): 1534-1540.

Condo I., Ventura N., Malisan F., *et al.* (2006). "A pool of extramitochondrial frataxin that promotes cell survival." J Biol Chem **281**(24): 16750-16756.

Cooper J. M., Korlipara L. V., Hart P. E., *et al.* (2008). "Coenzyme Q10 and vitamin E deficiency in Friedreich's ataxia: predictor of efficacy of vitamin E and coenzyme Q10 therapy." Eur J Neurol **15**(12): 1371-1379.

Cooper J. M. and Schapira A. H. (2007). "Friedreich's ataxia: coenzyme Q10 and vitamin E therapy." Mitochondrion **7 Suppl**: S127-135.

Cossee M., Puccio H., Gansmuller A., *et al.* (2000). "Inactivation of the Friedreich ataxia mouse gene leads to early embryonic lethality without iron accumulation." Hum Mol Genet **9**(8): 1219-1226.

Cossee M., Schmitt M., Campuzano V., *et al.* (1997). "Evolution of the Friedreich's ataxia trinucleotide repeat expansion: founder effect and premutations." Proc Natl Acad Sci U S A **94**(14): 7452-7457.

Cummings C. J. and Zoghbi H. Y. (2000). "Fourteen and counting: unraveling trinucleotide repeat diseases." Hum Mol Genet **9**(6): 909-916.

Davis T. W., Wilson-Van Patten C., Meyers M., *et al.* (1998). "Defective expression of the DNA mismatch repair protein, MLH1, alters G2-M cell cycle checkpoint arrest following ionizing radiation." Cancer Res **58**(4): 767-778.

De Biase I., Rasmussen A., Endres D., *et al.* (2007). "Progressive GAA expansions in dorsal root ganglia of Friedreich's ataxia patients." Ann Neurol **61**(1): 55-60.

De Biase I., Rasmussen A., Monticelli A., *et al.* (2007). "Somatic instability of the expanded GAA triplet-repeat sequence in Friedreich ataxia progresses throughout life." Genomics **90**(1): 1-5.

De Pas T., Martinelli G., De Braud F., *et al.* (1999). "Friedreich's ataxia and intrathecal chemotherapy in a patient with lymphoblastic lymphoma." Ann Oncol **10**(11): 1393.

de Souza-Pinto N. C., Wilson D. M., 3rd, Stevnsner T. V., *et al.* (2008). "Mitochondrial DNA, base excision repair and neurodegeneration." DNA Repair (Amst) **7**(7): 1098-1109.

de Wind N., Dekker M., Berns A., *et al.* (1995). "Inactivation of the mouse Msh2 gene results in mismatch repair deficiency, methylation tolerance, hyperrecombination, and predisposition to cancer." Cell **82**(2): 321-330.

de Wind N., Dekker M., Claij N., *et al.* (1999). "HNPCC-like cancer predisposition in mice through simultaneous loss of Msh3 and Msh6 mismatch-repair protein functions." Nat Genet **23**(3): 359-362.

Delatycki M. B., Williamson R. and Forrest S. M. (2000). "Friedreich ataxia: an overview." J Med Genet **37**(1): 1-8.

Denver D. R., Feinberg S., Steding C., *et al.* (2006). "The relative roles of three DNA repair pathways in preventing Caenorhabditis elegans mutation accumulation." Genetics **174**(1): 57-65.

Dhe-Paganon S., Shigeta R., Chi Y. I., *et al.* (2000). "Crystal structure of human frataxin." J Biol Chem **275**(40): 30753-30756.

Di Prospero N. A., Baker A., Jeffries N., *et al.* (2007). "Neurological effects of high-dose idebenone in patients with Friedreich's ataxia: a randomised, placebo-controlled trial." Lancet Neurol **6**(10): 878-886.

Di Prospero N. A. and Fischbeck K. H. (2005). "Therapeutics development for triplet repeat expansion diseases." Nat Rev Genet **6**(10): 756-765.

Dillin A., Hsu A. L., Arantes-Oliveira N., *et al.* (2002). "Rates of behavior and aging specified by mitochondrial function during development." Science **298**(5602): 2398-2401.

Ditch S., Sammarco M. C., Banerjee A., *et al.* (2009). "Progressive GAA.TTC repeat expansion in human cell lines." PLoS Genet **5**(10): e1000704.

Djian P., Hancock J. M. and Chana H. S. (1996). "Codon repeats in genes associated with human diseases: fewer repeats in the genes of nonhuman primates and nucleotide substitutions concentrated at the sites of reiteration." Proc Natl Acad Sci U S A **93**(1): 417-421.

Dragileva E., Hendricks A., Teed A., *et al.* (2009). "Intergenerational and striatal CAG repeat instability in Huntington's disease knock-in mice involve different DNA repair genes." Neurobiol Dis **33**(1): 37-47.

Du J., Campau E., Soragni E., *et al.* (2012). "Role of Mismatch Repair Enzymes in GAA{middle dot}TTC Triplet-repeat Expansion in Friedreich Ataxia Induced Pluripotent Stem Cells." J Biol Chem **287**(35): 29861-29872.

Durr A., Cossee M., Agid Y., *et al.* (1996). "Clinical and genetic abnormalities in patients with Friedreich's ataxia." N Engl J Med **335**(16): 1169-1175.

Edelmann W., Cohen P. E., Kane M., *et al.* (1996). "Meiotic pachytene arrest in MLH1-deficient mice." Cell **85**(7): 1125-1134.

Egger G., Liang G., Aparicio A., *et al.* (2004). "Epigenetics in human disease and prospects for epigenetic therapy." Nature **429**(6990): 457-463.

Elgin S. C. and Grewal S. I. (2003). "Heterochromatin: silence is golden." Curr Biol **13**(23): R895-898.

Ellison A. R., Lofing J. and Bitter G. A. (2004). "Human MutL homolog (MLH1) function in DNA mismatch repair: a prospective screen for missense mutations in the ATPase domain." Nucleic Acids Res **32**(18): 5321-5338.

Epplen C., Epplen J. T., Frank G., *et al.* (1997). "Differential stability of the (GAA)n tract in the Friedreich ataxia (STM7) gene." Hum Genet **99**(6): 834-836.

Ezzatizadeh V., Pinto R. M., Sandi C., *et al.* (2012). "The mismatch repair system protects against intergenerational GAA repeat instability in a Friedreich ataxia mouse model." Neurobiol Dis **46**(1): 165-171.

Feng J., Bussiere F. and Hekimi S. (2001). "Mitochondrial electron transport is a key determinant of life span in Caenorhabditis elegans." Dev Cell **1**(5): 633-644.

Ferrante R. J., Kubilus J. K., Lee J., *et al.* (2003). "Histone deacetylase inhibition by sodium butyrate chemotherapy ameliorates the neurodegenerative phenotype in Huntington's disease mice." J Neurosci **23**(28): 9418-9427.

Festenstein R. (2006). "Breaking the silence in Friedreich's ataxia." Nat Chem Biol **2**(10): 512-513.

Filla A., De Michele G., Cavalcanti F., *et al.* (1996). "The relationship between trinucleotide (GAA) repeat length and clinical features in Friedreich ataxia." Am J Hum Genet **59**(3): 554-560.

Fishel M. L., Vasko M. R. and Kelley M. R. (2007). "DNA repair in neurons: so if they don't divide what's to repair?" Mutat Res **614**(1-2): 24-36.

Foiry L., Dong L., Savouret C., *et al.* (2006). "Msh3 is a limiting factor in the formation of intergenerational CTG expansions in DM1 transgenic mice." Hum Genet **119**(5): 520-526.

Foury F. (1999). "Low iron concentration and aconitase deficiency in a yeast frataxin homologue deficient strain." FEBS Lett **456**(2): 281-284.

Fujita R., Agid Y., Trouillas P., *et al.* (1989). "Confirmation of linkage of Friedreich ataxia to chromosome 9 and identification of a new closely linked marker." Genomics **4**(1): 110-111.

Gakh O., Park S., Liu G., *et al.* (2006). "Mitochondrial iron detoxification is a primary function of frataxin that limits oxidative damage and preserves cell longevity." Hum Mol Genet **15**(3): 467-479.

Gardian G., Browne S. E., Choi D. K., *et al.* (2005). "Neuroprotective effects of phenylbutyrate in the N171-82Q transgenic mouse model of Huntington's disease." J Biol Chem **280**(1): 556-563.

Gasche C., Chang C. L., Rhees J., *et al.* (2001). "Oxidative stress increases frameshift mutations in human colorectal cancer cells." Cancer Res **61**(20): 7444-7448.

Gaspari Z., Ortutay C. and Toth G. (2007). "Divergent microsatellite evolution in the human and chimpanzee lineages." FEBS Lett **581**(13): 2523-2526.

Gomes-Pereira M., Fortune M. T., Ingram L., *et al.* (2004). "Pms2 is a genetic enhancer of trinucleotide CAG.CTG repeat somatic mosaicism: implications for the mechanism of triplet repeat expansion." Hum Mol Genet **13**(16): 1815-1825.

Gomes-Pereira M. and Monckton D. G. (2004). "Mouse tissue culture models of unstable triplet repeats." Methods Mol Biol **277**: 215-227.

Goncalves S., Paupe V., Dassa E. P., *et al.* (2008). "Deferiprone targets aconitase: implication for Friedreich's ataxia treatment." BMC Neurol **8**: 20.

Gottesfeld J. M. (2007). "Small molecules affecting transcription in Friedreich ataxia." Pharmacol Ther **116**(2): 236-248.

Grabczyk E., Mancuso M. and Sammarco M. C. (2007). "A persistent RNA.DNA hybrid formed by transcription of the Friedreich ataxia triplet repeat in live bacteria, and by T7 RNAP in vitro." Nucleic Acids Res **35**(16): 5351-5359.

Grabczyk E. and Usdin K. (2000). "The GAA*TTC triplet repeat expanded in Friedreich's ataxia impedes transcription elongation by T7 RNA polymerase in a length and supercoil dependent manner." Nucleic Acids Res **28**(14): 2815-2822.

Grant L., Sun J., Xu H., *et al.* (2006). "Rational selection of small molecules that increase transcription through the GAA repeats found in Friedreich's ataxia." FEBS Lett **580**(22): 5399-5405.

Greene E., Mahishi L., Entezam A., *et al.* (2007). "Repeat-induced epigenetic changes in intron 1 of the frataxin gene and its consequences in Friedreich ataxia." Nucleic Acids Res **35**(10): 3383-3390.

Guccini I., Serio D., Condo I., *et al.* (2011). "Frataxin participates to the hypoxia-induced response in tumors." Cell Death Dis **2**: e123.

Guo S., Presnell S. R., Yuan F., *et al.* (2004). "Differential requirement for proliferating cell nuclear antigen in 5' and 3' nick-directed excision in human mismatch repair." J Biol Chem **279**(17): 16912-16917.

Gylling A., Abdel-Rahman W. M., Juhola M., *et al.* (2007). "Is gastric cancer part of the tumour spectrum of hereditary non-polyposis colorectal cancer? A molecular genetic study." Gut **56**(7): 926-933.

Hadnagy A., Beaulieu R. and Balicki D. (2008). "Histone tail modifications and noncanonical functions of histones: perspectives in cancer epigenetics." Mol Cancer Ther **7**(4): 740-748.

Hadziahmetovic M., Song Y., Wolkow N., *et al.* (2011). "The oral iron chelator deferiprone protects against iron overload-induced retinal degeneration." Invest Ophthalmol Vis Sci **52**(2): 959-968.

Halabi A., Ditch S., Wang J., *et al.* (2012). "DNA Mismatch Repair Complex MutSbeta Promotes GAA{middle dot}TTC Repeat Expansion in Human Cells." J Biol Chem **287**(35): 29958-29967.

Hanauer A., Chery M., Fujita R., *et al.* (1990). "The Friedreich ataxia gene is assigned to chromosome 9q13-q21 by mapping of tightly linked markers and shows linkage disequilibrium with D9S15." Am J Hum Genet **46**(1): 133-137.

Hart P. E., Lodi R., Rajagopalan B., *et al.* (2005). "Antioxidant treatment of patients with Friedreich ataxia: four-year follow-up." Arch Neurol **62**(4): 621-626.

Hausse A. O., Aggoun Y., Bonnet D., *et al.* (2002). "Idebenone and reduced cardiac hypertrophy in Friedreich's ataxia." Heart **87**(4): 346-349.

Herman D., Jenssen K., Burnett R., *et al.* (2006). "Histone deacetylase inhibitors reverse gene silencing in Friedreich's ataxia." Nat Chem Biol **2**(10): 551-558.

Hockly E., Richon V. M., Woodman B., *et al.* (2003). "Suberoylanilide hydroxamic acid, a histone deacetylase inhibitor, ameliorates motor deficits in a mouse model of Huntington's disease." Proc Natl Acad Sci U S A **100**(4): 2041-2046.

Hsieh P. and Yamane K. (2008). "DNA mismatch repair: molecular mechanism, cancer, and ageing." Mech Ageing Dev **129**(7-8): 391-407.

Jascur T. and Boland C. R. (2006). "Structure and function of the components of the human DNA mismatch repair system." Int J Cancer **119**(9): 2030-2035.

Jasinska A. J., Kozlowski P. and Krzyzosiak W. J. (2008). "Expression characteristics of triplet repeat-containing RNAs and triplet repeat-interacting proteins in human tissues." Acta Biochim Pol **55**(1): 1-8.

Jaworski A., Rosche W. A., Gellibolian R., *et al.* (1995). "Mismatch repair in Escherichia coli enhances instability of (CTG)n triplet repeats from human hereditary diseases." Proc Natl Acad Sci U S A **92**(24): 11019-11023.

Jun S. H., Kim T. G. and Ban C. (2006). "DNA mismatch repair system. Classical and fresh roles." FEBS J **273**(8): 1609-1619.

Junop M. S., Obmolova G., Rausch K., *et al.* (2001). "Composite active site of an ABC ATPase: MutS uses ATP to verify mismatch recognition and authorize DNA repair." Mol Cell **7**(1): 1-12.

Jurka J. and Pethiyagoda C. (1995). "Simple repetitive DNA sequences from primates: compilation and analysis." J Mol Evol **40**(2): 120-126.

Kathe S. D., Shen G. P. and Wallace S. S. (2004). "Single-stranded breaks in DNA but not oxidative DNA base damages block transcriptional elongation by RNA polymerase II in HeLa cell nuclear extracts." J Biol Chem **279**(18): 18511-18520.

Kidd A., Coleman R., Whiteford M., *et al.* (2001). "Breast cancer in two sisters with Friedreich's ataxia." Eur J Surg Oncol **27**(5): 512-514.

Kirches E., Andrae N., Hoefer A., *et al.* (2011). "Dual role of the mitochondrial protein frataxin in astrocytic tumors." Lab Invest **91**(12): 1766-1776.

Klockgether T. (2007). "Ataxias." Parkinsonism Relat Disord **13 Suppl 3**: S391-394.

Kobayashi K., Karran P., Oda S., *et al.* (2005). "The Involvement of mismatch repair in transcription-coupled nucleotide excision repair." Hum Cell **18**(3): 103-115.
Koeppen A. H. (2011). "Friedreich's ataxia: Pathology, pathogenesis, and molecular genetics." J Neurol Sci.
Koeppen A. H., Michael S. C., Knutson M. D., *et al.* (2007). "The dentate nucleus in Friedreich's ataxia: the role of iron-responsive proteins." Acta Neuropathol **114**(2): 163-173.
Kondo Y., Shen L. and Issa J. P. (2003). "Critical role of histone methylation in tumor suppressor gene silencing in colorectal cancer." Mol Cell Biol **23**(1): 206-215.
Koshiji M., To K. K., Hammer S., *et al.* (2005). "HIF-1alpha induces genetic instability by transcriptionally downregulating MutSalpha expression." Mol Cell **17**(6): 793-803.
Koutnikova H., Campuzano V., Foury F., *et al.* (1997). "Studies of human, mouse and yeast homologues indicate a mitochondrial function for frataxin." Nat Genet **16**(4): 345-351.
Koutnikova H., Campuzano V. and Koenig M. (1998). "Maturation of wild-type and mutated frataxin by the mitochondrial processing peptidase." Hum Mol Genet **7**(9): 1485-1489.
Kovtun I. V. and McMurray C. T. (2001). "Trinucleotide expansion in haploid germ cells by gap repair." Nat Genet **27**(4): 407-411.
Kovtun I. V. and McMurray C. T. (2008). "Features of trinucleotide repeat instability in vivo." Cell Res **18**(1): 198-213.
Ku S., Soragni E., Campau E., *et al.* (2010). "Friedreich's Ataxia Induced Pluripotent Stem Cells Model Intergenerational GAATTC Triplet Repeat Instability." Cell Stem Cell **7**(5): 631-637.
Kuismanen S. A., Holmberg M. T., Salovaara R., *et al.* (2000). "Genetic and epigenetic modification of MLH1 accounts for a major share of microsatellite-unstable colorectal cancers." Am J Pathol **156**(5): 1773-1779.
Kunkel T. A. and Erie D. A. (2005). "DNA mismatch repair." Annu Rev Biochem **74**: 681-710.
Kuranaga N., Shinomiya N. and Mochizuki H. (2001). "Long-term cultivation of colorectal carcinoma cells with anti-cancer drugs induces drug resistance and telomere elongation: an in vitro study." BMC Cancer **1**: 10.
Labuda M., Labuda D., Miranda C., *et al.* (2000). "Unique origin and specific ethnic distribution of the Friedreich ataxia GAA expansion." Neurology **54**(12): 2322-2324.
Leadon S. A. and Avrutskaya A. V. (1997). "Differential involvement of the human mismatch repair proteins, hMLH1 and hMSH2, in transcription-coupled repair." Cancer Res **57**(17): 3784-3791.
Lee S. S., Lee R. Y., Fraser A. G., *et al.* (2003). "A systematic RNAi screen identifies a critical role for mitochondria in C. elegans longevity." Nat Genet **33**(1): 40-48.
Lehtonen H. J., Makinen M. J., Kiuru M., *et al.* (2007). "Increased HIF1 alpha in SDH and FH deficient tumors does not cause microsatellite instability." Int J Cancer **121**(6): 1386-1389.
Li D. S., Ohshima K., Jiralerspong S., *et al.* (1999). "Knock-out of the cyaY gene in Escherichia coli does not affect cellular iron content and sensitivity to oxidants." FEBS Lett **456**(1): 13-16.
Li F., Liu Q., Chen Y. Y., *et al.* (2008). "Escherichia coli mismatch repair protein MutL interacts with the clamp loader subunits of DNA polymerase III." Mutat Res **637**(1-2): 101-110.
Li G. M. (2008). "Mechanisms and functions of DNA mismatch repair." Cell Res **18**(1): 85-98.

Lin Y. and Wilson J. H. (2009). "Diverse effects of individual mismatch repair components on transcription-induced CAG repeat instability in human cells." DNA Repair (Amst) **8**(8): 878-885.

Liu J., Verma P. J., Evans-Galea M. V., *et al.* (2011). "Generation of induced pluripotent stem cell lines from Friedreich ataxia patients." Stem Cell Rev **7**(3): 703-713.

Llorens J. V., Navarro J. A., Martinez-Sebastian M. J., *et al.* (2007). "Causative role of oxidative stress in a Drosophila model of Friedreich ataxia." FASEB J **21**(2): 333-344.

Lobmayr L., Brooks D. G. and Wilson R. B. (2005). "Increased IRP1 activity in Friedreich ataxia." Gene **354**: 157-161.

Lodi R., Hart P. E., Rajagopalan B., *et al.* (2001). "Antioxidant treatment improves in vivo cardiac and skeletal muscle bioenergetics in patients with Friedreich's ataxia." Ann Neurol **49**(5): 590-596.

Lodi R., Taylor D. J. and Schapira A. H. (2001). "Mitochondrial dysfunction in friedreich's ataxia." Biol Signals Recept **10**(3-4): 263-270.

Long S., Jirku M., Mach J., *et al.* (2008). "Ancestral roles of eukaryotic frataxin: mitochondrial frataxin function and heterologous expression of hydrogenosomal Trichomonas homologues in trypanosomes." Mol Microbiol **69**(1): 94-109.

Lu C. and Cortopassi G. (2007). "Frataxin knockdown causes loss of cytoplasmic iron-sulfur cluster functions, redox alterations and induction of heme transcripts." Arch Biochem Biophys **457**(1): 111-122.

Maguire K. K. and Kmiec E. B. (2007). "Multiple roles for MSH2 in the repair of a deletion mutation directed by modified single-stranded oligonucleotides." Gene **386**(1-2): 107-114.

Manley K., Shirley T. L., Flaherty L., *et al.* (1999). "Msh2 deficiency prevents in vivo somatic instability of the CAG repeat in Huntington disease transgenic mice." Nat Genet **23**(4): 471-473.

Mariappan S. V., Catasti P., Silks L. A., 3rd, *et al.* (1999). "The high-resolution structure of the triplex formed by the GAA/TTC triplet repeat associated with Friedreich's ataxia." J Mol Biol **285**(5): 2035-2052.

Marquez V. E., Kelley J. A., Agbaria R., *et al.* (2005). "Zebularine: a unique molecule for an epigenetically based strategy in cancer chemotherapy." Ann N Y Acad Sci **1058**: 246-254.

Martelli A., Wattenhofer-Donze M., Schmucker S., *et al.* (2007). "Frataxin is essential for extramitochondrial Fe-S cluster proteins in mammalian tissues." Hum Mol Genet **16**(22): 2651-2658.

McMurray C. T. (2008). "Hijacking of the mismatch repair system to cause CAG expansion and cell death in neurodegenerative disease." DNA Repair (Amst) **7**(7): 1121-1134.

Meier T. and Buyse G. (2009). "Idebenone: an emerging therapy for Friedreich ataxia." J Neurol **256 Suppl 1**: 25-30.

Mellon I. and Champe G. N. (1996). "Products of DNA mismatch repair genes mutS and mutL are required for transcription-coupled nucleotide-excision repair of the lactose operon in Escherichia coli." Proc Natl Acad Sci U S A **93**(3): 1292-1297.

Mellon I. and Hanawalt P. C. (1989). "Induction of the Escherichia coli lactose operon selectively increases repair of its transcribed DNA strand." Nature **342**(6245): 95-98.

Mellon I., Rajpal D. K., Koi M., *et al.* (1996). "Transcription-coupled repair deficiency and mutations in human mismatch repair genes." Science **272**(5261): 557-560.

Merlo D., Di Stasi A. M., Bonini P., *et al.* (2005). "DNA repair in post-mitotic neurons: a gene-trapping strategy." Cell Death Differ **12**(3): 307-309.

Michalowski J., Seavey S. E., Mendrysa S. M., *et al.* (2001). "Defects in transcription coupled repair interfere with expression of p90(MDM2) in response to ultraviolet light." Oncogene **20**(41): 5856-5864.

Mihaylova V. T., Bindra R. S., Yuan J., *et al.* (2003). "Decreased expression of the DNA mismatch repair gene Mlh1 under hypoxic stress in mammalian cells." Mol Cell Biol **23**(9): 3265-3273.

Minucci S. and Pelicci P. G. (2006). "Histone deacetylase inhibitors and the promise of epigenetic (and more) treatments for cancer." Nat Rev Cancer **6**(1): 38-51.

Miranda C. J., Santos M. M., Ohshima K., *et al.* (2002). "Frataxin knockin mouse." FEBS Lett **512**(1-3): 291-297.

Montermini L., Andermann E., Labuda M., *et al.* (1997). "The Friedreich ataxia GAA triplet repeat: premutation and normal alleles." Hum Mol Genet **6**(8): 1261-1266.

Moyer M. P., Manzano L. A., Merriman R. L., *et al.* (1996). "NCM460, a normal human colon mucosal epithelial cell line." In Vitro Cell Dev Biol Anim **32**(6): 315-317.

Mrazek J., Guo X. and Shah A. (2007). "Simple sequence repeats in prokaryotic genomes." Proc Natl Acad Sci U S A **104**(20): 8472-8477.

Nardin R. A. and Johns D. R. (2001). "Mitochondrial dysfunction and neuromuscular disease." Muscle Nerve **24**(2): 170-191.

Navarro J. A., Ohmann E., Sanchez D., *et al.* (2010). "Altered lipid metabolism in a Drosophila model of Friedreich's ataxia." Hum Mol Genet.

Niessen R. C., Kleibeuker J. H., Westers H., *et al.* (2009). "PMS2 involvement in patients suspected of Lynch syndrome." Genes Chromosomes Cancer **48**(4): 322-329.

O'Neill H. A., Gakh O. and Isaya G. (2005). "Supramolecular assemblies of human frataxin are formed via subunit-subunit interactions mediated by a non-conserved amino-terminal region." J Mol Biol **345**(3): 433-439.

O'Neill H. A., Gakh O., Park S., *et al.* (2005). "Assembly of human frataxin is a mechanism for detoxifying redox-active iron." Biochemistry **44**(2): 537-545.

Ohshima K., Montermini L., Wells R. D., *et al.* (1998). "Inhibitory effects of expanded GAA.TTC triplet repeats from intron I of the Friedreich ataxia gene on transcription and replication in vivo." J Biol Chem **273**(23): 14588-14595.

Owen B. A., Yang Z., Lai M., *et al.* (2005). "(CAG)(n)-hairpin DNA binds to Msh2-Msh3 and changes properties of mismatch recognition." Nat Struct Mol Biol **12**(8): 663-670.

Pandolfo M. (1998). "Molecular genetics and pathogenesis of Friedreich ataxia." Neuromuscul Disord **8**(6): 409-415.

Pandolfo M. (1999). "Molecular pathogenesis of Friedreich ataxia." Arch Neurol **56**(10): 1201-1208.

Pandolfo M. (2002). "Frataxin deficiency and mitochondrial dysfunction." Mitochondrion **2**(1-2): 87-93.

Pandolfo M. (2008). "Drug Insight: antioxidant therapy in inherited ataxias." Nat Clin Pract Neurol **4**(2): 86-96.

Pandolfo M. (2009). "Friedreich ataxia: the clinical picture." J Neurol **256 Suppl 1**: 3-8.

Pandolfo M. and Montermini L. (1998). "Prenatal diagnosis of Friedreich ataxia." Prenat Diagn **18**(8): 831-833.

Park S., Gakh O., O'Neill H. A., *et al.* (2003). "Yeast frataxin sequentially chaperones and stores iron by coupling protein assembly with iron oxidation." J Biol Chem **278**(33): 31340-31351.

Pearson C. E., Nichol Edamura K. and Cleary J. D. (2005). "Repeat instability: mechanisms of dynamic mutations." Nat Rev Genet **6**(10): 729-742.

Pianese L., Cavalcanti F., De Michele G., *et al.* (1997). "The effect of parental gender on the GAA dynamic mutation in the FRDA gene." Am J Hum Genet **60**(2): 460-463.

Pianese L., Turano M., Lo Casale M. S., *et al.* (2004). "Real time PCR quantification of frataxin mRNA in the peripheral blood leucocytes of Friedreich ataxia patients and carriers." J Neurol Neurosurg Psychiatry **75**(7): 1061-1063.

Pineda M., Arpa J., Montero R., *et al.* (2008). "Idebenone treatment in paediatric and adult patients with Friedreich ataxia: long-term follow-up." Eur J Paediatr Neurol **12**(6): 470-475.

Pizzi C., Di Maio M., Daniele S., *et al.* (2007). "Triplet repeat instability correlates with dinucleotide instability in primary breast cancer." Oncol Rep **17**(1): 193-199.

Pollard L. M., Bourn R. L. and Bidichandani S. I. (2008). "Repair of DNA double-strand breaks within the (GAA*TTC)n sequence results in frequent deletion of the triplet-repeat sequence." Nucleic Acids Res **36**(2): 489-500.

Pook M. A., Al-Mahdawi S., Carroll C. J., *et al.* (2001). "Rescue of the Friedreich's ataxia knockout mouse by human YAC transgenesis." Neurogenetics **3**(4): 185-193.

Potaman V. N., Oussatcheva E. A., Lyubchenko Y. L., *et al.* (2004). "Length-dependent structure formation in Friedreich ataxia (GAA)n*(TTC)n repeats at neutral pH." Nucleic Acids Res **32**(3): 1224-1231.

Puccio H. and Koenig M. (2000). "Recent advances in the molecular pathogenesis of Friedreich ataxia." Hum Mol Genet **9**(6): 887-892.

Puccio H., Simon D., Cossee M., *et al.* (2001). "Mouse models for Friedreich ataxia exhibit cardiomyopathy, sensory nerve defect and Fe-S enzyme deficiency followed by intramitochondrial iron deposits." Nat Genet **27**(2): 181-186.

Radisky D. C., Babcock M. C. and Kaplan J. (1999). "The yeast frataxin homologue mediates mitochondrial iron efflux. Evidence for a mitochondrial iron cycle." J Biol Chem **274**(8): 4497-4499.

Rai M., Soragni E., Jenssen K., *et al.* (2008). "HDAC inhibitors correct frataxin deficiency in a Friedreich ataxia mouse model." PLoS One **3**(4): e1958.

Rea S. L., Ventura N. and Johnson T. E. (2007). "Relationship between mitochondrial electron transport chain dysfunction, development, and life extension in Caenorhabditis elegans." PLoS Biol **5**(10): e259.

Rindler P. M. and Bidichandani S. I. (2011). "Role of transcript and interplay between transcription and replication in triplet-repeat instability in mammalian cells." Nucleic Acids Res **39**(2): 526-535.

Ristow M. (2004). "Neurodegenerative disorders associated with diabetes mellitus." J Mol Med (Berl) **82**(8): 510-529.

Ristow M., Mulder H., Pomplun D., *et al.* (2003). "Frataxin deficiency in pancreatic islets causes diabetes due to loss of beta cell mass." J Clin Invest **112**(4): 527-534.

Ristow M., Pfister M. F., Yee A. J., *et al.* (2000). "Frataxin activates mitochondrial energy conversion and oxidative phosphorylation." Proc Natl Acad Sci U S A **97**(22): 12239-12243.

Rodriguez-Jimenez F. J., Moreno-Manzano V., Lucas-Dominguez R., *et al.* (2008). "Hypoxia causes downregulation of mismatch repair system and genomic instability in stem cells." Stem Cells **26**(8): 2052-2062.

Rotig A., de Lonlay P., Chretien D., *et al.* (1997). "Aconitase and mitochondrial iron-sulphur protein deficiency in Friedreich ataxia." Nat Genet **17**(2): 215-217.

Sakamoto N., Chastain P. D., Parniewski P., *et al.* (1999). "Sticky DNA: self-association properties of long GAA.TTC repeats in R.R.Y triplex structures from Friedreich's ataxia." Mol Cell **3**(4): 465-475.

Sakamoto N., Ohshima K., Montermini L., *et al.* (2001). "Sticky DNA, a self-associated complex formed at long GAA*TTC repeats in intron 1 of the frataxin gene, inhibits transcription." J Biol Chem **276**(29): 27171-27177.

Sancar A., Lindsey-Boltz L. A., Unsal-Kacmaz K., *et al.* (2004). "Molecular mechanisms of mammalian DNA repair and the DNA damage checkpoints." Annu Rev Biochem **73**: 39-85.

Santos M. M., Ohshima K. and Pandolfo M. (2001). "Frataxin deficiency enhances apoptosis in cells differentiating into neuroectoderm." Hum Mol Genet **10**(18): 1935-1944.

Sarsero J. P., Li L., Wardan H., *et al.* (2003). "Upregulation of expression from the FRDA genomic locus for the therapy of Friedreich ataxia." J Gene Med **5**(1): 72-81.

Sas K., Robotka H., Toldi J., *et al.* (2007). "Mitochondria, metabolic disturbances, oxidative stress and the kynurenine system, with focus on neurodegenerative disorders." J Neurol Sci **257**(1-2): 221-239.

Savas S., Kim D. Y., Ahmad M. F., *et al.* (2004). "Identifying functional genetic variants in DNA repair pathway using protein conservation analysis." Cancer Epidemiol Biomarkers Prev **13**(5): 801-807.

Saveliev A., Everett C., Sharpe T., *et al.* (2003). "DNA triplet repeats mediate heterochromatin-protein-1-sensitive variegated gene silencing." Nature **422**(6934): 909-913.

Savouret C., Brisson E., Essers J., *et al.* (2003). "CTG repeat instability and size variation timing in DNA repair-deficient mice." EMBO J **22**(9): 2264-2273.

Schmucker S., Argentini M., Carelle-Calmels N., *et al.* (2008). "The in vivo mitochondrial two-step maturation of human frataxin." Hum Mol Genet.

Schmucker S. and Puccio H. (2010). "Understanding the molecular mechanisms of Friedreich's ataxia to develop therapeutic approaches." Hum Mol Genet **19**(R1): R103-110.

Schulz T. J., Thierbach R., Voigt A., *et al.* (2006). "Induction of oxidative metabolism by mitochondrial frataxin inhibits cancer growth: Otto Warburg revisited." J Biol Chem **281**(2): 977-981.

Schweitzer J. K. and Livingston D. M. (1997). "Destabilization of CAG trinucleotide repeat tracts by mismatch repair mutations in yeast." Hum Mol Genet **6**(3): 349-355.

Seguin A., Sutak R., Bulteau A. L., *et al.* (2010). "Evidence that yeast frataxin is not an iron storage protein in vivo." Biochim Biophys Acta **1802**(6): 531-538.

Semenza G. L. (2010). "Defining the role of hypoxia-inducible factor 1 in cancer biology and therapeutics." Oncogene **29**(5): 625-634.

Shahi A., Lee J. H., Kang Y., *et al.* (2011). "Mismatch-repair protein MSH6 is associated with Ku70 and regulates DNA double-strand break repair." Nucleic Acids Res **39**(6): 2130-2143.

Shan Y. and Cortopassi G. (2012). "HSC20 interacts with frataxin and is involved in iron-sulfur cluster biogenesis and iron homeostasis." Hum Mol Genet **21**(7): 1457-1469.

Shell S. S., Putnam C. D. and Kolodner R. D. (2007). "The N terminus of Saccharomyces cerevisiae Msh6 is an unstructured tether to PCNA." Mol Cell **26**(4): 565-578.

Shimodaira H., Yoshioka-Yamashita A., Kolodner R. D., *et al.* (2003). "Interaction of mismatch repair protein PMS2 and the p53-related transcription factor p73 in apoptosis response to cisplatin." Proc Natl Acad Sci U S A **100**(5): 2420-2425.

Siehler S. Y., Schrauder M., Gerischer U., *et al.* (2009). "Human MutL-complexes monitor homologous recombination independently of mismatch repair." DNA Repair (Amst) **8**(2): 242-252.

Silva F. C., Valentin M. D., Ferreira Fde O., *et al.* (2009). "Mismatch repair genes in Lynch syndrome: a review." Sao Paulo Med J **127**(1): 46-51.

Simon D., Seznec H., Gansmuller A., *et al.* (2004). "Friedreich ataxia mouse models with progressive cerebellar and sensory ataxia reveal autophagic neurodegeneration in dorsal root ganglia." J Neurosci **24**(8): 1987-1995.

Smith J. A., Bannister L. A., Bhattacharjee V., *et al.* (2007). "Accurate homologous recombination is a prominent double-strand break repair pathway in mammalian chromosomes and is modulated by mismatch repair protein Msh2." Mol Cell Biol **27**(22): 7816-7827.

Son L. S., Bacolla A. and Wells R. D. (2006). "Sticky DNA: in vivo formation in E. coli and in vitro association of long GAA*TTC tracts to generate two independent supercoiled domains." J Mol Biol **360**(2): 267-284.

Sonneveld E., Vrieling H., Mullenders L. H., *et al.* (2001). "Mouse mismatch repair gene Msh2 is not essential for transcription-coupled repair of UV-induced cyclobutane pyrimidine dimers." Oncogene **20**(4): 538-541.

Soragni E., Herman D., Dent S. Y., *et al.* (2008). "Long intronic GAA*TTC repeats induce epigenetic changes and reporter gene silencing in a molecular model of Friedreich ataxia." Nucleic Acids Res **36**(19): 6056-6065.

Spurling C. C., Godman C. A., Noonan E. J., *et al.* (2008). "HDAC3 overexpression and colon cancer cell proliferation and differentiation." Mol Carcinog **47**(2): 137-147.

Steffan J. S., Bodai L., Pallos J., *et al.* (2001). "Histone deacetylase inhibitors arrest polyglutamine-dependent neurodegeneration in Drosophila." Nature **413**(6857): 739-743.

Stehling O., Elsasser H. P., Bruckel B., *et al.* (2004). "Iron-sulfur protein maturation in human cells: evidence for a function of frataxin." Hum Mol Genet **13**(23): 3007-3015.

Surtees J. A. and Alani E. (2006). "Mismatch repair factor MSH2-MSH3 binds and alters the conformation of branched DNA structures predicted to form during genetic recombination." J Mol Biol **360**(3): 523-536.

Sutak R., Xu X., Whitnall M., *et al.* (2008). "Proteomic analysis of hearts from frataxin knockout mice: marked rearrangement of energy metabolism, a response to cellular stress and altered expression of proteins involved in cell structure, motility and metabolism." Proteomics **8**(8): 1731-1741.

Sweder K. S., Verhage R. A., Crowley D. J., *et al.* (1996). "Mismatch repair mutants in yeast are not defective in transcription-coupled DNA repair of UV-induced DNA damage." Genetics **143**(3): 1127-1135.

Tautz D. (1989). "Hypervariability of simple sequences as a general source for polymorphic DNA markers." Nucleic Acids Res **17**(16): 6463-6471.

Thierbach R., Florian S., Wolfrum K., *et al.* (2012). "Specific alterations of carbohydrate metabolism are associated with hepatocarcinogenesis in mitochondrially impaired mice." Hum Mol Genet **21**(3): 656-663.

Thierbach R., Schulz T. J., Isken F., *et al.* (2005). "Targeted disruption of hepatic frataxin expression causes impaired mitochondrial function, decreased life span and tumor growth in mice." Hum Mol Genet **14**(24): 3857-3864.

Tome S., Holt I., Edelmann W., *et al.* (2009). "MSH2 ATPase domain mutation affects CTG*CAG repeat instability in transgenic mice." PLoS Genet **5**(5): e1000482.

Toth G., Gaspari Z. and Jurka J. (2000). "Microsatellites in different eukaryotic genomes: survey and analysis." Genome Res **10**(7): 967-981.

Tournier I., Vezain M., Martins A., *et al.* (2008). "A large fraction of unclassified variants of the mismatch repair genes MLH1 and MSH2 is associated with splicing defects." Hum Mutat **29**(12): 1412-1424.

Tozzi G., Nuccetelli M., Lo Bello M., *et al.* (2002). "Antioxidant enzymes in blood of patients with Friedreich's ataxia." Arch Dis Child **86**(5): 376-379.

van den Broek W. J., Nelen M. R., Wansink D. G., *et al.* (2002). "Somatic expansion behaviour of the (CTG)n repeat in myotonic dystrophy knock-in mice is differentially

affected by Msh3 and Msh6 mismatch-repair proteins." Hum Mol Genet **11**(2): 191-198.

Vasen H. F., Moslein G., Alonso A., *et al.* (2007). "Guidelines for the clinical management of Lynch syndrome (hereditary non-polyposis cancer)." J Med Genet **44**(6): 353-362.

Vasen H. F., Stormorken A., Menko F. H., *et al.* (2001). "MSH2 mutation carriers are at higher risk of cancer than MLH1 mutation carriers: a study of hereditary nonpolyposis colorectal cancer families." J Clin Oncol **19**(20): 4074-4080.

Vazquez-Manrique R. P., Gonzalez-Cabo P., Ros S., *et al.* (2006). "Reduction of Caenorhabditis elegans frataxin increases sensitivity to oxidative stress, reduces lifespan, and causes lethality in a mitochondrial complex II mutant." FASEB J **20**(1): 172-174.

Ventura N., Rea S., Henderson S. T., *et al.* (2005). "Reduced expression of frataxin extends the lifespan of Caenorhabditis elegans." Aging Cell **4**(2): 109-112.

Vetcher A. A., Napierala M., Iyer R. R., *et al.* (2002). "Sticky DNA, a long GAA.GAA.TTC triplex that is formed intramolecularly, in the sequence of intron 1 of the frataxin gene." J Biol Chem **277**(42): 39217-39227.

Vivas E., Skovran E. and Downs D. M. (2006). "Salmonella enterica strains lacking the frataxin homolog CyaY show defects in Fe-S cluster metabolism in vivo." J Bacteriol **188**(3): 1175-1179.

Waldvogel D., van Gelderen P. and Hallett M. (1999). "Increased iron in the dentate nucleus of patients with Friedrich's ataxia." Ann Neurol **46**(1): 123-125.

Walsh M. D., Cummings M. C., Buchanan D. D., *et al.* (2008). "Molecular, pathologic, and clinical features of early-onset endometrial cancer: identifying presumptive Lynch syndrome patients." Clin Cancer Res **14**(6): 1692-1700.

Wells R. D. (2008). "DNA triplexes and Friedreich ataxia." FASEB J **22**(6): 1625-1634.

Wheeler V. C., Lebel L. A., Vrbanac V., *et al.* (2003). "Mismatch repair gene Msh2 modifies the timing of early disease in Hdh(Q111) striatum." Hum Mol Genet **12**(3): 273-281.

White P. J., Borts R. H. and Hirst M. C. (1999). "Stability of the human fragile X (CGG)(n) triplet repeat array in Saccharomyces cerevisiae deficient in aspects of DNA metabolism." Mol Cell Biol **19**(8): 5675-5684.

Wilson A. J., Byun D. S., Popova N., *et al.* (2006). "Histone deacetylase 3 (HDAC3) and other class I HDACs regulate colon cell maturation and p21 expression and are deregulated in human colon cancer." J Biol Chem **281**(19): 13548-13558.

Wilson R. B. and Roof D. M. (1997). "Respiratory deficiency due to loss of mitochondrial DNA in yeast lacking the frataxin homologue." Nat Genet **16**(4): 352-357.

Wong A., Yang J., Cavadini P., *et al.* (1999). "The Friedreich's ataxia mutation confers cellular sensitivity to oxidant stress which is rescued by chelators of iron and calcium and inhibitors of apoptosis." Hum Mol Genet **8**(3): 425-430.

Wong A., Yang J., Danielson S., *et al.* (2000). "Sensitivity of FRDA lymphoblasts to salts of transition metal ions." Antioxid Redox Signal **2**(3): 461-465.

Yoon T. and Cowan J. A. (2003). "Iron-sulfur cluster biosynthesis. Characterization of frataxin as an iron donor for assembly of [2Fe-2S] clusters in ISU-type proteins." J Am Chem Soc **125**(20): 6078-6084.

Yoon T. and Cowan J. A. (2004). "Frataxin-mediated iron delivery to ferrochelatase in the final step of heme biosynthesis." J Biol Chem **279**(25): 25943-25946.

Yoon T., Dizin E. and Cowan J. A. (2007). "N-terminal iron-mediated self-cleavage of human frataxin: regulation of iron binding and complex formation with target proteins." J Biol Inorg Chem **12**(4): 535-542.

Zarse K., Schulz T. J., Birringer M., *et al.* (2007). "Impaired respiration is positively correlated with decreased life span in Caenorhabditis elegans models of Friedreich Ataxia." FASEB J **21**(4): 1271-1275.

Zhang Y. and Reinberg D. (2001). "Transcription regulation by histone methylation: interplay between different covalent modifications of the core histone tails." Genes Dev **15**(18): 2343-2360.

Zhang Y., Rohde L. H. and Wu H. (2009). "Involvement of nucleotide excision and mismatch repair mechanisms in double strand break repair." Curr Genomics **10**(4): 250-258.

Zhang Y., Yuan F., Presnell S. R., et al. (2005). "Reconstitution of 5'-directed human mismatch repair in a purified system." Cell 122(5): 693-705.

Zhao J., Bacolla A., Wang G., et al. (2010). "Non-B DNA structure-induced genetic instability and evolution." Cell Mol Life Sci 67(1): 43-62.

Journal publications

Sandi C, Pinto RM, Al-Mahdawi S, **Ezzatizadeh V**, Barnes G, Jones S, Rusche JR, Gottesfeld JM and Pook MA (2011) Prolonged treatment with pimelic o-aminobenzamide HDAC inhibitors ameliorates the disease phenotype of a Friedreich ataxia mouse model. *Neurobiol Dis*, 42(3):496-505.

Ezzatizadeh V, Pinto RM, Sandi C, Al-Mahdawi S, Te Riele H and Pook MA (2012) The mismatch repair system protects against intergenerational GAA repeat instability in a Friedreich ataxia mouse model. *Neurobiol Dis*, 46(1):165-71.

Tomassini B, Arcuri G, Fortuni S, Sandi C, **Ezzatizadeh V**, Casali C, Condo I, Malisan F, Al-Mahdawi S, Pook M, Testi R (2012) Interferon gamma upregulates frataxin and corrects the functional deficits in a Friedreich ataxia model. *Hum Mol Genet*, 21(13):2855-61.

Presented posters

Ezzatizadeh V, Mouro Pinto R, Sandi C, Al-Mahdawi S and Pook M (2011) Analysis of intergenerational GAA repeat instability in FRDA transgenic mouse models- Poster presented at "**4th FARA International Scientific Conference**", Strasbourg, France.

Ezzatizadeh V, Sandi C, Anjomani Virmouni S, Sandi M, Al-Mahdawi S and Pook M (2012) Mismatch repair gene effects on somatic GAA repeat instability and *FXN* gene expression in FRDA transgenic mice- Poster presented at "**International Ataxia Research Conference**", London, UK.